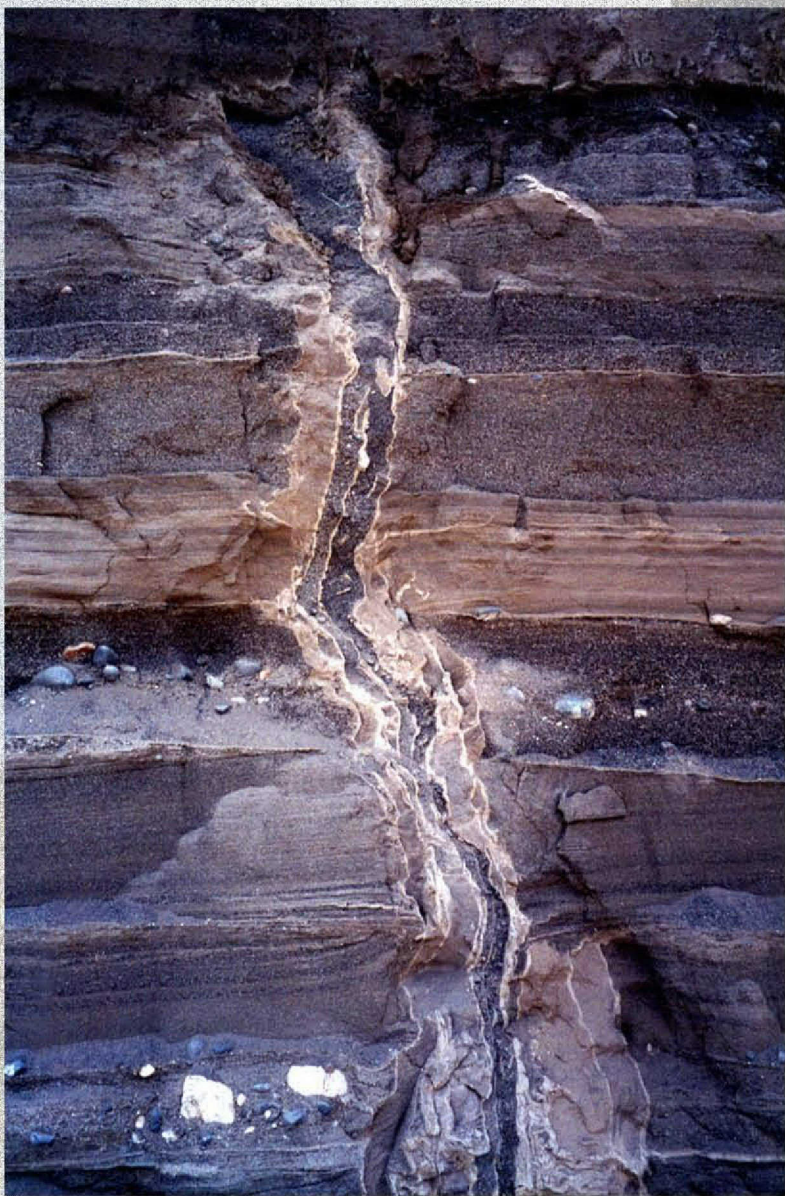


Geologic Atlas Series

Clastic Injection Dikes of the Pasco Basin and Vicinity



E9809105

Prepared for the
U.S. Department of Energy
Office of Environmental
Restoration



Clastic Injection Dikes of the Pasco Basin and Vicinity

Geologic Atlas Series

K. R. Fecht
Bechtel Hanford, Inc.
Richland, Washington

K. A. Lindsey
Daniel B. Stephens and Associates, Inc.
Richland, Washington

B. N. Bjornstad
D. G. Horton
G. V. Last
S. P. Reidel
Pacific Northwest National Laboratory
Richland, Washington

July 1999

PREFACE

The atlas provides a summary of the current understanding of clastic injection dikes in the Pasco Basin and vicinity. The atlas is a compilation of photographs, maps, tables, illustrations, and text that provides a summary of the physical description, emplacement history and mechanisms, and hydrologic characteristics of clastic injection dikes. The information that has been assembled is based on geologic, geophysical, and geohydrologic investigations conducted in the Pasco Basin and vicinity.

The atlas is organized as follows.

Introduction: This section provides an introduction to the study of clastic injection dikes, defines the purposes of the study, identifies the area of investigation, describes the geologic setting of the Pasco Basin and vicinity, and references previous studies.

Methods of Investigation: This section identifies and summarizes the methods used to identify and investigate clastic injection dikes. The section also identifies applications for testing the properties of clastic injection dikes.

Physical Description of Clastic Injection Dikes: This section describes the physical attributes of clastic injection dikes, including components, width, depth, lateral extent, and termination of dikes.

Distribution of Clastic Injection Dikes: This section describes the distribution of clastic injection dikes with respect to elevation, geomorphic terrain, and rock types.

Clastic Dike Networks: This section describes four types of clastic injection dike networks, including regular-shaped, polygonal-patterned ground; irregular-shaped, polygonal-patterned ground; pre-existing fissure; and random occurrence.

Age and Timing of Emplacement: This section defines the ages of the dikes and the timing of emplacement.

Origin of Clastic Injection Dikes: This section describes the approach, defines the constraints, evaluates the theories, and presents a discussion on the origin of clastic injection dikes and dike networks.

Geophysical Methods Testing: This section describes the test results of surface-based, nonintrusive geophysical surveys over buried clastic injection dikes. The test methods used are ground-penetrating radar and electromagnetic induction.

Hydraulic Testing: This section presents the results of hydraulic tests in and adjacent to clastic injection dikes. The test methods used in the study include Guelph permeameter, small-scale infiltration, and unsaturated flow apparatus.

Summary and Conclusions: This section summarizes the information from each section of the atlas and presents the conclusions of this study.

References: This section lists the references cited in the atlas.

Appendices: The appendices provide the lists of figures and tables used in this atlas.

C O N T E N T S

Preface.....	i
1.0 INTRODUCTION.....	1-1
1.1 Background.....	1-1
1.2 Purposes of the Study.....	1-3
1.3 Area of Investigation.....	1-4
1.4 Site Location Description.....	1-6
1.5 Geologic Setting.....	1-7
1.6 Previous Studies.....	1-16
2.0 METHODS OF INVESTIGATION.....	2-1
2.1 General.....	2-1
2.2 Standard Field and Trench Mapping.....	2-2
2.3 Mapping of Vegetation Patterns.....	2-3
2.4 Aerial Photogrammetric Imagery.....	2-4
2.5 Borehole Coring and Split-Tube Sampling.....	2-6
2.6 Geophysical Methods.....	2-7
2.7 Infiltration/Permeameter Methods.....	2-8
3.0 PHYSICAL DESCRIPTION OF INDIVIDUAL CLASTIC INJECTION DIKES.....	3-1
3.1 General Description.....	3-1
3.2 Components.....	3-2
3.3 Width, Depth, and Lateral Extent.....	3-13
3.4 Termination of Dikes.....	3-14
4.0 DISTRIBUTION OF CLASTIC INJECTION DIKES.....	4-1
4.1 Occurrence by Elevation.....	4-1
4.2 Geographic Distribution.....	4-2
4.3 Occurrence by Rock Type.....	4-3
4.4 Occurrence in Multiple Sediment/Rock Types.....	4-13
5.0 CLASTIC INJECTION DIKE NETWORKS.....	5-1
5.1 Types Of Networks.....	5-1
5.2 Regular-Shaped, Polygonal-Patterned Ground.....	5-2
5.3 Irregular-Shaped, Polygonal-Patterned Ground.....	5-16

5.4	Pre-Existing Fissure	5-22
5.5	Random Occurrence	5-29
5.6	Distribution of Networks	5-34
6.0	AGE AND TIMING OF EMPLACEMENT	6-1
6.1	Approach	6-1
6.2	Age of Dike Networks	6-2
6.3	Summary of Age and Timing of Emplacement	6-8
7.0	ORIGIN OF CLASTIC INJECTION DIKES	7-1
7.1	Approach	7-1
7.2	Constraints on Origin	7-2
7.3	Evaluation of Geologic Processes in Fissure Development	7-3
7.4	Evaluation of Geologic Processes in Sediment Transportation and Deposition	7-17
7.5	Origin of Dikes	7-19
7.6	Origin of Dike Networks	7-24
8.0	GEOPHYSICAL METHODS TESTING	8-1
8.1	Nonintrusive Electromagnetic Induction	8-1
8.2	Ground-Penetrating Radar	8-2
9.0	HYDRAULIC TESTING	9-1
9.1	Background	9-1
9.2	Abbreviations and Symbols	9-2
9.3	Guelph Permeameter	9-3
9.4	Small-Scale Infiltration Tests	9-13
9.5	Unsaturated Flow Apparatus (UFA™) Method - Moisture	9-33
9.6	Unsaturated Flow Apparatus (UFA™) Method - Gas	9-45
9.7	Discussion	9-47
10.0	SUMMARY AND CONCLUSIONS	10-1
11.0	REFERENCES	11-1
	APPENDIX A LIST OF FIGURES	A-1
	APPENDIX B LIST OF TABLES	B-1

ACKNOWLEDGMENTS

Many individuals assisted the authors over the past several years in planning field investigations, collecting field data, analyzing samples, and interpreting results associated with clastic injection dikes. The authors thank the many people who supported the field activities and preparation of this atlas. Some of the support included:

- Guelph permeameter measurements:
 - Brent Barnett, Greg Kasza, and Chris Kemp
- Field and trench mapping of dikes:
 - Heidi Stenner, Dave Watson, and Dave Weekes
- Electromagnetic induction and ground penetrating radar surveys:
 - Kevin Bergstrom, Tom Mitchell, and Greg Szwartz
- Field discussions:
 - Don Brown and Terry Tolan
- Borehole investigations:
 - Kent Reynolds and Dave Weekes
- Structural analysis:
 - Virginia Rohay
- Hydraulic property measurements by UFA™ methods:
 - Jim Conca, Xiaobing Chen, and Virginia Rohay
- Support to field investigations:
 - Judy Fecht
 - Steve and Cathy Thosath
- Review of drafts of the atlas, which helped significantly improve the final report:
 - Mike Connelly, Mike Fayer, Raz Khaleel, and Virginia Rohay
- Special thanks to Leslie Brown and the Bechtel Hanford, Inc. Publications and Graphic Services Department for the document preparation, editing, and graphic support in development of the atlas.

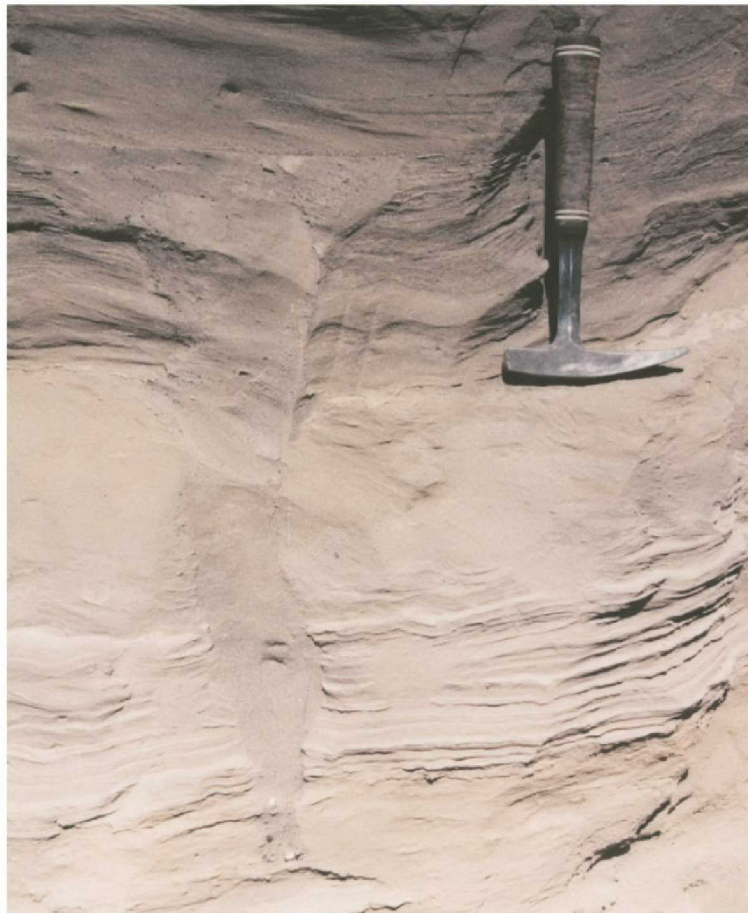
1.0 INTRODUCTION

1.1 BACKGROUND

- Clastic dikes are common structures that occur in many geologic units in the Pasco Basin and vicinity. Clastic dikes are tabular and tapered intrusive bodies that are composed of continental clastic sediments.
- Clastic dikes in the Pasco Basin and vicinity can be classified into two basic types. The types of clastic dikes are based on field observations that were made during geologic mapping of the Pasco Basin and vicinity by Reidel and Fecht (1994a, 1994b) and from unpublished information:
 - Type I dikes occur within fissures that formed by several mechanisms involving pedogenic, seismic, and mass wasting processes and are filled with clastic sediments from air and by moving water. The dike infilling process involves transport of sediments in a low-pressure, gravity-dominated system. Sills have not been observed in Type I dikes in the Pasco Basin.
 - Type II dikes occur within fissures that formed by several mechanisms involving multigenetic processes and are filled with clastic sediments deposited. Sediments are deposited in this type of dike by the injection of sediments by primarily water escape and/or water invasion processes. This process involves the injection of sediments and water in a predominantly moderate- to high-pressure system. Gravitational processes may also be a significant component in Type II dikes. Type II dikes commonly form as sills.
- This atlas addresses the Type II dikes that formed as a result of hydraulic injection of sediments in fissures. These dikes are termed “clastic injection dikes” in this study.
- Clastic injection dikes are fissures filled with sand, silt, clay, and minor coarser debris. Many dikes occur as near-vertical tabular and tapered bodies filled with multiple layers of unconsolidated sediments. The margins of most dikes and internal layers within dikes are separated by thin clay/silt linings.
- Clastic injection dikes are common in pre-Holocene sediments and rocks in the Pasco Basin and vicinity and throughout south-central Washington. Similar clastic injection dikes occur beyond the Pasco Basin, in sedimentary units up the Snake River drainage as far east as Lewiston, Idaho; up the Yakima River drainage as far west as Yakima, Washington; and down the Columbia River in the Umatilla, The Dalles, and Portland basins of Oregon.
- Clastic injection dikes are commonly associated with hydraulic injection during or immediately following Pleistocene cataclysmic flooding, mass wasting, earthquakes, and other geologic processes. Clastic injection dikes occur in geologic units ranging from Miocene to Pleistocene in age.
- Clastic injection dikes occurring in vadose zone sediments have the potential to influence the movement of soil moisture and contaminants.
- Numerous workers have observed and studied clastic injection dikes in south-central Washington, starting with the first study of clastic dikes by Jenkins in 1925.

1.1 BACKGROUND

Figure 1-1: Photograph of a Type I clastic dike that commonly occurs in the sand facies of the Hanford Formation in the central Pasco Basin. The photograph is from the north wall of an excavation at Keene/Kennedy Road (9/28-22M).



0 20
cm

E9803054.205

Figure 1-2: Typical Type II clastic injection dike exposed in a wall of the Environmental Restoration Disposal Facility excavation exposed during construction. The facility is located on the 200 Area Pleistocene Glaciofluvial Flood Bar in the central Hanford Site (12/26-7K).



0 30
cm

E9803054.8

1.2 PURPOSES OF THE STUDY

- The primary purposes of this atlas are to:
 - Describe the physical characteristics of clastic injection dikes
 - Define the known distribution of clastic injection dikes
 - Improve understanding of the emplacement history of clastic injection dikes.
- The secondary purposes of the atlas are to:
 - Constrain the origin of clastic injection dikes
 - Identify and test methods for detecting and determining hydraulic properties of clastic injection dikes.
- The atlas includes a compilation, analysis, and interpretation of existing information on clastic injection dikes in the Pasco Basin and vicinity. The atlas also includes extensive unpublished geological and hydrologic data collected during field investigations.
- The atlas includes numerous locations of clastic injection dikes. Accessible locations that exhibit some of the best physical characteristics of clastic injection dikes and associated host rock are identified as “reference locations.” Many locations require permission from the land owner to gain access.

Table 1-1: List of typical geological and geotechnical investigations that were sources for much of the published and unpublished data used in this study. The authors were directly or indirectly involved in many of these investigations.

Surface geologic mapping projects

Skagit/Hanford Nuclear Project (Reactor)
 WNP #1, #2, and #4 Nuclear Projects (Reactors)
 Fast Flux Test Facility (Reactor)
 Fuels and Materials Examination Facility (Testing Facility)
 Basalt Waste Isolation Project (Geologic Repository)
 Washington Division of Geology and Earth Resources Mapping Project
 US Ecology and Richland Landfills

Environmental restoration activities

CERCLA remedial investigations, engineering design, and remedial actions
 RCRA facility investigations, engineering design, and corrective actions

Geologic engineering studies

Geologic hazards analysis
 Foundation studies
 Natural resource evaluations for road material and surface barrier material
 Age and style of faulting
 Landslide evaluations

Geohydrologic investigations

High-level waste tank integrity assessments
 Restart of liquid waste disposal facilities
 Characterization to support vadose and groundwater monitoring

Geotechnical investigations

Roadways, bridges, and overpasses
 Irrigation canals and dams
 Underground utilities
 Potable water supply wells and distribution systems

1.3 AREA OF INVESTIGATION

- Clastic injection dikes are widespread in the Pasco Basin and vicinity.
 - More than 80 clastic injection dike sites, typically with multiple dikes at each site, were selected for inclusion in the atlas.
 - The dikes occur in a variety of rock types.
 - The dikes represent multiple ages of emplacement.
 - Dike emplacement is controlled by a variety of geologic mechanisms.
- The emphasis of this atlas is clastic injection dikes within the Pasco Basin because:
 - Some of the most extensive exposures of clastic injection dikes and dike networks in south-central Washington occur in the Pasco Basin.
 - There is a need to determine if clastic injection dikes are preferential pathways and/or barriers for flow and transport of contaminants at the U.S. Department of Energy's Hanford Site.
 - The authors have more than 30 years of experience with the surface and subsurface geology of the basin and have examined dozens of trenches, deep pit excavations (several over 20 m deep), and natural outcrops exposing clastic injection dikes.

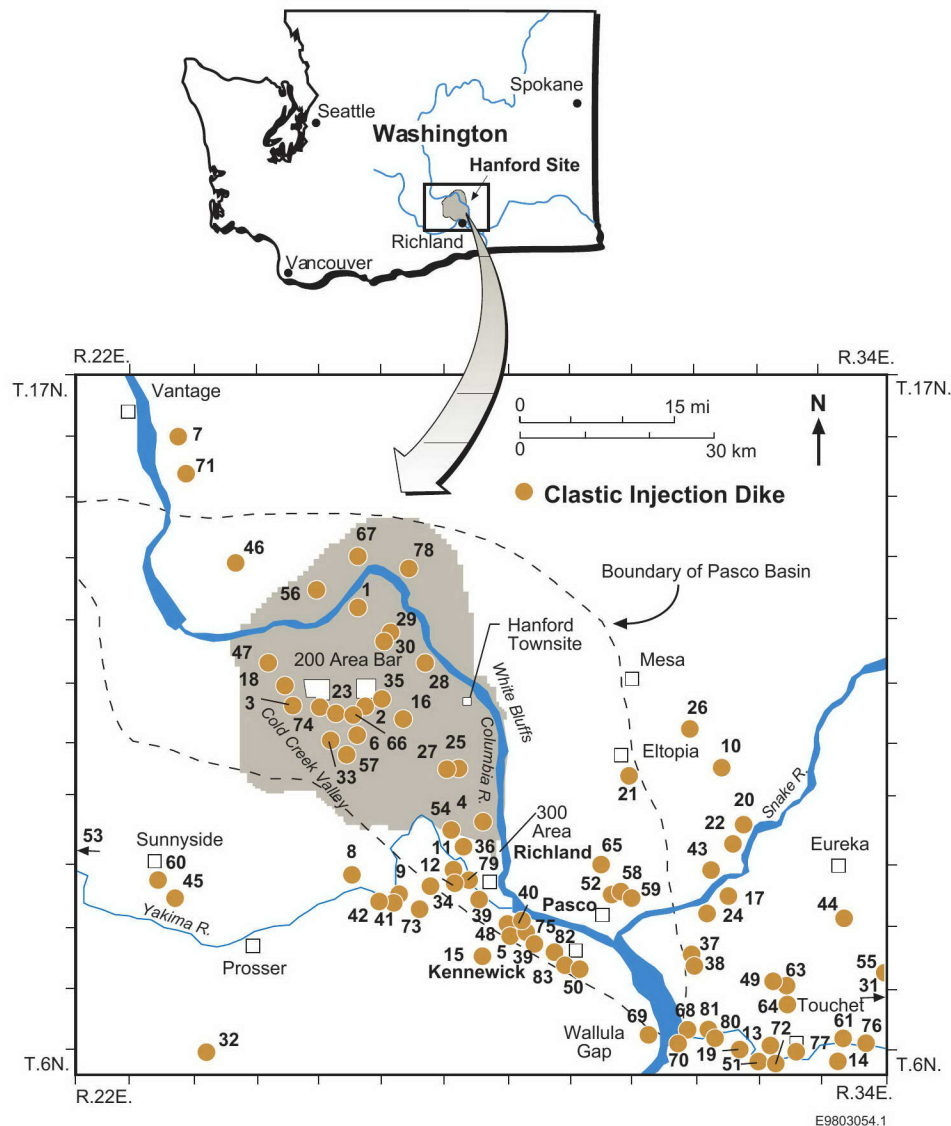


Figure 1-3: Map showing locations of selected clastic injection dike sites in the Pasco Basin and vicinity that were investigated as part of this study. Two clastic injection dike sites used in the study are located beyond the boundary of the map area (Locations #31 and #53).

1.3 AREA OF INVESTIGATION (Continued)

Figure 1-3 (Continued).

Clastic Injection Dike Sites	Location	Clastic Injection Dike Sites	Location	Clastic Injection Dike Sites	Location
1. 100-N Area	14/26-28C	32. Glade Creek East	6/24-11	64. Touchet Road	7/33-22Q
2. 216-BC Cribs	12/26-10K	33. Goose Egg Hill	12/26-33C	65. Transtate Gravel Pit	9/30-6F
3. 216-S-16 Pond	12/25-14E	34. Goose Gap	9/27-13E	66. US Ecology	9/26-9R
4. 300 Area	10/28-11G	35. Grout	12/26-1N	67. Wahluke Landing Road	14/26-3N
5. Amon Wasteway South	8/28-1A	36. Horn Rapids Ditch	10/28-29F	68. Wallula Gap East	7/31-27N
6. Army Loop Road	12/26-34C	37. Iowa Beef North	8/31-36D	69. Wallula Gap West	7/31-29J
7. Babcock Bench South	17/23-28	38. Iowa Beef South	8/31-36D	70. Wallula Junction	7/31-27J
8. Badlands	9/26-9N	39. Keene/Kennedy Road	9/28-22M	71. Wanapum East	16/23-8
9. Benton City Bluff	9/27-20D	40. Kennewick Railroad Cut	8/29-6B	72. Weaver Pit	6/33-17H
10. Blackman/Snake Road	11/32-11C	41. Kiona Gravel Pit	9/27-20K	73. Webber Canyon Road	9/27-33C
11. Bombing Range North	9/28-8E	42. Kiona Railroad Cut	9/27-19G	74. Well 699-32-72	12/26-18F
12. Bombing Range South	9/28-8M	43. Levey Park	9/32-8	75. West Highlands	9/29-34E
13. Brynes Road	7/32-36G	44. Luckenbill Road	9/34-33B	76. West Lowden	7/34-30J
14. Burlingame Canyon	6/34-5M	45. Mabton	9/23-34	77. West Touchet	7/33-29M
15. Burlington Northern 605	8/28-16Q	46. Mattawa East	14/24	78. White Bluffs North	14/27-8R
16. Central Landfill	12/27-20P	47. McGee Ranch	13/25-30	79. Yakima Bluffs	9/28-16G
17. Charbonneau Park	9/32	48. Meadow Hills	9/28-35R	80. Zangar Junction	7/31-25
18. Corehole DH-24	12/25-3A	49. Nine Mile/Dodd Road	8/33-81	81. Zangar Junction West	7/32-19K
19. Cummings Bridge	7/32-35Q	50. Oak Street	8/30-18R	82. Zintel Canyon Dam	8/29-16J
20. Dalton Lake West	9/32-4A	51. Oxbow Bend	6/32-12A	83. Zintel Canyon Road	8/29-24N
21. Eltopia South	11/30-23C	52. Pasco Landfill	9/30-22		
22. Emma Lake	10/32-23J	53. Pumphouse Road	10/18		
23. Environmental Restoration Disposal Facility	12/26-7K	54. Richland Landfill	10/28-17N		
24. Eureka Flats	9/31-36K	55. Rulo	8/34-24L		
25. Fast Flux Test Facility	11/28-18P	56. Saddle Mountains Lakes Area	14/26-7R		
26. Five Corners	12/31-24R	57. Sand Blowout	11/26-3G		
27. Fuels and Materials Exami- nation Facility	11/28-18N	58. Smith Canyon North	9/30-13N		
28. Gable Mountain Bar	13/27-28R	59. Smith Canyon South	9/30-24D		
29. Gable Mountain North	13/27-19A	60. Snipes Mountain	10/22-34		
30. Gable Mountain South	13/27-19N	61. South Lowden	7/34-29L		
31. Garrett	7/38-28J	62. Thiel South	8/35-31		
		63. Touchet Bridge South	7/33-2F		

1.4 SITE LOCATION DESCRIPTION

- The method of identifying site locations that is used throughout this atlas follows the designation used by the U.S. Geological Survey to locate wells. The designation is based on the rectangular system for subdivision of public land.
- The designation is illustrated using the elastic injection dikes at the Environmental Restoration Disposal Facility (ERDF) excavation in the central portion of the Hanford Site. The site location is designated as 12/26-7K. The numbers before the hyphen indicate the township and range north and east of the Willamette meridian and baseline, respectively (i.e., T. 12 N. and R. 26 E.). The number after the hyphen indicates the square-mile section in which the site is located (i.e., Section 7). The letter indicates the 40-acre tract within the section that the site is located (i.e., K or the northwest quarter of the southeast quarter).

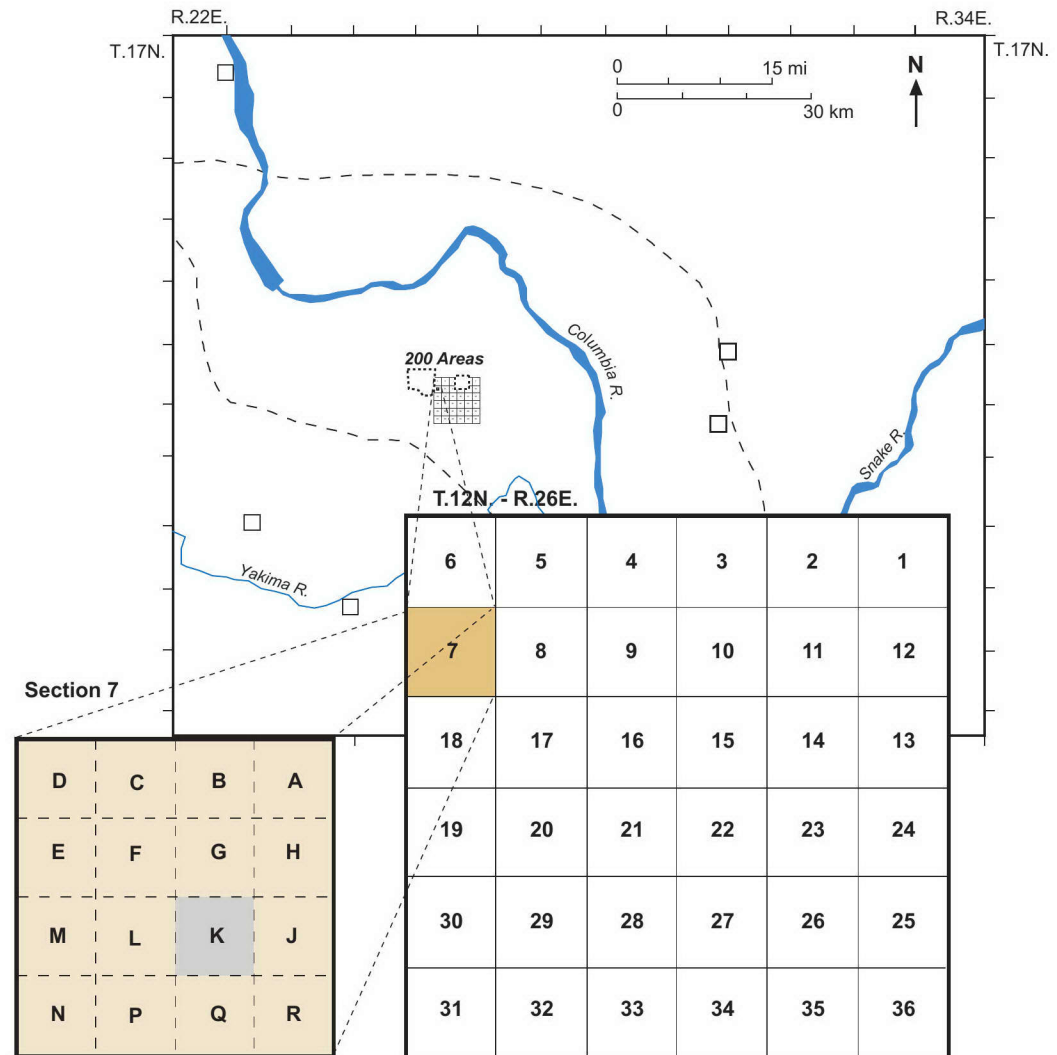


Figure 1-4: Example of the site location designation for the elastic injection dikes at the Environmental Restoration Disposal Facility.

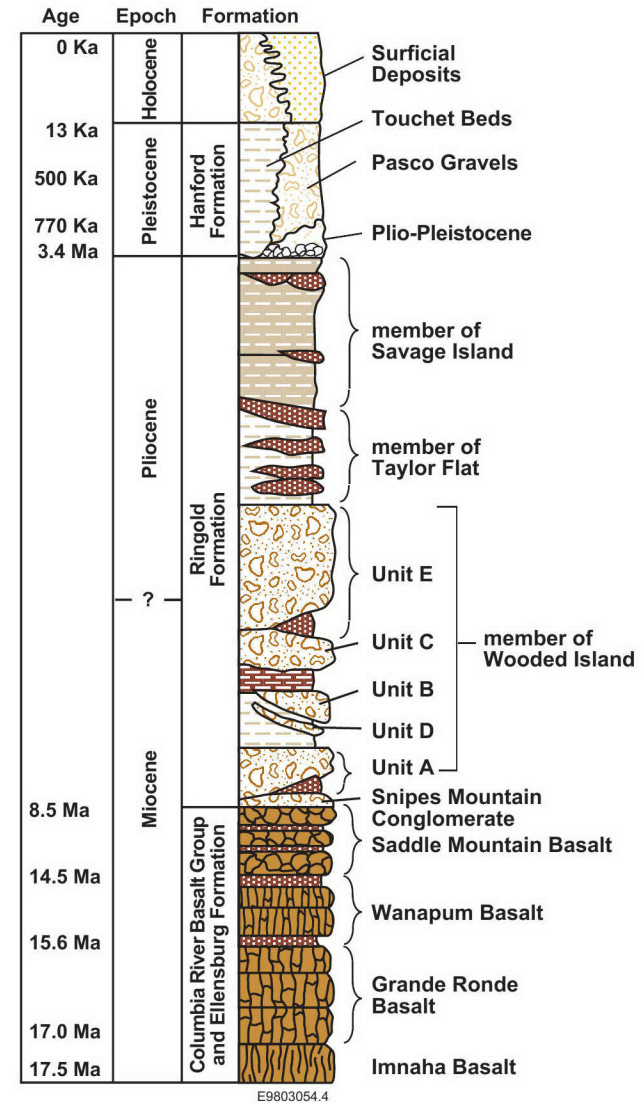
E9803054.3

1.5 GEOLOGIC SETTING

Stratigraphic Nomenclature

- The major stratigraphic units of the investigation area are as follows (listed from the youngest to oldest geologic unit):
 - Surficial deposits
 - Hanford Formation
 - Plio-Pleistocene deposits
 - Ringold Formation
 - Ellensburg Formation
 - Columbia River Basalt Group (CRBG).
- Sources: Lindsey (1991, 1995, 1996) and Reidel and Fecht (1994a, 1994b).

Figure 1-5: Late Cenozoic stratigraphy of the Pasco Basin and vicinity with emphasis on the post-CRBG sequence.

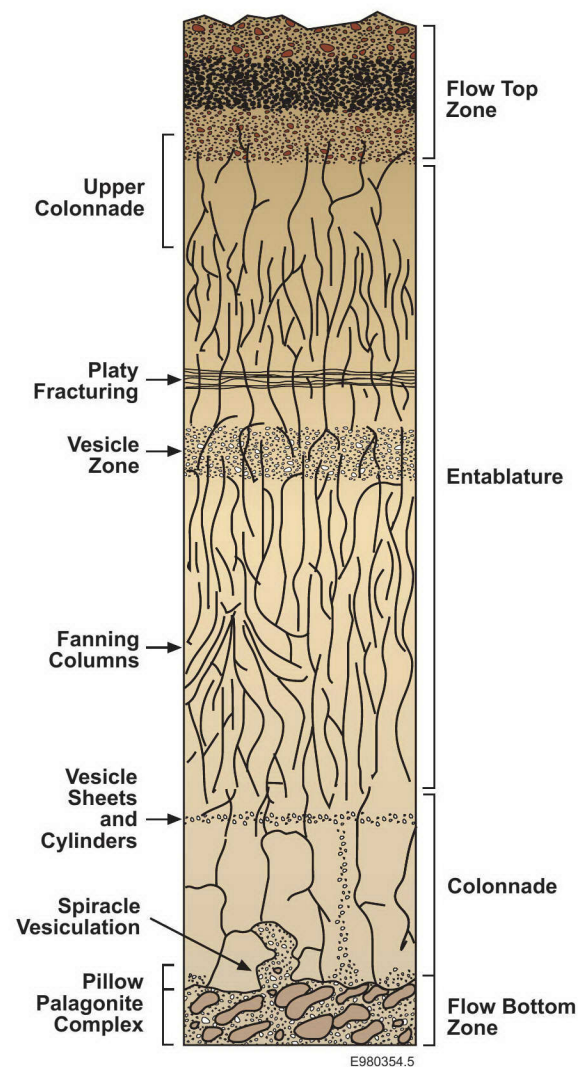


1.5 GEOLOGIC SETTING

Columbia River Basalt Group (CRBG)

- The CRBG forms the bedrock of the investigation area and crops out on the ridges (Yakima Fold Belt) that surround and trend into the Pasco Basin.
- The CRBG was erupted 8.5×10^6 to 17.0×10^6 years ago during the Miocene epoch within the investigation area.
- The CRBG consists of more than 300 tholeiitic basalt flows. Individual basalt flows range from a few meters to more than 100 m in thickness. The maximum accumulated thickness of the CRBG is more than 5,000 m.
- Many CRBG flows are laterally continuous over south-central Washington. Some flows originated in the investigation area and/or thin and pinch out across the area.
- The CRBG flows have complex internal structures. The internal structures include an extensive fracture network (e.g., entablatures, colonnade) that formed during cooling of the lava.
- Sources: Reidel and Fecht (1981, 1994a, 1994b), Long and Wood (1986), and Tolan et al. (1989).

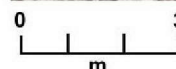
Figure 1-6: Schematic diagram showing the intraflow structures in a CRBG flow.



1.5 GEOLOGIC SETTING

Ellensburg Formation

- The Ellensburg Formation in the Pasco Basin and vicinity consists of continental fluvial and lacustrine sediments deposited by the ancestral Columbia and Clearwater-Salmon River systems.
- The Ellensburg Formation was deposited 8.5×10^6 to $>15.6 \times 10^6$ years ago during the Miocene epoch within the investigation area.
- The Ellensburg Formation includes epiclastic main channel sands and gravels, epiclastic overbank sands and silts, volcanoclastic ashes, other volcanoclastics, and paleosols.
- The Ellensburg Formation overlies and is interbedded within the CRBG and represents periods of quiescence or nondeposition in CRBG volcanism.
- The lateral extent and thickness of the Ellensburg sediments in the investigation area generally increase upward in the section. Individual interbeds intercalated with the Saddle Mountains Basalt are up to 45 m in thickness in the central Pasco Basin and thin onto anticlinal ridges.
- Sources: Reidel and Fecht (1981), Fecht et al. (1987), and Smith et al. (1989).



E9803054.7

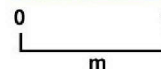
Figure 1-7: Photograph of the main-channel, epiclastic sands of the Rattlesnake Ridge interbed of the Ellensburg Formation. The exposure is located in the Badlands west of Benton City (9/26-9N).

1.5 GEOLOGIC SETTING

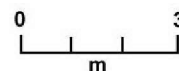
Ringold Formation

- The Ringold Formation consists of continental fluvial and lacustrine sediments deposited by the ancestral Columbia and Clearwater-Salmon River systems.
- The Ringold Formation was deposited between 3.4×10^6 and 8.5×10^6 years ago during the Miocene and Pliocene epochs.
- The Ringold Formation is up to 300 m thick in the north-central Pasco Basin and pinches out on the structural ridges in and around the basin.
- The Ringold Formation is divided into three informal members:
 - **Wooded Island:** Dominated by multiple fluvial gravels (Units A through E) that are separated by finer grained, widespread overbank, paleosol, and lacustrine deposits.
 - **Taylor Flat:** Dominated by thick sequences of fluvial sands, overbank sands and silts, and paleosols.
 - **Savage Island:** Consists of three sequences of lacustrine sand, silt, and diatomite deposits.
- Sources: Newcomb et al. (1972), Fecht et al. (1987), Reidel et al. (1994), and Lindsey (1995, 1996).

Figure 1-8: Photograph of the member of Savage Island (top) and member of Wooded Island (bottom) of the Ringold Formation. The photographs were taken above the Columbia River along the White Bluffs.



E9803054.9



E9803054.10

1.5 GEOLOGIC SETTING

Plio-Pleistocene Deposits

- The Plio-Pleistocene deposits consist of fluvial sediments deposited by the ancestral Columbia, Snake or Clearwater-Salmon (?) and Yakima River systems, eolian and sidestream sediments, and calcic paleosols.
- The Plio-Pleistocene deposits were laid down between 3.4×10^6 and 1×10^6 years ago during the late Pliocene to early Pleistocene epochs.
- The Plio-Pleistocene deposits are up to about 30 m thick. The thickest sections are present south of Gable Mountain in the central Hanford Site, on Wahluke Slope in the northern Pasco Basin, and on the Yakima Bluffs along the Yakima River west of Richland.
- For purposes of this atlas, deposits are divided into four units based on texture, lithology, and geographic position:
 - **Deposits of the Yakima River:** Consist of an upward fining sequence of mainstream sand and gravels, fluvial sands, and overbank and lacustrine sands and silts that occur on the Yakima Bluffs.
 - **Deposits of the Columbia River:** Consist of mainstream sand and gravels that occur south of Gable Mountain. Also referred to as Pre-Missoula gravels.
 - **Deposits of the Upper Cold Creek:** Consist of eolian silty sand (early Palouse soil) mixed with sidestream sands and basalt-rich granules and extensive calcic paleosols that occur primarily on the margins of the basin.
 - **Deposits of the Wahluke Slope:** Sidestream sands and basaltic debris with minor eolian loess and extensive calcic paleosols that occur in sidestream drainages on the margins of the basin.
- Sources: Reidel and Fecht (1994b), Lindsey et al. (1994), Slate (1996), and this study.



0 50
cm

E9803054.11



0 50
cm

E9803054.12

Figure 1-9: Photographs of the Plio-Pleistocene deposits of the Yakima River. The top photograph is of the upper overbank deposits. The bottom photograph is of the lower main channel gravel facies. The deposits are located on the Yakima Bluffs (9/28-16G).

1.5 GEOLOGIC SETTING

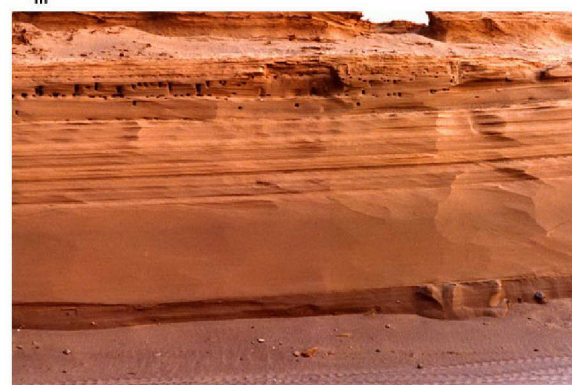
Hanford Formation

- The Hanford Formation consists of glaciofluvial sediments deposited by cataclysmic floods from Glacial Lake Missoula, Pluvial Lake Bonneville, and ice-margin lakes.
- The Hanford Formation formed about 1.3×10^4 to 1×10^6 years ago during the Pleistocene epoch.
- The Hanford Formation is divided locally and regionally into three interfingering sediment facies:
 - **Gravel facies:** Consists of sand and gravel deposited in major flood channels and as large-scale bars.
 - **Sand facies:** Dominated by plane-laminated sand and minor gravel and silt. The sand facies was deposited adjacent to major flood channels and, in plan view, between the gravel and silt facies.
 - **Silt facies:** Consists of graded beds of sand to silt with minor gravel. The silt facies was deposited on basin margins and backflooded tributary valleys.
- Individual beds within each sediment facies represent either separate cataclysmic outbursts or surges from floodwaters entering the Pasco Basin through multiple channelways from glacier-impounded lakes. Other beds were likely deposited as a result of pulses within an individual flood.
- The gravel facies is commonly referred to as the Pasco Gravels of Brown (1975); the sand and silt facies comprise the Touchet Beds of Flint (1938).

Figure 1-10: Photographs of the gravel (top), sand (middle), and silt (bottom) facies of the Hanford Formation.



E9803054.13



E9803054.14



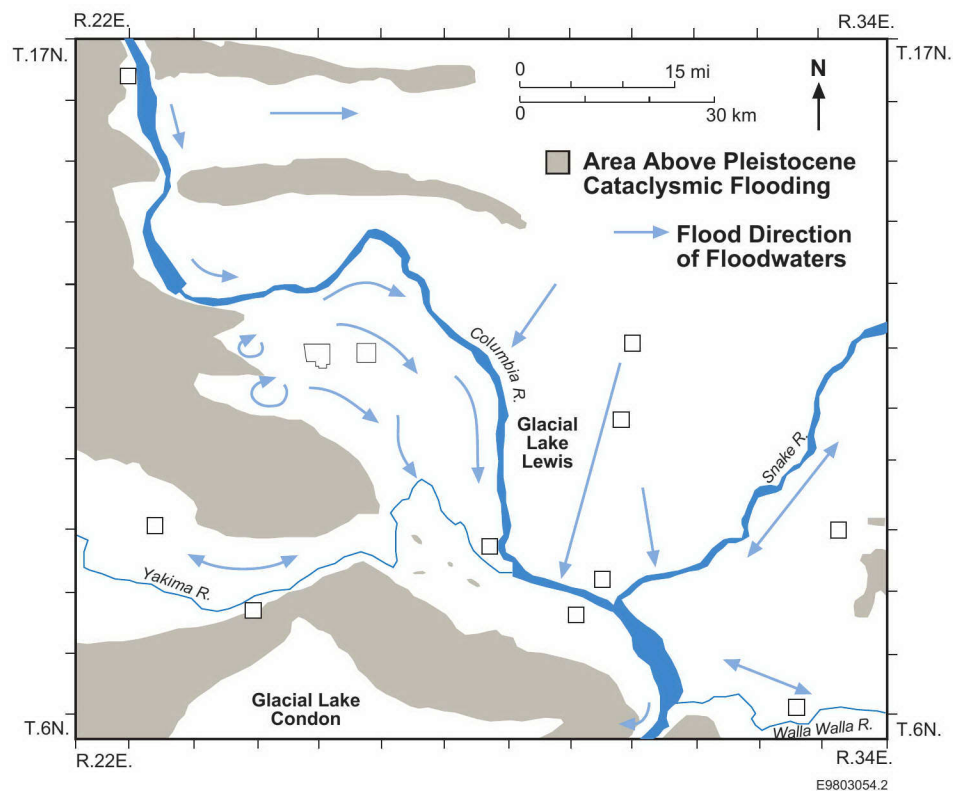
E9803054.15

1.5 GEOLOGIC SETTING

Hanford Formation (Continued)

- Floods from at least four different Pleistocene glacial events deposited sediments in the Pasco Basin. Sedimentary deposits from these floods are divided into four field mapping units based on paleomagnetic data, soil development, tephrochronology, and stratigraphic position. Cycles of floods occur with each field mapping unit. The field mapping units are, from youngest to oldest:
 - Field mapping unit #4 (Qh₄):** Unconsolidated sediments associated with late Wisconsin floods and includes the last low-volume outbursts from Glacial Lake Missoula and other ice margin lakes.
 - Field mapping unit #3 (Qh₃):** Unconsolidated sediments associated with late Wisconsin floods containing Mount St. Helens set ash tephra. The floods include large-scale cataclysmic outbursts from Glacial Lake Missoula and pluvial Lake Bonneville.
 - Field mapping unit #2 (Qh₂):** Unconsolidated sediments from an older Glacial Lake Missoula flood(s) with normal magnetic polarity and commonly capped by a superimposed petrocalcic horizon.
 - Field mapping unit #1 (Qh₁):** Consolidated to semiconsolidated sediments with reversed polarity from the oldest Glacial Lake Missoula floods.
- Floodwaters from Pleistocene floods entered the Pasco Basin through coulees of the channeled scabland, which are located north and northeast of the basin.

Figure 1-11: Map illustrating the extent of Glacial Lake Lewis in the Pasco Basin and vicinity.



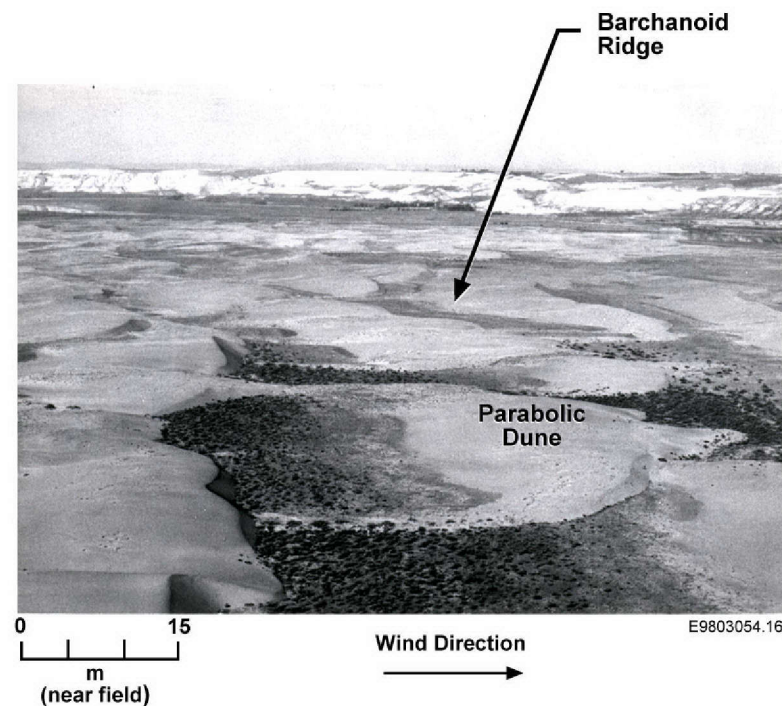
- Hydraulic damming of floodwaters behind the constriction at Wallula Gap formed temporary Glacial Lake Lewis in the Pasco Basin, lower Yakima Valley, and Walla Walla Valley. The maximum elevation of the surface of Glacial Lake Lewis was approximately 380 m above mean sea level based on the maximum elevation of ice-rafted erratics found along the margins of the Pasco Basin.
- The maximum depth of Glacial Lake Lewis in the Pasco Basin was approximately 285 m above mean sea level.
- Sources: Bretz (1923), Flint (1938), Bretz et al. (1956), Brown (1975), Bjornstad (1980), Waitt (1980), Fecht et al. (1987), Baker et al. (1991), Smith (1993), Lindsey et al. (1994), and Reidel and Fecht (1994a, 1994b).

1.5 GEOLOGIC SETTING

Surficial Deposits

- Surficial deposits of Holocene and nonglacial Pleistocene age occur throughout the Pasco Basin.
- Surficial deposits consist of the following:
 - Alluvium from the Columbia, Snake, Walla Walla, and Yakima Rivers and tributaries.
 - Alluvial fan debris consisting of poorly sorted sediments that accumulate where tributary streams leave the highlands and enter the major river valleys.
 - Eolian loess at higher elevations and dune sand in the valley terrain.
 - Mass-wasting debris found along steep slopes of anticlinal ridges and high bluffs adjacent to rivers and abandoned glaciofluvial flood channels.
- Surficial deposits veneer and obscure older deposits over much of the investigation area.
- Sources: Baker et al. (1991) and Reidel and Fecht (1994a, 1994b).

Figure 1-12: Aerial photograph of active parabolic dunes and barchanoid ridges migrating eastward across the central Pasco Basin (12/28). Dune deposits obscure much of the younger host sediments and rocks that contain clastic injection dikes.



1.5 GEOLOGIC SETTING

Geologic Structures

- The Pasco Basin area has been deformed into asymmetrical anticlines and synclines of the Yakima Fold Belt due to north-south compression. Deformation started prior to the CRBG volcanism, before 17 million years ago and continues into the present.
- The structural ridges are folded, faulted, and segmented by cross structures. Faulting on the structural ridges occurred as recently as the Holocene epoch.
- The synclinal lows are areas of sediment accumulation for the major depositional systems. The Miocene- and Pliocene-age sediments and the CRBG in structural lows are gently folded.
- The most prominent structural trends in the Pasco Basin and vicinity are oriented in the following directions:
 - Northwest-southeast (typically N55°W) [e.g., Rattlesnake Wallula Alignment (RAW)]
 - East-west (e.g., Saddle Mountains)
 - North-south (e.g., Hog Ranch).
- Sources: Tolan and Reidel (1989), Reidel and Fecht (1994a, 1994b), and Reidel et al. (1994).

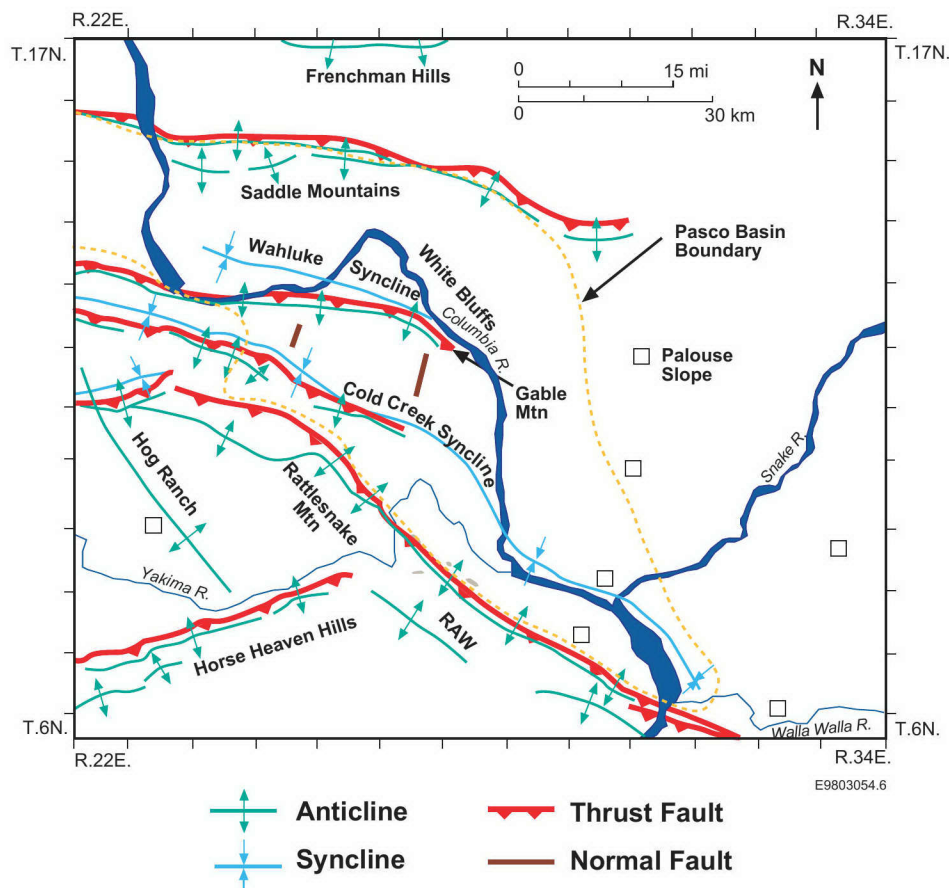


Figure 1-13: Map of the major structural elements of the Pasco Basin and vicinity (modified from Tolan and Reidel 1989).

1.6 PREVIO US STUDIES

- Previous workers found that clastic injection dikes tend to be vertical or near-vertical tabular bodies, with multiple layers of sand, silt, and clay, and minor coarser debris, and that the dikes are bounded by thin clay/silt linings.
- Previous workers in the region found that clastic injection dikes occur in a variety of host sediments and rocks and in numerous locations in south-central Washington and north-central Oregon. Workers agree that clastic injection dikes were formed during the Pleistocene epoch.
- Several explanations have been proposed for the origin of the fissures, the origin of the infilling materials, and the direction of infilling the fissures (i.e., from the top or bottom).
- Key observations and conclusions from earlier studies on clastic injection dikes are summarized in Table 1-2.
- Sources: See Table 1-2.

Table 1-2: A summary of selected information from previous studies on clastic injection dikes.

Study	Origin of Fissures	Origin of Sediment Filling	Direction of Filling	Geologic Units Penetrated			Study Location
				B	S	H	
Alwin 1970; Alwin & Scott 1970	• Thermal contraction of permafrost	• Water	D			●	Southeastern Washington
Baker 1973	• Slumping	• Water	D			●	Tucanón River Valley
Bechtel 1971	• Slumping	• ND	D			●	Central Pasco Basin
Black 1979	• Loading from Pleistocene flooding • Pre-existing fractures	• Water	D U		●	●	Pasco Basin
Brown & Brown 1962	• Seismically induced	• ND	D		●	●	White Bluffs
Brown & Brown 1968	• Seismically induced • Slumping	• Water	D	●	●	●	Pasco Basin
Bunker 1980	• Slumping	• Water (liquefaction)	U			●	Badger Coulee
Grolier & Bingham 1978	• Desiccation cracks • Deep frost cracks	• Water	D		●	●	Columbia Irrigation Project
Jenkins 1925	• Seismically induced	• Water	D		●	●	Eastern Washington
Jones & Deacon 1966	• Seismically induced	• ND	U			●	Pasco Basin
Last & Fecht 1986	• Loading from Pleistocene flooding • Seismically induced	• Water	U/D	●	●	●	Central Pasco Basin
Lupher 1944	• Melting of buried ice • Erosion from underground streams • Landslides in basalt	• Wind • Water	D	●	●	●	Columbia Basin
Newcomb 1962	• ND	• Water	U			●	Columbia Basin
PSPL 1981	• Slumping • Seismically induced • Slumping	• Water	D	●			Gable Mountain
Shannon & Wilson 1974	• Loading from Pleistocene flooding	• Water	U/D	●	●	●	Umatilla Basin
WCC 1981	• Seismically induced • Other unnamed processes	• Water • Water (liquefaction)	D U	●	●	●	Pasco Basin and Vicinity

B = Columbia River Basalt Group
 S = Older clastic sediments (pre-Hanford Formation)
 ND = Not determined
 D = Downward
 H = Hanford Formation
 U = Upward

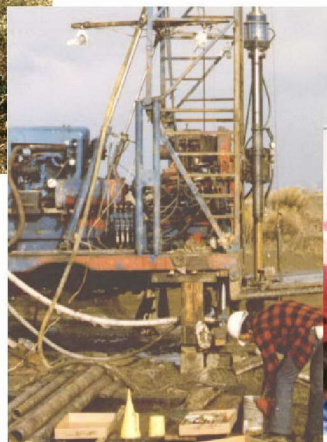
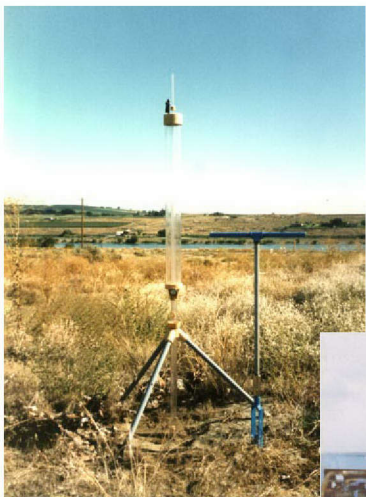
2.0 METHODS OF INVESTIGATION

2.1 GENERAL

- This section summarizes the methods used (1) to investigate clastic injection dikes and (2) to test techniques for future studies of dikes.

Figure 2-1: Photographs illustrating several of the methods used to investigate clastic injection dikes including, from left to right, Guelph permeameter testing equipment, sediment coring, ground-penetrating radar survey, aerial photogrammetric imagery (vertical view angle), mapping vegetation patterns, and field mapping.

- The methods of investigation that were used in this study are:
 - Standard field and trench mapping
 - Mapping of vegetation patterns
 - Aerial photogrammetric imagery
 - Surface geophysical techniques
 - Borehole coring and split-tube sampling
 - Infiltration tests and permeameter measurements.



2.2 STANDARD FIELD AND TRENCH MAPPING

- Standard geologic mapping techniques were used to map surface outcrops and vertical exposures of host rock and clastic injection dikes.
- Mapped areas included about 60 natural exposures and about 20 man-made excavations. The mapped areas selected for this study were based on the results of geologic mapping, which is documented in Reidel and Fecht (1994a, 1994b), and siting studies for nuclear facilities.
- Topographic maps by the U.S. Geological Survey, geologic maps compiled in Reidel and Fecht (1994a, 1994b), and altimeters were used for geographic, geologic, and vertical control.
- Aerial photographs were used to locate and map large areas of clastic injection dike network patterns. Also see Section 2.4, “Aerial Photogrammetric Imagery.”
- Sources: CDA (1969, 1971), PSPL (1981), Reidel and Fecht (1994a, 1994b), and this study.



E9803054.27

Figure 2-2: Photograph of a clastic injection dike exposed in the south wall of Trench CD-5 excavated in the central Gable Mountain area (13/27-19A). The trench walls were logged by CDA (1969, 1971) and relogged by PSPL (1981). The clastic injection dike occurs along a reverse fault in Elephant Mountain basalt of the Columbia River Basalt Group.

2.3 MAPPING OF VEGETATION PATTERNS

- An increase in the density of vegetation (e.g., grasses and shrubs) commonly occurs on the ground surface along clastic injection dikes in sedimentary environments. The increase is most pronounced where clastic injection dikes are greater than 0.3 m wide and host sediments are from the silt and sand facies of the Hanford Formation.
- Vegetation patterns can mark the location of clastic injection dikes covered by up to about 1 m of surficial deposits.
- The sediments in clastic injection dikes commonly have a higher field capacity than the host sediments. Clastic injection dikes can have more moisture-holding capacity in comparison to adjacent host sediments. The increased moisture promotes growth of more lush vegetation.
- The contrast in vegetation density between the dikes and host sediments is most pronounced in early spring, autumn, and up to 5 years after a range fire. As the thickness of surficial cover increases and the grain size of the host sediment fines, vegetation tends to be more disperse and linear trends become less obvious to completely obscured.
- Sources: Grolier and Bingham (1978) and this study.

Figure 2-3: Photograph of a linear trend of dense, green vegetation atop a clastic injection dike in the lower Cold Creek Valley [Goose Egg Hill (12/26-33C)].

Figure 2-4: Photograph of vegetation growing along two clastic injection dikes along the bottom of an excavation in the southeastern Pasco Basin [Iowa Beef South (8/31-36D)]. The dikes are exposed in the vertical cut along the north wall of the gravel quarry.



E9803054.25



E9803054.26

2.4 AERIAL PHOTOGRAMMETRIC IMAGERY

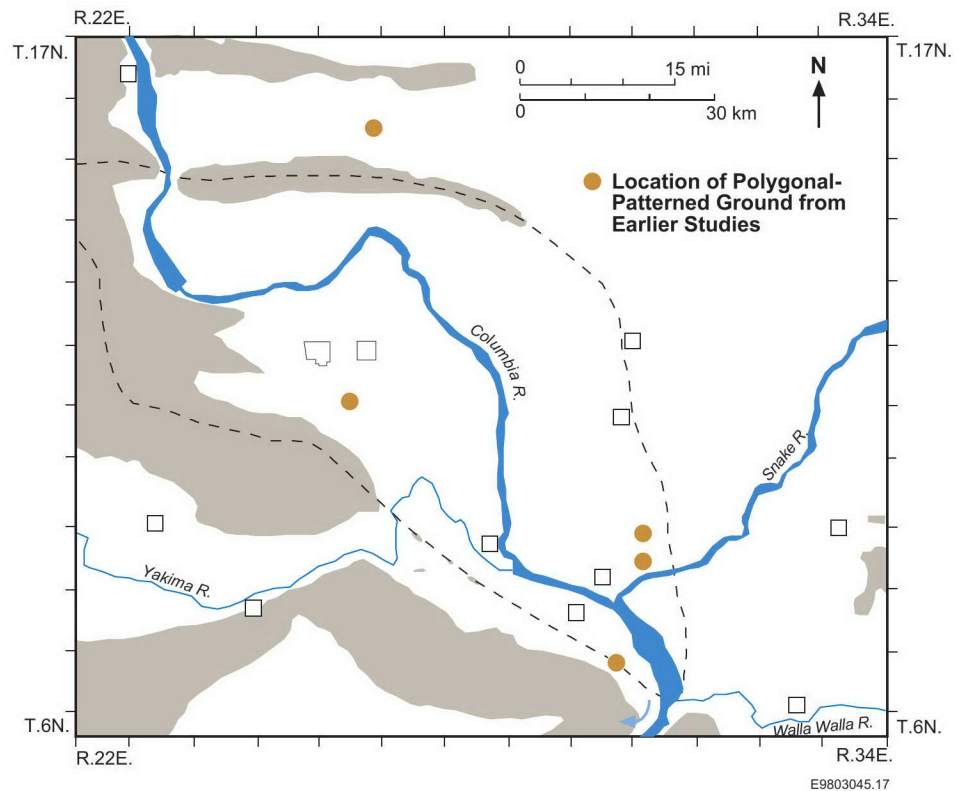
- Vertical and oblique view-angle photogrammetric imagery has been used by investigators to identify polygonal-patterned ground that marks the occurrence of clastic injection dikes in the Pasco Basin and vicinity.
- The polygonal-patterned ground stands out due to contrasts in the density of vegetation (see Section 2.3, “Mapping of Vegetation Patterns”).
- Polygonal-patterned ground has been identified on a variety of photogrammetric images (e.g., color, black and white, color near-infrared, and black and white near-infrared).

Table 2-1: Location of polygonal-patterned ground in the Pasco Basin and vicinity identified from aerial photographs from several earlier studies.

Location of Patterned Ground	Township/Range	Study	View Angle
Crab Creek	16/26	Jones and Deacon 1966	Vertical
Goose Egg Hill	12/26	Jones and Deacon 1966	Vertical
Wallula	7/31	Jones and Deacon 1966	Vertical
Smith Coulee North	10/30	Grolier and Bingham 1978	Oblique
Smith Coulee South	9/30	Grolier and Bingham 1978	Oblique

Figure 2-5: Map showing the locations of polygonal-patterned ground in the Pasco Basin and vicinity that are presented in Table 2-1.

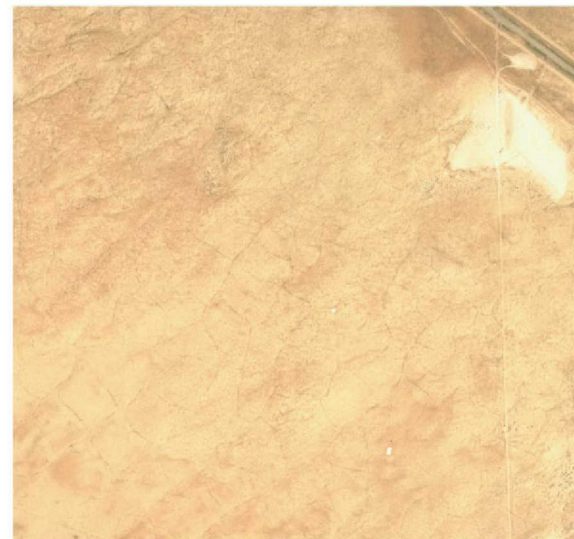
Figure 2-6: Aerial photograph (vertical view angle) of polygonal-patterned ground at an old liquid waste disposal site (216-S-16 Pond) near the 200 West Area on the Hanford Site (12/25-14E).



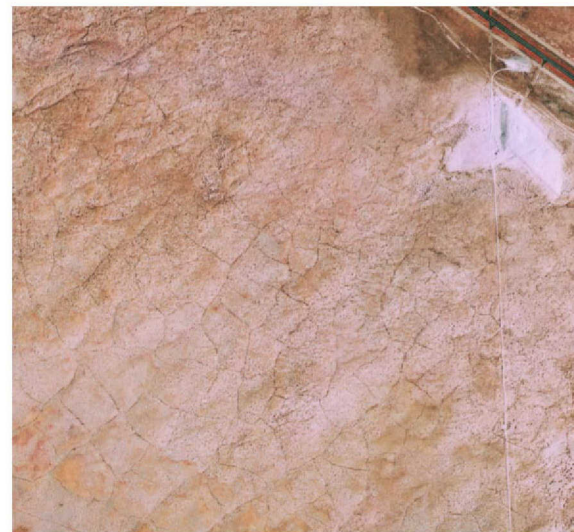
E9803054.21

2.4 AERIAL PHOTOGRAMMETRIC IMAGERY

- This study primarily used vertical view-angle, high-resolution, color, and near-infrared photogrammetric images to map the distribution of large polygonal-patterned ground networks in the central Pasco Basin (scale 1:19,900). Patterned ground was traced from aerial photographs, rescaled, and corrected for distortion due to oblique angle of view and lens effects, and then superimposed onto topographic maps for analysis.
- The photogrammetric images are from the U.S. Department of Energy Remote Sensing Laboratory, located at the Nevada Test Site, Las Vegas, Nevada. The imagery is from an aerial survey flown over the Hanford Site on May 7, 1987, at an altitude of 3,280 m (10,000 ft).
- Wild Heerbrugg RC-10 photogrammetric aerial cameras with a 153-mm lens (f/4), a normal angle field, and 9- by 9-in. format film size were used for the photographs.
- Near-infrared photogrammetric images provide better definition of the polygonal-patterned ground than visible light images because of the near-infrared sensitivity to changes in vegetation.
- Sources: Jones and Deacon (1966), Grolier and Bingham (1978), U.S. Department of Energy Remote Sensing Laboratory, and this study.



E9803054.22



E9803054.23

Figure 2-7: Polygonal-patterned ground in vertical view-angle color (top) and near-infrared (bottom) aerial photographs of a portion of the lower Cold Creek Valley (11/26-3 and 12/26-34). The imagery has a pixel resolution of less than 7.6 m (25 ft).

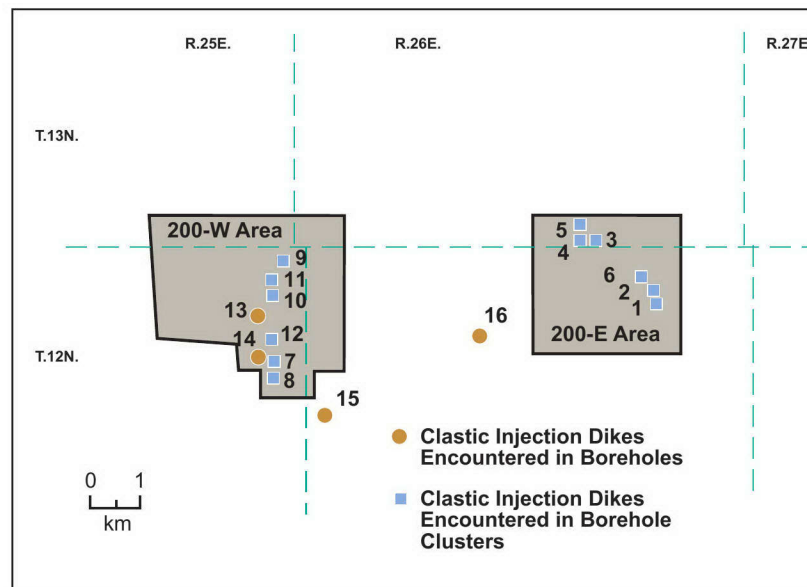
2.5 BOREHOLE CORING AND SPLIT-TUBE SAMPLING

- Clastic injection dikes have been encountered during drilling and sampling of boreholes in vadose sediments of the Pasco Basin.
- Sampling techniques used to sample clastic injection dikes include:
 - Solid, thick-wall drill pipe
 - Split-tube and shelby-tube samplers
 - Wire-line coring.
- Drilling systems used in conjunction with the sampling devices include:
 - Cable-tool percussion
 - Hollow-stem auger
 - Rotary, commonly with air hammer
 - Sonic
 - Tri-pod percussion
 - Vibratory.
- Sources: Price and Fecht (1976a), Singleton and Lindsey (1994), Weekes et al. (1995), and this study.

Table 2-2: List of borehole clusters and boreholes that are known to have encountered clastic injection dikes during drilling.

Figure 2-8: Map showing the location of boreholes and borehole clusters on the 200 Area Pleistocene Glaciofluvial Flood Bar that encountered clastic injection dikes during well installation (from Table 2-2).

Boreholes		
Clusters (listed by facility)		
1.	241-A Tank Farm	Price & Fecht 1976a
2.	241-AX Tank Farm	Price & Fecht 1976b
3.	241-B Tank Farm	Price & Fecht 1976c
4.	241-BX Tank Farm	Price & Fecht 1976d
5.	241-BY Tank Farm	Price & Fecht 1976e
6.	241-C Tank Farm	Price & Fecht 1976f
7.	241-S Tank Farm	Price & Fecht 1976g
8.	241-SX Tank Farm	Price & Fecht 1976h
9.	241-T Tank Farm	Price & Fecht 1976i
10.	241-TX Tank Farm	Price & Fecht 1976j
11.	241-TY Tank Farm	Price & Fecht 1976k
12.	241-U Tank Farm	Price & Fecht 1976l
Individual Wells		
13.	299-W15-14	
14.	299-W23-16	Singleton & Lindsey 1994
15.	699-32-72B	Weekes et al. 1995
16.	699-38-61	Weekes et al. 1995



E9803054.18

2.6 GEOPHYSICAL METHODS

- Prior to this study, nonintrusive techniques had not been used to detect clastic injection dikes in the subsurface of the Pasco Basin and vicinity.
- A nonintrusive testing program for detecting clastic injection dikes was developed to locate clastic injection dikes beneath the ground surface.
- The two geophysical methods tested in the study were electromagnetic induction (EMI) and ground-penetrating radar (GPR).
- The geophysical methods were selected for the following reasons:
 - The equipment was readily available.
 - Extensive experience has been gained using the equipment in various geologic environments in the Pasco Basin.
 - A large database of geophysical surveys exists for much of the central Pasco Basin.
 - The equipment can be economically used in field applications.
- Source: This study.



E9803054.24

Figure 2-9: Photograph of a ground-penetrating radar system being pulled along a survey grid that crosses a clastic injection dike. Ground-penetrating radar systems are used to detect contrasts in electrical conductivity in the upper 4 to 5 m of the soil column in the central Pasco Basin.

2.7 INFILTRATION / PERMEAMETER METHODS

- Hydraulic properties have not been determined previously for clastic injection dikes in the Pasco Basin and vicinity.
- A testing program for clastic injection dikes was developed to gather hydraulic data for the following purposes:
 - To determine initial hydraulic properties over a variety of geohydrologic conditions, but primarily in conditions representative of the central basin. (Note: Most hazardous and radioactive contaminants in the environment are present in the central Hanford Site, which is located in the central basin.)
 - To estimate unsaturated and saturated flow velocities for use in numerical flow modeling.
 - To support design of follow-on hydrologic tests.
- Three methods used in the study were:
 - Guelph permeameter
 - Small-scale infiltrometer
 - Unsaturated flow apparatus (UFA, a trademark of UFA Ventures Inc.).
- The methods were selected for the following reasons:
 - The equipment was available.
 - The equipment was portable (except the UFA).
 - The equipment is economically deployed.
- Source: This study and work in preparation.

Figure 2-10: Photograph of Jim Conca, from UFA Ventures Inc. in Richland, Washington, collecting a sample from the host sediment adjacent to a clastic injection dike (located <1 m to the left of photograph) at an exposure in a railroad cut west of Kiona, Washington (9/27-19G).



E9803054.190

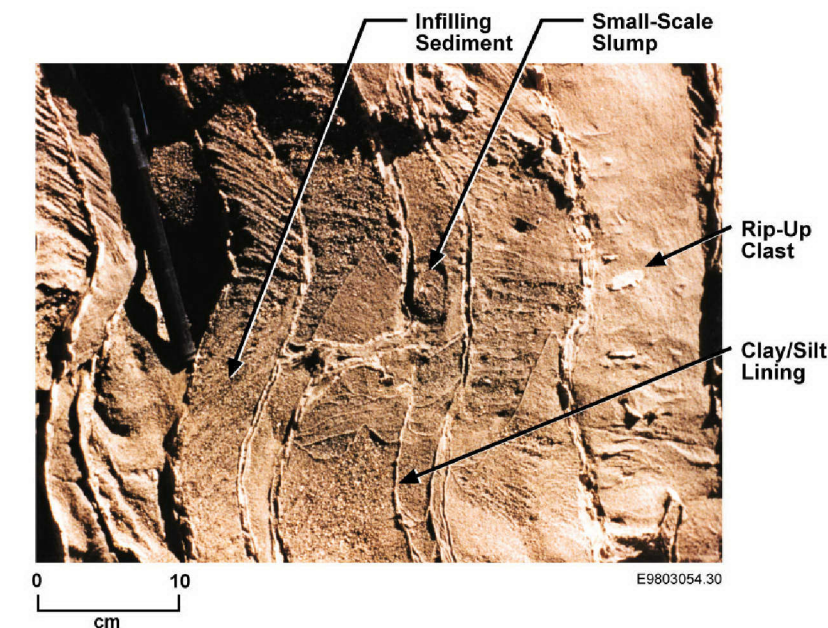
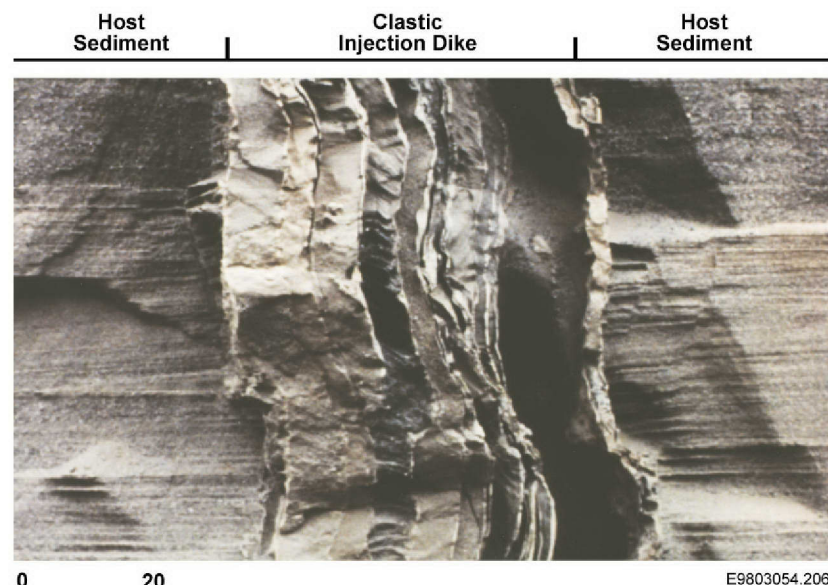
3.0 PHYSICAL DESCRIPTION OF INDIVIDUAL CLASTIC INJECTION DIKES

3.1 GENERAL DESCRIPTION

- Clastic injection dikes include both dike and sill structures that are filled with single or multiple infilling units. The infilling units are composed of clastic sediments. The walls of the dikes and infilling units are bounded by clay/silt linings. Most infilling units and clay/silt linings trend parallel or subparallel to the dike walls.
- The components of a clastic injection dike are as follows:
 - Clay/silt linings
 - Infilling sediments
 - Small-scale slumps
 - Small-scale faults and shears
 - Slickensides
 - Rip-up clasts
 - Soft-sediment flow features.
- This section describes the physical attributes of clastic injection dikes, including the following items:
 - General description
 - Key components
 - Width, depth, and lateral extent
 - Termination of dikes.
- Sources: Lupher (1944), Alwin (1970), Black (1979), and this study.

Figure 3-1: Photograph of a typical clastic injection dike in the Pasco Basin. The dike occurs within the sand facies of the Hanford Formation at the US Ecology excavation (12/26-9R).

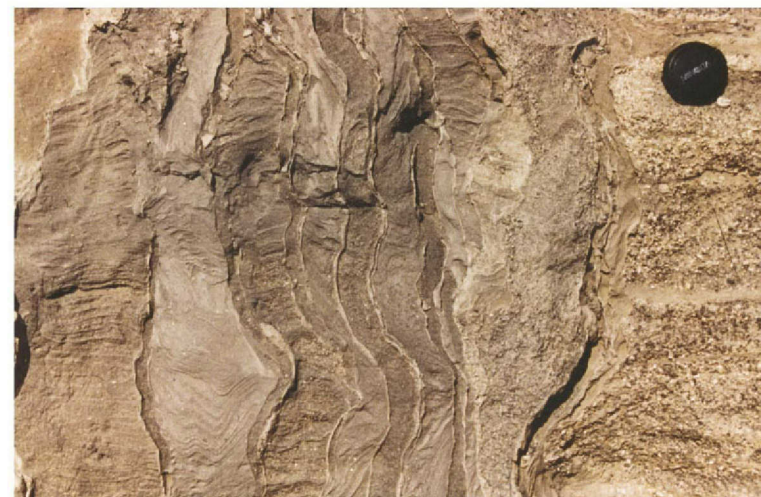
Figure 3-2: Photograph showing several key components of clastic injection dikes.



3.2 COMPONENTS

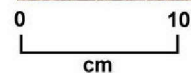
Clay/ Silt Linings

- Clay- and silt-sized particles form layers that line the walls of clastic injection dikes and line each infilling unit of sediments. The clay/silt linings are also called “clay skins.”
- The thickness of the clay/silt linings generally ranges between 0.03 and 1.0 mm, but occur up to 10 mm in width.
- The linings occur either as massive clay/silt material or as very thin laminae (0.01 mm).
- Clay/silt stringers also occur that cross-cut infilling sediments. These linings are typically less than 0.03 mm.
- Sources: Lupper (1944), Alwin (1970), Black (1979), and this study.



E9803054.39

Figure 3-3: Top: Thin clay/silt linings along the margins of infilling sediments and across infilling units in a clastic injection dike in south Richland [Keene/Kennedy Road (9/28-22M)]. Bottom: Thick clay/silt linings that comprise the majority of the clastic injection dikes in a coarse sand and granule unit in north Pasco [Transtate Gravel Pit (9/30-6F)]. Both clastic injection dikes are located in the Hanford Formation.



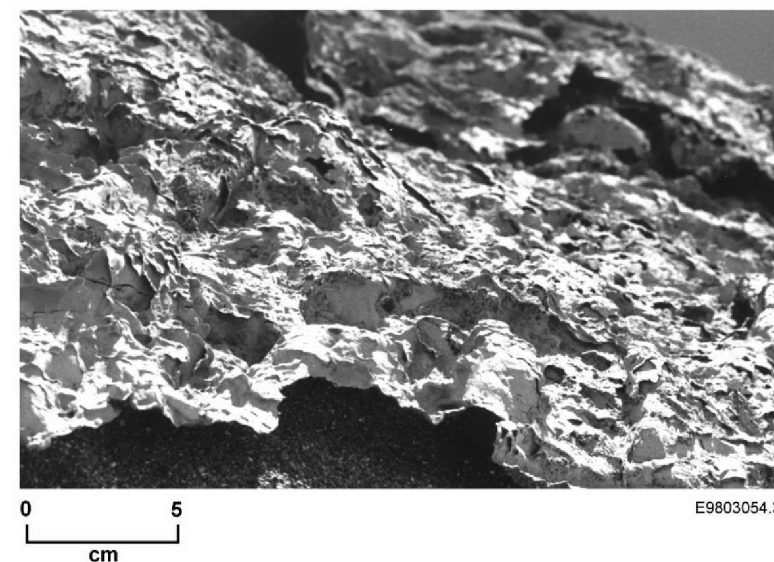
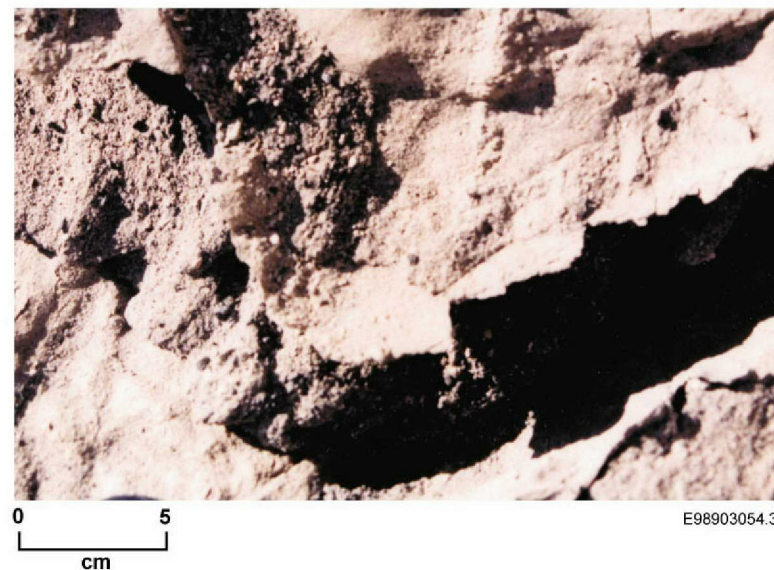
E9803054.40

3.2 COMPONENTS

Clay/Silt Linings (C ontinued)

- The surfaces of clay/silt linings can have a variety of forms, including the following:
 - Relatively smooth and flat or undulating planes.
 - Polygonal patterns formed by desiccation fissure networks (mudcracks). The polygons vary in width from 5 to 8 cm. Fissures may be open or subsequently filled with sediments. Fissures vary in width from 5 to 10 mm. The infilling sediments are similar in grain size and general texture to silt/clay linings, the surrounding host sediments, or consist of calcareous mud.
 - Small-scale structures that are deformed into ridge and trough structures, V-tapered ridges, and bulbous ridges. Amplitudes of the structures are commonly 1.5 to 10 mm with wave lengths of 10 mm to 2 cm.
 - Highly contorted structures.
- Small-scale structures on clay/silt linings tend to be parallel over surface areas from several square centimeters to several square meters.
- The trend of small-scale structures on the clay/silt linings along one infilling unit may not coincide with the trends on clay/silt linings of other infilling units.
- Sources: Alwin (1970) and this study.

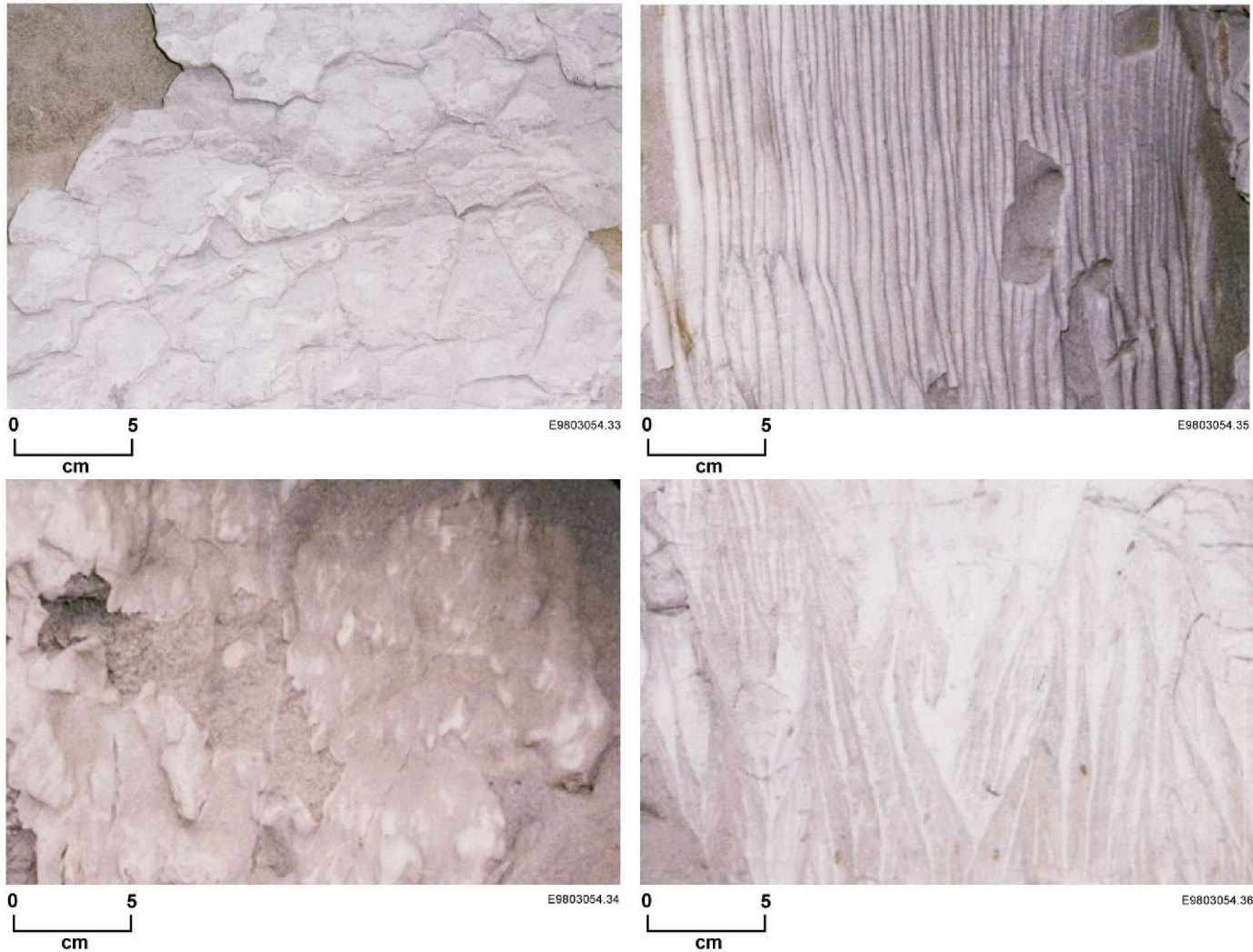
Figure 3-4: Photographs of relatively smooth and flat (top) and undulating clay/silt linings (bottom) in vertical exposures of clastic injection dikes.



3.2 COMPONENTS

Clay/Silt Linings (Continued)

Figure 3-5: Photographs of deformed surfaces of clay/silt linings in vertical exposures that occur in the Pasco Basin and vicinity (clockwise from upper right): ridge and trough, V-tapered ridges, bulbous ridges, and filled mudcracks.



3.2 COMPONENTS

Infilling Sediments

- Infilling sediments are divided into individual coarser grained packages bounded by the clay/silt linings. An individual package of infilling sediments is termed an infilling unit.
- Clastic injection dikes consist of one or more infilling unit.
- Infilling units trend parallel or subparallel to the walls of clastic injection dikes.
- Sand is the dominant grain size of infilling sediments, but minor clay, silt, and gravel are found.
- The particle sizes of dike infilling sediments may be similar or different from host sediments.
- Infilling sediments vary from poorly to well sorted, but are more commonly moderately well to well sorted.
- The width of infilling units ranges from 0.01 mm to greater than 30 cm.
- The vertical length of infilling units in vertical exposures ranges from approximately 0.2 m to greater than 20 m; wider infilling units average about 2 m in vertical length.
- The lateral lengths of infilling units (i.e., the length along strike) are similar to vertical lengths, which is based on few observations.

Figure 3-6: Photographs of vertical exposures showing dike infilling sediments and host rock with similar particle sizes at the Keene/Kennedy Road exposure located at 9/28-22M (top) and different particle sizes at the Yakima Bluffs site located at 9/28-16G (bottom).

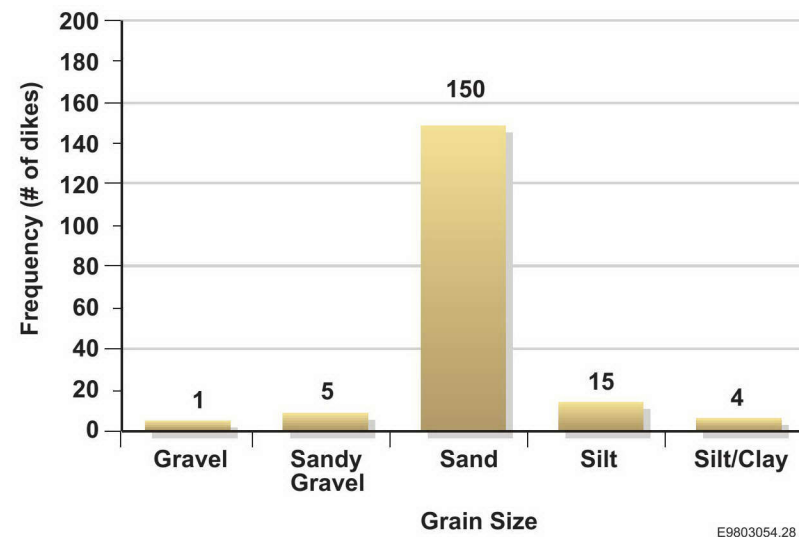
Figure 3-7: Frequency of grain sizes within infilling sediments encountered in clastic injection dikes in the Pasco Basin.



E9709055.48



E9709087.5



E9803054.28

3.2 COMPONENTS

Infilling Sediments (Continued)

- Sedimentary structures are common within infilling units and include the following:
 - Graded beds (both normal and reverse grading)
 - Cross-laminations and bedding
 - Massive bedding with no internal structure
 - Complex bedding forms (e.g., chevron or V-shaped patterns).
- Infilling units terminate as follows:
 - Truncation against another infilling unit or another clastic injection dike
 - Truncation at bedding planes, faults, or slumps
 - Thinning and pinching out at the top, bottom, or lateral extent of a dike
 - Bending and merging with another dike or sill.
- Sources: Lupher (1944), Alwin (1970), Black (1979), WCC (1981), and this study.



0 10
cm

E9803054.39



0 10
cm

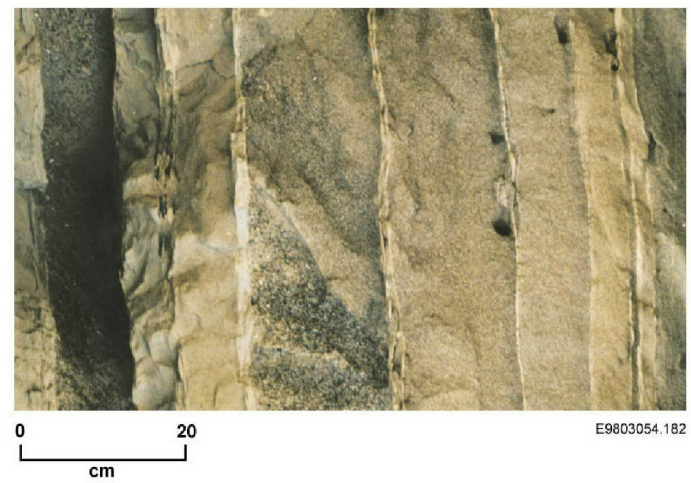
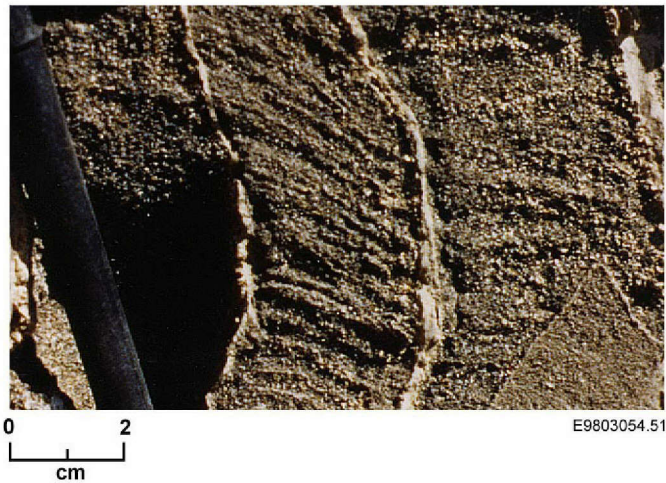
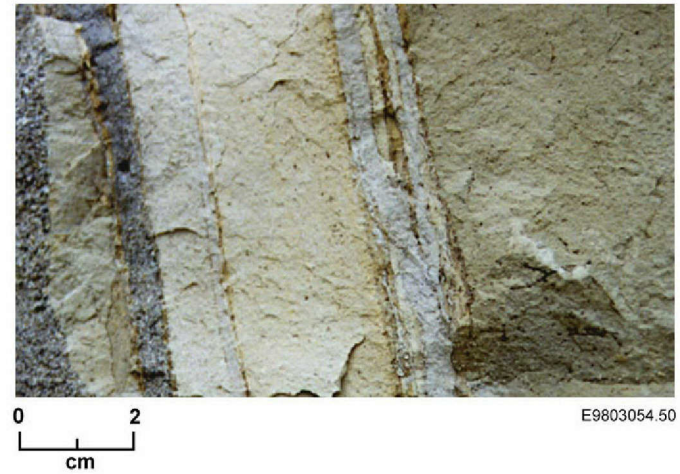
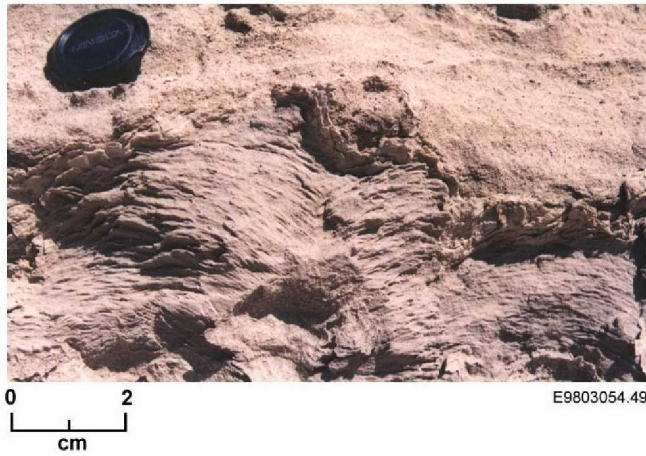
E9709055.41

Figure 3-8: Photographs of a vertical exposure (top) and surface exposure (bottom) of infilling sediments from a clastic injection dike in the sand facies of the Hanford Formation at Keene/Kennedy Road (9/28-22M).

3.2 COMPONENTS

Infilling Sediments (Continued)

Figure 3-9: Photographs of bedding structures of infilling sediments (clockwise from upper right): massive, normally graded, cross-laminated, and complex bed form.

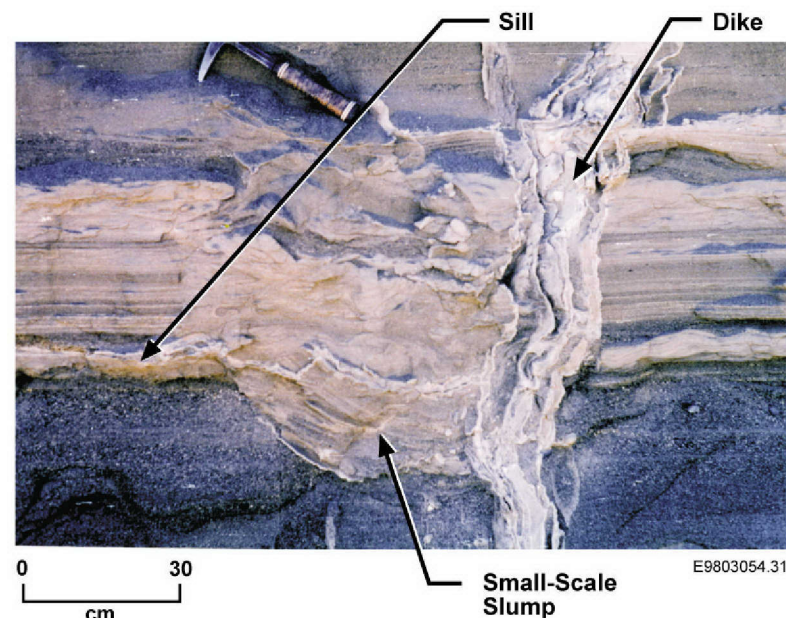


3.2 COMPONENTS

Small-Scale Slumps

- Small-scale slumps are commonly found in and adjacent to clastic injection dikes. Large-scale slumps that are associated with clastic injection dikes are discussed in the section on dike networks (Section 5.3.)
- Small-scale slumps are generally less than about 1 m³.
- Small-scale slumps can be divided into two basic types:
 - Block slumps, which occur as slightly rotated, intact deformed clastic debris. Block slumps occur partially in or across clastic injection dikes, but are most commonly adjacent to dikes.
 - Flow slumps, which occur as moderately deformed clastic debris as a result of fluidized flow. Flow slumps are common both in clastic injection dikes and in the host sediments adjacent to dikes.
- Small-scale slumps are often bounded by clay/silt linings.
- Most slumps are associated with clastic injection dikes with widths greater than 30 cm; few small-scale slumps are associated with narrower dikes.
- Sources: Lupher (1944), Alwin (1970), Fecht and Weekes (1996), and this study.

Figure 3-10: Photograph of a small-scale slump adjacent to a clastic injection dike at the Environmental Restoration Disposal Facility excavation on the 200 Area Pleistocene Glaciofluvial Flood Bar, Hanford Site (12/26-7K).



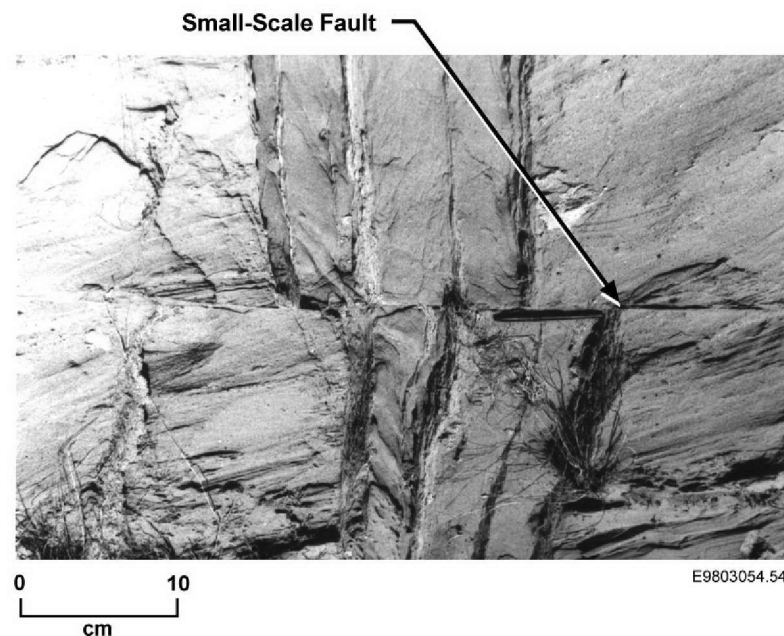
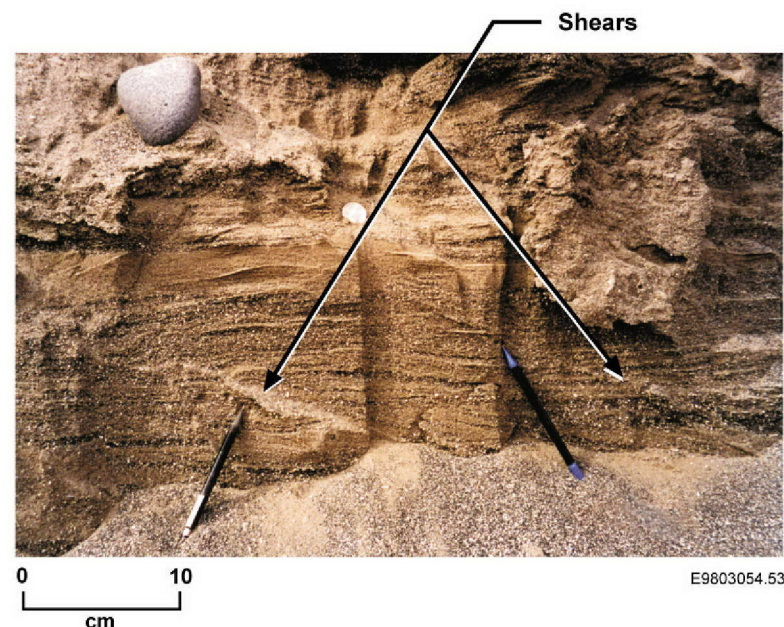
3.2 COMPONENTS

Small-Scale Faults and Shears

- Small-scale faults and shears occur in clastic injection dikes and the surrounding host material. Small-scale faults and shears are most common in dikes that occur in the sand and silt facies of the Hanford Formation.
- Small-scale faults and shears are primarily low angle ($<30^\circ$) to bedding plane.
- In cross section, small-scale faults and shears occur as:
 - Single structures
 - Two or more parallel structures
 - Conjugate sets.
- Individual faults and shears may have splays of secondary faults and shears.
- Small-scale faults may offset:
 - Clastic injection dikes including a single infilling unit, multiple infilling units, or the total dike
 - Host sediments including a single lamination, several sets of laminations, a single bed, or several beds.
- Offset across faults range from shears (with no observable offset) to greater than 2 m. Offset is generally less than 10 cm.
- Many small-scale faults and shears are lined or partially lined with clay/silt skins.
- Sources: Luper (1944), Alwin (1970), Black (1981), WCC (1981), and this study.

Figure 3-11: Photograph of shears adjacent to a clastic injection dike in the sand facies (field mapping unit #3) of the Hanford Formation in the Environmental Restoration Disposal Facility excavation (12/26-7K). The clastic injection dike is located 2 m to the left of the photograph.

Figure 3-12: Photograph of a small-scale horizontal fault with 8 cm of offset that cuts across a clastic injection dike.

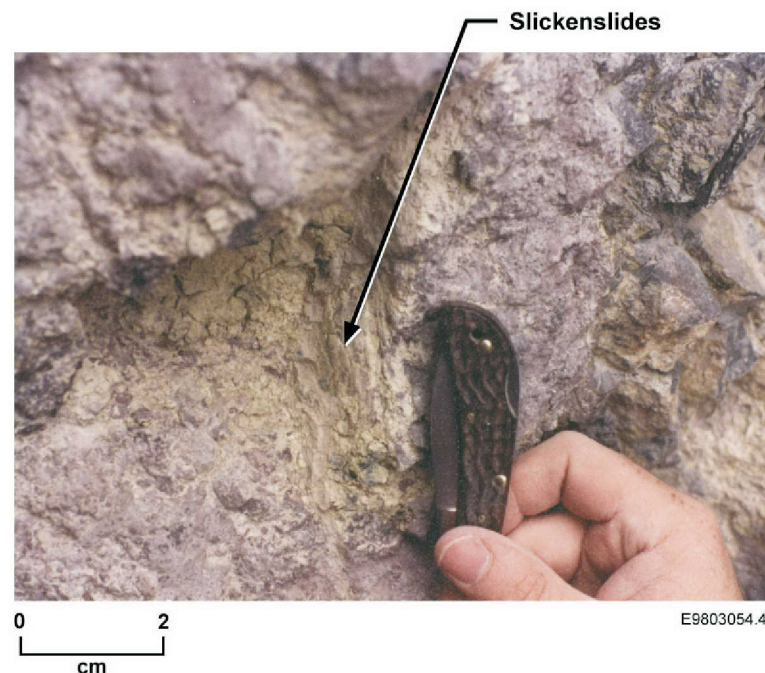


3.2 COMPONENTS

Slickensides

- Slickensides occur on the clay/silt linings that bound both clastic injection dikes and infilling units. Slickensides are most common on the clay/silt linings bounding the dikes.
- Slickensides also occur on multiple clay/silt lining surfaces within an individual clastic injection dike. The trends of slickensides are usually parallel or subparallel on all striated surfaces of a given dike.
- Slickensides are common on clay/silt linings in clastic injection dikes that occur within CRBG basalt in fault zones and sedimentary units in large-scale slumps.
- Slickensides also occur along clay/silt linings in small-scale faults/shears and small-scale slumps.
- Slickensides commonly occur sporadically along the surfaces of clay/silt linings; they are rarely continuous along the entire length of clay/silt lining surfaces.
- Sources: Farooqui (1979), PSPL (1981), WCC (1981), and this study.

Figure 3-13: Photograph of slickensides on a clay/silt lining of a thin clastic injection dike along a preexisting tear fault on the north-central flank of Gable Mountain, Hanford Site [Gable Mountain North (13/27-19A)]. Several clay/silt linings of the clastic injection dike have slickensides, which would indicate movement along the fault during or since formation of the clastic injection dike.



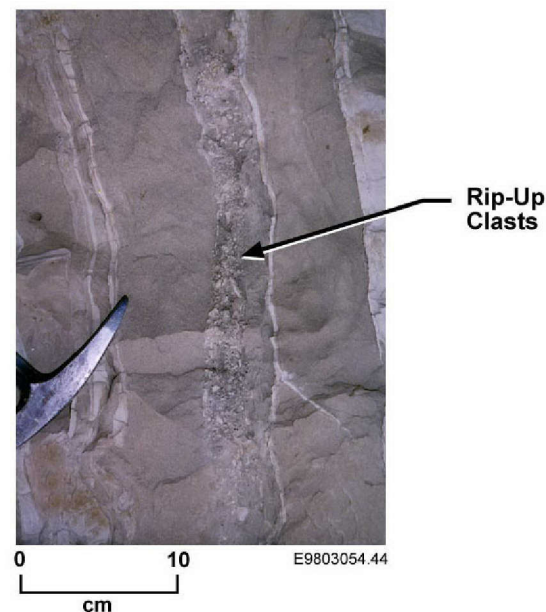
E9803054.42

3.2 COMPONENTS

Rip-Up Clasts

- Rip-up clasts frequently occur within infilling sediments of clastic injection dikes.
- Rip-up clasts are commonly disk-shaped clasts less than 1 cm across.
- Rip-up clasts are composed of moderately well- to well-sorted very fine sand, silt, and clay-sized particles, and are compact sediments or sediments cemented by calcium carbonate.
- The matrix surrounding clasts is composed of unconsolidated, poorly sorted to well-sorted sediments.
- Rip-ups occur as scattered clasts or comprise a majority of the sediments in an infilling unit.
- The sources of the rip-up clasts are eroded fragments of silt/clay linings of clastic injection dikes, silt and sandy silt from loess deposits, and silt and clay from the Ringold Formation based on sediment textures and mineralogy.
- Sources: Alwin (1970) and this study.

Figure 3-14: Photographs of multiple rip-up clasts in infilling units at two clastic injection dikes located along Touchet Road, north of Touchet [Touchet Road (7/33-22Q)].



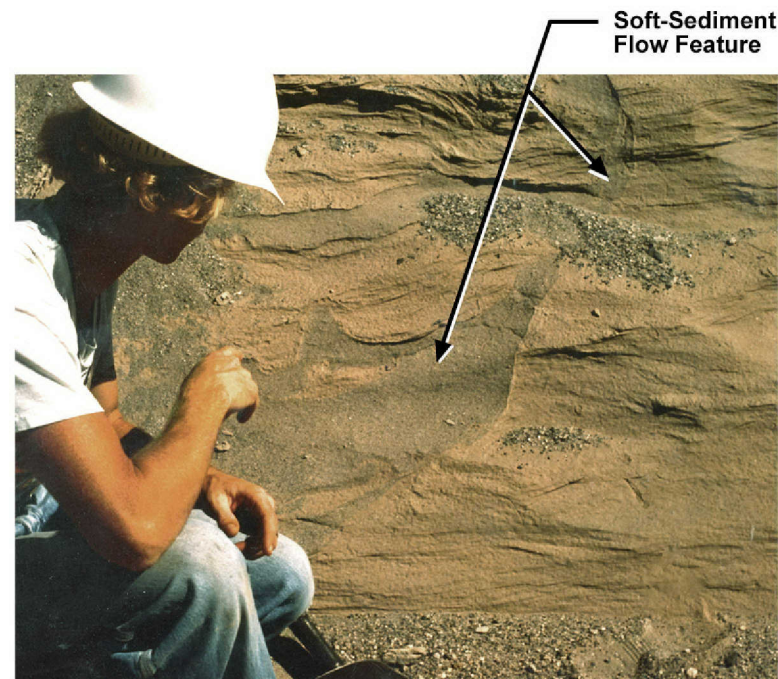
3.2 COMPONENTS

Soft-Sediment Flow Features

- Soft-sediment flow features frequently occur in the host sediments adjacent to clastic injection dikes. These features are commonly bounded by clay/silt linings.
- Soft-sediment flow features have been observed emanating from:
 - Clastic injection sills and dikes
 - Beds of the silt and sand facies of the Hanford Formation.
- The soft-sediment flow features are highly variable in width, but are generally less than 2 m in length.
- Some fine-grained, ripple-laminated beds in the sand and silt facies of the Hanford Formation adjacent to clastic injection dikes have been deformed into contorted beds. The contorted beds commonly merge with clastic dikes at one end and taper out at the other end. Contorted beds extend laterally up to about 20 m and are generally less than 30 cm in thickness.
- Source: This study.

Figure 3-15: Photograph of soft-sediment flow features in the sand facies of the Hanford Formation (field mapping unit #3). Pictured is George Last, one of the authors investigating clastic injection dikes in the Fuels and Materials Examination Facility (11/28-18N) (Last and Fecht 1986).

Figure 3-16: Photograph of contorted bedding associated with a laminated silty sand in the sand facies of the Hanford Formation (field mapping unit #2) at Keene/Kennedy Road (9/28-22M). The contorted bedding merges with a clastic injection dike 2 m to the left of the photograph.



E9803054.45



E9803054.46

3.3 WIDTH, DEPTH, AND LATERAL EXTENT

- The width, depth, and lateral extent of clastic injection dikes are highly variable.
- Clastic injection dikes range in vertical (continuous) extent from less than 30 cm to more than 45 m. There are more than 30 known localities in the Pasco Basin and vicinity where clastic injection dikes can be traced from the surface to a depth of at least 20 m.
- The deepest known occurrence of clastic injection dikes below the ground surface in the Pasco Basin and vicinity is greater than 75 m on the 200 Area Pleistocene Glaciofluvial Flood Bar in the 200 West Area on the Hanford Site (12/25-12F). The total vertical extent of this clastic injection dike is not known, although dikes have been observed in samples from boreholes that were collected 75 m below the ground surface as noted above.
- In cross-section, clastic injection dikes range from less than 1 mm to more than 2 m in width. The millimeter-scale dikes consist entirely of clay/silt linings.
- In plan view, clastic injection dikes range from less than 0.3 m to more than 100 m along strike. Many of the most laterally extensive dikes observed in the Columbia Basin occur in the Goose Egg Hill area, Hanford Site (12/26-33C).
- Sources: Brown and Brown (1962), CDA (1969, 1971), Bechtel (1971), Price and Fecht (1976a, 1976b), Last and Fecht (1986), Singleton and Lindsey (1994), Weekes et al. (1995), Fecht and Weekes (1996), and this study.

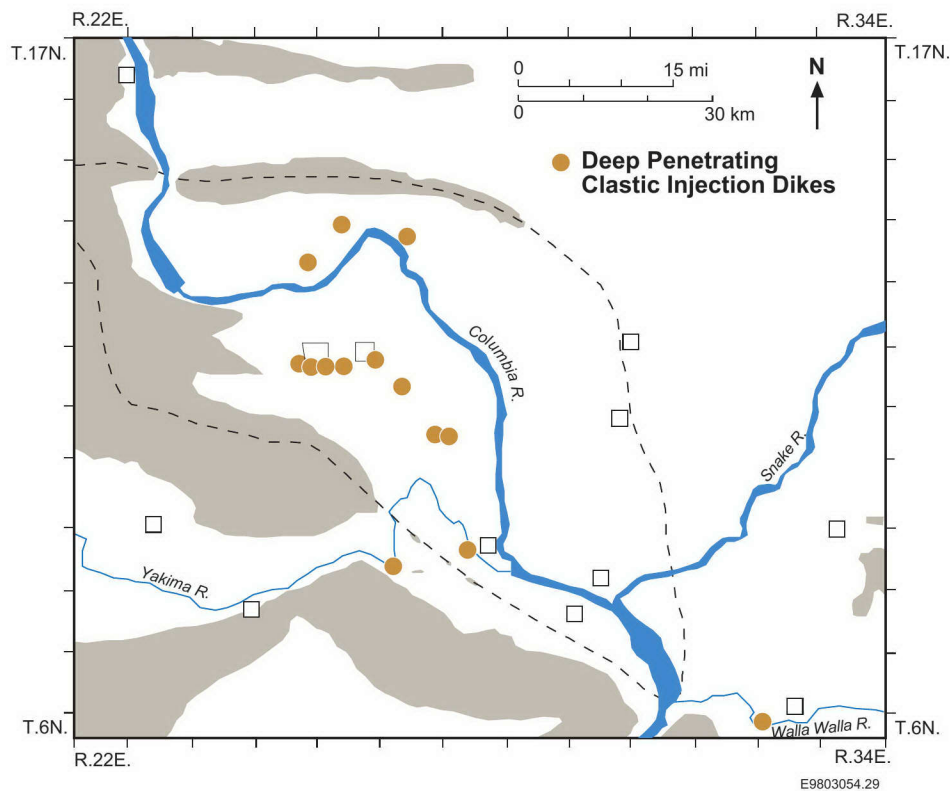


Figure 3-17: Map showing several localities of clastic injection dikes that extend more than 20 m in depth. The localities on the map are based on excavations and natural exposures that have been investigated and are not necessarily representative of the distribution of clastic injection dikes that extend to depth.

Figure 3-18: Photograph of a clastic injection dike complex that exceeds 2 m in width. The dike occurs in the sand facies (field mapping unit #2) in the Hanford Formation at the Fuels and Materials Examination Facility excavation (11/28-18N).

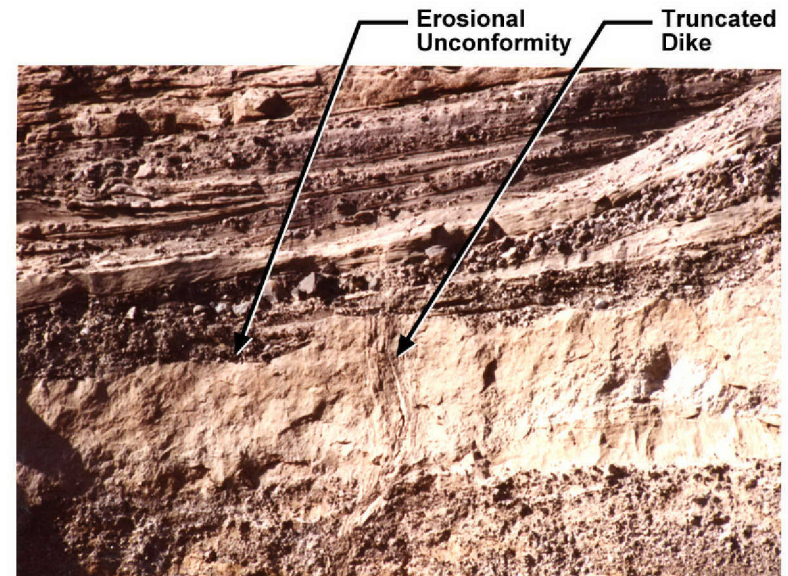


3.4 TERMINATION OF DIKES

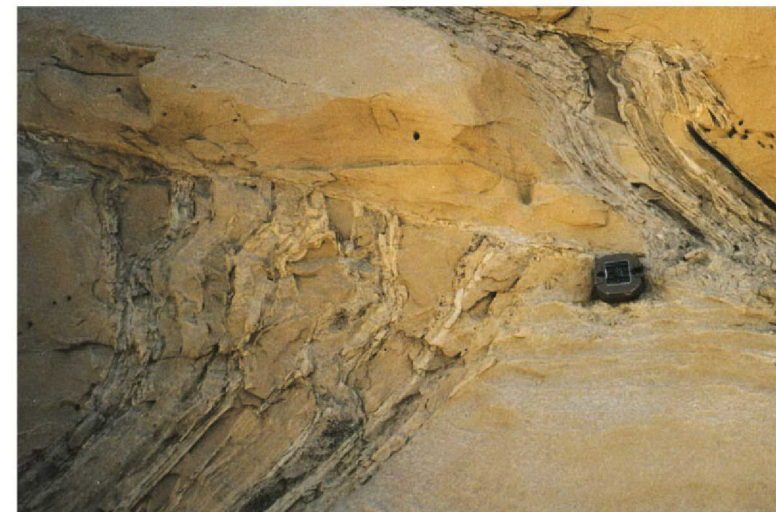
- Clastic injection dikes terminate as follows:
 - Truncation against another clastic injection dike, at bedding planes, at small-scale faults, or at small-scale slumps.
 - Thinning and pinching out at the top, bottom, or lateral extent of a dike.
 - Gradually losing definition into the host sediment or a superimposed soil horizon. The soil horizon is associated with Holocene soils or older paleosols.
 - Bending and merging with another dike or sill.
 - Splaying into dikelets (i.e., narrow dikes) and sills.
- Sources: Lupher (1944), Alwin (1970), Bjornstad (1980), WCC (1981), and this study.

Figure 3-19: Truncation of a clastic injection dike at a bedding plane at Cummings Bridge (7/32-35Q). The truncation is along a major erosional unconformity in the silt facies of the Hanford Formation (from Bjornstad 1980).

Figure 3-20: Truncation of a clastic injection dike at a small-scale fault at Touchet Road (7/33-22Q).



E9803054.32



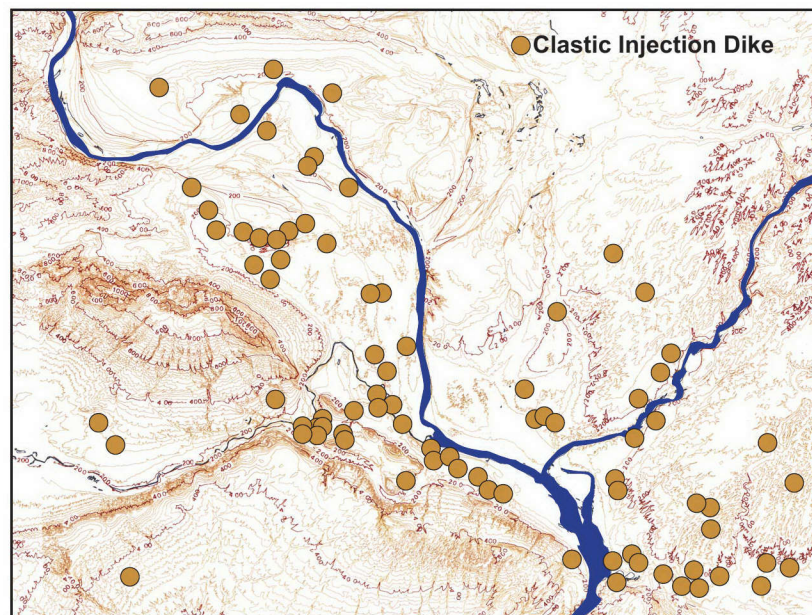
0 30
cm

E9803054.183

4.0 DISTRIBUTION OF CLASTIC INJECTION DIKES

4.1 OCCURRENCE BY ELEVATION

- The upper limit of clastic injection dikes is higher than 275 m elevation. Clastic injection dikes are scarce above 275 m and are often obscured by developing soils (bioturbation), deposition of a veneer of loess, and disking of farm land.
- Clastic injection dikes are not found above the maximum Pleistocene glaciofluvial flood level, which is about 380 m elevation.
- The lower limit of clastic injection dikes is about river level or near the elevation of the historic water table in the southern Pasco Basin prior to filling of reservoirs behind Ice Harbor, McNary, Priest Rapids, and Wanapum Dams (i.e., 104 m).
- Observations of the lower limit are infrequent and restricted to:
 - Several deep burrow pits in which water was pumped from the pit once excavations reached the water table
 - A few scattered exposures along the banks of rivers and streams in the Pasco Basin.
- Sources: Newcomb (1962), WCC (1981), Baker et al. (1991), and this study.



E9803054.5f

Figure 4-1: Map showing the distribution of clastic injection dikes used in this study on a topographic map of the Pasco Basin and vicinity.

4.2 GEOGRAPHIC DISTRIBUTION

- Clastic injection dikes occur in several geomorphic terrains in the Pasco Basin and vicinity, including the following geographic areas:
 - River and basin terrain that occurs in topographic low, sediment-filled areas of the central Pasco Basin and synclinal valleys.
 - Lower slope terrain that is the middle and lower slopes of the anticlinal ridges of the Yakima Fold Belt.
 - Coulees and scabland terrain that is the southwestern extent of the area eroded by floodwaters crossing the Columbia Plateau. This terrain is the area where floodwaters eroded the loess cover, scoured channelways into the CRBG and Ringold Formation, and deposited glaciofluvial sediments.
 - Low-relief areas (e.g., Gable Mountain and part of the Horse Heaven Hills) of the ridge terrain that are the upper slopes of the topographic highs associated with the anticlinal structures of the Yakima Fold Belt.
- Clastic injection dikes have not been observed in the high-relief areas (e.g., Saddle Mountains, Rattlesnake Mountain, Umtanum Ridge, Yakima Ridge) of the ridge terrain.
- Source: Myers/Price et al. (1979) and this study.

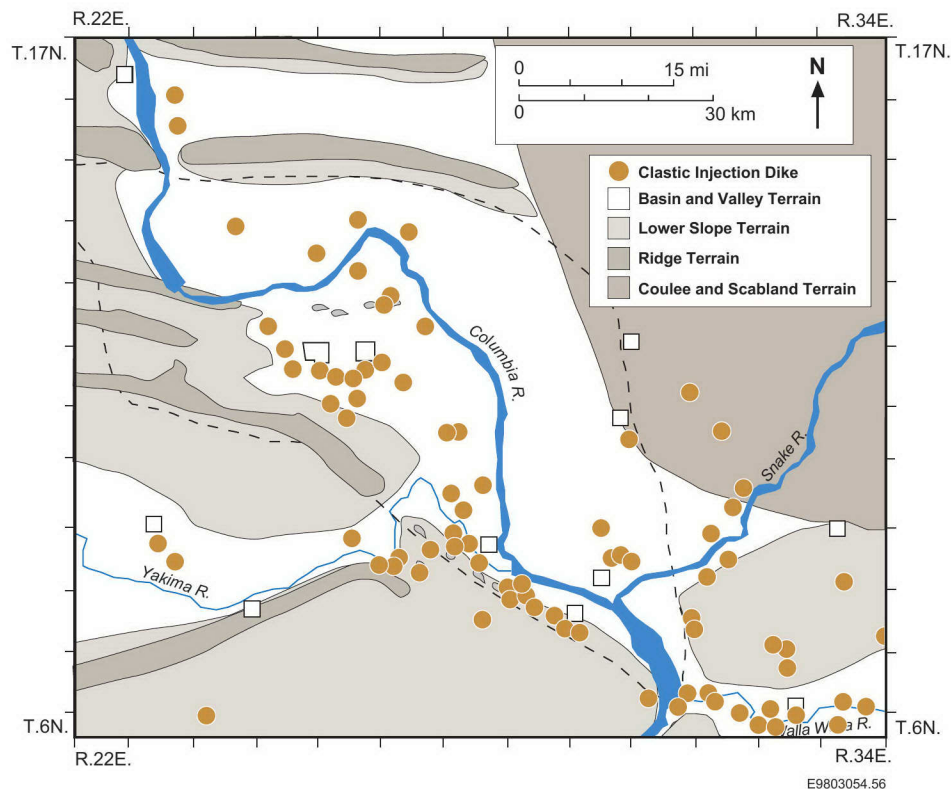


Figure 4-2: Map showing the geographic distribution of clastic dikes used in this study associated with geomorphic terrains in the Pasco Basin.

4.3 OCCURRENCE BY ROCK TYPE

General

- As part of a geologic mapping project of the Pasco Basin and vicinity for the State of Washington, Reidel and Fecht (1994a, 1994b) noted the presence of clastic injection dikes in many of the major stratigraphic units in the basin.
- The major stratigraphic units that were inspected for clastic injection dikes are presented in Table 4-1.
- Sources: Reidel and Fecht (1994a, 1994b) and this study.

Table 4-1: Stratigraphic units in the Pasco Basin that are known to be intruded by clastic injection dikes. It is important to note that although clastic injection dikes are not known to occur in older geologic units, it does not mean that they do not occur in that unit.

Stratigraphic Unit	Clastic Injection Dike	
	Yes	No ^a
Surficial sediments		●
Hanford Formation	●	
Silt Facies	●	
Sand Facies	●	
Gravel Facies	●	
Plio-Pleistocene Unit	●	
Deposits of the Yakima River	●	
Deposits of the Columbia River		●
Deposits of the Upper Cold Creek	●	
Deposits of the Wahluke Slope	●	
Ringold Formation	●	
Member of Savage Island	●	
Member of Taylor Flat	b	
Member of Wooded Island	●	
Columbia River Basalt Group	●	
Saddle Mountains Basalt	●	
Wanapum Basalt	●	
Grande Ronde Basalt		●
Ellensburg Formation	●	
Levey Interbed		●
Rattlesnake Ridge Interbed	●	
Selah Interbed	●	
Cold Creek Interbed	●	
Mabton Interbed		●

^aClastic injection dike(s) not known to be present.

^bClastic injection dikes have recently been observed in the member of Taylor Flat. Dikes within this member are not discussed further in this study.

4.3 OCCURRENCE BY ROCK TYPE

Columbia River Basalt Group

- Clastic injection dikes are infrequently observed in Saddle Mountains and Wanapum Basalts. Clastic injection dikes have not been observed in Grande Ronde Basalt in the Pasco Basin. Grande Ronde Basalt is poorly exposed in the Pasco Basin and vicinity except in Umtanum Ridge west of Midway and in the Saddle Mountains around Sentinel Gap.
- Clastic injection dikes have been observed in the following members of the CRBG:
 - Ice Harbor
 - Elephant Mountain
 - Pomona
 - Priest Rapids
 - Frenchman Springs.
- Clastic injection dikes occur in fissures and fractures of rubbly flow tops, entablatures, and colonnades of basalt flows. Clastic injection dikes most commonly occur in the CRBG where basalt is folded and/or faulted. Clastic injection dikes typically do not penetrate more than 30 cm into cooling fractures of basalt flows that have not been folded and/or faulted.
- Reference Location: Weaver Pit (6/33-17H).
- Sources: Jones and Deacon (1966), CDA (1969, 1971), Farooqui (1979), PSPL (1981), WCC (1981), and this study.

Figure 4-3: Photograph of a clastic injection dike along cooling fractures in the interior of a basalt flow from the Frenchman Springs Member. The clastic injection dike is located along the east wall of Weaver Pit (6/33-17H) on the north flank of the Horse Heaven Hills.



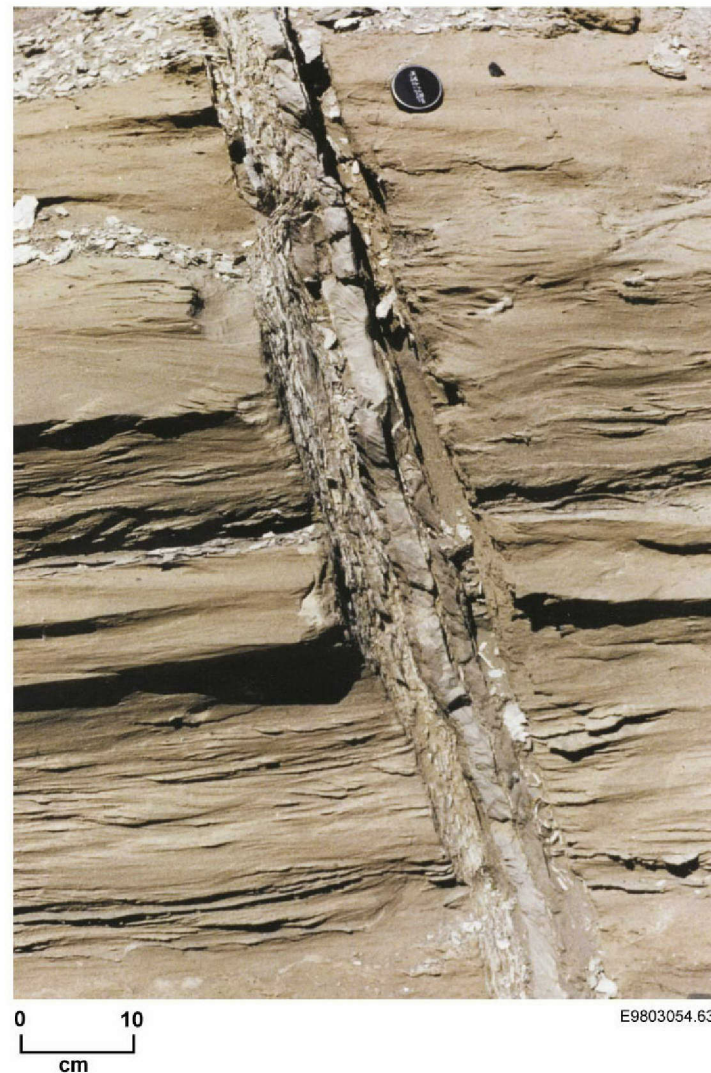
E9803054.60

4.3 OCCURRENCE BY ROCK TYPE

Ellensburg Formation

- Clastic injection dikes are infrequently observed in the Rattlesnake Ridge, Selah, and Cold Creek interbeds of the Ellensburg Formation. These interbeds are exposed in surface outcrops in the Pasco Basin and vicinity more frequently than other interbeds.
- The clastic injection dikes are generally thin (<5 cm) and vary in length from less than 1 m to greater than 10 m.
- Clastic injection dikes have not been observed in other interbeds. However, only a cursory examination of other interbeds has occurred to date.
- Reference Location: Badlands (9/26-9N).
- Sources: CDA (1969,1971), Black (1979), and this study.

Figure 4-4: Photograph of a clastic injection dike in the main channel sand facies of the Rattlesnake Ridge interbed of the Ellensburg Formation. The dike is located in the Badlands (9/26-9N) within a low-amplitude, anticlinal structure.



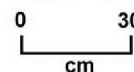
4.3 OCCURRENCE BY ROCK TYPE

Ringold Formation

Member of Wooded Island

- Clastic injection dikes are commonly observed in the member of Wooded Island in the southeastern Pasco Basin [e.g., Eureka Flats (9/31-36K) and Iowa Beef North and South (8/31-36D)].
- Clastic injection dikes rarely occur in exposures of the member of Wooded Island along the White Bluffs and in the western Pasco Basin.
- Clastic injection dikes are commonly 10 to 15 cm in width and are near-vertical in cross section.
- Reference Location: Iowa Beef South (8/31-36D).
- Source: Richman (1981) and this study.

Figure 4-5: Photograph of a clastic injection dike that extends down from lacustrine deposits of the member of Savage Island into a conglomerate unit of the member of Wooded Island. The dike is located in a gravel pit west of Eureka Flats (9/31-36K), southeastern Pasco Basin. The member of Taylor Flat is not present in this part of the Pasco Basin. The dike is exposed for 10 m and averages 12 cm in width.



E9803054.70

4.3 OCCURRENCE BY ROCK TYPE

Ringold Formation (Continued)

Member of Savage Island

- Clastic injection dikes have been observed in the member of Savage Island of the Ringold Formation.
- Brown and Brown (1962) observed clastic injection dikes in the northern White Bluffs along the Columbia River at Wahluke Landing Road (14/26-3N). The dikes extend 45 m through a petrocalcic horizon superimposed on top of the Ringold Formation and down into the member of Savage Island. This is the greatest known vertical extent of a continuously exposed clastic injection dike that has been observed in the Pasco Basin.
- Clastic injection dikes in the member of Savage Island commonly occur in the north-central Pasco Basin around the Saddle Mountain Lakes area (14/26-7R) and White Bluffs North (14/27-8R) and in the southeastern Pasco Basin, south of the Snake River.
- Clastic dikes are frequently observed at the top of the member of Savage Island along the White Bluffs from near Richland to south of Locke Island, but these dikes are associated with Type I dikes and are not clastic injection dikes.
- Reference Location: Wahluke Landing Road (14/26-3N).
- Sources: Brown and Brown (1962) and this study.

Figure 4-6: Photograph of the upper portion of the greatest known continuous vertical exposure of a clastic injection dike in the Pasco Basin (45 m). The dike occurs in the member of Savage Island, along Wahluke Landing Road (14/26-3N). Pictured is Don Brown, a geologist at the Hanford Site for over 40 years, investigating clastic injection dikes in the early 1960s.

Figure 4-7: Photograph of a clastic injection dike that penetrates the member of Savage Island along the Wahluke Landing Road (14/26-3N).



E9803054.71



E9803054.66

4.3 OCCURRENCE BY ROCK TYPE

Plio-Pleistocene Deposits

- Clastic injection dikes have been observed in deposits of the Yakima River, upper Cold Creek, and Wahluke Slope. Dikes have not been observed in deposits of the Columbia River.
- In the deposits of the Yakima River, clastic injection dikes are common to the overbank and fluvial silt and sand sequences, but do not penetrate through the main channel gravel sequence [e.g., Yakima Bluffs (9/28-16G)].
- In deposits of the upper Cold Creek, clastic injection dikes have been observed penetrating through the eolian loess and calcic paleosol sequence in many areas along the margins of the basin [e.g., Iowa Beef South (8/31-36D)] and occasionally in the central basin [e.g., Borehole 299-W23-16 (12/25-12G)].
- In deposits of the Wahluke Slope, clastic injection dikes are commonly observed penetrating sidestream basaltic sandy gravels mixed with calcic paleosols and minor eolian loess in the north-central Pasco Basin, north of the Saddle Mountain Lakes [e.g., Wahluke Landing Road (14/26-3N)].
- The deposits of the Columbia River are poorly exposed in the Pasco Basin and vicinity. Drilling and sampling techniques used to install boreholes and wells into and through this unit were not suitable to detect the presence of clastic injection dikes.
- Reference Location: Yakima Bluffs (9/28-16G).
- Source: This study.

Figure 4-8: Photograph of a clastic injection dike in the deposits of the Yakima River. The exposure is along the Yakima Bluffs west of the Yakima River (9/28-16G).

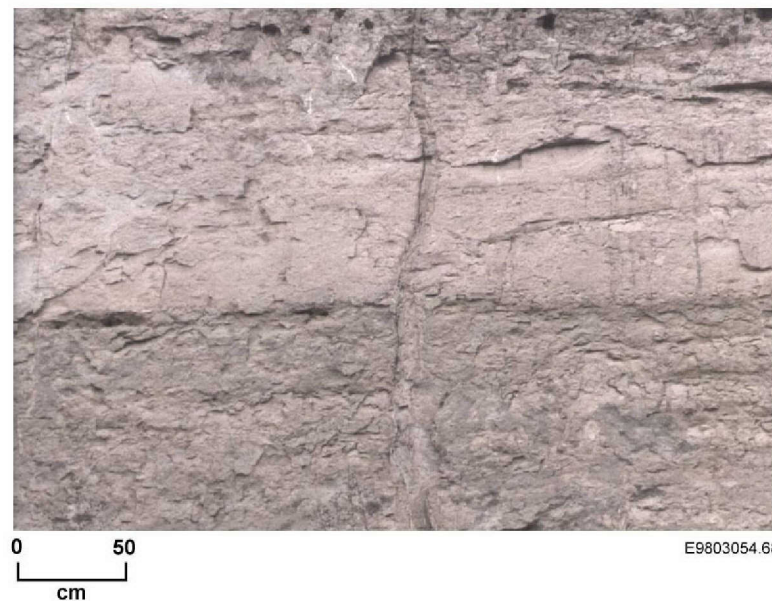
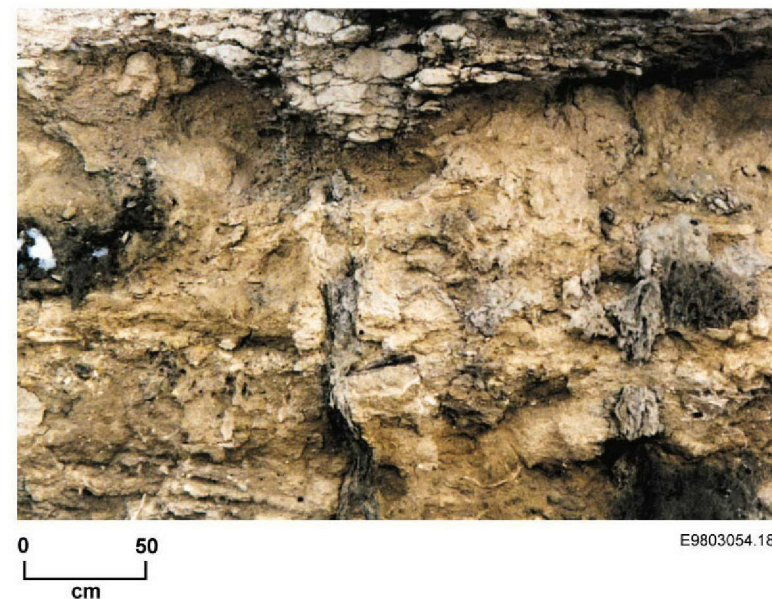


Figure 4-9: Photograph of a clastic injection dike in deposits of the upper Cold Creek located in an interfluvial area between sidestreams near Wahluke Landing Road (14/26-3N).



4.3 OCCURRENCE BY ROCK TYPE

Hanford Formation

Gravel Facies

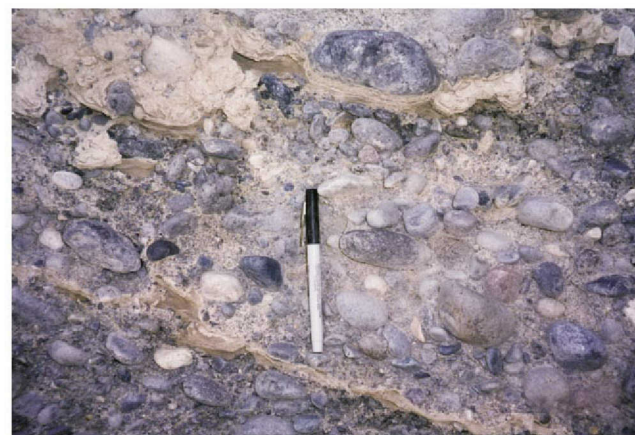
- Clastic injection dikes are occasionally observed in the gravel facies of the Hanford Formation.
- Clastic injection dikes have been observed in gravel deposits in field mapping units #1(?), #2, and #3 of the Hanford Formation.
- Clastic injection dikes occur in clast-supported gravels with sand and/or silt matrix and in matrix-supported, gravelly sands.
- Clastic injection dikes occur in thin deposits (i.e., <2 m) of open-framework gravels. Dikes that form in these gravels have the following characteristics:
 - Squeeze or ooze into the open spaces among clasts
 - Partially fill the interstices
 - Gradually lose definition in the gravels.
- Clastic injection dikes have not been found penetrating through thick deposits (i.e., >2 m) of open-framework gravels.
- Reference Location: Not designated due to the inaccessibility of good exposures.
- Source: This study.

Figure 4-10: Photograph of a clastic injection dike in the gravel facies of the Hanford Formation (field mapping unit #3) along the Columbia River at the 100-N Area, Hanford Site (14/26-28C).



0 5
cm
E9803054.61

Figure 4-11: Photograph of a clastic injection dike that filled open-framework gravels at the top of a pre-13,000-year-old gravel facies of the Hanford Formation (field mapping unit #1 or #2?). The dike occurs in a gravel quarry near the south end of Lower Smith Canyon [Smith Canyon North (9/30-13N)].



0 5
cm
E9803054.62

4.3 OCCURRENCE BY ROCK TYPE

Hanford Formation (Continued)

Sand Facies

- Clastic injection dikes are abundant in the sand facies of the Hanford Formation. The dikes in these deposits are more widely spaced than are dikes in the silt facies.
- Clastic injection dikes in the sand facies are commonly found in two areas of field mapping unit #3:
 - Between the southern 200 Area Pleistocene Glaciofluvial Flood Bar in the central Hanford Site and west Kennewick [e.g., US Ecology (12/26-9R)]
 - Between lower Esquatzel Coulee and the mouth of the Snake River [e.g., Pasco Landfill (9/30-22)].
- Clastic injection dikes are also present in sand facies in field mapping units #1(?) and #2 [e.g., West Highlands (9/29-34E) and Fast Flux Test Facility (11/28-18P), respectively].
- Clastic injection dikes have not been observed in late-stage basalt-rich sands of field mapping unit #4 that are located in abandoned glaciofluvial flood channelways north and south of Gable Mountain, between the old Hanford townsite and the 300 Area on the Hanford Site, and lower Esquatzel Coulee northwest of Pasco.
- Reference Location: Richland Landfill (10/28-17N).
- Sources: Bechtel (1971), Price and Fecht (1976m), Fecht and Weekes (1996), and this study.

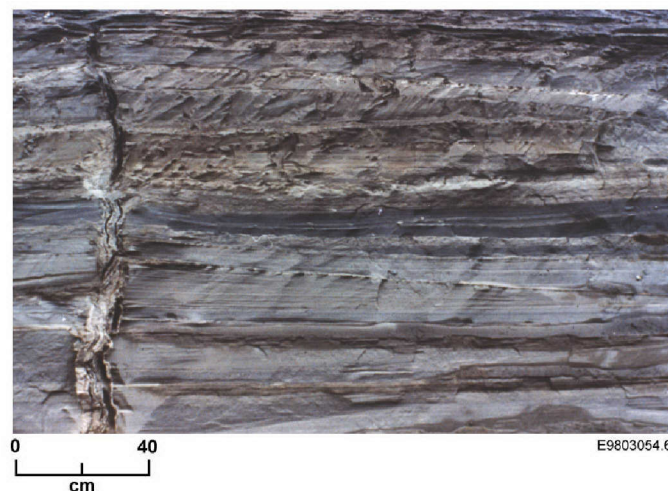
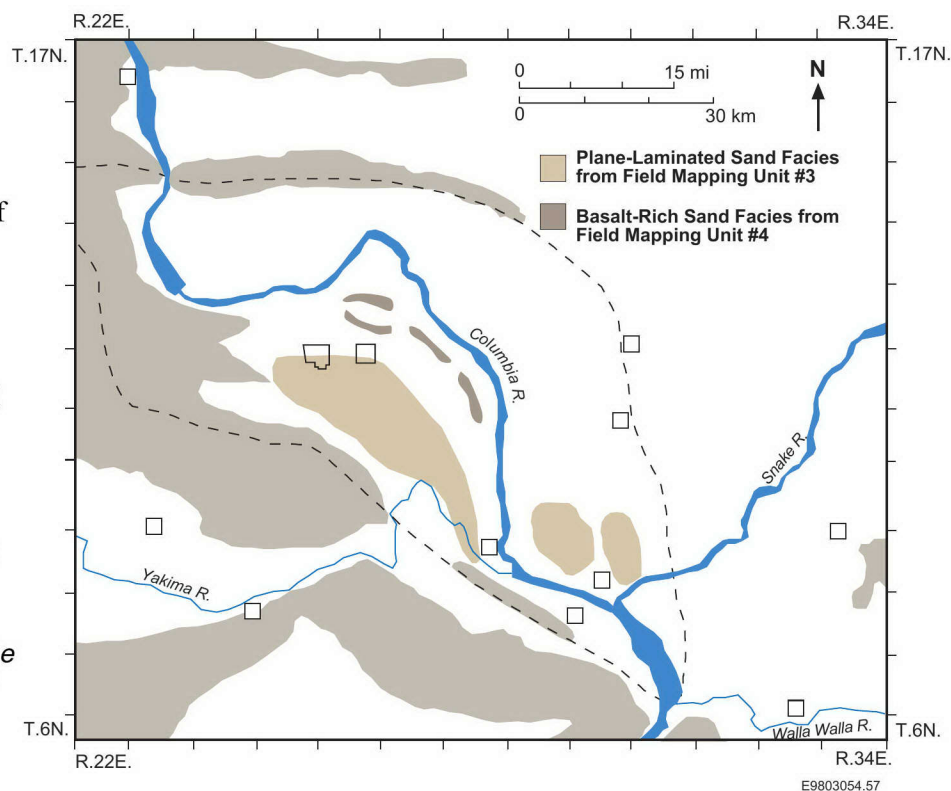


Figure 4-12: Photograph of a clastic injection dike in the sand facies of the Hanford Formation (field mapping unit #3) at the US Ecology excavation on the 200 Area Pleistocene Glaciofluvial Flood Bar, Hanford Site (12/26-9R).

Figure 4-13: Map showing the location of the major deposits of the sand facies of the Hanford Formation (field mapping units #3 and #4).



4.3 OCCURRENCE BY ROCK TYPE

Hanford Formation (Continued)

Silt Facies

- Clastic injection dikes are ubiquitous in the silt facies in field mapping units #1, #2, and #3 of the Hanford Formation throughout the Pasco Basin and vicinity [e.g., Yakima Bluffs (9/28-16G), Cummings Bridge (7/32-35Q), and Burlingame Canyon (6/34-5M), respectively].
- Clastic injection dikes have not been observed in some younger silt facies of field mapping unit #3 at lower elevations along the Columbia and Yakima Rivers (e.g., 7/31-27J). The silts were deposited by late Glacial Lake Missoula floods or from other ice-margin lakes on the Columbia River system.
- Reference Location: Burlingame Canyon (6/34-5M).
- Sources: Jenkins (1925), Lupher (1944), Newcomb (1962), Alwin (1970), WCC (1981), and this study.

Figure 4-14: Photograph of clastic injection dikes in the silt facies of the Hanford Formation (field mapping unit #3) in the Burlingame Canyon (6/34-5M).

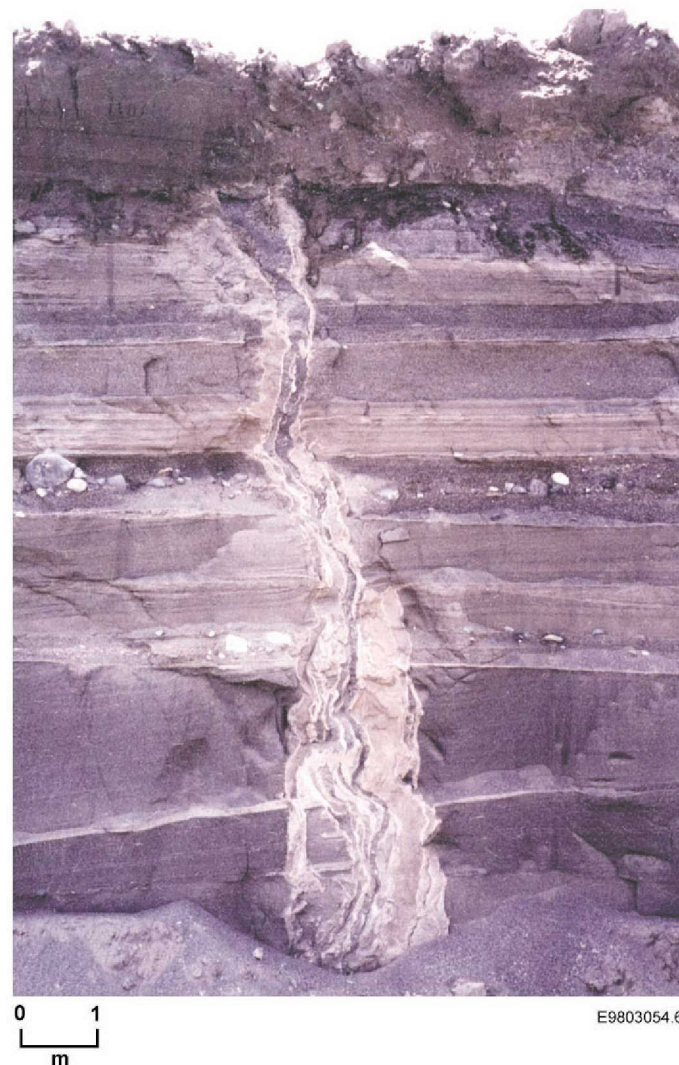


4.3 OCCURRENCE BY ROCK TYPE

Surficial Sediments

- Clastic injection dikes have not been observed in Holocene sediments. Holocene sedimentary deposits in the Pasco Basin and vicinity include the following:
 - Eolian loess and dune sand
 - Colluvium and talus
 - Sidestream and main stream alluvium
 - Mass wasting deposits.
- In all instances where clastic injection dikes and Holocene sediments occur in the same exposure, the clastic injection dikes are truncated at the base of the Holocene sediments.
- Source: WCC (1981), Fecht and Weekes (1996), and this study.

Figure 4-15: Photograph of clastic injection dikes in a host of glaciofluvial sediment at the Environmental Restoration Disposal Facility excavation (12/26-7K). The clastic injection dike does not penetrate Holocene surficial eolian sands (from Fecht and Weekes 1996).



4.4 OCCURRENCE IN MULTIPLE SEDIMENT/ROCK TYPES

- Clastic injection dikes commonly occur in more than one stratigraphic unit within many exposures in the Pasco Basin and vicinity. Exposures of clastic injection dikes in multiple stratigraphic units include:

1. Brynes Road	7/32-36G
2. Cummings Bridge	7/32-35Q
3. Eureka Flats	9/31-36K
4. Fast Flux Test Facility	11/28-18P
5. Gable Mountain South	13/27-19N
6. Garrett	7/35-28J
7. Grout	12/26-1N
8. Iowa Beef North	8/31-36D
9. Iowa Beef South	8/31-36D
10. Keene/Kennedy Road	9/28-22M
11. Kiona Gravel Pit	9/27-20K
12. Meadow Hills	9/28-35R
13. Pumphouse Road	10/18
14. Saddle Mountain Lakes Area	14/26-7R
15. Smith Canyon North	9/30-13N
16. Transtate Gravel Pit	9/30-6F
17. Wahluke Landing Road	14/26-3E&M
18. Weaver Pit	6/33-17H
19. Yakima Bluffs	9/28-16G
20. Borehole 299-W23-16	12/25-12G

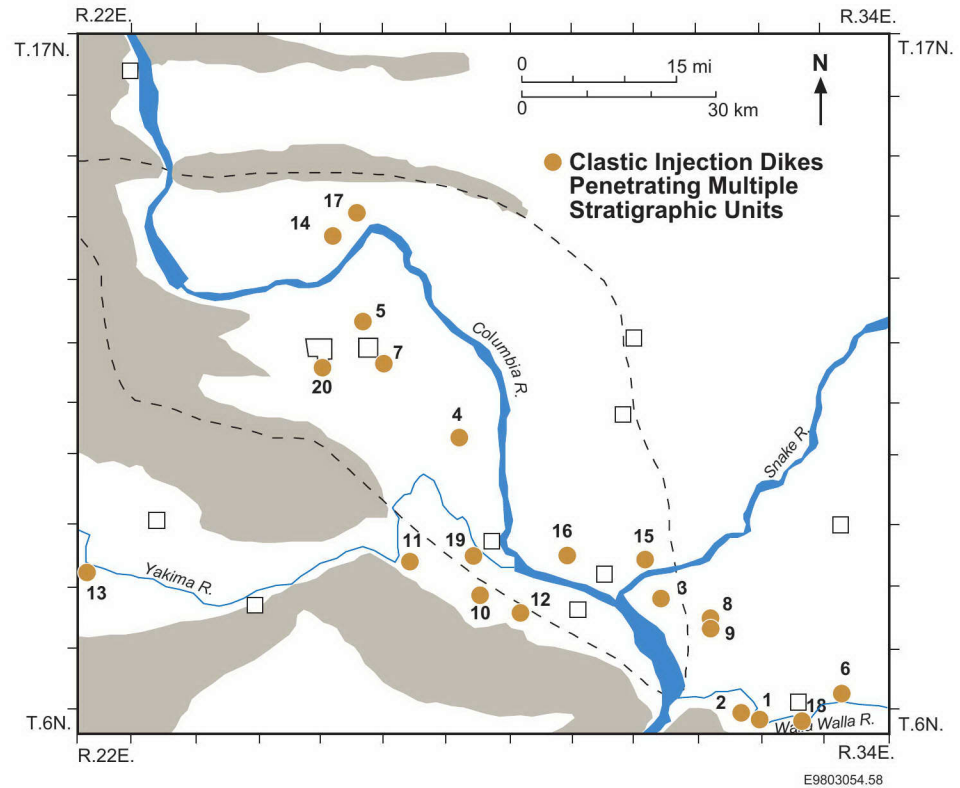


Figure 4-16: Map showing the locations of clastic injection dikes exposed in multiple stratigraphic units.

4.4 OCCURRENCE IN MULTIPLE SEDIMENT/ROCK TYPES

- In most exposures, Hanford Formation sediments form the uppermost unit in sequences that contain clastic injection dikes. The lower unit(s) may be the Hanford Formation, Plio-Pleistocene deposits, Ringold Formation, and/or CRBG.
- The number of dikes per linear distance is highest in the finer grained units and decreases with coarser grained units or rocks.
- In sequences of the silt or sand facies of the Hanford Formation that overlie the gravels of the Hanford Formation or Ringold Formation, or basalt of the CRBG, clastic injection dikes:
 - Fill vertical or near-vertical fractures in the gravel or basalt,
 - Form sills in fractures of the gravels or basalts near the contact with the overlying silt and sand facies, or
 - Terminate before entering the gravels or basalt.

Table 4-2: Selected geologic sequences within the Pasco Basin and vicinity that contain clastic injection dikes in multiple sediment/rock types and units in a single geologic section.

Location	Upper Unit	Lower Unit(s)
Weaver Pit (6/33-17H)	Silt facies, Hanford Formation (field mapping unit #3)	Frenchman Springs, CRBG
Iowa Beef South (8/31-36D)	Sand facies, Hanford Formation (field mapping unit not known)	Deposits of Upper Cold Creek, Plio-Pleistocene deposits and member of Wooded Island, Ringold Formation
Yakima Bluffs (9/28-16G)	Silt facies, Hanford Formation (field mapping unit #3)	Deposits of Yakima River, Plio-Pleistocene deposits
Garrett (7/35-28J)	Silt facies, Hanford Formation (field mapping unit #3)	Old loess/colluvium
Kiona Gravel Pit (9/27-20K)	Silt facies, Hanford Formation (field mapping unit #3)	Gravel facies, Hanford Formation (field mapping units #1 and #2)
Weaver Pit (6/33-17H)	Silt facies, Hanford Formation (field mapping unit #3)	Frenchman Springs Member, CRBG
Keene/Kennedy Road (9/28-22M)	Silt facies, Hanford Formation (field mapping unit #3)	Sand facies, Hanford Formation (field mapping unit #2)
Cummings Bridge (7/32-35Q)	Silt facies, Hanford Formation (field mapping unit #3)	Silt facies, Hanford Formation (field mapping unit #2?)
Fuels and Materials Examination Facility (11/28-18N)	Sand facies, Hanford Formation (field mapping unit #3)	Sand facies, Hanford Formation (field mapping units #1 and #2)
Fuels and Materials Examination Facility (11/28-18N)	Sand facies, Hanford Formation (field mapping unit #2)	Sand facies, Hanford Formation (field mapping unit #1)
Yakima Bluffs (9/28-16G)	Gravel facies, Hanford Formation (field mapping unit #2)	Silt facies, Hanford Formation (field mapping unit #1) and deposits of the Yakima River, Plio-Pleistocene deposits

4.4 OCCURRENCE IN MULTIPLE SEDIMENT/ROCK TYPES

- In clastic injection dikes that formed into two distinctly different time intervals, younger dikes have been observed to:
 - Use older clastic injection dikes as the pathway through the older material before intruding upward into the younger host sediments [e.g., Iowa Beef South (8/31-36D)].
 - Use a pathway through the older rock types other than older clastic injection dikes before entering into younger host sediments [e.g., Cummings Bridge (7/32-35Q)].
 - Use some older clastic injection dikes as pathways, but also use other pathways through the older sediments or rocks [e.g., Fuels and Materials Examination Facility excavation (11/28-18N) and Keene/Kennedy Road (9/28-22M)].
 - Use older clastic injection dikes, but bifurcate as the younger dikes intrude into the younger host sediments [e.g., Grout (12/26-1N)].
- The younger clastic injection dikes typically use older clastic injection dikes as pathways when:
 - The texture, composition, and bedding characteristics are similar between the older sediments intruded by older clastic injection dikes and the younger sediments intruded by the younger dikes.
 - They occur along the same tectonic structure (joint, shear, or fault).
- Reference Location: Yakima Bluffs (9/28-16G).
- Source: This study.

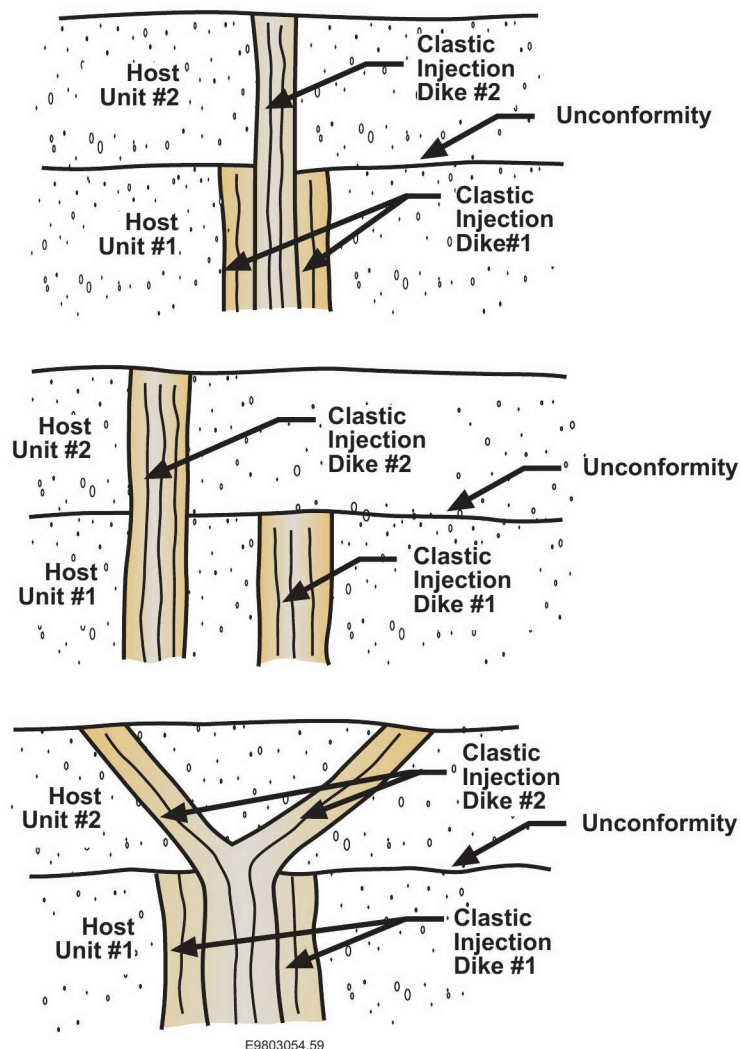
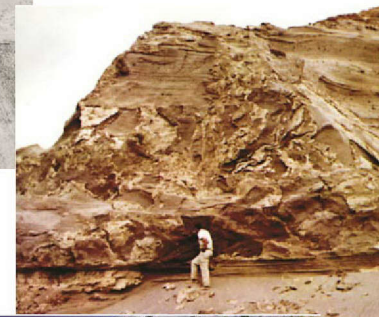


Figure 4-17: Figures illustrating the relationship of clastic injection dikes from two different intervals of emplacement, including (from top to bottom) older dike as host, older sediments as host, and bifurcation.

5.0 CLASTIC INJECTION DIKE NETWORKS

5.1 TYPES OF NETWORKS

- Clastic injection dikes in the Pasco Basin and vicinity can be divided into dike networks based on the context of the fissures and the interrelationship of individual clastic dikes. Dike networks occur where stratigraphic units have consistency in textural and bedding characteristics, topographic relief, and structural features or fabric.
- Types of networks defined by this study are:
 - Regular-shaped, polygonal-patterned ground: Clastic injection dikes form regular polygonal patterns in clastic host sediments in plan view. Dikes merge at intersections with other dikes in the network.
 - Irregular-shaped, polygonal-patterned ground: Clastic injection dikes form irregular and complex forms in clastic host sediments in plan view. Dikes merge, but primarily cross-cut at intersections with other dikes in the network.
 - Pre-existing fissure: Clastic injection dikes form along fissures that were established in the host sediments/rocks long before emplacement of the infilling dike material. Clastic injection dikes merge or cross-cut at intersections with other clastic injection dikes.
 - Random occurrence: Clastic injection dikes form in randomly oriented and distributed fissures in clastic host sediments in both plan view and cross-section. Few dikes have been observed intersecting with other dikes in the “network.”
- Source: This study.



E9803054.90

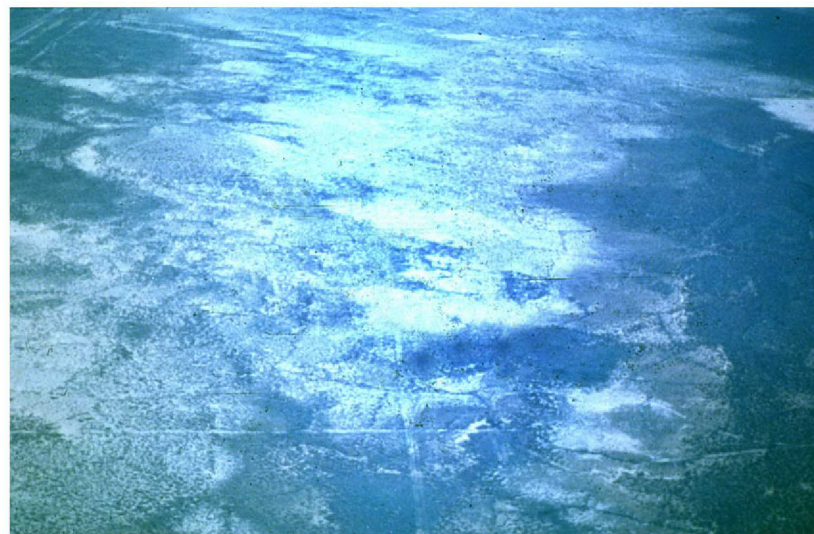
Figure 5-1: Photographs of clastic injection dike networks that occur in the Pasco Basin and vicinity (clockwise from top: regular-shaped polygons, irregular-shaped polygons, pre-existing fissures, and random dikes).

5.2 REGULAR-SHAPED, POLYGONAL-PATTERNED GROUND

General

- Previous studies have observed that clastic injection dikes form polygonal-patterned ground in several locations in the Pasco Basin and vicinity. These polygonal networks have been assigned to the regular-shaped, polygonal-patterned ground in this atlas. These studies include the following:
 - Newcomb (1962)
 - Jones and Deacon (1966)
 - Grolier and Bingham (1978)
 - Black (1979)
 - Last and Fecht (1986)
 - Fecht et al. (1994)
 - Fecht and Weekes (1996).
- The principal components of regular-shaped, polygonal-patterned ground dike networks from this study are:
 - Master dikes
 - Dikelets
 - Sills
 - Small-scale faults and shears.

Figure 5-2: Aerial oblique photographs of regular-shaped, polygonal-patterned ground from the Goose Egg Hill area (12/26-33C). The photographs were taken by George Last during a study of clastic injection dikes (Last and Fecht 1986).



E9803054.113



E9803054.114c

5.2 REGULAR-SHAPED, POLYGONAL-PATTERNED GROUND

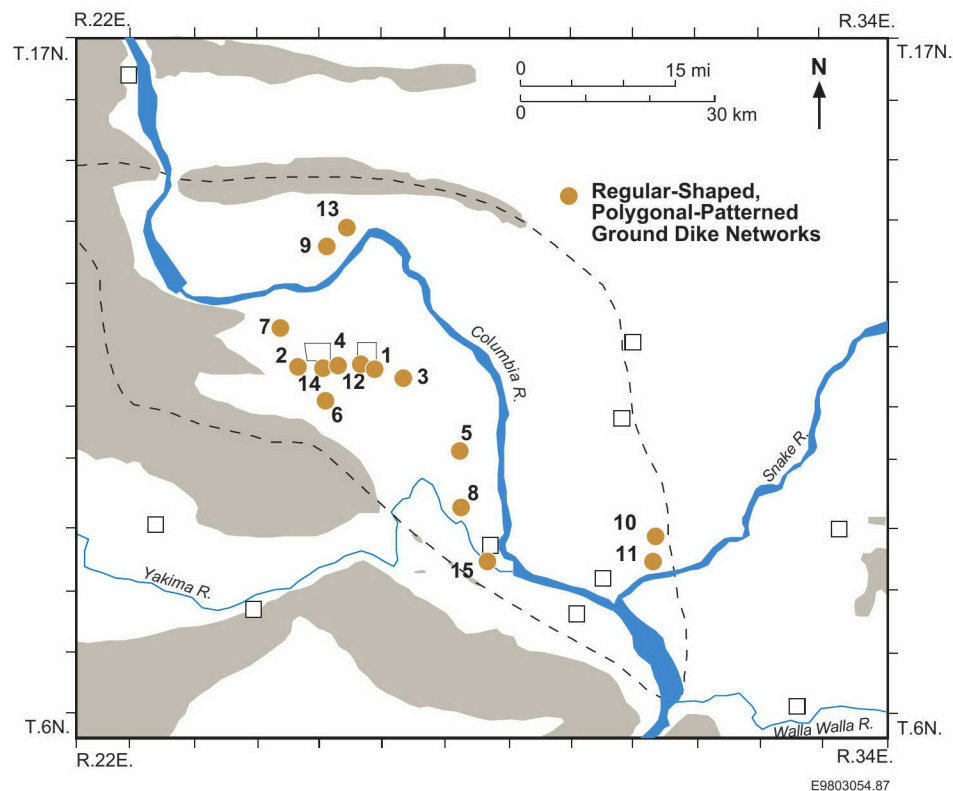
Locations

- Several large exposures of regular-shaped, polygonal-patterned ground dike networks occur in the Pasco Basin and vicinity. Large exposures of regular-shaped, polygonal-patterned ground are located at:

1.	216-BC Cribs	12/26-10K
2.	216-S-16 Pond	12/25-14E
3.	Central Landfill	12/27-20P
4.	Environmental Restoration Disposal Facility	12/26-7K
5.	Fast Flux Test Facility	11/28-18P
6.	Goose Egg Hill	12/26-33C
7.	McGee Ranch	13/25-30
8.	Richland Landfill	10/28-17N
9.	Saddle Mountain Lakes Area	14/26-7R
10.	Smith Coulee North	9/30-13N
11.	Smith Coulee South	9/30-24D
12.	US Ecology	12/26-9R
13.	Wahluke Landing Road	14/26-3N
14.	Well 699-32-72	12/26-18F
15.	Yakima Bluffs (fine-grained dikes)	9/28-16G

- The regular-shaped, polygonal-patterned ground has been located from photogrammetric images, field mapping of the Pasco Basin, and mapping of large construction excavations in the central basin.
- Reference Location: Goose Egg Hill (12/26-33C).

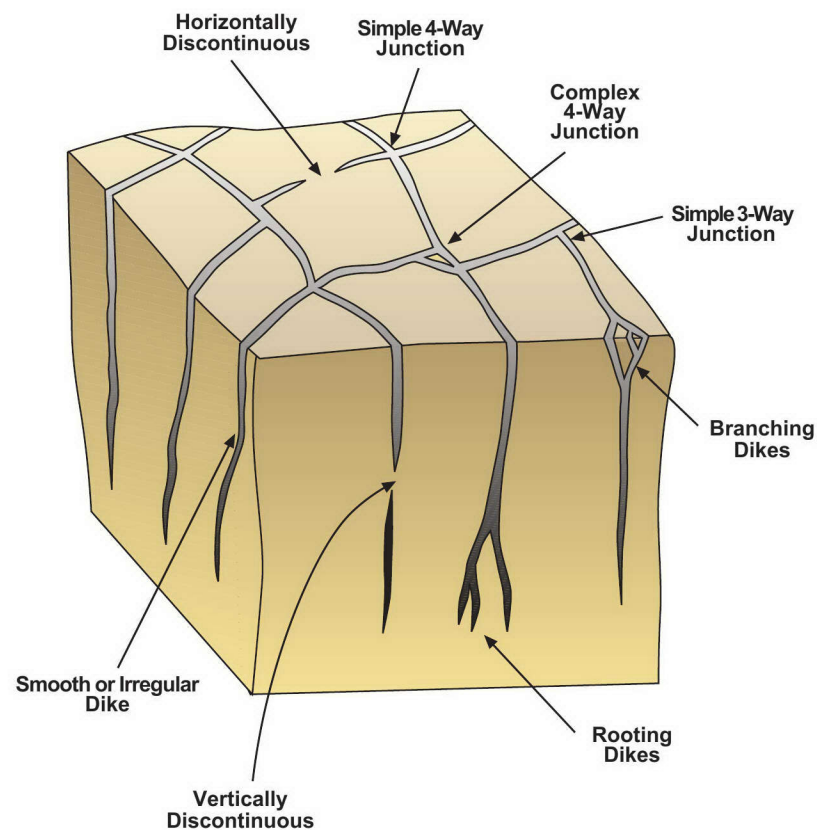
Figure 5-3: Map showing the location of large exposures of regular-shaped, polygonal-patterned ground dike networks in the Pasco Basin.



5.2 REGULAR-SHAPED, POLYGONAL-PATTERNED GROUND

Master Dikes

- Master dikes are clastic injection dikes that form boundaries of the regular-shaped polygonal patterns.
- Master dikes are defined as typically the widest, deepest, and most laterally extensive dikes in regular-shaped, polygonal-patterned ground dike networks.
 - Dike widths generally range from 3 cm to 1 m.
 - Dike depths range from 2 m to greater than 20 m.
 - Segment lengths in plan view generally range from 1.5 to 100 m.
- Master dikes may not completely enclose every polygon in a regular-shaped, polygonal-patterned ground dike network. Segments or portions of segments of individual polygons may not be complete.
- About 8% of master dikes do not form completely across a surface segment of a regular-shaped, polygonal-patterned ground dike network. Examples of this are found in field exposures in the regular-shaped, polygonal-patterned ground dike network around Goose Egg Hill in the lower Cold Creek Valley (12/26-33C).
- Between 10% and 20% of the vertical segments of master dikes are discontinuous based on examination of vertically extensive exposures in the central Pasco Basin.



E9803054.72

Figure 5-4: Schematic of master dikes associated with a regular-shaped, polygonal-patterned ground dike network. Only master dikes are depicted on the schematic.

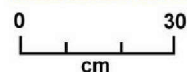
5.2 REGULAR-SHAPED, POLYGONAL-PATTERNED GROUND

Master Dikes (Continued)

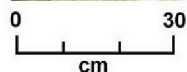
- A characteristic of regular-shaped, polygonal-patterned ground is the merging of master dikes at the intersection of dike segments. The merging is represented by master dike segments and individual infilling units changing orientation by bending or splaying into an adjoining segment(s) and associated infilling units. Truncation of master dike segments and associated infilling units only occasionally occurs in regular-shaped, polygonal-patterned ground dike networks.
- Master dikes generally merge at triple junctions (i.e., three master dike segments intersect at a single point). Four-way junctions also occur where four master dike segments intersect.
- Mergers of master dikes range from simple mergers with individual infilling units trending into adjoining segments to more complex mergers that often incorporate blocks of host sediments or slumps into the area of merging dike segments.
- In the regular-shaped, polygonal-patterned ground dike network around Goose Egg Hill in the lower Cold Creek Valley (12/26-33C), 77% of the master dike junctions are simple mergers and 23% are complex (278 junctions were evaluated).

Figure 5-5: Photograph of a simple merger of three master dikes segments at the Keene/Kennedy Road regular-shaped, polygonal-patterned ground dike network in the southern Pasco Basin (9/28-22M).

Figure 5-6: Photograph of a complex merger of three master dike segments at Touchet Road (7/33-22Q).



E9803054.91



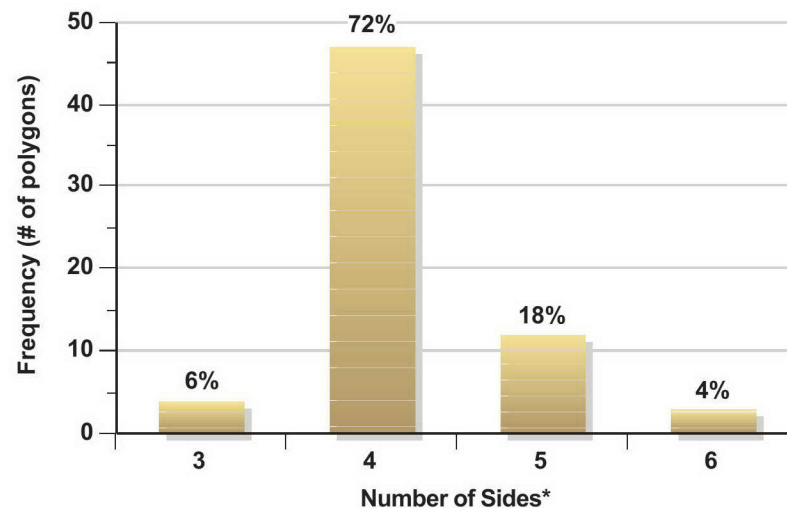
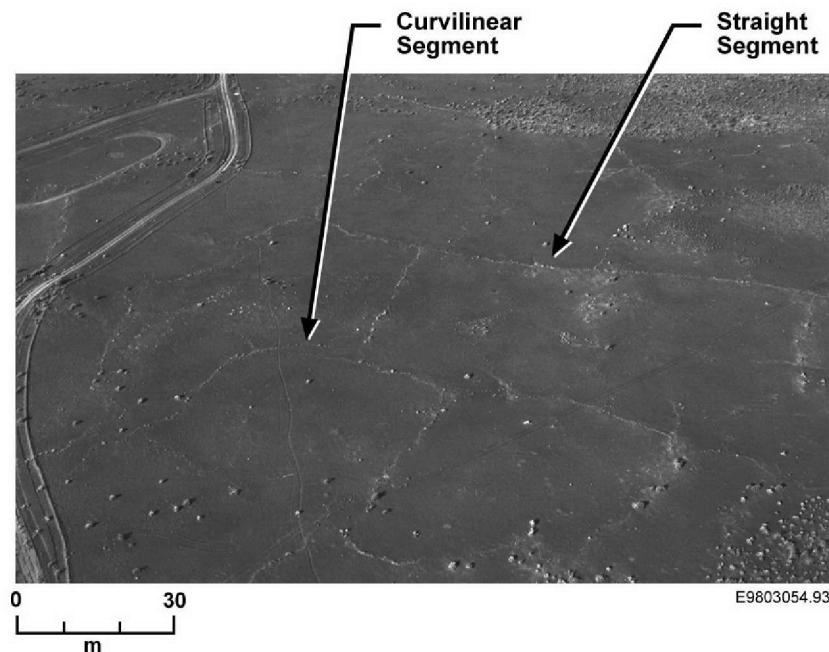
E9803054.92

5.2 REGULAR-SHAPED, POLYGONAL-PATTERNED GROUND

Master Dikes (Continued)

- Master dike segments occur as either straight linear structures or curvilinear structures. Curvilinear segments commonly have a single, gradual, or sharp obtuse bend. In the regular-shaped, polygonal-patterned ground dike network around Goose Egg Hill in the lower Cold Creek Valley (12/26-33C), 55% of the master dike segments were mapped as straight-trending structures, and 45% were mapped as curvilinear structures based on a population of 282 master dike segments that were evaluated. Similar results were found at other regular-shaped, polygonal-patterned ground dike networks [e.g., Central Landfill (12/27-20P), Richland Landfill (10/28-17N), McGee Ranch (13/25-30)].
- Master dike segments most commonly form three- to six-sided polygons; four-sided polygons are dominant in most regular-shaped, polygonal-patterned ground dike networks.
- The strike orientations were measured in dike networks with extensive ground surface exposure. The strike of master dike segments were found to be randomly oriented in the central basin area and in adjacent valleys.

Figure 5-7: Aerial photograph illustrating examples of straight and curvilinear master dike segments in the regular-shaped, polygonal-patterned ground dike network near the Richland Landfill (10/28-17N).



* Based on 66 polygons in Cold Creek Valley

E9803054.73

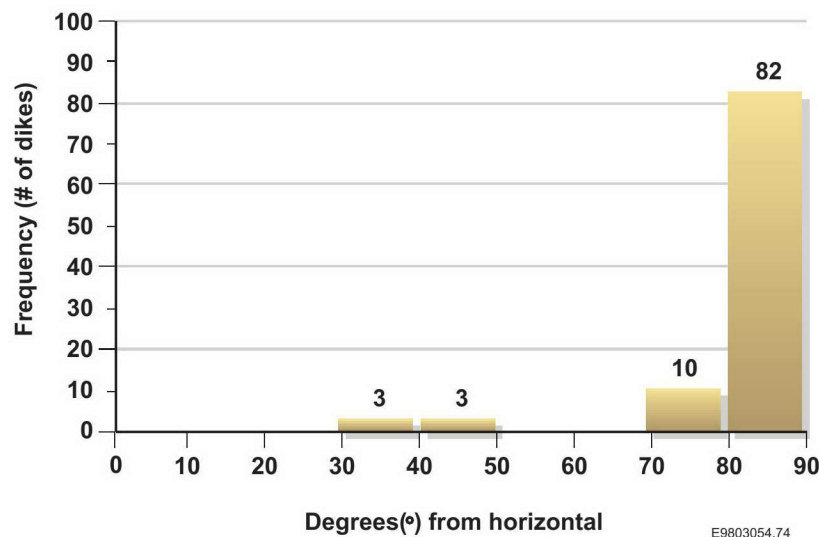
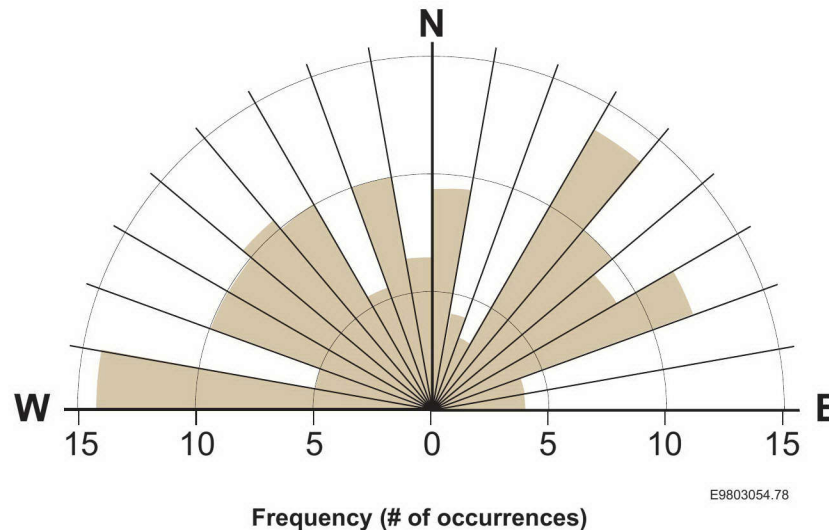
5.2 REGULAR-SHAPED, POLYGONAL-PATTERNED GROUND

Master Dikes (Continued)

- The strike of master dike segments may have preferred orientations adjacent to tectonic structures, but insufficient data are available for a definitive interpretation.
- The dip of master dikes range from vertical (90° from horizontal) to about 30° . Most master dikes (>80%) are near vertical between 80° and 90° from horizontal and perpendicular to the surface of the uppermost geologic unit intruded by dikes. Several of the master dikes that dip between 30° to 50° from horizontal occur in the sand facies of the Hanford Formation and are located on the margin of a large-scale glaciofluvial Pleistocene flood bar [e.g., master dikes at the Fast Flux Test Facility (11/28-18P) and Grout (12/26-1N)]. Low-angle dipping master dikes most commonly occur on the margins of topographic features (e.g., flood bars, escarpments, terraces).

Figure 5-9: Strike of master dikes in the Goose Egg Hill regular-shaped, polygonal-patterned ground dike network in the lower Cold Creek Valley (12/26-33C).

Figure 5-10: Dip of master dikes in regular-shaped, polygonal-patterned ground dike networks in the Pasco Basin and vicinity.



5.2 REGULAR-SHAPED, POLYGONAL-PATTERNED GROUND

Master Dikes (Continued)

- In regular-shaped, polygonal-patterned ground dike networks, the size of polygons varies throughout the Pasco Basin and vicinity.
- In areas where sediments are similar in texture and bedding characteristics, the size of polygons are generally similar. In areas where sediment texture and bedding are variable, the size of polygons also vary.
- For similar-sized polygons, the length of polygonal segments ranges considerably in a single regular-shaped, polygonal-patterned ground dike network, but generally most dikes are within 20% of median dike length of the segment.
- Four-sided polygons and associated segments typically have one pair of segments shorter than the other pair.
- The results of a study of a portion of the Goose Egg Hill regular-shaped, polygon-patterned ground dike network (12/26-33C) with similar-sized polygons is presented in Figures 5-11 and 5-12 and Table 5-1.



E9803054.114

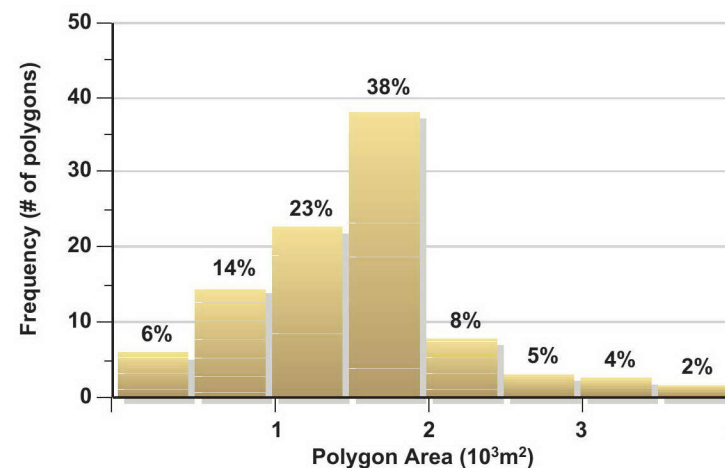
Measure	Dimension	
	Long	Short
Range	150 - 240	30 - 180
Arithmetic Mean	143	104
Median	152	98
Mode	171	85
Standard Deviation	34	32
Skewness	-0.80	0.58

Units in meters, unless dimensionless.

Figure 5-11: Color near-infrared photograph of a portion of the Goose Egg Hill regular-shaped, polygon-patterned ground dike network in the lower Cold Creek Valley (12/26-33C). The photograph and field observation were used as the basis for measurements of the length of dike segments.

Table 5-1: Geometric measurements of polygon segments in the Goose Egg Hill regular-shaped, polygonal-patterned ground dike network.

Figure 5-12: Frequency plot of the area of polygons in the Goose Egg Hill regular-shaped, polygonal-patterned ground dike network (12/26-33C).



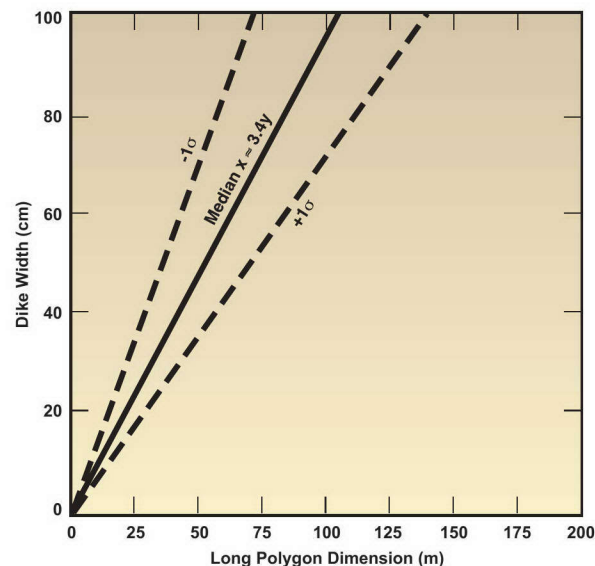
E9803054.84

5.2 REGULAR-SHAPED, POLYGONAL-PATTERNED GROUND

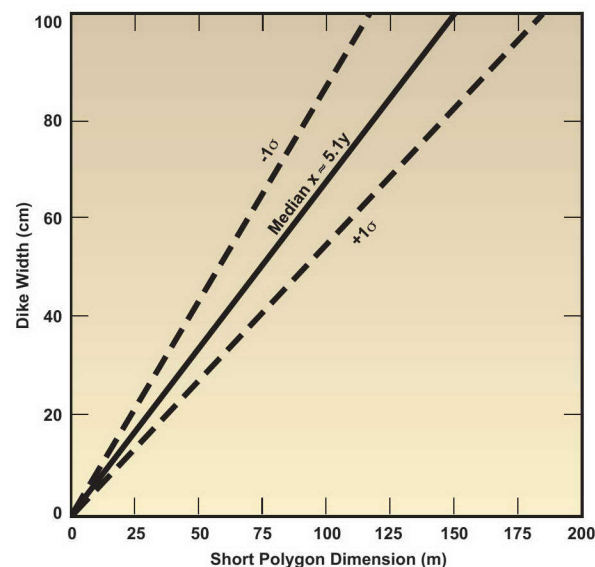
Master Dikes (Continued)

- In many regular-shaped, polygonal-patterned ground dike networks, the width of master dikes is related to the width of polygons. More than 40 regular-shaped, polygonal-patterned ground dike networks were examined, and the widths of dikes and polygons were measured (or in some cases estimated). The relationship between polygon width and dike width holds for a large range of widths from polygons 5 to 10 m across with master dikes 1 to 2 cm wide [e.g., Brynes Road (7/32-36G) and Pumphouse Road (10/18)] to polygons 100 to 150 m across with master dikes 100 cm wide [e.g., Goose Egg Hill (12/26-33C) and Fast Flux Test Facility (11/28-18P)].
- The relationship between dike width and polygon width (both short and long directions) is summarized in Figure 5-13.
- Master dikes comprise about 3% of the volume of regular-shaped, polygon-patterned ground dike networks. The remainder of the volume is composed of about 1% dikelets and 96% host sediments.
- Source: This study.

Figure 5-13: Relationship between dike width and the long (top) and short (bottom) polygon dimensions for regular-shaped, polygonal-patterned ground dike networks in the Pasco Basin and vicinity.



E9803054.82

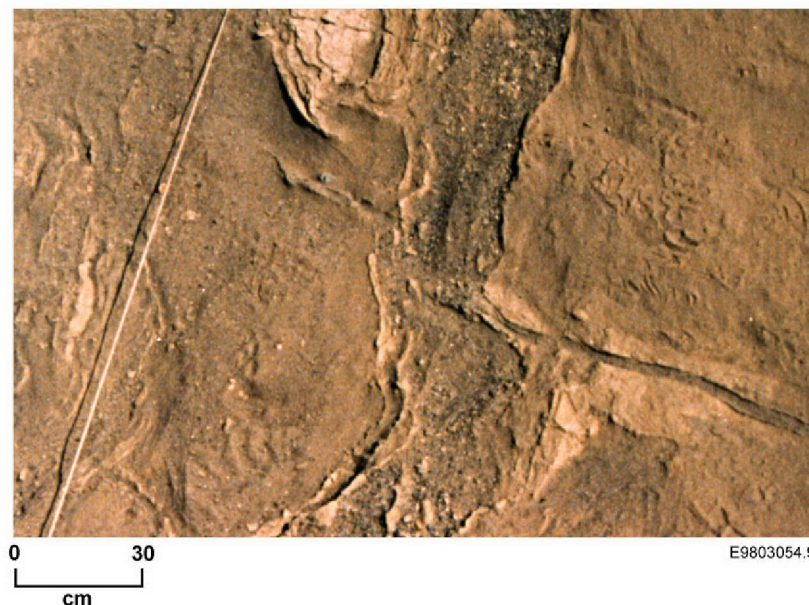


E9803054.83

5.2 REGULAR-SHAPED, POLYGONAL-PATTERNED GROUND

Dikelets

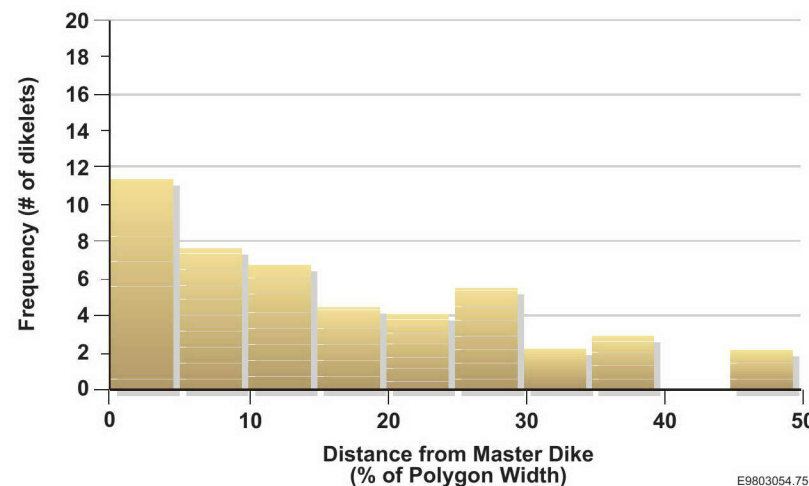
- Dikelets are smaller than master dikes and are typically contained within individual regular-shaped polygons; that is, dikelets typically do not cross from one polygon into an adjacent polygon.
- Dikelets in host sediments adjacent to master dikes typically merge with the infilling sediments of the master dike.
- Dikelets decrease in abundance toward the center of the regular-shaped polygons and are often not present in the central polygonal area.
- Dikelets are often most abundant where master dikes splay near the upper or lower boundaries of the dike. Dikelets also occur locally as a dikelet complex in which numerous dikelets (up to as many as 30 dikelets) emanate from a master dike.
- Dikelets commonly occur along shears that are present in the master dike and host sediments (see section on shears in regular-shaped, polygonal-patterned ground dike networks).



E9803054.94

Figure 5-14: Vertical photograph of a dikelet (right side of photograph) merging with a master dike (center of photograph) in a regular-shaped, polygonal-patterned ground dike network at Keene/Kennedy Road (9/28-22M).

Figure 5-15: Frequency of dikelets across a polygon as a function of distance from a master dike in a regular-shaped, polygonal-patterned ground dike network at Keene/Kennedy Road (9/288-22M). The frequency is based on the number of dikelets measured vertically at intervals across the polygon.



E9803054.75

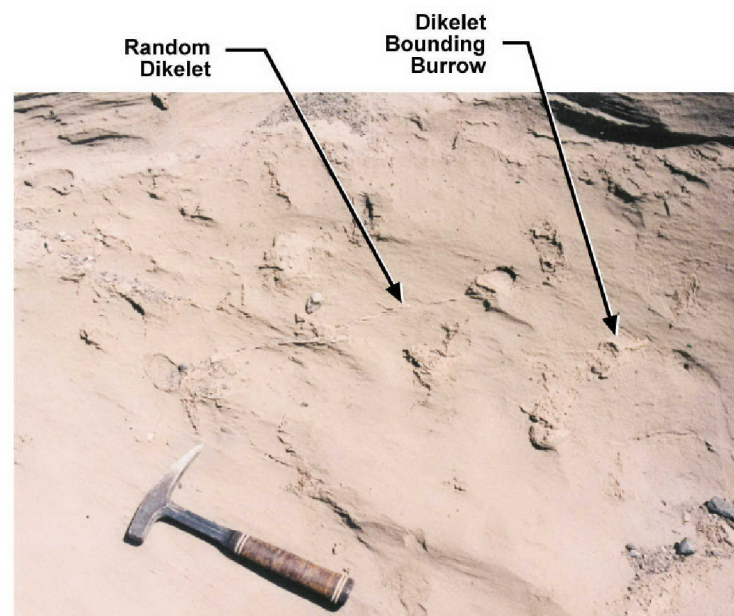
5.2 REGULAR-SHAPED, POLYGONAL-PATTERNED GROUND

Dikelets (Continued)

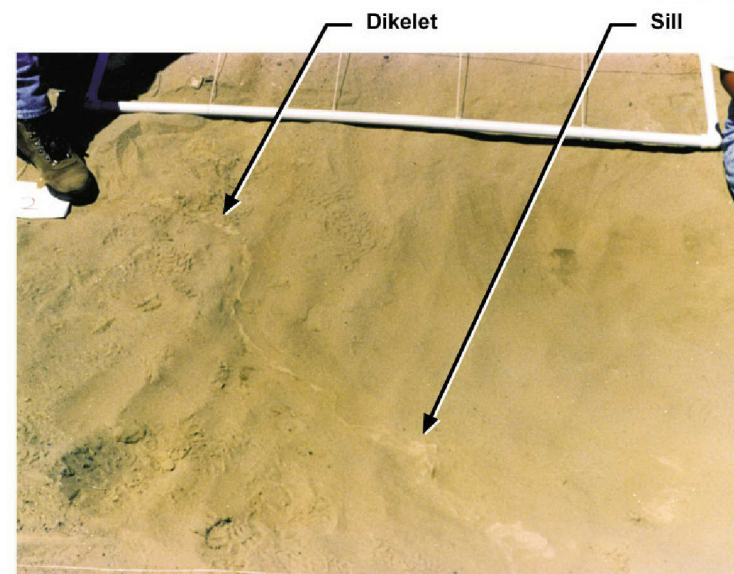
- Dikelets can occur near the center of regular-shaped polygons and are commonly isolated, randomly distributed, and only occasionally merge with other dikelets in the polygon.
- Dikelets commonly occur along pre-existing small-scale structures in host sediments (e.g., soil joints, burrows, root tubes), but not all such structures are bounded by dikelets.
- Dikelets generally decrease in width toward the center of regular-shaped polygons where they commonly branch into even smaller dikelets.
- Dikelets commonly terminate by merging with sills within sandy silt and silt lenses or by branching into small, dendritic dikelets. The small, dendritic dikelets gradually taper out or terminate in small silt nodules.

Figure 5-16: Photograph of random dikelets in a central polygonal area at a regular-shaped, polygonal-patterned ground dike network at Keene/Kennedy Road (9/28-22M). The photograph also shows dikelets occurring between several burrows and host sediments.

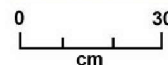
Figure 5-17: Photograph of a dikelet merging on the left side of the photograph that changes orientation into a sill in a silt lens. The dikelet terminates in the silt lens on the right side of the photograph. The photograph was taken at the regular-shaped, polygonal-patterned ground dike network at Keene/Kennedy Road (9/28-22M).



E9803054.95



E9803054.95



5.2 REGULAR-SHAPED, POLYGONAL-PATTERNED GROUND

Sills

- Sills have many of the characteristics of dikelets, except that they trend parallel to the bedding.
- Sills are narrower clastic injection dikes than are master dikes.
- Sills are typically contained within individual regular-shaped polygons and do not cross from one polygon into an adjacent polygon, except occasionally along bedding plane shears.
- Sills in the host sediments adjacent to master dikes typically merge with one or more infilling unit of the master dike.
- Sills decrease in abundance and width toward the center of regular-shaped polygons and typically pinch out less than about 30% of the distance across polygons.
- Sills commonly occur along bedding plane shears in the host sediments (see section on shears in regular-shaped, polygonal patterned ground).
- Sills commonly terminate by branching into small, dendritic sills that gradually taper out or terminate in small silt nodules (also see section on dikelets in regular-shaped, polygonal-patterned ground).

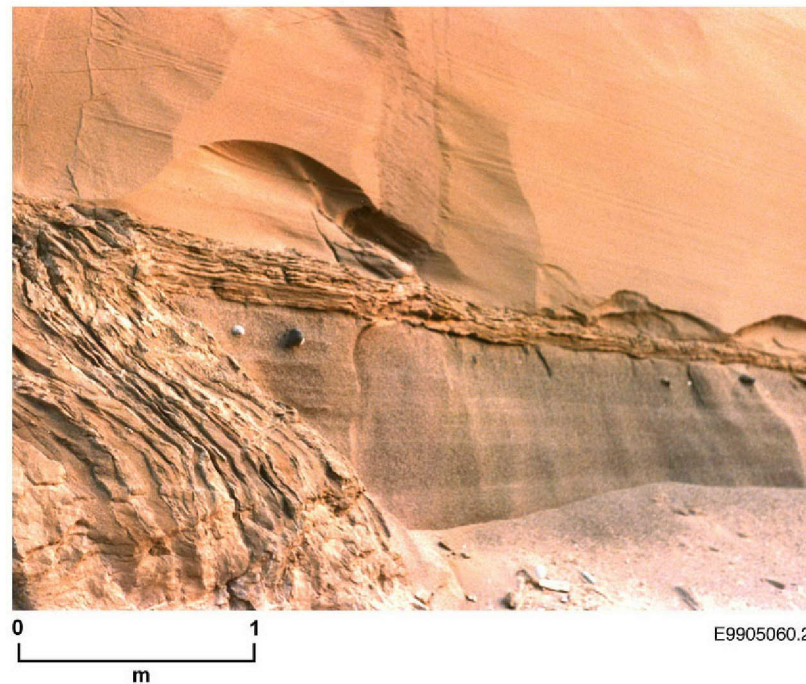


Figure 5-18: Photograph of a sill along a bedding plane between two plane-laminated sand units in the sand facies of the Hanford Formation (field mapping unit #3). The sill merges with a master dike at the left side of the photograph. The photograph was taken at the Richland Landfill regular-shaped, polygonal-patterned ground dike network (10/28-17N).

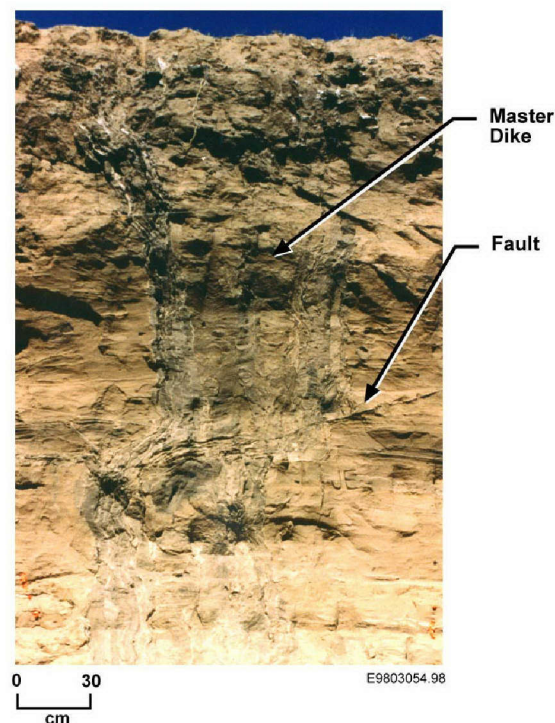
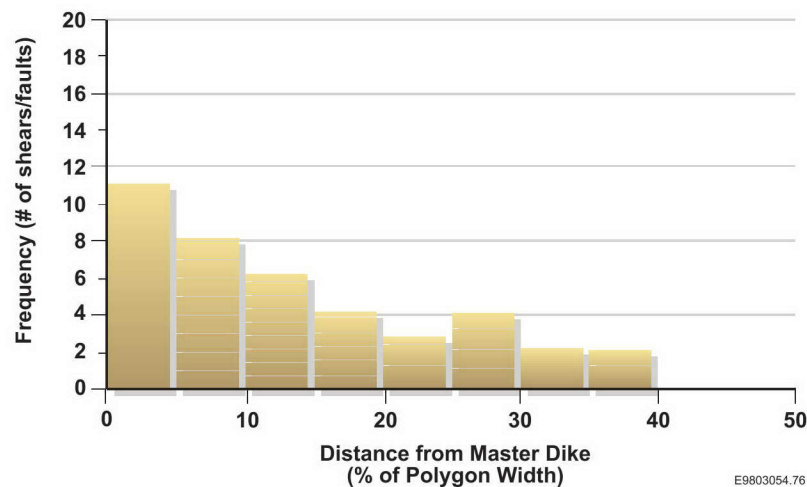
5.2 REGULAR-SHAPED, POLYGONAL-PATTERNED GROUND

Small-Scale Faults and Shears

- Faults and shears commonly occur in regular-shaped, polygonal-patterned ground dike networks. Faults and shears are more common in large regular-shaped polygons with wide master dikes than in small polygons with narrower master dikes.
- Faults and shears are typically low angle (e.g., $<30^\circ$). Bedding-plane faults also occur.
- Both normal and reverse sense of movement have been observed along faults associated with regular-shaped, polygonal-patterned ground.
- The offset along faults is generally less than 10 cm and rarely more than 30 cm; offset decreases down dip. The maximum observed offset is about 2 m.
- Near master dikes, faults and shears can dip either into or away from the center of a regular-shaped polygon. Away from the master dikes, faults and shears generally dip toward the center of the polygon.
- The number of faults and shears decreases toward the center of regular-shaped polygons.
- Faults and shears commonly occur in sand units of sand and silt facies of the Hanford Formation. Fewer faults and shears generally occur in silt lenses within the sand facies.

Figure 5-19: Frequency of small-scale faults and shears as a function of distance across a regular-shaped polygon from the master dike at Keene/Kennedy Road (9/28-22M). The frequency is based on the number of shears/faults measured vertically at intervals across the polygon.

Figure 5-20: Photograph of small-scale faults and shears in a master dike and sand facies (field mapping unit #2) sequence at Keene/Kennedy Road (9/28-22M).



5.2 REGULAR-SHAPED, POLYGONAL-PATTERNED GROUND

Small-Scale Faults and Shears (Continued)

- Small-scale faults and shears may occur as single structures, parallel sets, or conjugate sets.
- Clay skins and small dikelets may occur along part or all of a fault or shear. In five regular-shaped polygons in the Walla Walla Valley, lower Yakima Valley, and Pasco Basin, about 50% of shears have clay skins along the shear surface.
- The extent of small-scale faults and shears across clastic injection dikes varies, that is:
 - Offset along a fault may change across individual infilling units.
 - A fault or shear may cross some infilling units, while not crossing others.
 - A fault or shear may or may not have similar offset across all infilling units.

Figure 5-21: Photographs of a conjugate shear set with minor faulting associated within a master dike in a regular-shaped, polygonal-patterned ground dike network. The master dike is located 1 m to the left of the top photograph. The photographs were taken at the Corehole DH-24 mud pit (12/25-3A). The hand tool is 45 cm long.



E9803054.99



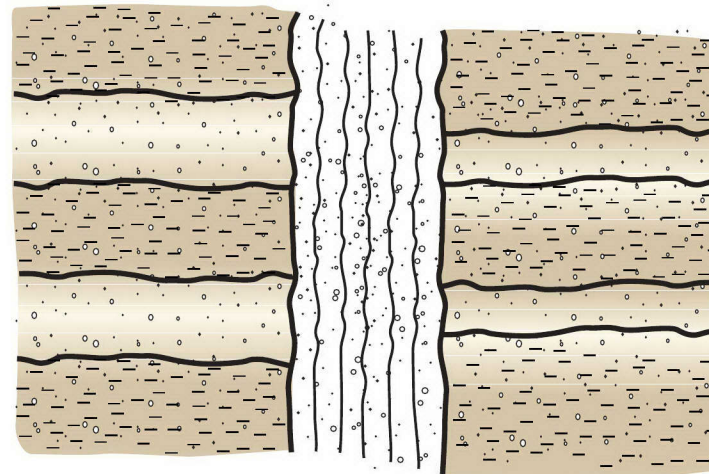
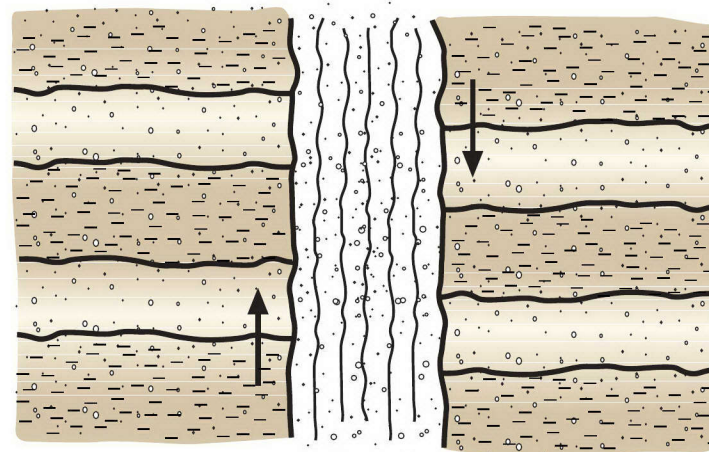
E9803054.100

5.2 REGULAR-SHAPED, POLYGONAL-PATTERNED GROUND

Small-Scale Faults and Shears (Continued)

- Vertical faulting is present in some master dikes, as shown by offset bedding features in the host rock on either side of the master dike. Vertical faulting, as associated with master dikes, is uncommon in most regular-shaped, polygon-patterned ground dike networks.
- The greatest observed vertical offset associated with vertical faults along major dikes is 40 cm.

Figure 5-22: Schematics of vertical offsets that have been observed at master dikes in regular-shaped, polygonal-patterned ground dike networks. The top schematic illustrates constant vertical offset on either side of the master dike [Kennewick Railroad Cut (8/29-6B)]. The bottom schematic illustrates variable vertical offset on either side of the master dike [Environmental Restoration Disposal Facility (12/26-7K)].



E9803054.77

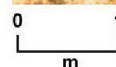
5.3 IRREGULAR-SHAPED, POLYGONAL-PATTERNED GROUND

General

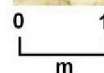
- Earlier studies identified clastic injection dikes that form irregular-shaped, polygonal-patterned ground. The dike networks have tension fractures associated with the slumping of sediments. Studies assigned to the irregular-shaped, polygonal-patterned ground dike networks include the following:
 - Baker (1973)
 - Bunker (1980)
 - Lupher (1944).
- The key components of irregular-shaped, polygonal-patterned ground dike networks used in this study are:
 - Dikes
 - Sills
 - Faults and shears
 - Slumps.

Figure 5-23: Photograph of cross-cutting clastic injection dikes in an irregular-shaped, polygonal-patterned dike network in the silt facies of the Hanford Formation from the Touchet Road area (7/33-22Q).

Figure 5-24: Photograph of deformed (slumped) sediments and clastic injection dikes in an irregular-shaped, polygonal-patterned ground dike network along Touchet Road (7/33-22Q).



E9803054.103



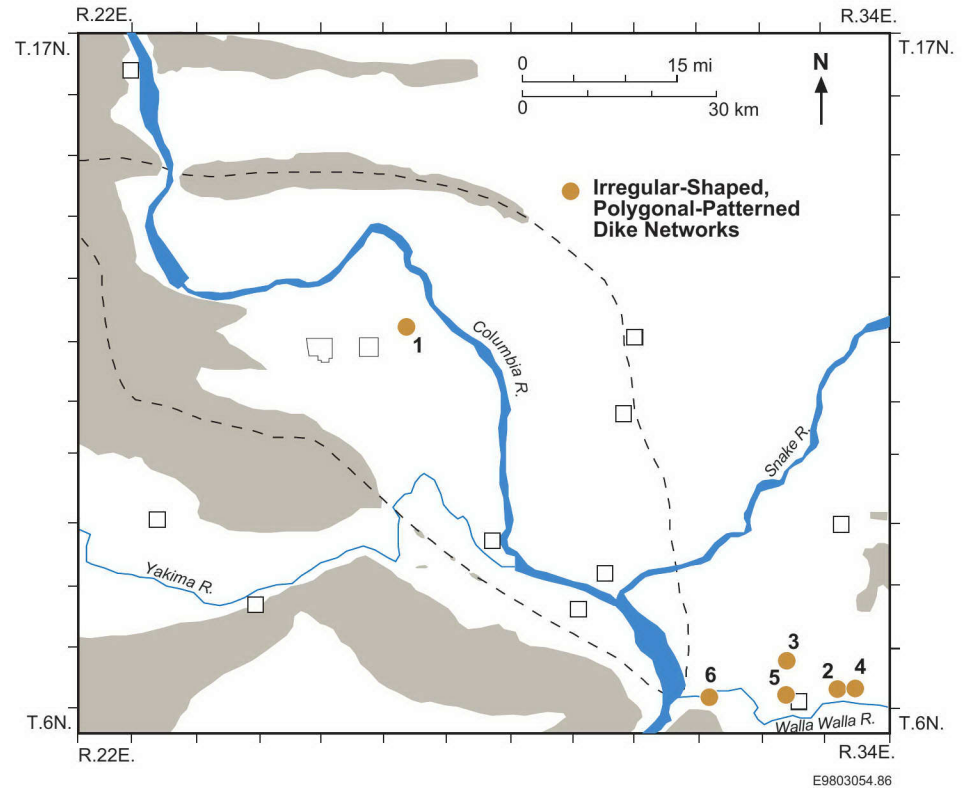
E9803054.189

5.3 IRREGULAR-SHAPED, POLYGONAL-PATTERNED GROUND

Location

- Numerous exposures of irregular-shaped, polygonal-patterned ground dike networks occur around the Pasco Basin and vicinity. Several exposures of irregular-shaped, polygonal-patterned dike networks include:
 - Gable Mountain Bar 13/27-28R
 - South Lowden 7/34-29L
 - Touchet Road 7/33-22Q
 - West Lowden 7/34-30J
 - West Touchet 7/33-29M
 - Zangar Junction 7/31-25
- Irregular-shaped, polygonal-patterned ground dike networks have been found in the Pasco Basin and vicinity through mapping of vertical or near-vertical sediment exposures.
- Reference Location: Touchet Road (7/33-22Q).

Figure 5-25: Map showing the location of several irregular-shaped, polygonal-patterned ground dike networks in the Pasco Basin and vicinity.



5.3 IRREGULAR-SHAPED, POLYGONAL-PATTERNED GROUND

Dikes

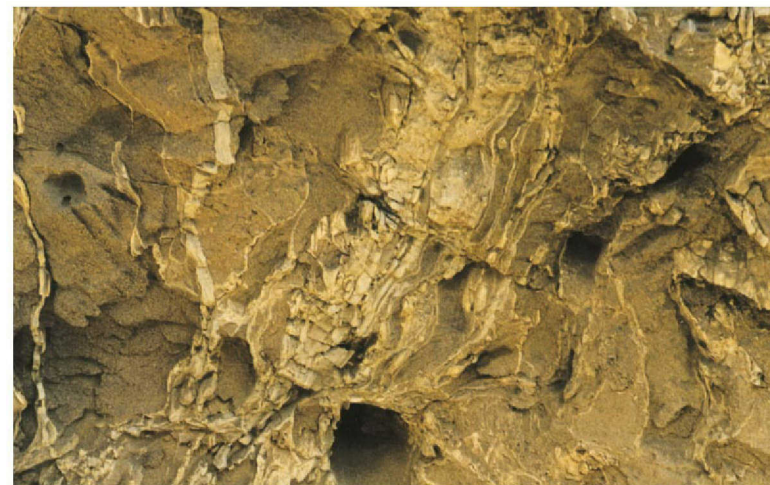
- Clastic injection dikes are a dominant component of irregular-shaped, polygonal-patterned dike networks.
- A characteristic of irregular-shaped, polygonal-patterned ground is the cross-cutting nature of dikes at the intersection of clastic injection dikes in plan view and vertical exposures. Clastic injection dikes are commonly highly deformed with very irregular shapes.
- The cross-cutting relationship results in extensive segmentation of clastic injection dikes. Individual dike segments are generally highly variable in shape (e.g., linear, curvilinear, sinuous) and lateral extent (from about 30 cm to >20 m).
- The bedding adjacent to the dikes is commonly gently folded or highly contorted.
- The width of dikes in irregular-shaped, polygonal-patterned ground dike networks range from less than 1 mm to about 1.5 m. There does not appear to be any obvious relationships among dike widths and dike patterns in exposures examined in irregular-shaped, polygonal-patterned ground dike networks.
- The strike of dikes in irregular-shaped, polygonal-patterned ground dike networks does not have a preferred orientation in the Pasco Basin and northern Walla Walla Valley.

Figure 5-26: Photograph showing cross-cutting relationships among clastic injection dikes associated with irregular-shaped, polygonal-patterned ground. The photograph was taken along Touchet Road (7/33-22Q).

Figure 5-27: Photograph of highly deformed and contorted clastic injection dikes in an irregular-shaped, polygonal-patterned ground dike network along Touchet Road (7/33-22Q).



E9803054.101



E9803054.184

5.3 IRREGULAR-SHAPED, POLYGONAL-PATTERNED GROUND

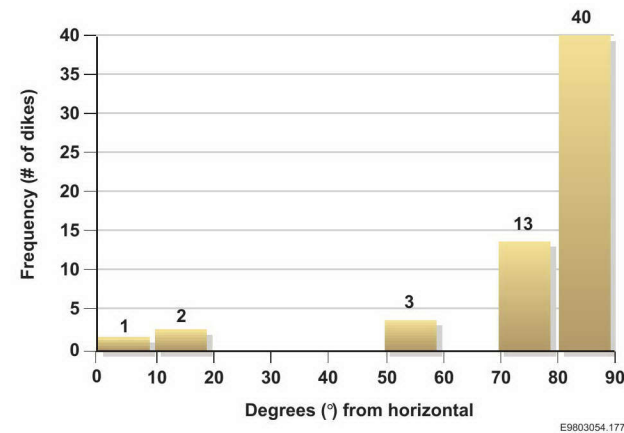
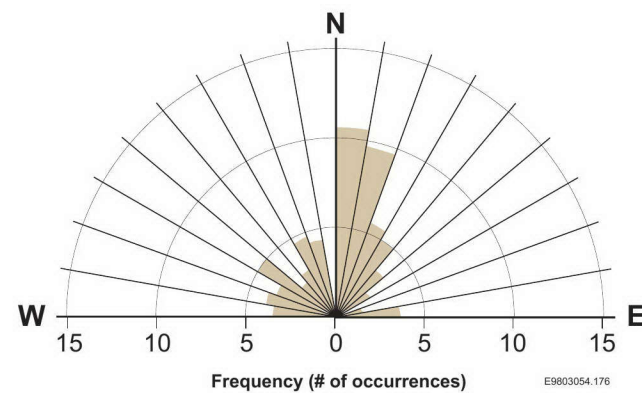
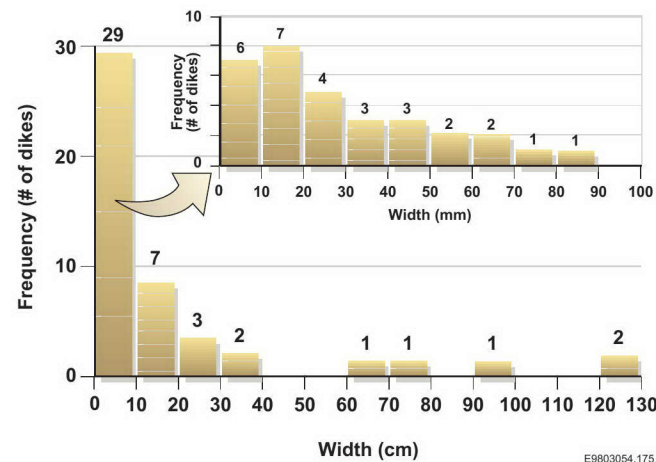
Dikes (Continued)

- The dips of dikes in irregular-shaped, polygonal-patterned ground dike networks are generally very steep. Most dips are near vertical ($>70^\circ$), although shallower dips also occur in most irregular-shaped, polygonal-patterned ground dike networks.
- The spacing between clastic injection dikes in irregular-shaped, polygonal-patterned ground dike networks are typically narrow (i.e., <1 m), although wider spacings (i.e., >1 m) are common.
- Ground surface (plan view) exposures of irregular-shaped, polygonal-patterned ground dike networks are relatively uncommon. The shape of individual polygons is highly variable in the number of sides and the length of segments. The size among polygons in the dike network is highly variable and independent of grain size. The size of polygons is typically significantly smaller than polygons in regular-shaped, polygonal-patterned ground dike networks.
- Dikes in irregular-shaped, polygonal-patterned ground also occasionally merge at intersections with other dikes. These intersections have many of the characteristics observed in intersects of regular-shaped, polygon-patterned ground dike networks.

Figure 5-28: Frequency of dike widths from a segment of an irregular-shaped, polygonal-patterned ground dike network along Touchet Road (7/33-22Q).

Figure 5-29: Strike of clastic injection dikes in a segment of an irregular-shaped, polygonal-patterned ground dike network along Touchet Road (7/33-22Q).

Figure 5-30: Dip of clastic injection dikes in a segment of an irregular-shaped, polygonal-patterned ground dike network along Touchet Road (7/33-22Q).

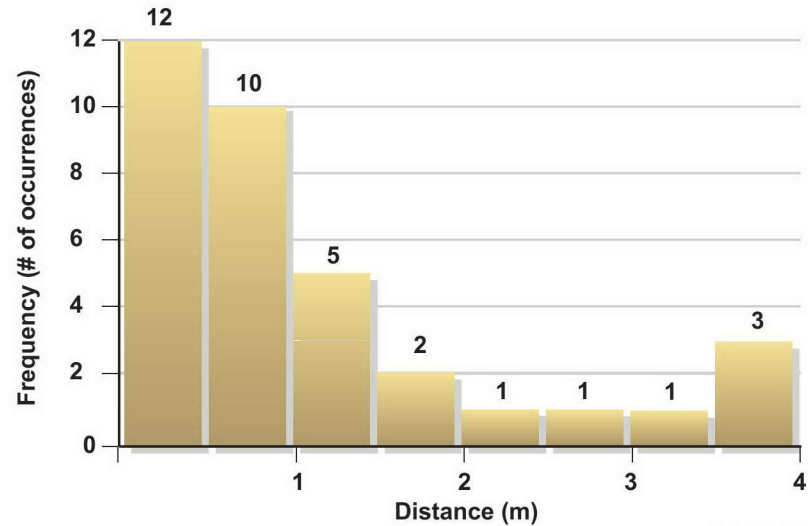


5.3 IRREGULAR-SHAPED, POLYGONAL-PATTERNED GROUND

Dikes (Continued)

- Clastic injection dikes in irregular-shaped, polygonal-patterned ground dike networks commonly terminate:
 - Against other cross-cutting dikes
 - Abut up to bedding planes
 - Cut by small-scale faults
 - Splay into smaller dikes and pinch out.

Figure 5-31: Frequency of distance between clastic injection dikes in a segment of an irregular-shaped, polygonal-patterned ground dike network along Touchet Road (7/33-22Q).



E9803054.178

Figure 5-32: Photograph of the clastic injection dikes in an irregular-shaped, polygonal-patterned ground dike network in the sand facies of the Hanford Formation. The dike network is located in a glaciofluvial flood bar on the east end of Gable Mountain (13/27-28R).



E9803054.102

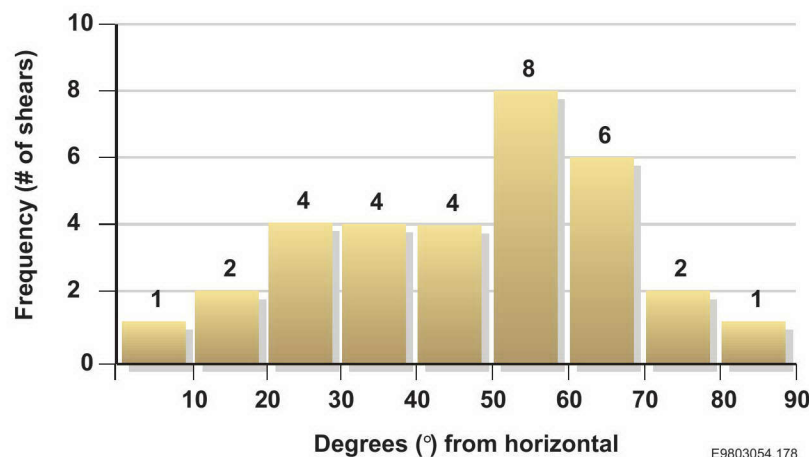
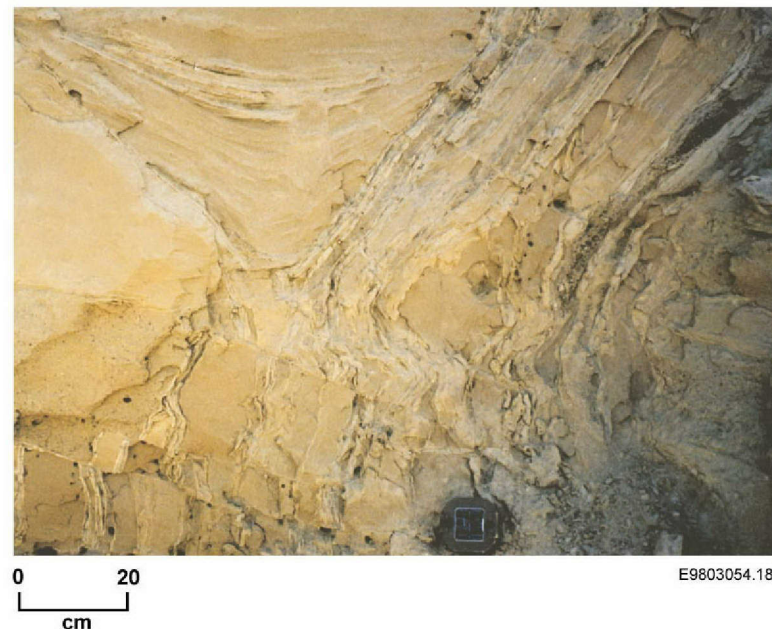
5.3 IRREGULAR-SHAPED, POLYGONAL-PATTERNED GROUND

Faults and Shears

- Faults and shears are much more abundant and larger scale in irregular-shaped, polygonal-patterned ground dike networks than faults and shears in regular-shaped, polygonal-patterned ground dike networks.
- The strikes and dips of faults and shears are commonly highly variable in irregular-shaped, polygonal-patterned ground dike networks.
- Most faults and shears typically form the primary fissures in irregular-shaped, polygonal-patterned ground dike networks that are associated with clastic injection dikes.
- The length of faults and shears may exceed 20 m. The length of clastic injection dikes not truncated by faults and shears is generally short (i.e., <2 m).
- The extent of small-scale faults and shears varies in a similar manner as small-scale faults and shears in regular-shaped, polygonal-patterned ground dike networks.

Figure 5-33: Photograph of slumped sediments with deformed beds and low-angle, small-scale faults cutting across a clastic injection dike at an irregular-shaped, polygonal-patterned ground dike network along Touchet Road (7/33-22Q).

Figure 5-34: Dip of shears in an irregular-shaped, polygonal-patterned ground dike network along Touchet Road (7/33-27).



5.4 PRE-EXISTING FISSURE

General

- In earlier geological studies, clastic injection dikes were observed in fissures that were formed long before they were used as a pathway for infilling of sediments associated with dikes. Geologic studies that describe clastic injection dikes assigned to pre-existing fissure dike networks are:
 - Black (1979)
 - CDA (1969, 1971)
 - Farooqui (1979)
 - Grolier and Bingham (1978)
 - PSPL (1981)
 - WCC (1981).
- Pre-existing structures formed fissures in joints, shears, and faults. These fissures occur in older sediments and rocks of the Pasco Basin and vicinity.
- Key components of pre-existing fissure dike networks used in this study are:
 - Dikes
 - Sills
 - Joints, shears, and faults
 - Breccias.



Figure 5-35: Photograph of clastic injection dikes in the hanging wall of the Horse Heaven Hills fault zone. The clastic injection dikes occur in a pre-existing fissure dike network that trends parallel to the Horse Heaven Hills (N50° W) and dips between 85° and 75° to the south (i.e., perpendicular to the flow top of the CRBG). The clastic injection dike is located in the east wall of Weaver Pit (6/33-17H).

5.4 PRE-EXISTING FISSURE

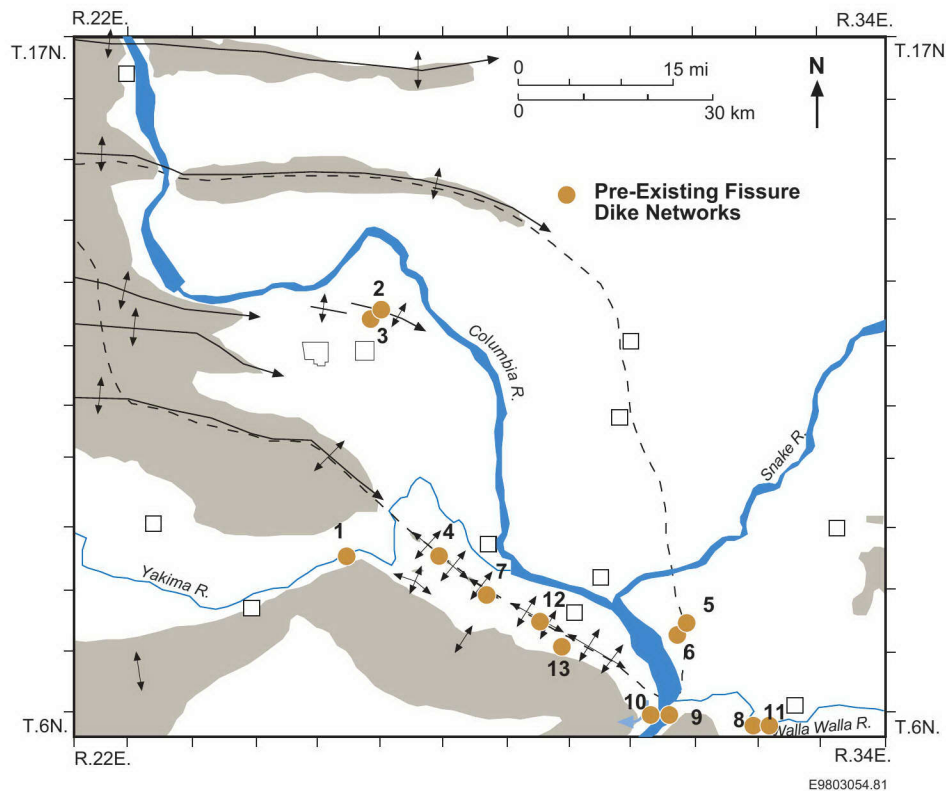
Locations

- Locations of several exposures of clastic injection dikes filling pre-existing fissures are:

1. Badlands	9/26-9N
2. Gable Mountain North	13/27-19A
3. Gable Mountain South	13/27-19N
4. Goose Gap	9/27-13E
5. Iowa Beef North	8/31-36D
6. Iowa Beef South	8/31-36D
7. Meadow Hills	9/28-35R
8. Oxbow Bend	6/32-12A
9. Wallula Gap East	7/31-27N
10. Wallula Gap West	7/31-29J
11. Weaver Pit	6/33-17H
12. Zintel Canyon Dam	8/29-16J
13. Zintel Canyon Road	8/29-24N

- Reference Locations: Iowa Beef South (8/31-36D) and Weaver Pit (6/33-17H).

Figure 5-36: Map showing locations of key exposures of pre-existing fissure dike networks in the Pasco Basin and vicinity.



5.4 PRE-EXISTING FISSURE

Dikes

- Clastic injection dikes in pre-existing fissure dike networks range from 0.03 mm to approximately 60 cm in width. The widest known dikes occur in the Horse Heaven Hills. The narrowest dikes are the thickness of clay/silt linings and are found at numerous locations. In general, dikes in joint- and fault-controlled dike networks range from 1 to 5 cm in width.
- Clastic injection dikes within pre-existing fissure dike networks display many of the components typical of clastic injection dikes (i.e., clay/silt linings, infilling sediments, slickensides, and rip-up clasts). In addition, tectonic breccias are commonly observed along with clastic injection dikes in shears, joints, and faults. Small-scale slumps and soft-sediment flow features have not been observed in pre-existing fissure dike networks, except within the clastic injection dikes.
- Clastic injection dikes commonly occur as thinly laminated, fine to very fine sand, silt, and clay. Occasionally, coarse-grained sediments are present [e.g., Meadow Hills (9/28-35R)]. The composition of the infilling units and clay/silt linings is similar to the composition of the overlying sedimentary units.
- Infilling units have been observed to range from less than 0.03 mm to about 4 cm wide. Sedimentary structures common to infilling units include:
 - Graded beds
 - Cross laminations
 - Massive bedding with no internal structure.
- Clastic injection dikes generally occur as single dikes or numerous subparallel dikes. Many dikes splay, but do not often intersect other dikes, except for dikes in faults and shears associated with doubly plunging anticlines [e.g., Zintel Canyon Dam (8/29-16J)].

Figure 5-37: Photograph of 40-cm-wide dike with multiple infilling units located in a pre-existing fracture within the CRBG. Infilling units vary from cross-laminated to massive bedded. The dike occurs in Weaver Pit (6/33-17H).



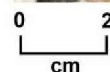
5.4 PRE-EXISTING FISSURE

Dikes (Continued)

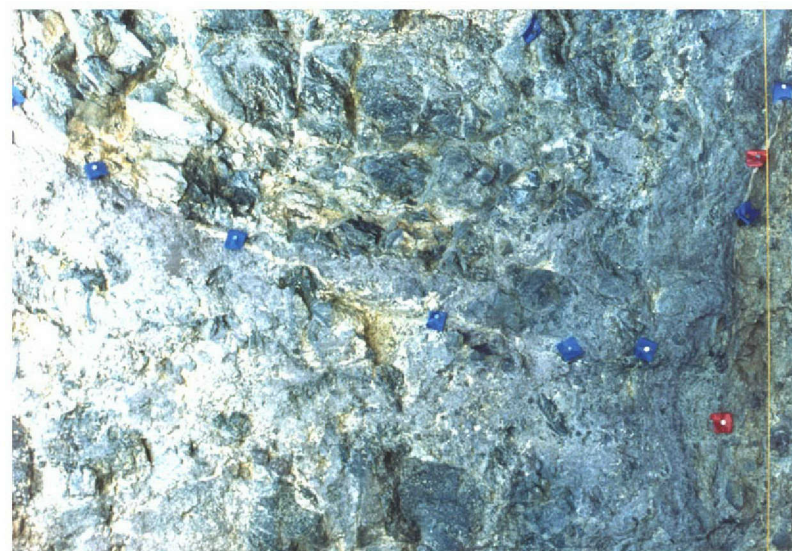
- Some clastic injection dikes join as simple mergers, with individual infilling units trending into adjoining segments. Cross-cutting relationships are rarely observed at dike intersections.
- Clastic injection dikes in pre-existing fissure dike networks occur primarily in older sediments and rocks. Examples include exposures in the Ringold Formation at Iowa Beef South (8/31-36D), CRBG at Weaver Pit (6/33-17H), and Rattlesnake Ridge interbed at the Badlands (9/26-9N).
- Clastic injection dikes that occur in pre-existing fissures associated with joints and shears of anticlinal ridges and in the hanging walls of faults generally vary from 3 m to more than 15 m in length.
- Clastic injection dikes along pre-existing fault planes have been observed to be more than 150 m in length [e.g., Gable Mountain North (13/27-19A)].
- Clastic injection dikes rarely penetrate more than 1 m into undeformed rocks of the CRBG or Ellensburg Formation.
- Pre-existing fissure dike networks do not have master dikes as do regular-shaped, polygonal-patterned ground dike networks.
- Clastic injection dikes in pre-existing fissure dike networks terminate by:
 - Tapering and pinching out
 - Truncating at the contact with intact (undeformed) basalt
 - Splaying into multiple dikelets that follow cooling joints and quickly pinch out.
- Source: CDA (1969, 1971) and this study.

Figure 5-38: Photograph of a clastic injection dike within a fault of a flow-top breccia in the Elephant Mountain flow [Gable Mountain North (13/27-19A)]. The dike is exposed in a trench wall.

Figure 5-39: Photograph of clastic injection dike that splays and pinches out downward into enhanced, pre-existing fissures in the Elephant Mountain flow of the CRBG. The exposure is located in the hanging wall of the central Gable Mountain cross fault [Gable Mountain North (13/27-19A)].



E9803054.192



E9803054.106

5.4 PRE-EXISTING FISSURE

Sills

- Clastic injection dikes that form sills are uncommon in pre-existing fissure dike networks.
- Sills have been observed in the following:
 - Along bedding planes in the Rattlesnake Ridge interbed of the Ellensburg Formation in the hanging wall of a fault on the south-central Gable Mountain [Gable Mountain South (13/27-19N)] and in fault zones [e.g., fault in Goose Gap (9/27-13E) along the Rattlesnake Hills].
 - Along parting surfaces in the uppermost flow of the CRBG in several areas [e.g., in the Frenchman Springs member at Weaver Pit (6/33-17H)].
- Sills are typically narrow, ranging from about 1 to 5 cm wide. In several localities, sills are composed only of thin clay skins.
- Sills are generally less than 3 m in length.
- Sills typically consist of thinly laminated, fine to very fine sand, silt, and clay. The sands infilling the sills are quartzose-feldspathic sands from the surrounding host sediments.
- Sills in pre-existing fissure dike networks often do not intersect with other injection sills and dikes.

Figure 5-40: Photograph of a clastic injection dike penetrating vertically through the silt facies of the Hanford Formation. The clastic injection dike abruptly changes orientation at the top of the undeformed CRBG to trend as a sill parallel to the CRBG surfaces. The locality of the dike is at the south wall of the Weaver Pit (6/33-17H).

Figure 5-41: Photograph of clastic injection dikes that occur as a set of sills trending parallel to the surface of the CRBG at the south end of Weaver Pit (6/33-17H).



0 30
cm

E9803054.107



0 20
cm

E9803054.108

5.4 PRE-EXISTING FISSURE

Joints and Shears

- Sources: CDA (1969, 1971), Black (1979), Farooqui (1979), PSPL (1981), WCC (1981), and this study.

Figure 5-42: Extended cooling joints in a Frenchman Springs flow of the CRBG filled with a clastic injection dike. The dike occurs in the hanging wall of the Horse Heaven Hills fault zone in Weaver Pit (6/33-17H).

Figure 5-43: Photograph of clastic injection dikes in tectonic joints within the member of Wooded Island, Ringold Formation. The dikes are located at Iowa Beef South (8/31-36D).

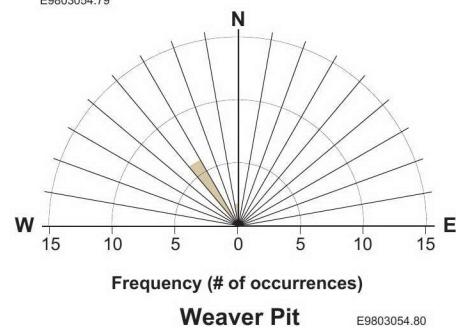
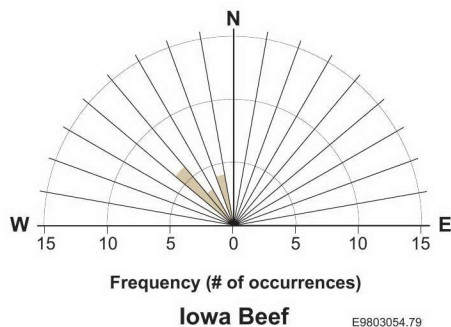
Figure 5-44: Orientation of joints and shears that are filled with clastic injection dikes at Iowa Beef South (8/31-36D) and Weaver Pit (6/33-17H).



0 3
cm
E9803054.109



0 2
m
E9803054.110



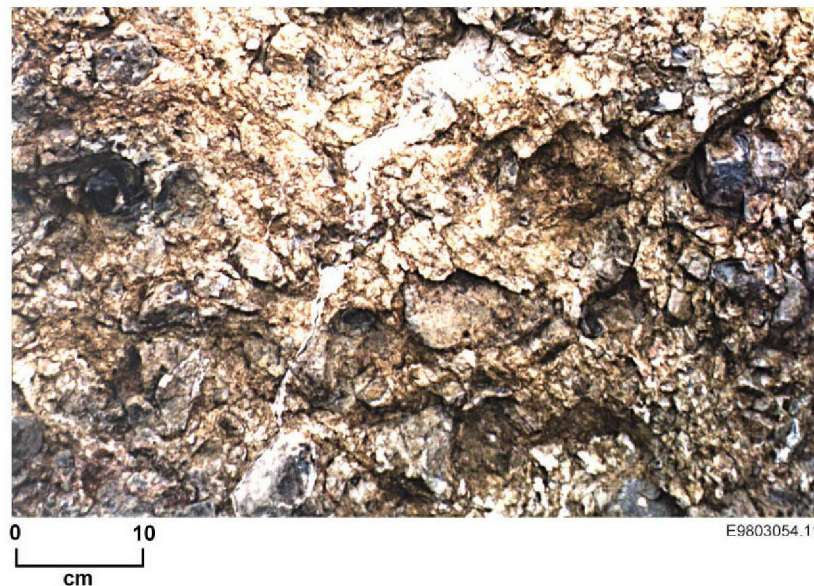
5.4 PRE-EXISTING FISSURE

Breccias

- Breccias are commonly associated with joints, shears, and faults in pre-existing fissure dike networks in the CRBG.
- The extent of brecciation is a function of the extent of movement in the basalt flows. The steeper dip basalt flows generally are more brecciated.
- Clastic injection dikes commonly occur along:
 - Zones of weakness within breccia zones
 - Shear surfaces within highly brecciated basalt
 - Joints and shears that have extended openings.
- Breccias consist of angular fragments of basalt of varying sizes that formed as a result of cataclasis. The breccia clasts (and the wall rock adjacent to the breccias) typically have thick, stained alteration rinds (often >5 mm thick) and are coated with dark smectite clays as a result of long periods of ongoing weathering and movement. This is contrast to the infilling material of clastic injection dikes that commonly lack alteration rinds and contain a relatively small amount of clay. Also, breccias are commonly cemented with calcium carbonate, silica, and occasionally iron oxide. The alteration rinds and clays are evidence that the breccias formed in fissures long before the injection of sediment at clastic injection dikes.
- Source: Reidel et al. (1994), Reidel and Fecht (1994a, 1994b), and this study.

Figure 5-45: Photograph of a clastic injection dike along a zone of weakness in a brecciated zone within the Pomona Member, CRBG at Meadow Hills (9/28-35R).

Figure 5-46: Photograph of a clastic injection dike along a shear within a breccia zone. The dike and breccia occur within the Pomona Member, CRBG at Meadow Hills (9/28-35R).



5.5 RANDOM OCCURRENCE

General

- Clastic injection dikes have been observed that are not, or do not appear to be, associated with other dike networks (i.e., regular-shaped, polygonal-patterned ground; irregular-shaped, polygonal-patterned ground; or pre-existing fissure). Many previous studies have described individual clastic injection dikes, but generally do not include discussions of the relationships among clastic injection dikes.
- Key components of random occurrence dike networks in this study are:
 - Dikes
 - Sills
 - Small-scale slumps
 - Small-scale shears and faults
 - Soft-sediment deformation.
- The description of the key components of random occurrence dike networks is similar to the description of dikes in Section 3.0, “Physical Description of Clastic Injection Dikes.” Therefore, the discussion of principal components in this section is restricted to the location and key characteristics of random occurrence dike networks.



E9803054.193

Figure 5-47: Photograph of a random occurrence dike that penetrates an upper silt facies and a lower gravel facies of the Hanford Formation. The exposure is about 10 m high. The site is located in the Transtate Gravel Pit (9/30-6F) in lower Esquatzel Coulee north of Pasco.

5.5 RANDOM OCCURRENCE

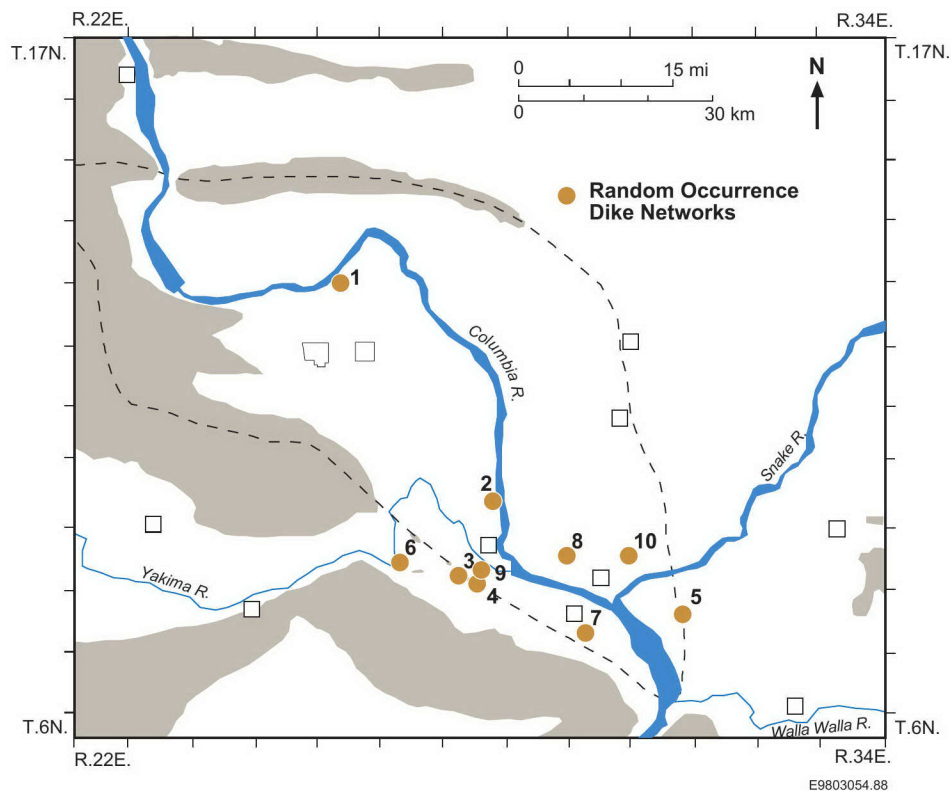
Location

- Random occurrences of clastic injection dikes have been observed in several areas of the Pasco Basin and vicinity. Exposures of random occurrences of clastic injection dikes are located at:

- | | | |
|-----|---|-----------|
| 1. | 100-N Area | 14/26-28C |
| 2. | 300 Area | 10/28-11G |
| 3. | Bombing Range Road North | 9/28-8E |
| 4. | Bombing Range Road South | 9/28-8M |
| 5. | Eureka Flats | 9/31-36K |
| 6. | Kiona Gravel Pit | 9/27-20K |
| 7. | Oak Street | 8/30-18R |
| 8. | Transtate Gravel Pit | 9/30-6F |
| 9. | Yakima Bluffs
(coarse-grained dikes) | 9/28-16G |
| 10. | Smith Canyon North
(gravel facies) | 9/30-13N |

- Reference Location: Not designated.

Figure 5-48: Map showing the location of several random occurrence dike networks.



5.5 RANDOM OCCURRENCE

Dikes

- The random occurrence dikes have been observed in the following sedimentary units:
 - Gravel facies of the Hanford Formation (field mapping units #1(?), #2, and #3) [e.g., Bombing Range Road North (9/28-8E), Oak Street (8/30-18R), and 300 Area (10/28-11G), respectively].
 - Silt facies of the Hanford Formation (field mapping unit #1) [e.g., Yakima Bluffs (9/28-16G)].
 - Deposits of the Yakima River associated with the Plio-Pleistocene deposits [e.g., same as Yakima Bluffs (9/28-16G) above].
 - Member of Wooded Island of the Ringold Formation [e.g., Eureka Flats (9/31-36K)].
 - Member of Savage Island of the Ringold Formation [e.g., same as Eureka Flats (9/31-36K) above].
- Most clastic injection dikes with random occurrences form tabular vertical bodies and sinuous near-vertical bodies.
- The random occurrence dikes observed in the Pasco Basin and vicinity may belong to another type of dike network or transition from another type of dike network, but the field evidence is inadequate to assign dikes to other networks.

Figure 5-49: Photograph of a random occurrence clastic injection dike (coarse-grained dike) that penetrates the upper gravel facies (field mapping unit #2) of the Hanford Formation, middle silt facies (field mapping unit #3) of the Hanford Formation, and the overbank sediments of the deposits of the Yakima River, Plio-Pleistocene deposits [Yakima Bluffs (9/28-16G)].



5.5 RANDOM OCCURRENCE

Dikes (Continued)

- Random dikes typically occur as isolated clastic injection dikes that do not intersect. Relationships of intersecting dikes are not known primarily due to the limited exposure or heterogeneous textural characteristics in the host sedimentary sequence.
- Random dikes occur as:
 - Single clastic injection dikes:

100-N Area	14/26-28C
300 Area	10/28-11G
Eureka Flats	9/31-36K
 - Multiple clastic injection dikes:

Bombing Range North	9/28-8E
Oak Street	8/30-18R
Yakima Bluffs (coarse-grained dikes)	9/28-16G
 - Dike complexes:

Smith Canyon North (gravel facies)	9/30-13N
------------------------------------	----------
- Single clastic injection dikes that occur as random dikes are generally fine-grained, narrow (<20 cm in width), and highly variable in vertical extent (1 m to >10 m).
- Multiple clastic injection dikes that occur in random dike networks commonly are coarse-grained (sands and pebbles) and taper downward with a vertical extent of less than about 2 m.



Figure 5-50: Photograph of a single, random-occurrence clastic injection dike in bedded sand and silt sequence within a gravel facies of the Hanford Formation (field mapping unit #3). The photograph was taken at an excavation in the central Hanford Site.

5.5 RANDOM OCCURRENCE

Dikes (Continued)

- Dike complexes occur as isolated series of dikes that commonly form in the fine-grained silt and/or sand facies of the Hanford Formation and are surrounded by coarse-grained sediments. The coarse-grained sediments can be of the same age as the fine-grained host or in part older. The coarse-grained sediments are commonly from the gravel facies of the Hanford Formation.

Figure 5-51: Photograph of an isolated clastic injection dike complex associated with a random dike in Smith Coulee North (9/30-13N).



E9803054.191

5.6 DISTRIBUTION OF NETWORKS

General

- In stratigraphic units containing clastic injection dikes, the type of dike network that occurs in the Pasco Basin and vicinity is primarily dependent on the:
 - Elevation
 - Textural and bedding characteristics
 - Topography (primarily slope)
 - Structural fabric.
- All dike networks occur below the 380-m elevation that is the maximum level of glaciofluvial flooding of the Pasco Basin area. Clastic injection dikes may not be present below a lower elevation of about 104 m. This approximate elevation may represent the water table at the time clastic injection dikes were formed (at least for clastic dikes that occur in field mapping unit #3).
- Clastic injection dikes that occur in sedimentary sequences with highly variable textures and bedding features are likely to have complex dike formations. The highly variable sedimentary sequences generally are local features and are not laterally or vertically continuous over significant areas of the Pasco Basin and vicinity.
- The best developed dike networks form in sedimentary sequences with similar textures and have laterally continuous and uniform thick beds (as discussed in Sections 5.2 through 5.5).
- Regular-shaped, polygonal-patterned ground dike networks occur in:
 - Sand, silt, and occasionally gravel (i.e., gravelly sand) facies of the Hanford Formation or stratigraphic sections with sedimentary sequences that are (or were) capped by sand and silts of the Hanford Formation.
 - Sedimentary sequences with laterally continuous beds that are relatively uniform in thickness and are free of pre-existing structural features or fabric.
 - Low-relief, relatively flat topography in the basins and valley floors, atop broad expansive glaciofluvial flood bars, and in flood-scoured coulees.
- Irregular-shaped, polygonal-patterned ground dike networks occur in:
 - Sand, silt, and occasionally gravel (i.e., sandy gravel) facies of the Hanford Formation or stratigraphic sections with sedimentary sequences that are capped by sand and silts of the Hanford Formation (similar to regular-shaped, polygonal-ground dike networks).
 - Sedimentary sequences that are free of extensive pre-existing linear structural features.
 - Gentle to moderate dipping ($>5^\circ$) slopes along the margins of the basin, valleys, flood bars, and small topographic rises.
 - Terrain that, with the cross-cutting nature of clastic injection dikes, indicates these networks form as a result of ground failure through slumping.
- Pre-existing fissure dike networks occur in:
 - Deformed basalts of CRBG and sediments of the Ellensburg and Ringold Formations.
 - Tectonic shears that are part of the regional structural fabric and generally trend $N50^\circ-55^\circ W$. The trend is parallel to the Rattlesnake Wallula Alignment (RAW) (see Section 1.5).
 - Conjugate shear and joint sets in anticlinal and synclinal folds associated with the Yakima Fold Belt.
 - Along fault zones in the Yakima Fold Belt that occur in near-surface areas and are associated with extensional stresses
 - Structural features that formed long before intrusion by clastic injection dikes.
- Random dikes occur in:
 - The sand and gravel facies (i.e., sands to sandy gravel textures) of the Hanford Formation and locally in the members of Wooded Island and Savage Island of the Ringold Formation
 - Sediments without pre-existing structural fabric
 - Low-relief, relatively flat topography on the basin floor and valley floors
 - Dike complexes that have limited extent.

5.6 DISTRIBUTION OF NETWORKS

Aerial Distribution

- The aerial distribution of dike networks in the Pasco Basin and vicinity is based primarily on field examinations of clastic injection dikes and associated dike networks and analysis of aerial photographs. The photographs used in this study were aerial photographs of the Pasco Basin. In areas with limited exposures or covered by Quaternary alluvium and eolian deposits, dike networks are defined by:

- Textural and bedding characteristics of stratigraphic units
- Topographic relief
- Structural features and fabric.

Most of the geologic information on stratigraphic units and structures is based on Reidel and Fecht (1994a, 1994b).

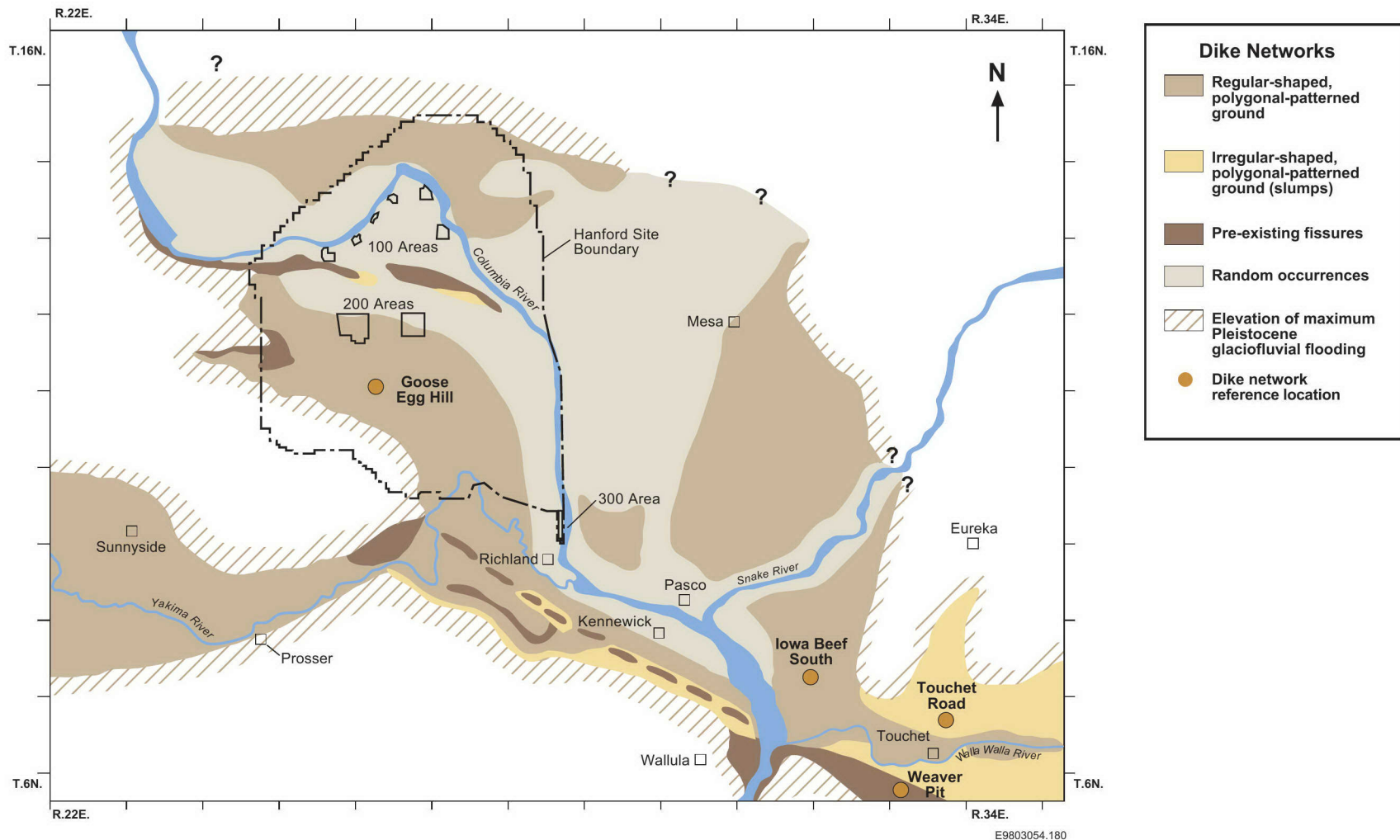
- The aerial distribution of dike networks is shown in Figure 5-52. The map is divided into areas based on the most abundant type of dike network. Several areas include multiple types of dike networks that occur as a result of local changes in geologic, topographic, or structural conditions. These networks are present over only small portions of the area.
- The interrelationship between adjacent dike networks in aerial view is not clearly displayed in most surface exposures in the Pasco Basin and vicinity. Some relationships are interpreted based on examination of more than 50 dike networks.

- For polygonal-patterned ground dike networks, the networks appear to be end members of a continuum from regular- to irregular-shaped polygons. This relationship is common in the Walla Walla River Valley where the slopes of the valley margins intersect the relatively flat, central valley area, and in the central valley where local topographic highs merge with flatter plain areas.
- There appears to be a transition from irregular-shaped, polygonal-patterned ground dike networks and pre-existing fissure dike networks. This occurs on basin margins where clastic injection dikes in sand and silt facies of the Hanford Formation lie adjacent to areas with established structural fabric in CRBG and pre-Hanford Formation sediments.
- There also appears to be a transition between regular-shaped, polygonal-patterned ground and random occurrence dike networks. The polygonal-patterned dike networks gradually lose definition, and clastic injection dikes narrow and pinch out. The change occurs as the texture of the host sediments coarsens from silts and sands to sandy gravels in the Hanford Formation. Clastic injection dikes that are present in the gravel facies (i.e., sandy gravels of the Hanford Formation) generally occur as isolated dikes in random occurrence dike networks. This relationship occurs in excavations of the east portion of the 200 East Area, Hanford Site.

5.6 DISTRIBUTION OF NETWORKS

Aerial Distribution (Continued)

Figure 5-52: Map of the Pasco Basin and vicinity showing the location of the types of dike networks that are identified in this atlas. The types of dike networks depicted on the map represent networks present in the near-surface geologic units.



5.6 DISTRIBUTION OF NETWORKS

Vertical Distribution

- Vertically, the type of dike network varies depending on the textural and bedding characteristics of the sediments or the extent of deformation of the CRBG and sediments of the Ellensburg and Ringold Formations.
- Examples of several vertical relationships of dike networks are discussed below.
 - Transtate Gravel Pit (9/30-6F): Clastic injection dikes of a regular-shaped, patterned-ground dike network in a silt facies of the Hanford Formation transition at the lower contact into a random occurrence dike network in a gravel facies of the Hanford Formation. The clastic injection dikes in both networks are the same age.
 - Weaver Pit/Oxbow Bend area (6/33-17H and 6/32-12A): Clastic injection dikes in an irregular-shaped, polygonal-patterned ground dike network within the silt facies of the Hanford Formation merge downward into a pre-existing fissure dike network in the CRBG. The transition of dike networks occurs at the contact of the two geologic units. The clastic injection dikes in both networks are the same age.
 - Keene/Kennedy Road (9/28-22M): Clastic injection dikes in a younger, small regular-shaped, polygonal-patterned ground dike network overlie another series of clastic injection dikes associated with an older, larger regular-shaped, polygonal-patterned ground dike network. The dike networks are two different ages.
 - Burlington Northern 605 (8/28-16Q): Clastic injection dikes in a small regular-shaped, polygonal-patterned ground dike network overlie a series of clastic injection dikes that occur in another small regular-shaped, polygonal-patterned ground dike network of similar size. The dike networks occur in the silt facies of the Hanford Formation. Both host sediments and associated dikes are associated with two different ages. The younger dike network penetrates sediments of both ages.
 - Yakima Bluffs (9/28-16G): Clastic injection dikes in a random occurrence dike network occurring primarily in the gravel facies of the Hanford Formation overlie a regular-shaped, polygonal-patterned ground dike network that occurs in the silt facies of the Hanford Formation and deposits of the Yakima River. Clastic injection dikes associated with the Yakima Bluffs exposure are two different ages. The younger dikes also penetrate into the older sediments.
 - Amon Wasteway South (8/28-1A): Clastic injection dikes in a regular-shaped, patterned-ground dike network in the silt facies of the Hanford Formation intrude downward and form clastic injection dikes in a random occurrence dike network within the gravel facies of the Hanford Formation. The dike networks are the same age. The sediments were deposited during two different glacial events.
 - Fast Flux Test Facility (11/28-18P) and Fuels and Materials Examination Facility (11/28-18N): Clastic injection dikes in two regular-shaped, polygonal-patterned ground occur that are about the same polygonal size and texture (sand facies of the Hanford Formation). The two networks and host sediments were formed during two different glacial events. The younger dike network penetrates into the older sediments.

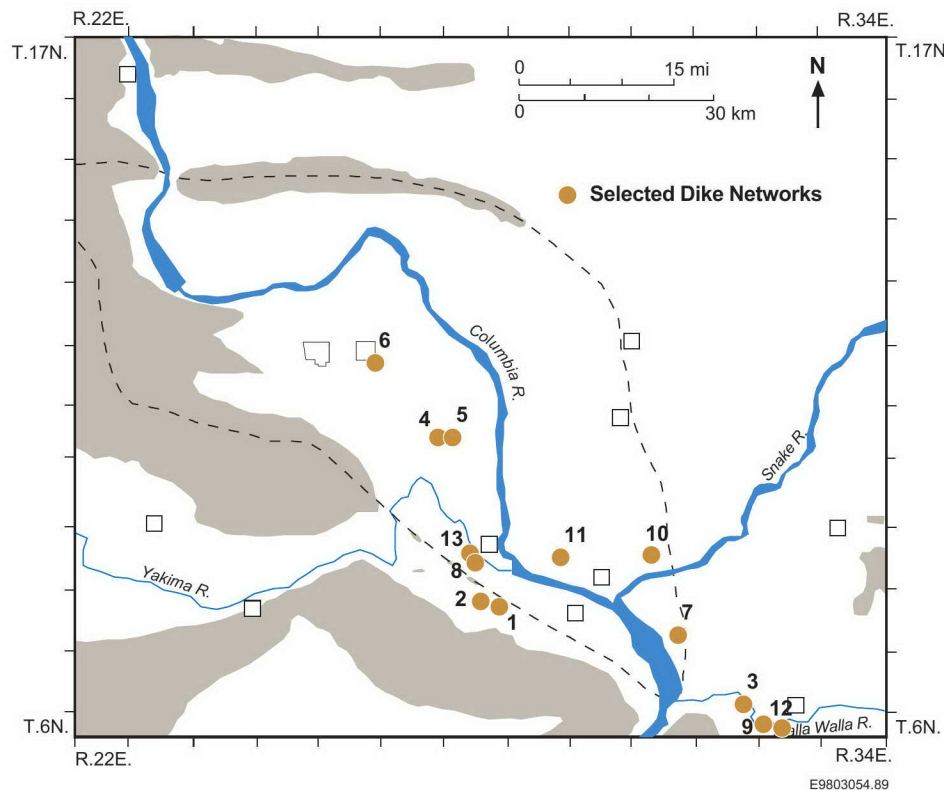
5.6 DISTRIBUTION OF NETWORKS

Vertical Distribution (Continued)

- Selected locations where clastic injection dikes and associated dike networks vary vertically include:

1.	Amon Wasteway South	8/28-1A
2.	Burlington Northern 605	8/28-16Q
3.	Cummings Bridge	7/32-35Q
4.	Fast Flux Test Facility	11/28-18P
5.	Fuels and Materials Examination Facility	11/28-18N
6.	Grout	12/26-1N
7.	Iowa Beef South	8/31-36D
8.	Keene/Kennedy Road	9/28-22M
9.	Oxbow Bend	6/32-12A
10.	Smith Coulee South	9/30-24D
11.	Transtate Gravel Pit	9/30-6F
12.	Weaver Pit	6/33-17H
13.	Yakima Bluffs	9/28-16G

Figure 5-53: Map showing the location of clastic injection dikes that occur vertically in more than one type of dike network.



6.0 AGE AND TIMING OF EMPLACEMENT

6.1 APPROACH

- This section provides a discussion of the age and timing of emplacement of clastic injection dikes.
- Dike networks were selected as a basis for evaluating the age and timing of clastic injection dikes. Individual clastic injection dikes can prove unreliable for use in age determinations. Individual dikes can terminate by truncation, splaying, pinching out, and gradually losing definition in a manner that is not representative of the age of the dikes. Whereas, dike networks are formed by an interrelated system of multiple dikes that can provide a better basis for determining age relationships among clastic injection dikes, host sediments, and dated horizons.
- The age and timing of clastic injection dikes are evaluated in this section for each type of dike network that is identified in Chapter 5.0:
 - Regular-shaped, polygonal-patterned ground
 - Irregular-shaped, polygonal-patterned ground
 - Pre-existing fissure
 - Random occurrence.
- The age and timing of clastic injection dikes in the following sections will be based on the:
 - Age of youngest host sediments/rocks penetrated by the dikes
 - Relationship between the host sediment/rock and the fissures of the clastic injection dikes
 - Relationship between the fissure and the injected sediments.
- The ages of key geologic units and horizons associated with the host sediments/rocks that are important in determining the age and timing of emplacement of clastic injection dikes are provided in Table 6-1.

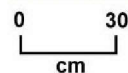
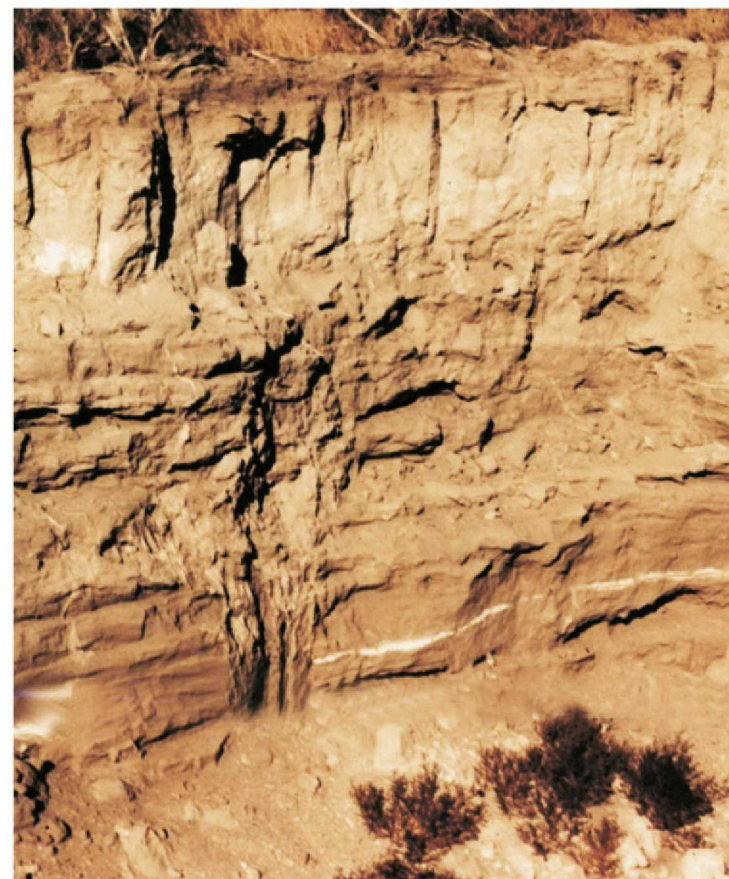
Table 6-1: Age of key stratigraphic units and tephra horizons in the Pasco Basin and vicinity important to determining the age and timing of emplacement of clastic injection dike networks.

Unit	Age	Dating Method	Source
Surficial deposits	0 - 12 Ka	Stratigraphic position	Reidel & Fecht 1994a, 1994b
<i>Mazama Tephra</i>	6.85 Ka	C ¹⁴ dating	Kittleman 1973
<i>Glacier Peak Tephra (B&G)</i>	11.25 Ka	C ¹⁴ dating	Mehring et al. 1984
Hanford Formation			
– Qh ₄	6.85 - 12.7 Ka	C ¹⁴ and varves	Waitt 1994
– Qh ₃	12.7 Ka - 15.7 Ka		
<i>Mount St. Helens Set S Tephra</i>	13 Ka	C ¹⁴ dating	Mullineaux et al. 1978
– Qh ₂	~200 Ka	Th-U dating	Baker et al. 1991
– Qh ₁	>770 Ka	Magnetic polarity	Baker et al. 1991
Plio-Pleistocene Deposits	>770 Ka - 3.4 Ma	Stratigraphic position	
Ringold Formation			
– Member of Savage Island	3.4 - 4.5 Ma	Vertebrate fossils Magnetic polarity	Packer & Johnson 1979
– Member of Taylor Flat	4.5 - 6 Ma	Vertebrate fossils	Gustafson 1978
– Member of Wooded Island	6 Ma - 8.5 Ma	Stratigraphic position	
CRBG and Ellensburg Formation			
– Ice Harbor Member	8.5 Ma	K/Ar dating	McKee et al. 1977
– Elephant Mountain Member	10.5 Ma	K/Ar dating	McKee et al. 1977
– Rattlesnake Ridge Interbed	10.5 Ma - 12 Ma	Stratigraphic position	
– Pomona Member	12 Ma	K/Ar dating	McKee et al. 1977
– Frenchman Springs Member	15.3 Ma	K/Ar dating	Tolan et al. 1989
Qh ₁ = field mapping unit #1 Qh ₂ = field mapping unit #2 Qh ₃ = field mapping unit #3 Qh ₄ = field mapping unit #4			

6.2 AGE OF DIKE NETWORKS

Regular-Shaped, Polygonal-Patterned Ground

- Clastic injection dikes of regular-shaped, polygonal-patterned ground dike networks intrude into sediments/rocks that range from Pleistocene to Pliocene age.
- The youngest geologic units penetrated by master dikes and dikelets are within the Hanford Formation. Master dikes and many dikelets intrude into silt and sand sequences in each of field mapping units #1, #2, and #3.
- Observations of regular-shaped, polygonal-patterned ground dike networks indicate that clastic injection dikes formed:
 - Near the end of glaciofluvial deposition of field mapping unit #3 based on master dikes and dikelets that penetrate to the top of the sequence along the basin margins. The clastic injection dikes do not penetrate the last several flood units in many of the major channelways along the Columbia, Walla Walla, and Yakima Rivers [e.g., at Wallula Junction (7/31-27J)].
 - Near the end of the glaciofluvial deposition of field mapping unit #2 based on master dikes and dikelets that penetrate to the top of the field mapping unit and truncate against an erosional surface. Clastic injection dikes do not penetrate younger glaciofluvial, fluvial, and eolian sediments [e.g., Keene/Kennedy Road (9/28-22M)].
 - Near the end of the glaciofluvial deposition of field mapping unit #1 based on characteristics similar to dikes associated with field mapping unit #2 [e.g., Yakima Bluffs - fine-grained sediments (9/28-16G)].



E9803054.117

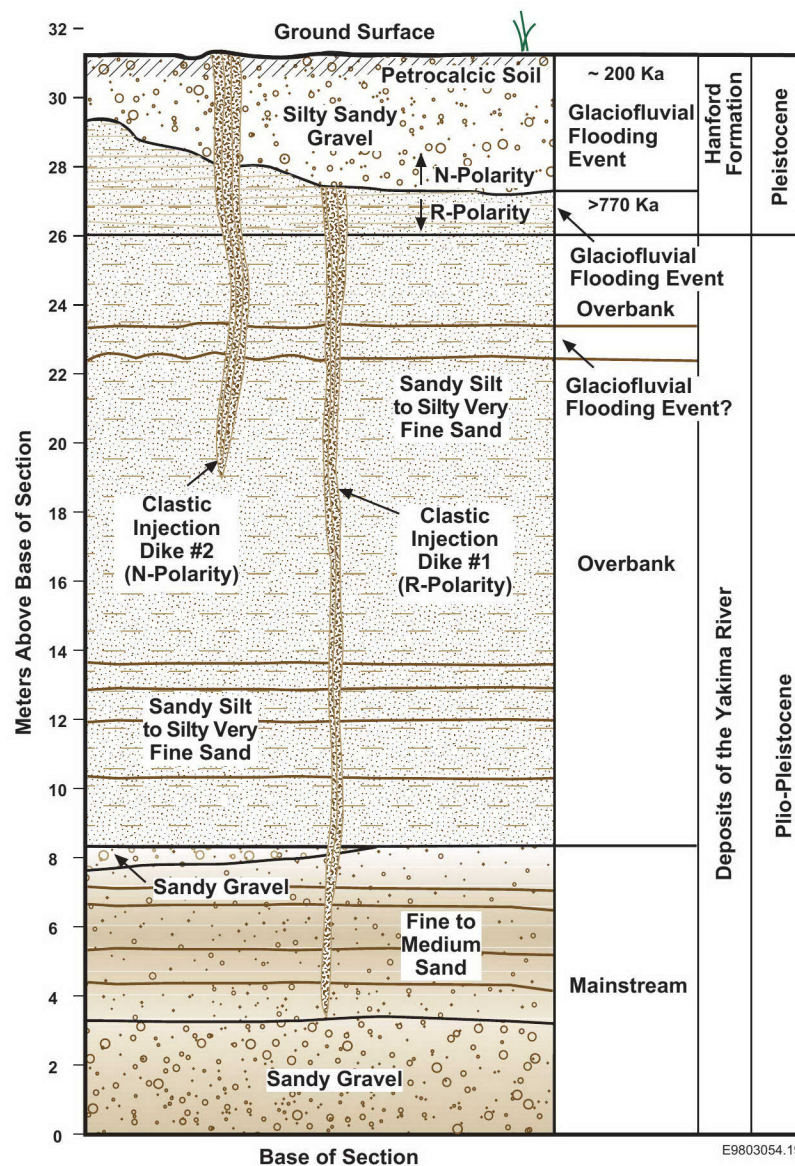
Figure 6-1: Photograph of a clastic injection dike in a regular-shaped, polygonal-patterned ground dike network. The clastic injection dike intrudes into the sand facies of the Hanford Formation (field mapping unit #3). Mount St. Helens Set S tephra (white couplet) occurs between plane-laminated sand beds. The dike does not penetrate the Holocene eolian sand unit that contains the Mazama tephra. The site is located in a railroad cut in Kennewick (8/29-6B).

6.2 AGE OF DIKE NETWORKS

Regular-Shaped, Polygonal-Patterned Ground (Continued)

- The development of fissures, widening of the fissure openings, and injection of sediments associated with this type of dike network are interpreted to have resulted in the emplacement of clastic injection dikes as a continuous process over a relatively short time span based on the:
 - Absence of significant time breaks (e.g., development of staining and alteration rinds) in the formation of clastic injection dikes from the initial fissure formation, through the deposition of all of the infilling units, and through associated structural deformation, indicating a relatively continuous process.
 - Presence of multiple sedimentary infilling units that are interpreted as separate and discrete dispositional events, indicating that a period of time is required for dikes to be emplaced rather than forming instantaneously.
 - Limited time span between the last glaciofluvial deposit penetrated by the dike and the next fluvial, eolian, or glaciofluvial (for field mapping unit #3) deposit, suggesting that the time span of dike formation was short.
- Based on the age information in Table 6-1 and relationships presented above, the age and timing of emplacement of clastic injection dikes in regular-shaped, polygonal-patterned ground dike networks is at or near the end of the deposition of three field mapping units of the Hanford Formation or:
 - 12.7 to 15.7 Ka Field mapping unit #3
 - Approximately 200 Ka Field mapping unit #2
 - Greater than 770 Ka Field mapping unit #1

Figure 6-2: Stratigraphic column of Yakima Bluffs (9/28-16G) with at least two older glaciofluvial events and two ages of clastic injection dike emplacement. The younger clastic injection dike was formed during the ~200 Ka glaciofluvial flooding event. The dike and youngest host sediment have normal magnetic polarity. The older clastic injection dike and second youngest host sediment in the exposure have reverse magnetic polarity (Van Alstine 1982).

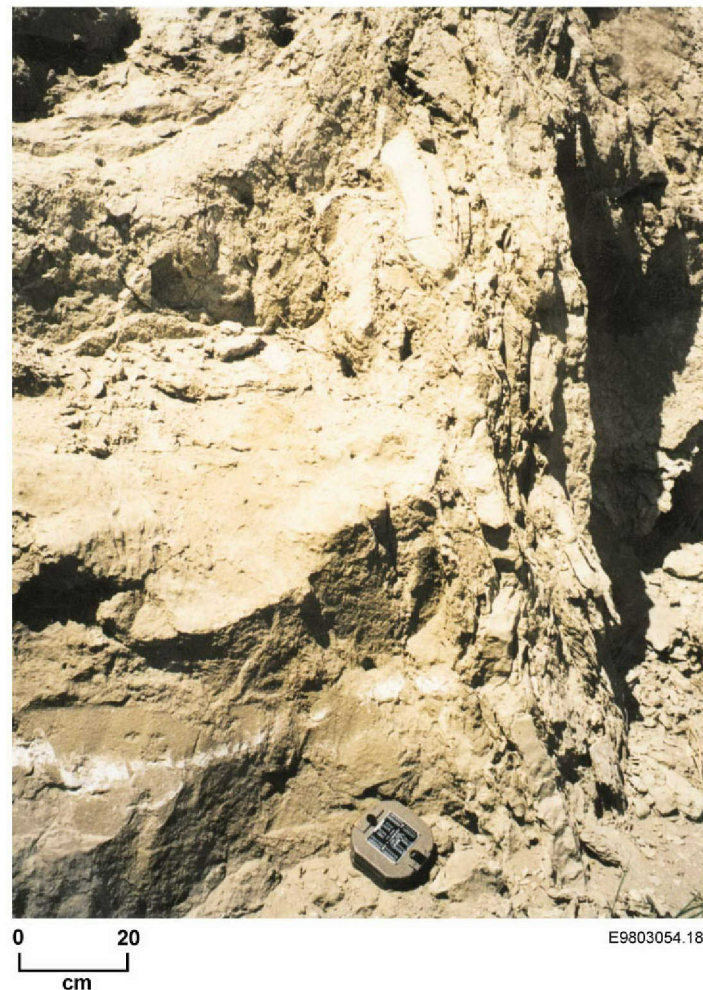


6.2 AGE OF DIKE NETWORKS

Irregular-Shaped, Polygonal-Patterned Ground

- Clastic injection dikes of irregular-shaped, polygonal-patterned ground dike networks intrude into sediments/rocks that range from Pleistocene to Miocene age.
- The youngest dikes in this type of dike network are found within the Hanford Formation. Clastic injection dikes intrude into silt and sand sequences in field mapping units #1(?), #2(?), and #3, indicating two or three periods of emplacement of clastic injection dikes in the Pasco Basin and vicinity.
- Clastic injection dikes appear to have formed:
 - At the end of glaciofluvial deposition of field mapping unit #3 based on the presence of dikes that penetrate to the top of the sequence in portions of the basin where irregular-shaped, polygonal-patterned ground dike networks occur [e.g., Gable Mountain Bar (13/27-28R) and Touchet Road (7/33-22Q)].
 - In older field mapping units [#1(?) and #2(?)] that are locally exposed near the base of glaciofluvial deposits in the Walla Walla and Touchet River Valleys. The dikes terminate at the top of an iron oxidized to calcic paleosols that cap the older geologic units. Clastic dikes associated with field mapping units #1(?) and #2(?) penetrate through an older field mapping units and intrude up to the paleosol capping each of field mapping units #1(?) and #2.

Figure 6-3: Photograph of a clastic injection dike in an irregular-shaped, polygonal-patterned ground dike network. The clastic injection dike intruded into the silt facies of the Hanford Formation (field mapping unit #3). Mount St. Helens Set S tephra (white couplet) occurs between silt beds. The dike does not penetrate the Holocene loess unit capping the exposure. The site is located on Touchet Road (7/33-22Q).



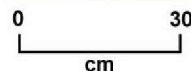
6.2 AGE OF DIKE NETWORKS

Irregular-Shaped, Polygonal-Patterned Ground (Continued)

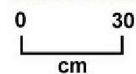
- The development of fissures, widening of the fissure openings, and injection of sediments into this type of dike network were emplaced as a continuous process over a relatively short time span similar to regular-shaped, polygonal-patterned ground dike networks.
- Based on the age information in Table 6-1 and provided above, the age and timing of emplacement of clastic injection dikes in irregular-shaped, polygonal-patterned ground dike networks is at or near the youngest age of the two or three field mapping units of the Hanford Formation or:
 - 12.7 to 15.7 Ka Field mapping unit #3
 - Possibly ~200 Ka Older field mapping units
and >770 Ka [possibly #1(?) and #2(?)]

Figure 6-4: Photograph of a clastic injection dike in silt facies of the Hanford Formation (field mapping unit #3) unconformably overlying an older clastic injection dike in an earlier silt facies of the Hanford Formation. The exposure occurs in an irregular-shaped, polygonal-patterned ground dike network along Touchet Road (7/33-22Q).

Figure 6-5: Photograph of an older clastic injection dike penetrating the silt facies of the Hanford Formation (equivalent to field mapping unit #1 or #2) and lower loess horizon in Touchet Valley (7/33-2F). The clastic injection dike is associated with an irregular-shaped, polygonal-patterned ground dike network.



E9803054.185



E9803054.186

6.2 AGE OF DIKE NETWORKS

Pre-Existing Fissures

- Clastic injection dikes associated with pre-existing fissures penetrate from rocks as old as Miocene up to the silt and sand facies of the Hanford Formation. The youngest sediments penetrated by dikes are associated with field mapping units #1(?) and #3.
- Dikes associated with pre-existing fissure dike networks penetrate to the top of the silt and sand sequences in each of field mapping units #1(?) [e.g., Iowa Beef North and South (8/31-36D)] and #3 [e.g., Gable Mountain North (13/27-19A)]. The clastic injection dikes were emplaced at the end or shortly after the end of the deposition of glaciofluvial sediments. Clastic injection dikes in pre-existing fissure dike networks associated with the older field mapping units are consolidated and locally cemented. The degree of cementation is consistent with dikes found elsewhere in field mapping unit #1. However, the dikes could be older than field mapping unit #1.
- The initial formation of fissures in pre-existing dike networks occurred long before injection of clastic sediments. The widening of the fissures and injection of sediments into the fissures occurred as a relatively continuous process. The time of emplacement was relatively short. Movement along fissures after injection of sediments was minimal with occasional shears present within clastic injection dikes and the formation of slickensides on the surfaces of clay/silt linings in dike walls along infilling units at several locations [e.g., Gable Mountain South (13/27-19N)].



E9803054.116

- This places the age of the emplacement of clastic injection dikes at:
 - 12.7 to 15.7 Ka Field mapping unit #3
 - >770 Ka Field mapping unit #1(?) or possibly older.

Figure 6-6: Photograph of clastic injection dikes of two different ages in the member of Wooded Island, Ringold Formation. The fine-grained infilling units are associated with field mapping unit #1(?). The coarser basalt-rich infilling unit is unconsolidated and is from a clastic injection dike of late Wisconsin age (field mapping unit #3) [Iowa Beef South (8/31-36D)].

6.2 AGE OF DIKE NETWORKS

Random Occurrence

- Clastic injection dikes associated with random occurrence dike networks penetrate into the sand and gravel facies of the Hanford Formation, which belong to field mapping units #1(?), #2, and #3 [e.g., Kiona Gravel Pit (9/27-20K)].
- These dikes intrude into various discrete portions of these field mapping units and typically do not intersect other clastic injection dikes except for dikes located in field mapping unit #3. Clastic injection dikes locally intrude older geologic units (i.e., loesses, Plio-Pleistocene units, and the Ringold Formation) [e.g., Eureka Flats (9/31-36K)].
- The infrequent occurrence and the lateral extent of random occurrence dike networks make this type of dike network of little value in determining the age and timing of emplacement of clastic injection dikes in the Pasco Basin and vicinity. Other dike networks are better suited for determining the age and timing of emplacement of clastic injection dikes.
- Several of the clastic injection dikes of the random occurrence dike network penetrate to the top of field mapping units #2 and #3, indicating that the youngest ages in this dike network are:
 - 12.7 to 15.7 Ka Field mapping unit #3
 - ~200 Ka Field mapping unit #2
 - >770 Ka(?) Field mapping unit #1(?).

Clastic dikes associated with field mapping unit #1(?) may not penetrate to the top of the unit, indicating that the dikes may have been emplaced near the end of glaciofluvial deposition, but before the final glaciofluvial sediments of the flooding cycle were deposited.

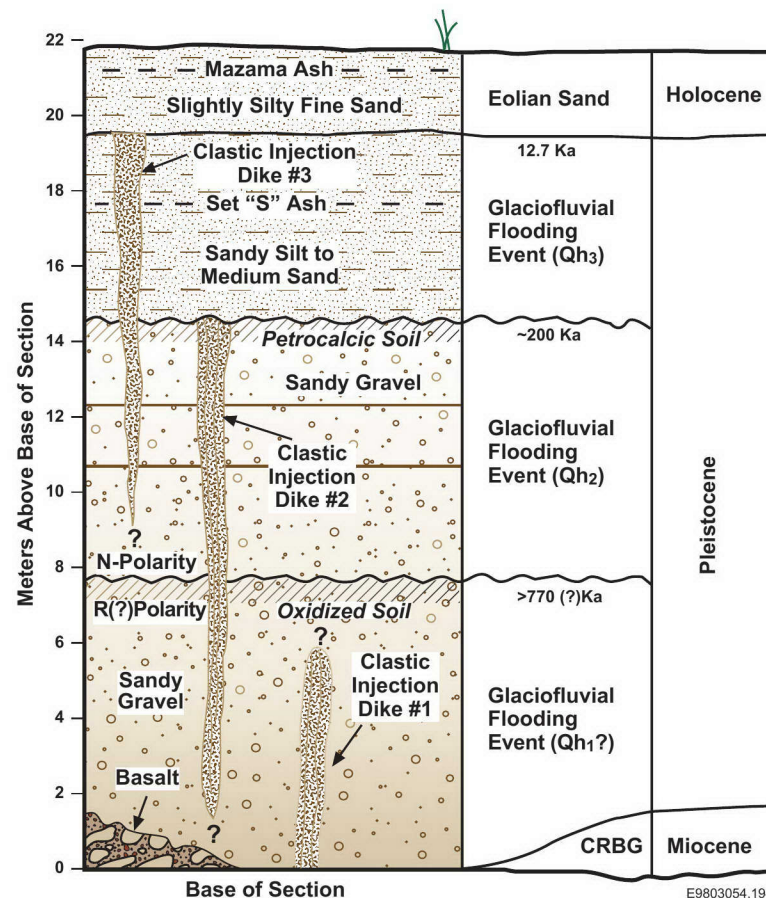


Figure 6-7: Stratigraphic column of Kiona Quarry (9/27-20K) with three glaciofluvial flooding events and two and perhaps three ages of clastic injection dike emplacement.

6.3 SUMMARY OF AGE AND TIMING OF EMPLACEMENT

- Clastic injection dikes are interpreted to have formed as a relatively continuous process of short duration in each of the ages of dikes and within each type of dike network:
 - Fissure systems formed immediately before sediment infilling, except for dikes associated with pre-existing fissure systems
 - Fissures gradually widening with apertures ranging from less than 1 mm to several tens of centimeters.
 - Injection of sediments that form individual infilling units. Each infilling unit is representative of separate flowpaths along the fissure opening. Textural variations within and across infilling units are due to changes in injection pressures and source sediments.

- Many clastic injection dikes penetrate to or very near the top of the three field mapping units of the Hanford Formation (field mapping units #1, #2, and #3) in most dike networks. Clastic injection dikes in random occurrence dike networks may not intrude to the top of field mapping units.

- Clastic injection dikes were emplaced during at least three different periods of injection based on evaluation of dike networks. The youngest ages of each emplacement are:
 - Between 12.5 and 15.7 Ka associated with field mapping unit #3
 - Approximately 200 Ka associated with field mapping unit #2
 - Greater than 770 Ka associated with field mapping unit #1.

Dike Network	Age of Emplacement		
	12.5 - 15.7 Ka	~200 Ka	>770 Ka
Regular-shaped, polygonal-patterned ground	●	●	●
Irregular-shaped, polygonal-patterned ground	●	●?	●?
Pre-existing fissures	●	(1)	●?
Random occurrence	●	●	●?

(1) Not observed in field exposures that were examined.

Table 6-2: Age of clastic injection dikes based on dike networks from the Pasco Basin and vicinity.

7.0 ORIGIN OF CLASTIC INJECTION DIKES

7.1 APPROACH

- This section presents a discussion of the origin of clastic injection dikes that are found in the Pasco Basin and vicinity. Emphasis is placed on the origin of the fissures and the infilling of sediments.
- The approach used in this section is to:
 - Screen the physical characteristics, location, and timing of emplacement of clastic injection dikes against theories on the origin of fissure development and sediment infilling to constrain the origin of dikes
 - Identify the geologic processes that are considered significant in fissure formation and sediment deposition associated with clastic injection dikes
 - Discuss the origin of clastic injection dikes and dike networks.
- Earlier workers proposed several theories for the origin of fissures and the emplacement of sediments associated with clastic injection dikes in eastern Washington, including the Pasco Basin and vicinity.
- The mechanisms that have been proposed for creation of fissures associated with clastic injection dikes include:
 - Desiccation
 - Deep frost/permafrost
 - Melting of buried ice
 - Loading/unloading due to Pleistocene flooding
 - Tectonism
 - Seismicity
 - Mass movement (slumping).
- The processes that have been proposed for the infilling of sediments into clastic injection dikes include:
 - Wind transportation and deposition/resorting
 - Water transportation and deposition/resorting/injection.
- For some dikes, the creation and infilling of fissures clearly have unrelated origins (e.g., many pre-existing fissure dikes). For other dikes, the creation and infilling of fissures are intimately related (e.g., polygonal-patterned dike networks).
- Advances in basin stratigraphy, particularly in the Pleistocene glaciofluvial deposits and study of the characteristics of dikes and dike networks, make it an appropriate time to reevaluate theories on the origin of clastic injection dikes.
- Sources: Table 1-2, references in Section 1.5, and this study.

7.2 CONSTRAINTS ON ORIGIN

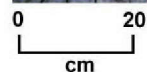
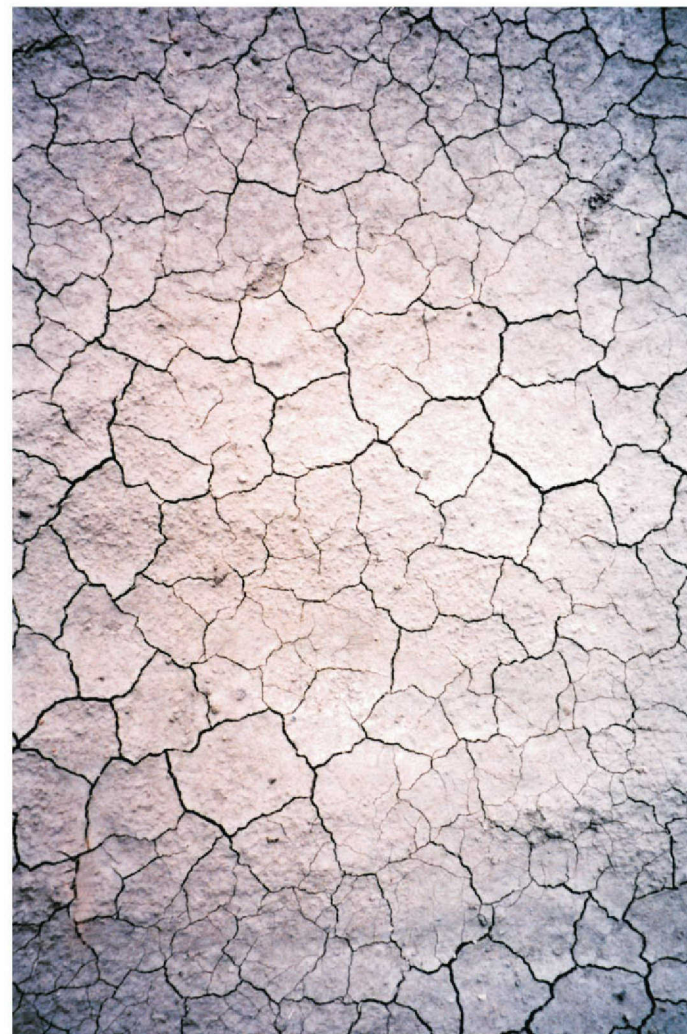
- This section presents a summary of information to evaluate theories on the origin of clastic injection dikes. The information is focused on observations and interpretations presented in this atlas that can constrain the origin of clastic injection dikes.
- Clastic injection dikes occur as true dikes (i.e., discordant to bedding), but also occur as sills (i.e., discordant to bedding). Clastic injection dikes are typically filled upward, downward, or horizontally with a single unit or multiple units of clay-to-gravel size sediments.
- The sediments of infilling units are variably sorted with a high percentage of units ranging from moderately well to well sorted. Dike walls and infilling units are commonly bounded by clay skins (Section 3.2).
- Clastic injection dikes are highly variable in width, depth, and lateral extent. Dikes range from less than 30 cm to more than 45 m in vertical extent, from less than 1 mm to greater than 2 m in width, and from 30 cm to greater than 100 m in lateral extent (Section 3.3).
- Clastic injection dikes have infilling units with bedding features that indicate water as the primary transport agent. The bedding features include laminations, cross laminations, graded and massive bedding, and complex bedding forms (e.g., chevron or V-shaped patterns) (Section 3.2).
- Clastic injection dikes are commonly associated with several types of small-scale geologic structures, including faults and shears, slumps, slickensides, and rip-up clasts (Section 3.2).
- Clastic injection dikes occur in several types of dike networks. These dike networks include regular-shaped, polygonal-patterned ground; irregular-shaped, polygonal-patterned ground; pre-existing fissures; and random occurrences. Clastic injection dikes crosscut and truncate, and/or merge at intersections based on the type of dike network (Section 5.0).
- Clastic injection dikes are known to occur in:
 - Several sediment and rock types, including loess, fine-to-coarse-grained alluvium, paleosols, and basalt, but do not pass across thick beds of open-framework gravel (Table 4-1).
 - Sediments and rocks from Miocene to Pleistocene in age, but not in sediments of Holocene age (Table 6-1).
 - Fissures that range from Miocene(?) to Pleistocene in age.
- Clastic injection dikes are associated with multiple ages of emplacement, including at least three different periods during the Pleistocene epoch. The last period occurred near the end of deposition of glaciofluvial sediments. Clastic injection dikes occur in glaciofluvial sediments and have not been observed in post-cataclysmic flood deposits, which suggests that dikes formed during or soon after glaciofluvial flooding (Section 6.3).
- Individual clastic injection dikes formed as a relatively continuous process that developed over a short time period. The process included formation of fissures, gradual widening of fissure apertures, and infilling of clastic sediments. Some fissures (e.g., fissures associated with pre-existing dike networks) initially formed long before injection of clastic sediments (Section 6.3).
- Clastic injection dikes are observed in several geomorphic areas including river and basin terrain, lower slope terrain, coulees, and lower regions of the ridge terrain. Clastic injection dikes have not been observed in the high-relief areas of the ridge terrain (Section 4.2).
- Clastic injection dikes occur between 104 m to greater than 275 m in elevation. The lower elevation is about the same as the present-day water table. The upper limit is below the maximum elevation of Pleistocene flooding (Section 4.1).

7.3 EVALUATION OF GEOLOGIC PROCESSES IN FISSURE DEVELOPMENT

Desiccation Cracks

- Desiccation cracks have been proposed as a mechanism for the formation of fissures associated with clastic injection dikes by Grolier and Bingham (1978).
- Desiccation cracks associated with polygonal patterns commonly form at the ground surface as sediments shrink and tension fractures are created. Desiccation cracks propagate until intersecting other cracks to form polygonal patterns. This process occurs in fine-grained sediments that are initially moist or wetted by precipitation, flooding, or fluctuating water table and followed by drying through evapotranspiration.
- Desiccation cracks found in sediments in the Pasco Basin and vicinity that are associated with polygons typically range from less than 1 mm to about 10 cm in width. The cracks are downward-tapering features that pinch out within a few centimeters. The lateral extent of cracks range from less than 10 cm to occasionally greater than 1 m. The width of desiccation cracks is similar to small clastic injection dikes, but significantly smaller than large dikes. The depth of penetration of desiccation cracks is significantly less (centimeters versus tens of meters) than the depth of most clastic injection dikes.
- The sediments that fill desiccation cracks are commonly massive, but may be vertically stratified. The sediments in desiccation cracks do not display banding of alternating clay skins and infilling units found in clastic injection dikes.
- Polygons associated with desiccation cracks are often three- to four-sided, but are primarily five- and six-sided. Polygons associated with clastic injection dikes in the central Pasco Basin are most commonly four-sided.
- Polygons associated with desiccation cracks vary from about 5 cm to 1.5 m across, which are significantly smaller than polygonal patterns in clastic injection dike networks. Polygons found in dike networks typically are tens of meters across.

Figure 7-1: Photograph of mud cracks on Pleistocene silt-dominated flood sediments in upper Cold Creek Valley (13/25-30M). Mud cracks of similar size and shape commonly occur on fine-grained Pleistocene flood sediments along the northern, western, and southern margins of the Pasco Basin.



E9803054.162

7.3 EVALUATION OF GEOLOGIC PROCESSES IN FISSURE DEVELOPMENT

Desiccation Cracks (Continued)

- Desiccation cracks and polygons are found at the ground surface on top of several different geologic units within the Pasco Basin and vicinity, including Holocene alluvium. Clastic injection dikes have not been observed to penetrate Holocene sediments.
- Mud cracks form in silt- and clay-dominated sediments, but do not occur in coarser sediments because coarse material does not decrease in volume upon drying. However, clastic injection dikes and polygonal-patterned ground have been observed in sand and gravelly sand units and within the Columbia River Basalt Group.
- Sills are not common features associated with desiccation cracks, whereas sills are common in clastic injection dike systems. The primary reason for the absence of sills associated with desiccation cracks is the limited vertical extent of desiccation cracks (i.e., less than a few centimeters).
- A vertical sequence of coalescent desiccation cracks that cross multiple silt units could account for deeper penetration of desiccation cracks. However, coalescing desiccation cracks are rarely observed in the Holocene sediment record in the Pasco Basin and vicinity, and the walls of clastic injection dikes do not display features to suggest significant repeated periods of desiccation associated with cyclic aggradation of sediments.
- Desiccation cracks do not appear to be a significant mechanism for the formation of fissures hosting clastic injection dikes.
- Sources: Fairbridge (1968) and this study.

Figure 7-2: Photograph of large recent mud cracks that formed in the bottom of a large excavation located within lower Smith Canyon in the southeastern Pasco Basin (9/30-13L).

Figure 7-3: Photograph of downward-tapering fissures in desiccation cracks in a Saddle Mountains wasteway pond [Saddle Mountain Lakes (14/26-18J)].



0 30
cm

E9803054.163



0 20
cm

E9803054.163

7.3 EVALUATION OF GEOLOGIC PROCESSES IN FISSURE DEVELOPMENT

Deep Frost/ Permafrost Cracks

- Fractures associated with deep frost and permafrost cracks were suggested as a mechanism to form fissures hosting clastic injection dikes (Alwin 1970, Alwin and Scott 1970, Grolier and Bingham 1978). These fractures are termed ice wedges.
- Ice wedges are confined to permafrost regions and are best developed in fine-grained sediments. Ice wedges form primarily by wetting and drying, freezing and thawing, slumping, and faulting mechanisms. Fossil ice wedges, or sand wedges, are commonly filled with silt- and sand-sized sediments.
- Fossil wedges are typically sediment-filled, wedged-shaped structures that are oriented near vertical with their apices downward and commonly contain crisscrossing narrow dikelets. Wedges range from a few millimeters to many meters wide at the top and are generally less than 10 m vertical length. Clastic injection dikes are also near vertical, but are commonly tabular and often splay into clastic injection sills. The ranges of the width of wedges and dikes overlap. Sand wedges commonly exceed the maximum width observed in dikes. Clastic injection dikes display banding that is associated with alternating clay skins and infilling units, but do not contain the crisscrossing dikelets found in sand wedges.
- In plan view ice wedges intersect to form polygonal-patterned ground with polygons that range from 5 to 20 m across. Polygons are commonly four-sided structures. The soil wedges display merging and crosscutting relationships at intersections. Polygonal-patterned ground associated with clastic injection dikes displays many of the same features as polygons in permafrost, but the dimensions of polygons associated with clastic injection dikes can be larger and typically range from 5 m to greater than 150 m.



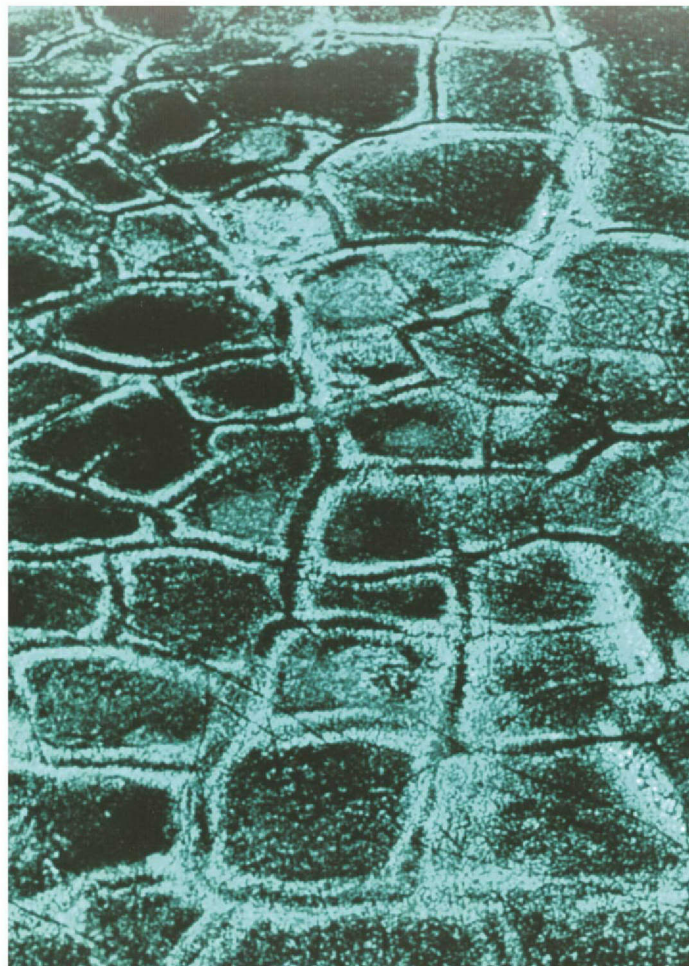
Figure 7-4: Photograph of an ice wedge in permafrost, Yukon Territory, Canada (<http://res.agr.ca/CANSIS/TAXA/LANDSCAPE/GROUND/yukon.html>).

7.3 EVALUATION OF GEOLOGIC PROCESSES IN FISSURE DEVELOPMENT

Deep Frost/ Permafrost Cracks (Continued)

- Sand wedges exhibit several features that are common to clastic injection dikes, including similar grain sizes, wedge shape, small-scale faults, shears, and slumps. The margins of sand wedges display the effects of pressure from repeated freezing and thawing. Pressure effects found in sand wedges have not been observed along the walls of clastic injection dikes.
- Ice wedges and associated polygonal-patterned ground form in permafrost environments. Fabrics associated with permafrost environments have not been observed in soils of the Pasco Basin and vicinity.
- Fossil ice wedges form in sediments. Fossil ice wedges are not typically present in bedrock, whereas clastic injection dikes commonly occur in Ringold and Ellensburg Formations and CRBG in the Pasco Basin and vicinity.
- Fractures associated with deep frost and permafrost cracks are not considered a significant mechanism for the formation of fissures in clastic injection dikes.
- Sources: Black (1976) for characteristics of ice wedge/polygons, Black (1979), and this study.

Figure 7-5: Aerial photograph of polygonal-patterned ground that occurs in a modern permafrost region south of Prudhoe Bay in northern Alaska, north of the Arctic Circle. Polygons are approximately 15 m across.

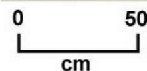


E9803054.165

7.3 EVALUATION OF GEOLOGIC PROCESSES IN FISSURE DEVELOPMENT

Melting of Buried Ice

- Fissures associated with melting of buried ice or frozen sediment were proposed as mechanisms to form the fractures enclosing clastic injection dikes (Lupher 1944).
- Ice-melt features have been observed in the Pasco Basin and vicinity. The debris-laden ice from continental glaciers and/or ice margin lakes was transported into the basin. Some ice became trapped in the glaciofluvial sediments. As the ice thawed, meltwater drained from the ice cavity, and debris contained in the ice fell to the bottom of the cavity. Glaciofluvial sediments above the cavity collapsed into the void with sharply defined margins between the undisturbed sediments and the cavity fill.
- Ice-melt cavities observed in the Pasco Basin range from 30 cm³ to 2 m³. The collapse chimneys located above the ice-melt cavities are similar in width to the ice-melt cavities. The chimneys are well defined near the ice-melt cavity but lose definition toward the top.
- Ice melt features do not contain near-vertical banding with multiple clay skins and infilling units. Clay skins do not form along the margin of the boundaries of the ice/melt cavities or collapse features. Small-scale faults, shears, and rip-up clasts have not been observed in ice-melt features. The ice-melt features have similar characteristics of soft-sediment flow features found in clastic injection dikes.
- Ice-melt features are observed in all sediment facies of the Hanford Formation, but have not been observed in other geologic units in the Pasco Basin and vicinity.



E9803054.166

Figure 7-6: Photograph of an ice-melt feature in the sand facies (field mapping unit #3) of the Hanford Formation in the Richland Landfill (10/28-17N).

7.3 EVALUATION OF GEOLOGIC PROCESSES IN FISSURE DEVELOPMENT

Melting of Buried Ice (Continued)

- Ice-melt cavities are observed with individual beds of the Hanford Formation, but have not been observed crossing multiple beds. Clastic injection dikes typically penetrate multiple beds or rock units.
- Ice-melt cavities are frequently observed within the Hanford Formation, but are relatively rare compared to ubiquitous occurrences of clastic injection dikes within the silt and sand facies.
- The sedimentary deposits in the Pasco Basin and vicinity were evaluated for the presence of large-scale ice-melt features. The basis of the evaluation is Dionne and Shilts (1974) and Dionne (1976). Mud boils and clastic dikes were formed by the melting of ice layers buried beneath sediments. The weight of the overlying sediments forced the trapped melted water from ice sheets to the surface. The water escape features that were formed included clastic dikes and small polygonal-patterned ground dike networks. Large-scale ice-melt features have not been observed in the Pasco Basin and vicinity. There is no evidence to indicate that extensive layers of frozen ground or ice sheets existed buried deep in the sediments of the basin area.
- The melting of buried ice is not considered a significant mechanism in the formation of fissures in clastic injection dikes.
- Source: Dionne and Shilts (1974), Dionne (1976), and this study.



Figure 7-7: Photograph of an ice-melt feature in the gravel facies (field mapping unit #2) of the Hanford Formation at a borrow pit located in Amon Canyon (9/28-25F).

7.3 EVALUATION OF GEOLOGIC PROCESSES IN FISSURE DEVELOPMENT

Loading/Unloading from Pleistocene Flooding

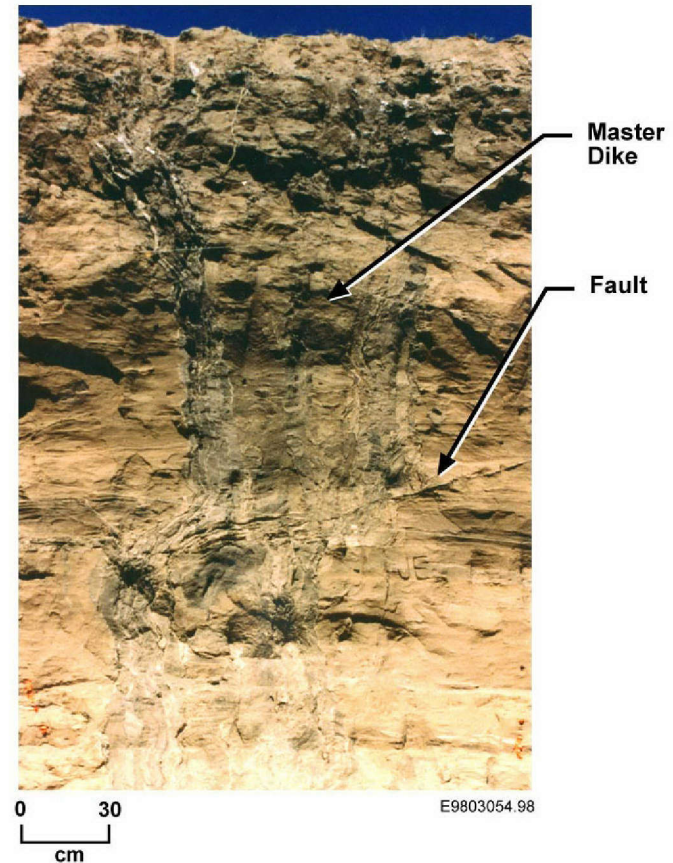
- Fractures resulting from rapid loading or unloading of Pleistocene floodwaters were suggested as the source for fissures containing clastic injection dikes by earlier workers, including Newcomb (1962), Black (1979), and Last and Fecht (1986).
- Rapid filling or draining of Glacial Lake Lewis would create temporary vertical gradients of pore-water pressures in the thick sequence of saturated, underconsolidated, semicohesive sediments. Differential settling could create vertical fissures that propagate into a network of polygons, form near-vertical to slightly inclined fissures in large-scale slumps, and enhance pre-flood tectonic fracture systems.
- The fissures in polygonal-patterned ground dike networks would be primarily due to a vertical component of compression caused by the weight of overlying sediments and a lateral component of tension caused by downslope movement or repacking of the sediments to a tighter arrangement of grains.
- Cataclysmic flooding of the Pasco Basin and vicinity occurred from at least four different glacial events during the Pleistocene epoch. Each flooding event (except from Pluvial Lake Bonneville) consisted of dozen(s) of individual cataclysmic floods. However, the emplacement of clastic injection dikes occurred only at or near the end of at least three of the four cataclysmic flooding events. Clastic injection dikes are not observed after each individual cataclysmic flood within an event.
- Surface loading by deposition of glaciofluvial sediments through Pleistocene cataclysmic flooding resulted in an increase in the weight of the soil mass. Consolidation of the metastable, semicohesive, glaciofluvial sediments and underlying units could form a network of fissures through which sediments are mobilized and resorted/transported.
- Lowering of the groundwater level in a sedimentary sequence increases the effective weight of the soil mass situated between the initial and final positions of the water table. This causes a corresponding additional consolidation of this soil mass and underlying deposits. Similar consolidation has been observed in marine sediments uplifted due to isostatic rebound and, on a smaller scale, in sediments associated with artificial drainage (Terzaghi and Peck 1948). Such consolidation can produce fissure systems associated with clastic injection dikes.
- The sedimentary sequences from earlier cataclysmic flooding events that inundated the basin (i.e., field mapping units #2 and #3) have similar bedding characteristics as sediments in the late Wisconsin-flooding event (field mapping unit #3). A key characteristic is the decrease in bed thickness in the upper portion of each sedimentary sequence in the basin associated with a cataclysmic flooding event. The similarities of bedding characteristics among these sequences suggest that the volume of floodwaters also decreased near the end of the cataclysmic flooding events. With clastic dikes forming during or shortly after small-scale cataclysmic flooding of temporary Glacial Lake Lewis, loading or unloading associated with Pleistocene flooding may not be the sole mechanism in the formation of fissures related to clastic injection dikes at the higher elevations of the basin.
- The volume of water released toward the end of cataclysmic flooding event during the late Wisconsin decreased relative to earlier floods in the event. The decrease in the volume of cataclysmic floods is a function of the size of the ice dam blocking the drainage system (Waitt 1994). As above, with the small volume of late-stage flooding, loading or unloading may not be the sole mechanism in the formation of fissures associated with clastic injection dikes.

7.3 EVALUATION OF GEOLOGIC PROCESSES IN FISSURE DEVELOPMENT

Loading/Unloading from Pleistocene Flooding (Continued)

- Loading or unloading during Pleistocene flooding may not be the sole mechanism in forming fissures associated with clastic injection dikes. However, since three episodes of clastic injection dike formation occurred during or soon after Pleistocene flooding, it is likely that loading or unloading associated with Pleistocene flooding is a significant contributing factor to fissure formation in clastic injection dikes.
- Source: Waitt (1994) and this study.

Figure 7-8: Photograph of clastic injection dikes that formed during two different cataclysmic flooding events and penetrate to the top of their respective sequence. The clastic injection dikes occur in field mapping units #2 and #3 at Keene/Kennedy Road (9/28-22M).



7.3 EVALUATION OF GEOLOGIC PROCESSES IN FISSURE DEVELOPMENT

Pre-Existing Fractures

- Pre-existing fractures were proposed by Black (1979) as fissures that were used for injection of sediments associated with clastic injection dikes.
- The structural fabric of the basin is expressed as a series of anticlinal and synclinal folds, faults, and fracture networks that were established early in the deformational history of the basin. The structural fabric is the result of north-south compression. This fabric was initiated over 17 million years ago and is commonly expressed in the basaltic bedrock, occasionally observed in the sediments of the Ringold Formation, and rarely displayed in sediments of Pleistocene and Holocene age. The faults and shears associated with the structural fabric are typically stained and have alteration rinds and clays that resulted from long periods of exposure to groundwater that percolated along the structures and tectonic movement. These structures formed long before the emplacement of clastic injection dikes (Sections 1.5 and 6.0).
- Uplift of the anticlinal ridges of the Yakima Fold Belt formed fault and shear networks in the basaltic bedrock, as well as in some sedimentary sequences that are incorporated into the folding. The fault and shear networks include conjugate joints and shears in the hanging wall of fault zones and doubly plunging anticlines; tension joints in the hanging wall of fault zones; and tear, thrust, and normal faults. Clastic injection dikes occur along faults and shears of the anticlinal ridges (Section 5.3).
- One of the major trends of the structural fabric of the Pasco Basin and vicinity is N55°W. Joints and shears associated with this trend are common in the Pasco Basin and vicinity. Two examples of joints and shears along this trend include Iowa Beef (8/31-36D) and Wallula Gap (7/31). Clastic injection dikes occur along several of the joints and shears at these localities (Section 5.3).



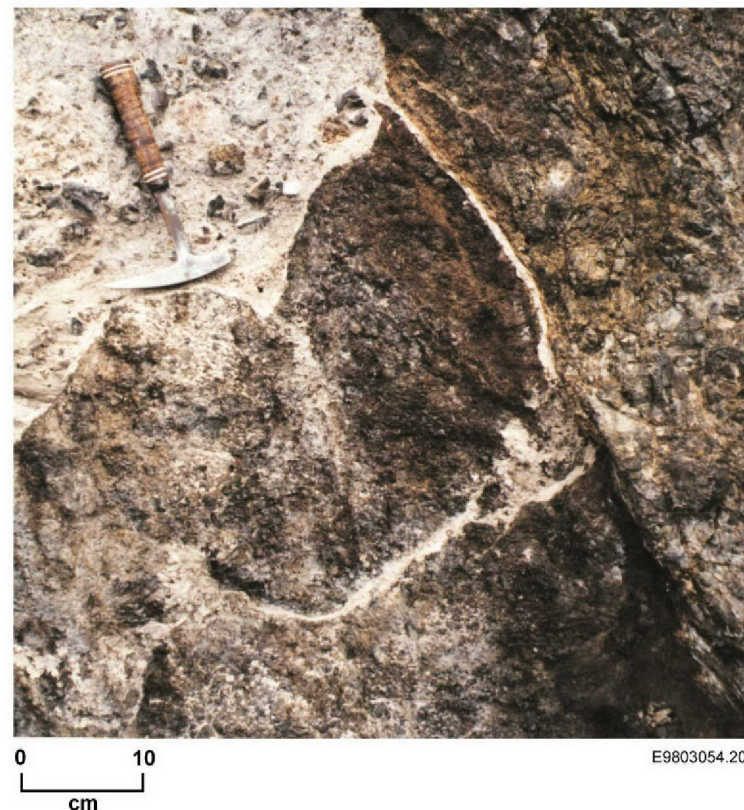
Figure 7-9: Photograph of clastic injection dikes along tectonic joints within the member of Wooded Island, Ringold Formation, that are oriented N50°W. The dikes are located at Iowa Beef South (8/31-36D).

7.3 EVALUATION OF GEOLOGIC PROCESSES IN FISSURE DEVELOPMENT

Pre-Existing Fractures (Continued)

- Black (1979) correctly interpreted that clastic injection dikes occupy pre-existing fractures associated with the structural fabric of the basin. Clastic injection dikes that occur within pre-existing fractures are classified as pre-existing fissure dike networks in this atlas (Section 5.3). Pre-existing fractures are a significant contributing structure in the origin of fissures associated with some clastic injection dikes.
- Sources: Black (1979), Farooqui (1979), WWC (1981), Reidel et al. (1994), and this study.

Figure 7-10: Photograph of tension fractures associated with the uplift of a doubly plunging anticline in the Rattlesnake Hills south of Richland at Meadow Hills (9/28-35R). The fractures were used as a fissure for injection of sediment that forms a clastic injection dike.



7.3 EVALUATION OF GEOLOGIC PROCESSES IN FISSURE DEVELOPMENT

Seismically Induced

- Several workers suggested fissures associated with clastic injection dikes were formed as a result of seismic activity (Jenkins 1925, Lupher 1944, Brown and Brown 1962, Jones and Deacon 1966, PSPL 1981, and Last and Fecht 1986).
- Seismicity could provide the catalyst for forming fissures occupied by clastic injection dikes. Seismic events can result in compaction of loosely consolidated sediments by vertical stresses from the weight of the overlying sediments. Coeval with compaction is volume reduction; both act to produce lateral tension stresses that can form vertically oriented tensional fissures. Turbid fluids from wetted sediments or ponded water could be forced into the fissures to form clastic injection dikes.
- Regional seismic events could have produced shock waves triggering compaction and volume reduction in sediments in the Glacial Lake Lewis. The March 27, 1964 Alaska earthquake (M_w 9.2) produced clastic injection dikes and polygonal-patterned ground in saturated overbank deposits along the reaches of rivers and streams in several areas of Alaska (Walsh et al. 1995).
- Moderate earthquakes are commonly associated with reservoir filling due to isostatic adjustment from the weight of water (Bolt 1978). Reservoir-induced seismicity is associated with very deep (>150 m) or very large (>1 x 10¹⁰ m³) man-made reservoirs (WCC 1980). Glacial Lake Lewis was up to 250 m deep and about 2 x 10¹² m³ in volume and could be responsible for reservoir-induced seismicity from the rapid filling and draining of glaciofluvial floodwaters.



E9803054.170

Reservoir	Country	Magnitude
Lake Mead	United States	5.0
Lake Kariba	Zambia	5.8
Koyna	India	6.5
Hsingfengkiang	China	6.1

Figure 7-11: Photograph of an excavation in floodplain alluvium exposing a clastic injection dike that formed in the 1964 Alaska earthquake. The photograph is taken near Kodiak, Alaska. The source of the photograph is Jones and Deacon (1966).

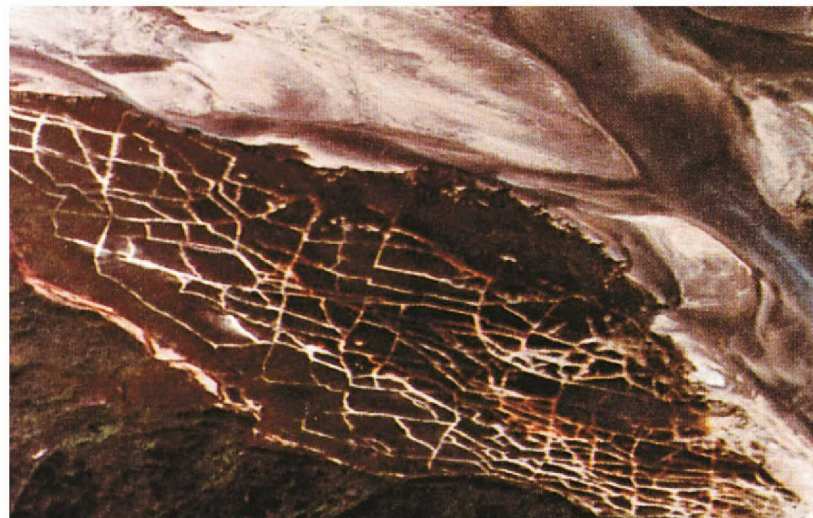
Table 7-1: Selected moderate-sized earthquakes detected with filling of large reservoirs (from Bolt 1978).

7.3 EVALUATION OF GEOLOGIC PROCESSES IN FISSURE DEVELOPMENT

Seismically Induced (Continued)

- The Pacific Northwest is tectonically active and is capable of generating large earthquakes (>7.0 M) based on geologic data, seismic measurements, and historical information. Large earthquakes could generate significant ground motion that could create fissures associated with clastic injection dikes.
- Sources: Jones and Deacon (1966), Bolt (1978), Kanamori (1977), WCC (1980, 1981), Walsh et al. (1995), and this study.

Figure 7-12: Photograph of an alluvium with polygonal-patterned ground that formed during the 1964 Alaska earthquake. The photograph was taken near Kodiak, Alaska. The source of the photograph is Jones and Deacon (1966).



E9803054.169

7.3 EVALUATION OF GEOLOGIC PROCESSES IN FISSURE DEVELOPMENT

Slumping

- Several earlier workers proposed that fissures associated with clastic injection dikes are the result of slumping (Lupher 1944, Bechtel 1971, Baker 1973, Black 1979, Bunker 1980, and PSPL 1981). Two workers specified mechanisms for slumping. Lupher (1944) attributed the slumping to landslides in the basalt sequence. Baker (1973) proposed that flood sediments were deposited as turbidites that slumped and formed fissures.
- Gravity-induced slumps can originate through the collapse of metastable, semicohesive silts and fine sands, which are generally saturated. Such collapse results from a sudden disturbance that produces transient, high pore pressures. This results in a brief semifluid character, increased shear stress, and subsequent failure of the host media associated with shear stresses. Shear stresses induced in the host sediments are typically associated with sediments that occur on inclined surfaces. The shear stresses are a function of slope geometry including slope inclination, slope height, and weight of the slope-forming material.
- Clastic injection dikes are present in sediments that occur on gently (5 to 10°) to highly (>20°) inclined slopes in the Pasco Basin and vicinity. The slopes are associated with a variety of geomorphic features and include:

Geomorphic Features	Inclination	Height	Dikes
Draped sediments over local topographic structures	Gentle	Low	Yes
Margins of basin	Gentle	High	Yes
Margins of Pleistocene flood bars	High	Low	Yes
Older landslides*	High	High	Not observed

*Slopes failed prior to formation of clastic injection dikes; clastic injection dikes have not been observed in poorly exposed debris of the landslides.

- Other aseismic factors that can affect shear stress (Schuster and Krizek 1978) and cause slumping include:
 - Removal of lateral support adjacent to the host media
 - Surcharge weight either by precipitation or flooding or through lowered water table
 - Inclined strata toward a free face
 - Structures such as faults, joints, and bedding planes.

Slumping would include fissures that form pathways for the injection of clastic sediments.

- Sediment failure is progressive and self-perpetuating; it usually starts in areas of greatest instability, and sliding slope movement continues until the causal factors (geologic, topographic, or climatic) have dissipated such that shear stresses are reduced and movement ceases. Clastic injection dikes in sediments with cross-cutting relationships are likely associated with sliding slope movement. The sliding and slumping may result in the host sediments being rotated such as at the Gable Mountain Bar (13/27-28R) or translated such as at Touchet Road (7/33-27).
- Slumping is a mechanism that likely created some fissures in sediments associated with clastic injection dikes in the Pasco Basin and vicinity.
- Sources: Baker (1973), Schuster and Krizek (1978), Black (1979), and this study.

7.3 EVALUATION OF GEOLOGIC PROCESSES IN FISSURE DEVELOPMENT

Summary

- The geologic processes considered significant in forming fissures containing clastic injection dikes are:
 - Loading and unloading by Pleistocene floodwaters
 - Pre-existing tectonic fractures
 - Seismically-induced ground motion
 - Slumping of sediment/rock masses.
- Processes not considered significant in the formation of fissures in clastic injection dikes are:
 - Desiccation cracks formed as a result of a volume decrease due to drying of wetted sediment
 - Deep frost/permafrost cracks formed by thermal expansion and contraction of sediments
 - Melting of ice buried beneath unconsolidated sediments.

7.4 EVALUATION OF GEOLOGIC PROCESSES IN SEDIMENT TRANSPORTATION AND DEPOSITION

Wind Transportation and Deposition

- Gravity filling of open fissures by wind transportation and deposition was proposed by Lupher (1944) as one of several processes for sediment infilling of the ubiquitous dikes of the silt facies of the Hanford Formation.
- Field investigations were initiated to find wind-filled fractures or analogs within the basin and valley terrain of the Pasco Basin and vicinity to evaluate infilling processes. The investigations did not reveal analogs for open fissures filled from the surface by wind processes. Most processes for modern fissure filling involved colluvial deposition by wind and water processes.
- The colluvial infilling by gravitational forces of open fissures resulted in clastic dikes that were poorly sorted, highly variable in grain sizes (silt to gravel), and massive to weakly stratified. The sediments do not display the banding of alternating clay skins and infilling units that are common to clastic injection dikes. The large grain sizes cannot be transported by wind processes.
- The clastic dikes filled with colluvial debris are typically wedge-shaped structures that are generally less than 5 m in depth and up to about 2 m in width.
- The source material for many of the colluvial-fill clastic dikes can be found adjacent to the dikes and are likely transported as slope wash and by gravitational processes.
- The characteristics of clastic dikes associated with colluvial filling of open fissures from the surface by gravitational forces are unlike those of clastic injection dikes present in this atlas.
- Wind processes may be involved in the infilling of clastic injection dikes, but are not the primary process for filling of dikes in the Pasco Basin and vicinity.
- Sources: Lupher (1944), WCC (1981), and this study.

Figure 7-13: Photograph of a clastic dike located south of Finley in the Rattlesnake Hills. The dike is an open tensional fissure in Umatilla basalt that has been filled with colluvium from above by gravitational forces.



E9803054.203

7.4 EVALUATION OF GEOLOGIC PROCESSES IN SEDIMENT TRANSPORTATION AND DEPOSITION

Water Transportation and Deposition

- Filling of open fissures by water transport and deposition has been proposed for infilling of clastic injection dikes by most earlier workers (see Table 1-2).
- Several key components of clastic injection dikes have characteristics that strongly indicate water as the transport agent for sediment infilling. The characteristics include:
 - Silt/clay linings commonly consist of thin laminae parallel to dike walls and infilling units, and have surfaces with undulating, ridge and trough structures, V-shaped tapers, and bulbous ridges.
 - Infilling sediments are variably sorted (from poorly to very well sorted or bimodally distributed when associated with gravel or rip-up clasts) and show elaborate internal structure (massive, cross-laminated, graded beds, and complex bed forms).
 - Clastic injection dikes commonly display complex and intricate multiple layers, bends, and folds of infilling units and silt/clay linings that formed during emplacement of dikes. Clastic injection dikes and components merge at intersections with other dikes in several types of dike networks.
 - Soft-sediment deformation features exist in the host sediments associated with formation of clastic injection dikes.
- Two basic types of water transport processes have been previously proposed for the infilling of fissures in clastic injection dikes.
 - Water infilling by the influx of water and sediment from gravitational drainage or transient loading of debris-laden waters (lake, fluvial or glaciofluvial).
 - Water escape by dewatering (likely entrapped water and air) of saturated and frequently underconsolidated sediments through seepage, liquefaction, and/or fluidization. This can result from mass movement (slumping), rapid consolidation of sediments from unloading, and/or seismic stress (earthquakes).
- Silt/clay linings that are present along the walls of clastic injection dikes and infilling units have been interpreted to form as the result of plugging pore spaces by debris-laden waters forced through fissures and dike sediments (Black 1979, Last and Fecht 1986). This process is termed filter pressing. Filter pressing of sediments indicates that high pressures were required to hydraulically emplace the sediment slurry into fissures (Black 1979, WCC 1981) and resort host sediments that became incorporated into fissures (Last and Fecht 1986).
- Many “roots” of silt/clay linings in dikelets splaying from master dikes in regular-shaped, polygonal-patterned ground dike networks, strongly suggest injection by water.
- The presence of sills along bedding planes and within beds also indicates the emplacement of sediments by water under hydraulic pressures.
- The primary process for the transportation of clastic sediments and infilling of fissures is by water under hydraulic pressure.
- Sources: Table 1-2 and this study.

7.5 ORIGIN OF DIKES

- This section presents a discussion on the origin of clastic injection dikes. The discussion is based on the description of clastic injection dikes (Section 3.0), constraints on origin (Section 7.2), and evaluation of the processes in fissure development (Section 7.3) and sediment injection (Section 7.4).
- **Fissures** associated with clastic injection dikes formed as a result of ground failure that was caused by the compaction (volume reduction) of the sedimentary sequence, translocation of the sediment/rock mass, and extensional stresses in the rock mass. Fissures formed in all ages of sediments and rocks in the Pasco Basin and vicinity from Miocene to late Pleistocene. Initial propagation and widening of fissures in unconsolidated sediment during ground failure required particle cohesion and hydraulic pressure to maintain fissure apertures. Particle cohesion is likely due to high moisture content in the sedimentary sequence. Frozen ground and cementation are ruled out as cohesive agents in underconsolidated sediments.
- Pre-existing **fissures** that are associated with some clastic injection dikes formed long before injection of sediments. This is based on extensive staining and alteration of fissure walls and breccias compared to relatively unaltered materials found in clastic injection dikes. These fissures typically occur along basaltic ridges of the Yakima Fold Belt and N50-55°W structural trends on the eastern margin of the Pasco Basin. Pre-existing fissures are only one type of fissure associated with clastic injection dikes of the Pasco Basin and vicinity.
- The **sources of the fluids** are (1) Pleistocene floodwaters that were hydraulically dammed behind bedrock narrows at Wallula Gap in the Horse Heaven Hills forming deep [up to about 243 m (800 ft)] temporary Glacial Lake Lewis and (2) the residual water (and probably air) trapped in the pore spaces of sediment/rock mass of vadose zone from infiltration due to Pleistocene flooding. Fluid movement was multidirectional within fissures due to the variable pressure gradients created by differential movement within the sediment/rock sequence. The greatest pressure gradients were created in areas of greatest compaction. These pressure gradients occurred in the underconsolidated sediments deposited by Pleistocene cataclysmic flooding.
- The **sources of sediments** in clastic injection dikes are primarily from unconsolidated sediments deposited by Pleistocene cataclysmic flooding based on the composition of the sand fraction. Sands within the dikes generally have a high percentage of unweathered basalt particles that is typical of flood deposits (Hanford Formation). Sediments from Plio-Pleistocene deposits, Ringold Formation, and Ellensburg Formation also are known to be incorporated into some clastic injection dikes, but make up a small percentage of dike material.
- **Clay/silt linings** are commonly thin, poorly sorted fine-grained sediments that line the walls of dikes and margins of infilling units. The clay and silt fractions of the linings are interpreted as deposits that formed by sediment-laden water that was forced into pore spaces along fissure walls. The filter press of silt- and clay-sized particles into pore spaces along fissure walls is consistent with concepts presented by Black (1979) and Last and Fecht (1986). Water injection into open fissures resulted from pressure gradients that were developed from hydraulic pressure from loading or unloading of Glacial Lake Lewis or from within wetted underconsolidated sediments and rock mass during mass movement.
- **Infilling units** are sediments deposited or resorted as sediment-laden water moved along open fissures. The movement in open fissures resulted from pressure gradients that are described above. The fluid velocities were sufficient to transport sediments. Most clastic injection dikes contain more than a single infilling unit. Multiple infilling units each separated by clay/silt linings give clastic injection dikes a banded appearance. Each band represents a discrete sediment infilling unit. As a pathway became blocked and sealed off by movement of small-scale structures (e.g., slumps, folds, and faults), tensional stresses created new fissures within the dike or, in some instances, in the host sediments adjacent to dikes to accommodate flow. Flow along pathways within a dike was essentially continuous until the pressure gradient dissipated.

7.5 ORIGIN OF DIKES

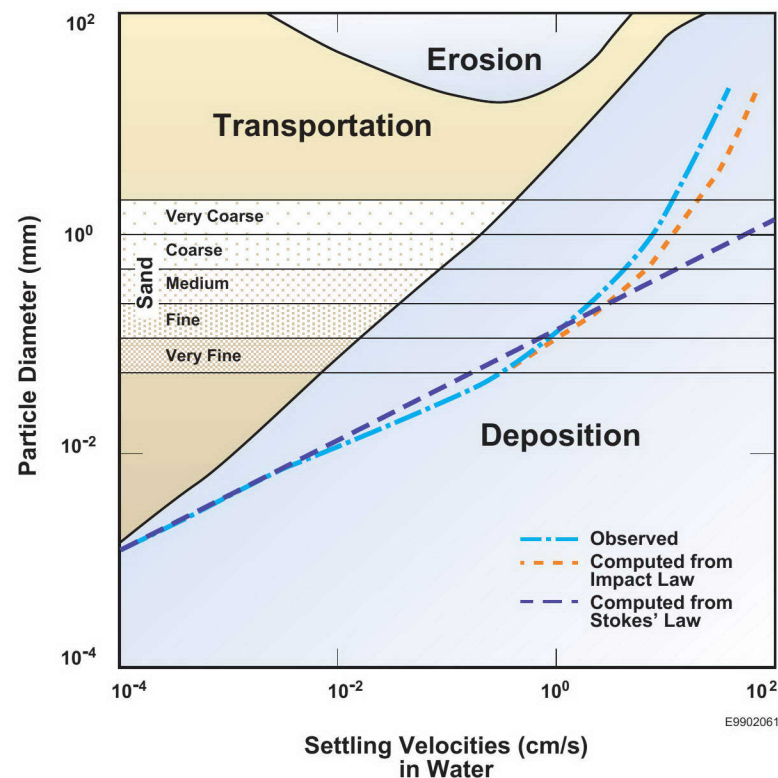
- Within **infilling units**, flow direction indicators are not abundant or obvious in clastic injection dike exposures. Flow direction indicators in the sand fraction such as direction to source beds and truncation of sedimentary structures suggest sediment transport in many different directions (i.e., upward, downward, and laterally) in most exposures. The multiple flow directions are expected based on the presence of extensive small-scale structures that formed due to locally induced stresses. These stresses created a complex system of pressure gradients. Coarser grained sediments (e.g., gravel-size clasts) within infilling units were transported with downward flow, but in upward flow large clasts settled downward due to gravitational forces.
- **Infilling unit** sediments vary from poorly sorted to very well-sorted materials, but are more commonly moderately well to well sorted. Deposition of well-sorted sediments requires either a well-sorted sediment source or sufficient time to rework poorly sorted sediments. In a floodwater-loading scenario, the fissures are relatively short, fill volume is relatively small, and time of deposition is limited to filling of the fissure as the pore spaces along fissure walls would be quickly plugged by clay/silt linings. Since Pleistocene cataclysmic floodwaters were likely very turbid with a poorly sorted admix of sediments, discharge of floodwaters directly into open fissures would likely deposit predominantly poor to moderately well-sorted sediments. This scenario is not conducive to rework poorly sorted sediments to create a more uniform particle size distribution of well-sorted sediments. However, in an unloading scenario, sediments that were wetted (and often saturated) from infiltration of Pleistocene floodwaters could discharge water along short flow paths, and have sufficient time to sort sediments as waters were discharged upward, downward, and laterally away from the wetted sediments.

The water flowing along fissures outward to the surface or at some locations into highly permeable horizons could be many times the volume of the fissure. Such a volume of water could be sufficient to create a reasonably well-sorted sediment, develop intricate bed forms, and create multiple infilling units within fissures of clastic injection dikes. These characteristics are key indicators that infilling units were likely deposited as a result of dewatering of the sediment/rock mass.

- Variability of particle sizes with and among **infilling units** can be used to determine general characteristics of flow conditions within clastic injection dikes. Uniform particle sizes within and among infilling units indicate a depositional environment under relatively constant flow and velocities. Dikes with variable grain sizes suggest changing flow velocities during deposition. Dikes with variable grain sizes also commonly have complex internal bed forms (e.g., cross-laminations, graded beddings, and complex folds), small-scale structures (e.g., slumps, faults, folds), and vary significantly in width of infilling units.

7.5 ORIGIN OF DIKES

- The **flow velocity** during sediment deposition within clastic injection dikes can be estimated based on the settling velocities of particle sizes within infilling units. The largest particle size transported with the water is generally very coarse sand. The most common particle sizes measured in infilling units range from medium to fine sand. Based on Stokes Law (Stokes 1851) and the Impact Law (Rubey 1933), the water velocities required for deposition in clastic injection dikes based on the particle sizes above are estimated to have been less than 20 cm/sec and most commonly ranged between 2 to 10 cm/sec.
- Extensive **small-scale structures** including slumps, faults and shears, slickensides, and associated soft-sediment flow features are related to the deformation of the host sediments and the clastic injection dike. Deformation resulted from differential movement in the sediment and rock mass (e.g., volume reduction through compaction of underconsolidated wetted sediments). The differential movement manifested itself in the formation of small-scale structures (e.g., slumps, faults, and shears) in the host sediments and clastic injection dikes. Small-scale structures indicate that deformation started with the initial propagation of fissures, continued during injection of sediments into dikes, and ended with primarily post-dike emplacement of shears and faults.



E9902061

Figure 7-14: Graph of Settling Velocities Versus Particle Size (from Dapples 1959). Stokes' Law holds for particles with diameters less than 0.1 mm, and the Impact Law controls velocities for larger particles.

7.5 ORIGIN OF DIKES

- **Small-scale structures** form on clay/silt linings including slickensides and deformed linings. Slickensides are observed on multiple surfaces of many clay/silt linings. The orientation of the slickensides varies on single surfaces or among different surfaces indicating multiple directions of movement. Deformation of clay/silt linings range from smooth, slightly undulating surfaces to highly contorted folds and slumps. These structures are small in scale (i.e., centimeter) and highly variable in orientation, which indicates a complex series of movement under locally induced stress conditions. These structures indicate continued micro-scale (i.e., centimeter) deformation through slumping, folding, and faulting of the clastic injection dike and adjacent host sediments. The small-scale structures indicate a deformational history that is initiated during formation of fissures, continued through injection of sediments, and ended shortly after the last sediments were injected.
- The **small-scale structures** were principally formed during sediment injection and widening of the fissures. Only minor deformation (e.g., slumps, faults, and shears) is observed during initial propagation of fissures or post-injection of sediments.
- **Geologic processes** (as discussed in Section 7.3) can create fissures associated with clastic injection dikes in many types of terrain in the Pasco Basin and vicinity. Only two geologic processes occur in all types of geographic terrain known to contain clastic injection dikes (i.e., unloading of Pleistocene floodwaters and seismically-induced ground motion).

Geologic Process	Present in All Geographic Terrain?	
	Yes	No
Loading of Pleistocene floodwaters		● Not viable in dewatering
Unloading of Pleistocene floodwaters	●	
Seismically-induced ground motion	●	
Slumping		● Limited primarily to slopes
Pre-existing fractures		● Limited to Pleistocene- and Miocene-aged sediments/rocks

- **Older Pleistocene-age clastic injection dikes** in the Pasco Basin are exposed in many different terrains in the Pasco Basin. Older clastic injection dikes are generally poorly exposed as younger Pleistocene and Holocene sediments extensively cover older dikes and host sediments/rocks in the basin. Older clastic injection dikes are known to occur in the:
 - Central and southern parts of the Pasco Basin
 - Eastern part of the lower Yakima Valley, and
 - Central and eastern Walla Walla valley.

7.5 ORIGIN OF DIKES

- **Older Pleistocene-age clastic injection dikes** formed over a relatively short time interval. Limited exposures make it difficult to determine whether the dikes formed simultaneously or whether dikes formed over multiple individual floods within a flooding event. Therefore, the process that formed fissures in the clastic injection dikes could be due to unloading from Pleistocene floodwaters, seismically-induced ground motion, or both. Both processes could result in extensional stresses that opened fissures and injected sediments during dewatering of the sediment/rock sequence.
- In the **youngest** period of cataclysmic flooding (i.e., late Wisconsin), most **clastic injection dikes** were formed over a large geographic area (Pasco Basin, Quincy Basin, Walla Walla Valley, lower Yakima Valley, Umatilla-Dalles syncline, and beyond), at essentially the same time. This suggests that the late episode of dike formation may be due to a single geologic event. Such an event may be required as a catalyst to initiate fissure formation (except in pre-existing fissure dike networks) and sediment injection processes in different terrains covering large geographic areas at essentially the same time. Only one geologic process considered in Section 7.3 could result in such a geologic event; i.e., seismically-induced ground motion.
- **Seismicity** (greater than magnitude 7.0) associated with strong ground motion has the potential to create fissures for the injection of sediments in clastic injection dikes. Coseismic ground motion in the Pasco Basin and vicinity could come from several sources (Geomatrix 1996 and this study):
 - Isostatic adjustments due to periodic filling and/or draining of Glacial Lake Lewis
 - A regional seismic event such as an event along the Cascadia subduction zone
 - Deep event (>15 km) in the crystalline basement rocks beneath the central Columbia Basin
 - Uplift or subsidence in the Yakima Fold Belt
 - Shallow event (<5 km) in the Columbia River Basalt Group.
- The frequency of clastic injection dikes can be controlled by physical properties and characteristics of host sediments/rocks and/or the proximity to active geologic structures or geologic events. Measurements of several clastic injection dike patterns in the Pasco Basin area suggest that over large geographic areas **dike frequency** appears to be controlled primarily by texture, bedding characteristics, and pre-existing fractures (i.e., type of dike network). Based on measurements of several clastic injection dike networks, dike frequency does not systematically increase in any preferred direction. Thus, clastic injection dikes may not be associated with a large local earthquake in the central plateau. If seismically-induced ground motion is the geologic catalyst in forming clastic injection dikes, then the seismic event may be a large regional earthquake with an epicenter located outside the central plateau. For example, a regional earthquake, such as along the Cascadian subduction zone that recurs at an interval of 450 years for earthquakes of magnitudes greater than 9.0 (see Geomatrix 1996), could produce sufficient ground motion to act as a catalyst in forming clastic injection dikes. Further studies on the frequency of clastic injection dikes in and beyond the Pasco Basin are needed to resolve the association of seismically-induced ground motion and clastic injection dikes.

7.6 ORIGIN OF DIKE NETWORKS

- This section presents a discussion on the origin of dike networks. The discussion is based on the description of dike networks (Section 5.0) and origin of clastic injection dikes (Section 7.5). Dike networks included regular-shaped, polygonal-patterned ground; irregular-shaped, polygonal-patterned ground; pre-existing fissure; and random occurrence.
- **Regular-shaped, polygonal-patterned ground dike networks** occur in valley bottoms and atop large Pleistocene flood bars. The similarity in size of regular-shaped patterns over large areas (square kilometers) requires uniformity in grain size and bedding characteristics over the area. As the grain size and bedding characteristics change, the patterns change. Gradual changes tend to result in changes to the size of regular-shaped patterns. Abrupt changes generally result in a change from regular-shaped polygons to other dike networks (i.e., irregular-shaped polygons, pre-existing fissures, or random occurrence).
- Master dikes in regular-shaped, polygonal-patterned ground formed in a network of interconnected fissures that was created by a reduction in volume of the sedimentary sequence. The volume reduction is estimated to be at least 3%, which represents the volume of the dikes in the sediment mass to perhaps 6% to allow for additional compaction for an underconsolidated sedimentary sequence. Initial sediment conditions included a wetted environment to provide sufficient particle cohesion and hydraulic pressure to form open tensional fissures. The fissures were the conduits for water flow and sediment transport.
- Volume reduction of the sedimentary sequence resulted in increased pore pressure and reduced grain stability. Grains supported by pore pressure had little strength and behaved as a fluid that flowed as a result of pressure gradients.
 - Sand, silt, and clay grains were mobilized due to reduced shear strength.
 - Sand grains, although set in motion, were not transported great distances. Sand grains were commonly reoriented, sorted, and redeposited in infilling units.
 - Large sand grains, gravel clasts, and rip-up debris moved downward by gravitational forces, perhaps even against the flow of water.
 - Fine grains, mainly very fine, silt and clay, appear to be fluidized and transported with the water. Silt lenses and silt and clay associated with laminated silty sand units appear to be the primary sources for clay/silt-size grains found in the linings.
- Soil moisture (near saturation) that was trapped in the sedimentary sequence was injected along thin fissures and into the major fissure system. The thin, filled fissures are preserved as dikelets, and the larger filled fissures formed master dikes. Flow and transport follow pressure gradients that can be any direction on a small scale (meters). On a larger scale, pressure reduction in this type of dike system formed by violently releasing water to lower pressure conditions. The dewatering process was primarily to the ground surface, but in some sedimentary conditions the water was transported laterally and/or downward.
- Pressure gradients in the host sediments/rocks created during mass movement rapidly dissipated in most sedimentary environments in the Pasco Basin and vicinity. Therefore, fissures were formed and sediments were injected and deposited in a very short time span. Several rough calculations of the time estimated to form clastic injection dikes (based on primarily parameters and concepts contained in this study) averaged about 1.5 to 3 hours for an individual polygon. The elevation of polygons varies among and across a polygon in a given network because of differential movement among polygons; the time to form the network would be more than the calculated average of 1.5 to 3 hours for an individual polygon.

7.6 ORIGIN OF DIKE NETWORKS

- **Irregular-shaped, polygonal-patterned ground dike networks** form in sedimentary sequences located on margins of valleys and large-scale Pleistocene flood bars. In these terrains, unstable sediments are susceptible to slumping. Sedimentary sequences were underconsolidated and wetted, similar to sediments in regular-shaped, polygonal-patterned ground dike networks. The fissures associated with clastic injection dikes are commonly formed in a two-part process:
 - Initially, many fissures form as regular-shaped, polygonal-patterned ground dike networks based on early formation of intersecting master dikes and rhombohedral shape that formed due to volume reduction of the sedimentary sequence from compaction;
 - Secondly, the irregular-shaped, polygonal-patterned ground formed as a result of lateral extension as the sediment mass moves down slope with coeval injection of sediments into fissures.
- Shapes of the polygons are highly variable in size due to the complex mass movement in this type of dike network. The vertical and horizontal length of dike segments and width of dikes are also highly variable because of the complex history.
- Dikes in irregular-shaped, polygonal-patterned ground formed along fissures created by lateral extension and volume reduction in sediment mass. Mass movement in this type of dike network is generally much greater than in regular-shaped, polygonal-patterned ground dike networks. The number of dikes in irregular-shaped, polygonal-patterned ground dike networks is also significantly higher, often comprising as much as 20% of the sediment mass. The fissures that formed the conduits for water flow and sediment transport primarily followed shear surfaces within the slumped material. The width of dikes was dependent on the volume of water released and the time fissures were open to flow before truncation by subsequent slumping or microfaulting.
- Slumping of the sedimentary sequence increased the pore pressure in the wetted underconsolidated sediments and reduced grain stability. Water trapped in the sedimentary sequence moved along the fissures due to pressure gradients created during the mass movement process. The grains moved in a similar manner to sediments in regular-shaped, polygonal-patterned ground dike networks. The thin fissures are preserved as clastic injection dikes with irregular patterns with common cross-cutting relationship to the dikes. The flow and transport of sediments follows the pressure gradients. The gradients can be virtually any direction in irregular-shaped, polygonal-patterned ground dike networks because of the complex movement that occurs within slumps. Clastic injection dikes formed in slumps as sediments were transported with soil water that was trapped in the sedimentary sequence. Dewatering of the sedimentary sequence can move turbid water upward to the top of the slump, laterally to the side of the slump, and downward along the base of the slump.
- In sedimentary sequences associated with extensive slumping, clastic injection dikes would be expected to form over a longer time. Calculations of the time required to form clastic injection dikes in complex slump environments used many of the same input parameters in the calculations for regular-shaped, polygonal-patterned ground dike networks, but included an increased abundance and extensive cross-cutting relationships of dikes. It is estimated that the clastic injection dike in a complex slump environment was four to eight times longer (or perhaps at least 12 hours) than in regular-shaped, polygonal-patterned ground dike networks.

7.6 ORIGIN OF DIKE NETWORKS

- **Pre-existing fissure dike networks** are located along major bedrock structures. These dike networks are found in bedrock units (Ringold Formation, Columbia River Basalt Group, and Ellensburg Formation) that have been incorporated in folding and faulting on Yakima folds or along a N50-55°W major structural trend on the eastern margin of the Pasco Basin. Fractures in pre-existing fissure dike networks were established as structural fabric that formed as a result of tectonism. The pre-existing faults and joints required tensional forces to enhance fissure apertures to allow for injection of clastic sediments. In near-surface environments, the structures are susceptible to tensional forces even though most structures are formed as the result of north-south compressional stresses.
- In most pre-existing fissure dike networks, the direction of sediment transport is laterally along or downward into open fissures based on sediment composition. The sediments in most pre-existing fracture networks are composed of quartzofeldspathic- and basaltic-rich particles. This composition is common in Pleistocene flood deposits. The basalt particles in dikes are not highly weathered, which is also consistent with flood deposits.
- The opening of fissures in bedrock to accommodate the injection of dike sediments could be from lateral flow associated with dewatering of the rock mass. However, the opening of fissures on bedrock structures across much of the Pasco Basin and vicinity may indicate greater stresses than could be generated from unloading floodwaters.
- **Random occurrence dike networks** occur as single or multiple clastic injection dikes or dike complexes. These networks represent isolated dike systems that are limited in spatial extent because of significant variations in bed characteristics and grain size or the exposures limit the ability to assign dikes to another network. It is reasonable to assume that the origin of random occurrence dike networks is similar to other dike networks.

8.0 GEO PHYSICAL METHODS TESTING

8.1 NON INTRUSIVE ELECTROMAGNETIC INDUCTION

- Two electromagnetic induction (EMI) tests were conducted in the Goose Egg Hill area (12/26-33C) at a regular-shaped, polygonal-patterned ground dike network to determine if EMI methods would be useful for detecting and mapping dikes.
- The EMI equipment used was a Geonics, Ltd., Model EM-31.
- Results:
 - The EMI survey detected clastic injection dikes in an area where the dikes were oriented vertically, greater than 30 cm wide, and the top of the dikes were approximately 1 m below the ground surface.
 - For a dry condition test, the clastic injection dikes displayed a prominent anomaly (conductor) that was three to four times above the 1 mmho/m background.
 - For a wet condition test (conducted following a rainy period), the same clastic injection dikes displayed higher readings due to the higher soil moisture (greater conductance), but the contrast between background and dike anomalies was similar to the dry condition test.
- Source: This study.

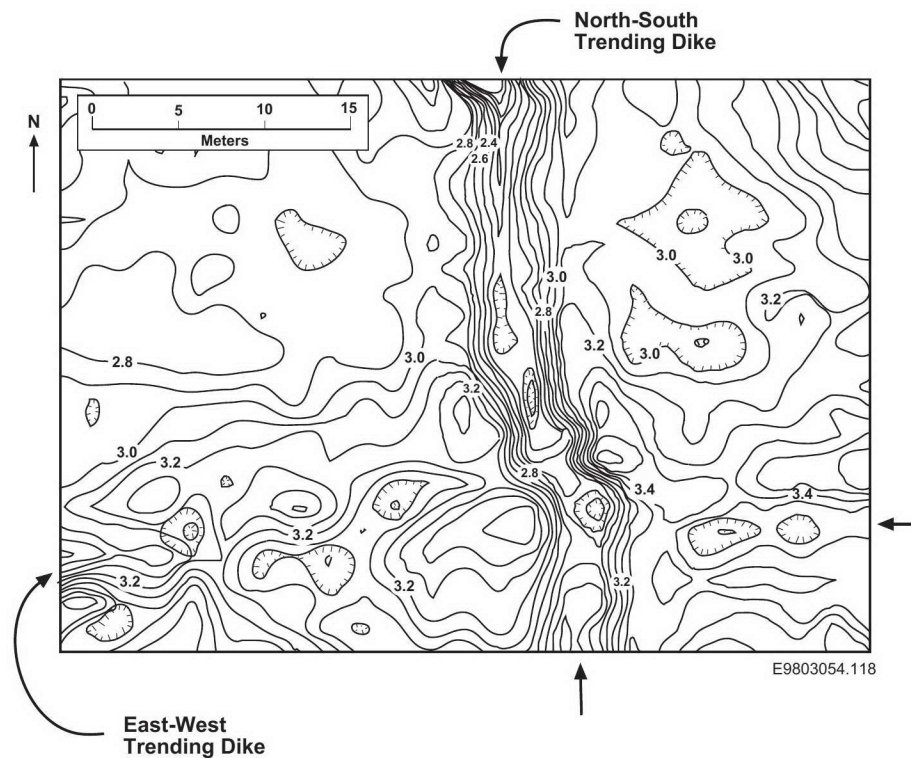
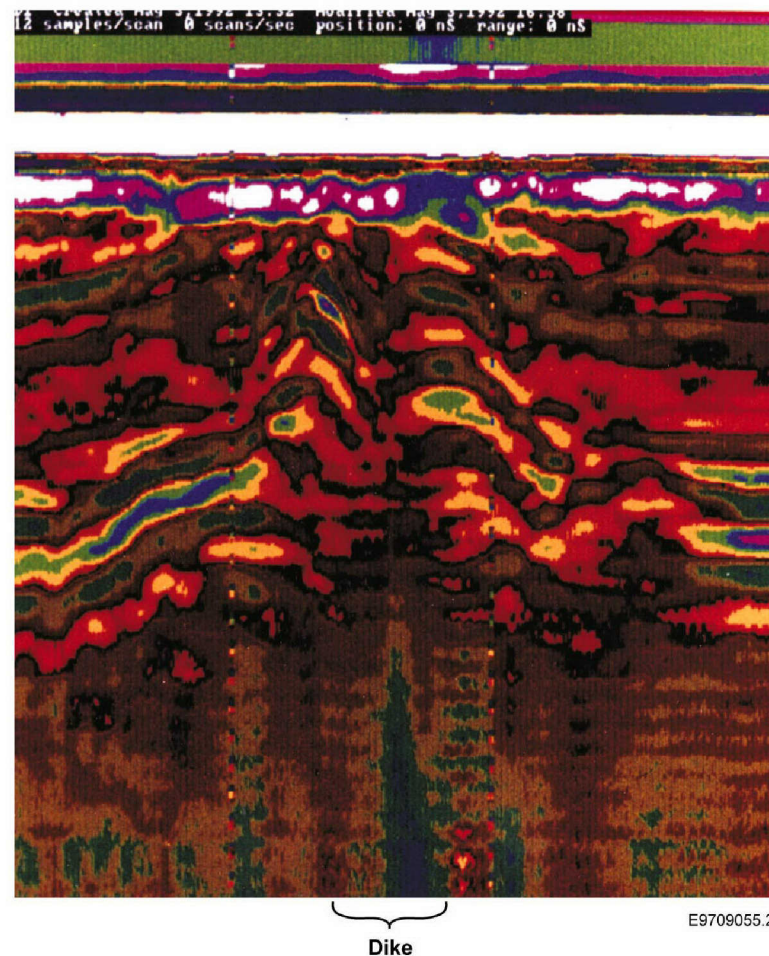


Figure 8-1: Map of EMI survey showing two orthogonal clastic injection dikes in the lower Cold Creek Valley [Goose Egg Hill area (12/26-33C)]. Host sediments are the sand facies of the Hanford Formation. Contour interval is 0.1 mmhos/m.

8.2 GROUND-PENETRATING RADAR

- A ground-penetrating radar (GPR) field test was conducted in the Goose Egg Hill area (12/26-33C) at a known clastic injection dike network to determine if GPR methods could be used to detect and map clastic injection dikes in the subsurface. The GPR test was conducted in the same area as the EMI tests.
- The GPR system used was a GSSI Model SIR-8, with a 300 MHz antenna.
- Results:
 - The GPR survey detected clastic injection dikes in an area where clastic injection dikes were oriented vertically, greater than 30 cm wide, and the top of the dikes were within 1 m of the ground surface
 - The clastic injection dike displayed a prominent anomaly that is easily distinguished from horizontally layered strata and low-angle cross bedding, both of which are common features found in the host sediments.
- Source: This study.

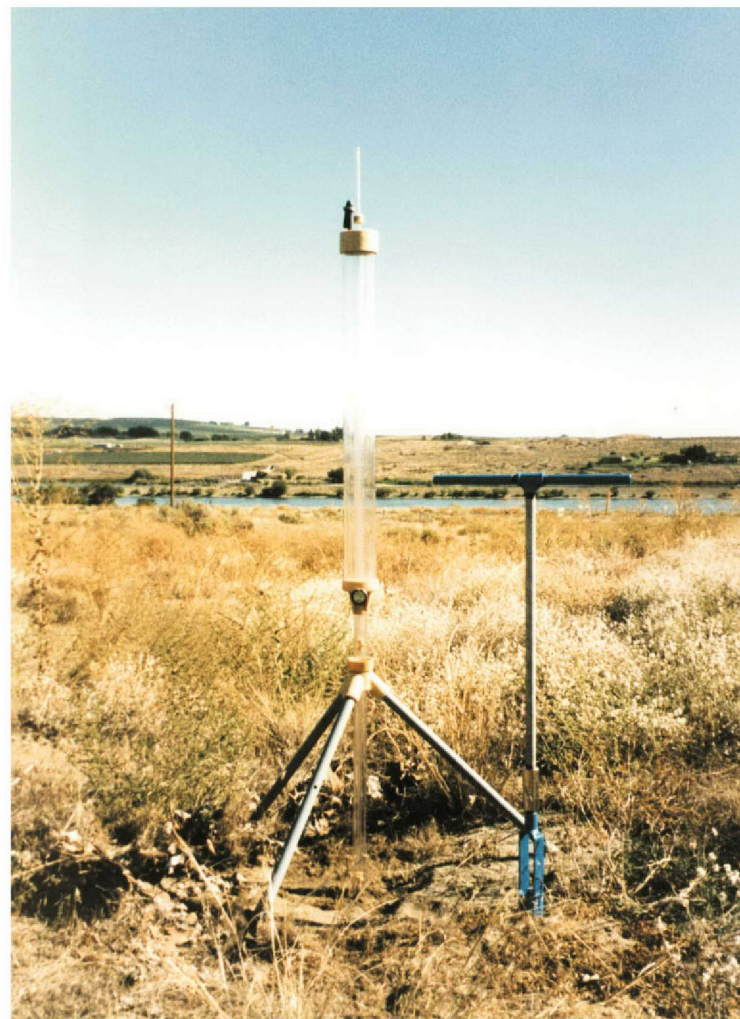
Figure 8-2: Cross-section of an anomaly associated with a clastic injection dike in the Goose Egg Hill area (12/26-33C). Host sediments are the sand facies of the Hanford Formation. Depth of investigation is approximately 4 m.



9.0 HYDRAULIC TESTING

9.1 BACKGROUND

- Clastic dikes have the potential to act as preferential pathways and/or barriers to movement of soil moisture in the vadose zone.
- Until this study, hydraulic properties have not been determined for clastic injection dikes in the Pasco Basin and vicinity.
- Simple field tests were designed for the following purposes:
 - Measure moisture movement rates in and adjacent to clastic injection dikes
 - Provide initial data for use in modeling of moisture flow in the Hanford Site vadose zone
 - Relate moisture flow in and adjacent to clastic injection dikes to physical properties of the dikes and host sediments (e.g., grain size, internal bedding)
 - Provide basis for more detailed follow-on field experiments.
- Three methods were selected for study because of their availability, portability (except the unsaturated flow apparatus), and economics:
 - Guelph permeameter
 - Small-scale infiltration
 - Unsaturated flow apparatus.
- This section presents the results of hydraulic and gas conductivity testing of clastic injection dikes followed by a summary of results and a discussion of test results.



E9803054.158

Figure 9-1: Photograph of Guelph permeameter equipment.

9.2 ABBREVIATIONS AND SYMBOLS

Grain Size

C	clay
C/P	clay laminations
G	gravel
S	sand
SZ	sandy silt
Z	silt
ZS	silty sand

Sand Sizes

[]	dominant grain sizes of sand
VC	very coarse
C	coarse
M	medium
F	fine
VF	very fine

Other Units and Symbols

cm	centimeters
cm ³	cubic centimeter
Dike	clastic injection dike
ft	feet
g	gram
GP	Guelph permeameter test
HF	Hanford Formation
hr	hours
in.	inch
IT	small-scale infiltrometer test
K _{fs}	field-saturated hydraulic conductivity
km	kilometers
m ²	square meters
MHz	megahertz
m	meters
mm	millimeters
P	partition (i.e., number of infilling units in an infilling group; number before P is the number of partitions in infilling group)
<u>S</u>	shear
sec	seconds
	relative direction of movement of host rock on either side of shear
UFA	unsaturated flow apparatus test

9.3 GUELPH PERMEAMETER

Test Plan

- Equipment - Model 2800K Guelph permeameter from Soil Moisture Equipment Corporation, Santa Barbara, California.
- General procedure:
 - Evaluate soils and select test sites.
 - Excavate 6-cm-diameter borehole, clean debris from bottom, and remove sidewall smear.
 - Assemble permeameter, fill with water, and lower into borehole until the water outlet tip rests on the bottom.
 - Raise the air tube until a well height of 5 cm is established.
 - Record the time and the water level in the reservoir at regular intervals until the rate of fall does not change over at least three consecutive time intervals.
 - Repeat last three steps for 10-cm well head height.
 - Calculate K_{fs} using the equations in Equation Set 1.
 - Note: There are limitations to using and interpreting Guelph permeameter data generated in this atlas. One basic assumption is that the sediments measured are uniform. Sediments in clastic injection dikes are typically not uniform, but are variably sorted and stratified.

Equation Set 1 – Equations used to calculate K_{fs} from Guelph permeameter data.

$$\text{Equation (1)} \quad \bar{R}_1 = (\Sigma R_1) \left(\frac{1}{n} \right) \left(\frac{1}{t} \right)$$

where

\bar{R}_1 = steady-state flow rate (cm/s) for first set of permeameter readings (5-cm height)

ΣR_1 = sum of steady-state Δ in centimeters for the first set of readings

n = number of steady-state measurements for the first set of readings

t = time interval in seconds.

$$\text{Equation (2)} \quad \bar{R}_2 = (\Sigma R_2) \left(\frac{1}{n} \right) \left(\frac{1}{t} \right)$$

where

\bar{R}_2 = steady-state flow (cm/s) for the second set of permeameter readings (10-cm height)

ΣR_2 = sum of steady-state Δ in centimeters for the second set of readings

n = number of steady-state measurements for the second set of readings

t = time interval in seconds.

$$\text{Equation (3)} \quad K_{fs} = [(0.0041)(R_c)(R_2)] - [(0.0054)(R_c)(R_1)]$$

where

R_c = reservoir constant (measured from the fluid reservoir on the Guelph permeameter)

\bar{R}_1 = steady-state flow rate for first set of permeameter readings (5-cm height)

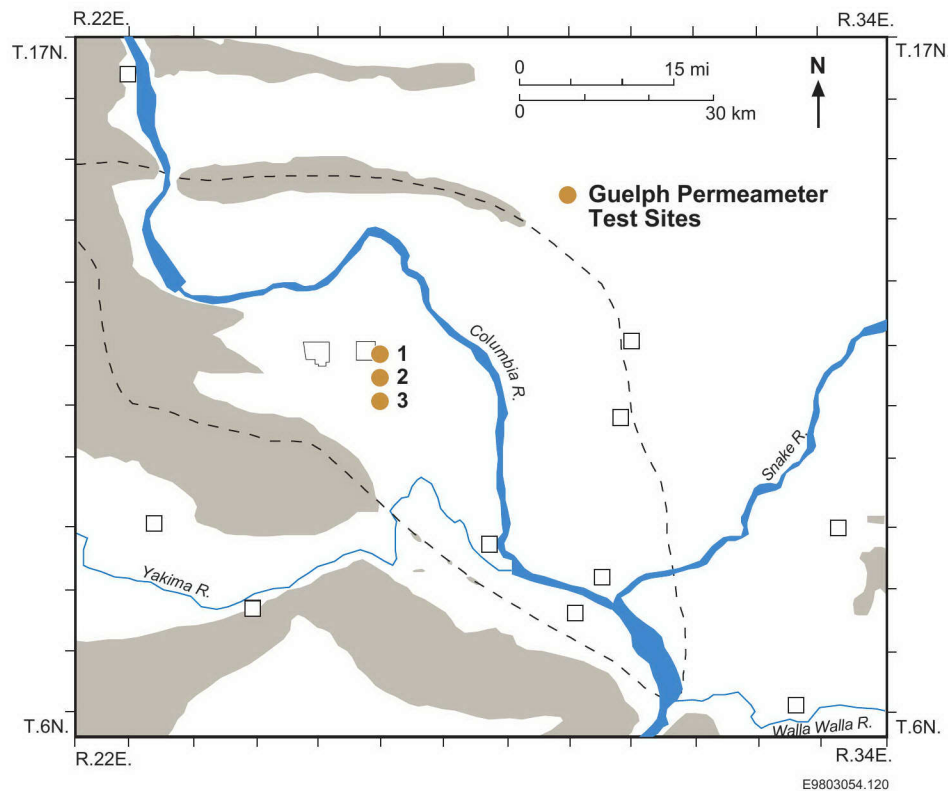
\bar{R}_2 = measured steady-state flow for the second set of permeameter readings (10-cm height).

9.3 GUELPH PERMEAMETER

Selection of Test Sites

- Three sites were selected to test the Guelph permeameter:
 1. The Grout excavation located east of the 200 East Area on the 200 Area Pleistocene Glaciofluvial Flood Bar of the Hanford Site (12/26-1N)
 2. An exposure located along Army Loop Road south of the 200 Areas and east of Goose Egg Hill (12/26-34C)
 3. A wind-scoured blowout located south of Goose Egg Hill in the lower Cold Creek Valley on the Hanford Site [Sand Blowout (11/26-3G)].
- The sites selected for testing were easily accessible with good surface exposures of clastic injection dikes and host sediments. The sites are located on the Hanford Site and require permission from the U.S. Department of Energy for entry. Both the dike and host sediments that were tested are of Wisconsin age.
- Source: This study.

Figure 9-2: Map showing the location of Guelph permeameter tests.



9.3 GUELPH PERMEAMETER

Guelph Permeameter Test #1

- Purpose: Test #1 was designed to measure the K_{fs} of a medium-to-fine-grained clastic injection dike.
- Location: Sand Blowout (11/26-3G).
- Test Area: The permeameter was inserted into a borehole 16 cm in depth and 6 cm in diameter. The borehole was located in a clastic injection dike with medium and fine sand infilling units and silt/clay linings. The dike strikes N65°E and dips nearly vertical and parallel to the borehole. The clastic injection dike and host sediments (field mapping unit #3, Hanford Formation) are Wisconsin, Pleistocene in age. The permeameter fluid volume reservoir constant (R_c) is 34.98.
- Results:

- The steady-state flow rate for \bar{R}_1 is:

$$\bar{R}_1 = (\Sigma R_1) \left(\frac{1}{n} \right) \left(\frac{1}{t} \right) = (4.4 \text{ cm}) \left(\frac{1}{7} \right) \left(\frac{1}{30 \text{ sec}} \right) = 2.1 \times 10^{-2} \text{ cm/sec}$$

and for \bar{R}_2 is:

$$\bar{R}_2 = (\Sigma R_2) \left(\frac{1}{n} \right) \left(\frac{1}{t} \right) = (7.9 \text{ cm}) \left(\frac{1}{7} \right) \left(\frac{1}{30 \text{ sec}} \right) = 3.8 \times 10^{-2} \text{ cm/sec}$$

- The calculated K_{fs} is:

$$\begin{aligned} K_{fs} &= [(4.1 \times 10^{-3})(R_c)(\bar{R}_2)] - [(5.4 \times 10^{-3})(R_c)(\bar{R}_1)] \\ &= [(4.1 \times 10^{-3})(3.498 \times 10^1)(3.8 \times 10^{-2} \text{ cm/sec})] \\ &\quad - [(5.4 \times 10^{-3})(3.498 \times 10^1)(2.1 \times 10^{-2} \text{ cm/sec})] = 1.4 \times 10^{-3} \text{ cm/sec} \end{aligned}$$

First Set of Readings ($H_1 = 5 \text{ cm}$)					
Reading Number	Time Interval (sec)	Reservoir Water Level		$\Delta(\text{cm})$	$\Sigma R_1 (\text{cm})$
		Start (cm)	End (cm)		
1	30	26.9	27.4	0.5	0.5
2	30	27.6	28.3	0.7	1.2
3	30	28.5	29.1	0.6	1.8
4	30	29.1	29.6	0.5	2.3
5	30	29.8	30.6	0.8	3.1
6	30	30.7	31.4	0.7	3.8
7	30	31.8	32.4	0.6	4.4
Second Set of Readings ($H_2 = 10 \text{ cm}$)					
Reading Number	Time Interval (sec)	Reservoir Water Level		$\Delta(\text{cm})$	$\Sigma R_2 (\text{cm})$
		Start (cm)	End (cm)		
1	30	13.0	14.4	1.4	
2	30	14.7	16.0	1.3	
3	30	16.2	17.4	1.2	1.2
4	30	17.6	18.7	1.1	2.3
5	30	18.8	20.0	1.2	4.5
6	30	20.1	21.2	1.1	5.6
7	30	21.2	22.3	1.1	6.7
8	30	22.4	23.4	1.0	7.7
9	30	23.9	25.1	1.2	7.9

Table 9-1: Summary of field measurements for Guelph permeameter test #1.

9.3 GUELPH PERMEAMETER

Guelph Permeameter Test #2

- Purpose: Test #2 was designed to measure the K_{fs} of a very fine-grained clastic injection dike.
- Location: Sand Blowout (11/26-3G).
- Test Area: The permeameter was inserted into a borehole 16 cm in depth and 6 cm in diameter that was located in a clastic injection dike with very fine sand infilling units and silt/clay linings. The dike is oriented near vertical and parallel to the borehole. The clastic injection dike and host sediment (sand facies, field mapping unit #3, Hanford Formation) are Wisconsin, Pleistocene in age. The permeameter fluid volume reservoir constant (R_c) is 35.4.

• Results:

- The steady-state flow rate for \bar{R}_1 is:

$$\bar{R}_1 = (\Sigma R_1) \left(\frac{1}{n} \right) \left(\frac{1}{t} \right) = (8.5 \text{ cm}) \left(\frac{1}{4} \right) \left(\frac{1}{30_{\text{sec}}} \right) = 7.1 \times 10^{-2} \text{ cm/sec}$$

and for \bar{R}_2 is:

$$\bar{R}_2 = (\Sigma R_2) \left(\frac{1}{n} \right) \left(\frac{1}{t} \right) = (10.3 \text{ cm}) \left(\frac{1}{3} \right) \left(\frac{1}{30_{\text{sec}}} \right) = 1.1 \times 10^{-1} \text{ cm/sec}$$

- The calculated K_{fs} is:

$$\begin{aligned} K_{fs} &= [(4.1 \times 10^{-3})(R_c)(\bar{R}_2)] - [(5.4 \times 10^{-3})(R_c)(\bar{R}_1)] \\ &= [(4.1 \times 10^{-3})(3.54 \times 10^1)(1.1 \times 10^{-1} \text{ cm/sec})] \\ &\quad - [(5.4 \times 10^{-3})(3.54 \times 10^1)(7.1 \times 10^{-2} \text{ cm/sec})] = 2 \times 10^{-3} \text{ cm/sec} \end{aligned}$$

Table 9-2: Summary of field measurements for Guelph permeameter test #2.

First Set of Readings ($H_1 = 5 \text{ cm}$)					
Reading Number	Time Interval (sec)	Reservoir Water Level		$\Delta(\text{cm})$	$\Sigma R_2 (\text{cm})$
		Start (cm)	End (cm)		
1	30	44.6	46.8	2.2	
2	30	46.8	49.2	2.4	
3	30	49.2	56.4	2.2	2.2
4	30	51.4	53.5	2.1	4.3
5	30	53.5	53.6	2.1	6.4
6	30	55.6	57.7	2.1	8.5
Second Set of Readings ($H_2 = 10 \text{ cm}$)					
Reading Number	Time Interval (sec)	Reservoir Water Level		$\Delta(\text{cm})$	$\Sigma R_2 (\text{cm})$
		Start (cm)	End (cm)		
1	30	12.0	18.7	6.7	
2	30	18.7	23.6	4.9	
3	30	23.6	28.1	4.5	
4	30	28.1	32.0	3.9	
5	30	32.0	35.5	3.5	3.5
6	30	35.5	39.0	3.5	7.0
7	30	39.0	42.3	3.3	10.3

9.3 GUELPH PERMEAMETER

Guelph Permeameter Test #3

- Purpose: Test #3 was designed to measure the K_{fs} of a fine-grained host sediment adjacent to Guelph permeameter tests #1 and #2.
- Location: Sand Blowout (11/26-3G).
- Test Area: The permeameter was inserted into a borehole 14 cm in depth and 6 cm in diameter. The borehole is located in a ripple-laminated silt and silty fine sand. The host sediments are the sand facies, field mapping unit #3, Hanford Formation, that are Wisconsin, Pleistocene in age. The permeameter fluid volume reservoir constant (R_c) is 34.98.
- Results:

- The steady-state flow rate for \bar{R}_1 is:

$$\bar{R}_1 = (\Sigma R_1) \left(\frac{1}{n} \right) \left(\frac{1}{t} \right) = (18.7 \text{ cm}) \left(\frac{1}{7} \right) \left(\frac{1}{30_{\text{sec}}} \right) = 8.9 \times 10^{-2} \text{ cm/sec}$$

and for \bar{R}_2 is:

$$\bar{R}_2 = (\Sigma R_2) \left(\frac{1}{n} \right) \left(\frac{1}{t} \right) = (18.8 \text{ cm}) \left(\frac{1}{5} \right) \left(\frac{1}{30_{\text{sec}}} \right) = 1.3 \times 10^{-1} \text{ cm/sec}$$

- The calculated K_{fs} is:

$$\begin{aligned} K_{fs} &= [(4.1 \times 10^{-3})(R_c)(\bar{R}_2)] - [(5.4 \times 10^{-3})(R_c)(\bar{R}_1)] \\ &= [(4.1 \times 10^{-3})(3.498 \times 10^1)(1.3 \times 10^{-1} \text{ cm/sec})] \\ &\quad - [(5.4 \times 10^{-3})(3.498 \times 10^1)(8.9 \times 10^{-2} \text{ cm/sec})] = 2.0 \times 10^{-3} \text{ cm/sec} \end{aligned}$$

First Set of Readings ($H_1 = 5 \text{ cm}$)					
Reading Number	Time Interval (sec)	Reservoir Water Level		$\Delta(\text{cm})$	$\Sigma R_1 (\text{cm})$
		Start (cm)	End (cm)		
1	30	48.0	50.9	2.9	
2	30	51.2	53.7	2.5	2.5
3	30	54.2	57.5	2.8	5.3
4	30	58.0	60.5	2.5	7.8
5	30	61.1	63.8	2.7	10.5
6	30	64.1	67.0	2.9	13.4
7	30	67.7	70.5	2.8	16.2
8	30	71.2	73.7	2.5	18.7

Second Set of Readings ($H_2 = 10 \text{ cm}$)					
Reading Number	Time Interval (sec)	Reservoir Water Level		$\Delta(\text{cm})$	$\Sigma R_2 (\text{cm})$
		Start (cm)	End (cm)		
1	30	8.1	13.0	4.9	
2	30	14.4	18.5	4.1	
3	30	19.3	23.2	3.9	3.9
4	30	23.8	27.6	3.8	7.7
5	30	28.2	32.0	3.8	11.5
6	30	32.7	36.3	3.6	15.1
7	30	37.7	41.3	3.7	18.8

Table 9-3: Summary of field measurements for Guelph permeameter test #3.

9.3 GUELPH PERMEAMETER

Guelph Permeameter Test #4

- Purpose: Test #4 was designed to measure the K_{fs} of a medium-to-fine-grained clastic injection dike.
- Location: Grout (12/26-1N).
- Test Area: The permeameter was inserted into a borehole 28 cm in depth and 6 cm in diameter. The borehole was located in a clastic injection dike with a medium-to-fine-grained sand infilling unit and silt/clay linings. The dike strikes generally east-west and dips to the south at about 40°. The clastic injection dike and host sediments (gravel facies, field mapping unit #3, Hanford Formation) are Wisconsin, Pleistocene in age. The permeameter fluid volume reservoir constant (R_c) is 35.4.
- Results:

- The steady-state flow rate for \bar{R}_1 is:

$$\bar{R}_1 = (\Sigma R_1) \left(\frac{1}{n} \right) \left(\frac{1}{t} \right) = (1.3 \text{ cm}) \left(\frac{1}{5} \right) \left(\frac{1}{30_{\text{sec}}} \right) = 8.7 \times 10^{-3} \text{ cm/sec}$$

and for \bar{R}_2 is:

$$\bar{R}_2 = (\Sigma R_2) \left(\frac{1}{n} \right) \left(\frac{1}{t} \right) = (4.8 \text{ cm}) \left(\frac{1}{9} \right) \left(\frac{1}{30_{\text{sec}}} \right) = 1.8 \times 10^{-2} \text{ cm/sec}$$

- The calculated K_{fs} is:

$$\begin{aligned} K_{fs} &= [(4.1 \times 10^{-3})(R_c)(\bar{R}_2)] - [(5.4 \times 10^{-3})(R_c)(\bar{R}_1)] \\ &= [(4.1 \times 10^{-3})(3.54 \times 10^1)(1.8 \times 10^{-2} \text{ cm/sec})] \\ &\quad - [(5.4 \times 10^{-3})(3.54 \times 10^1)(8.7 \times 10^{-3} \text{ cm/sec})] = 9 \times 10^{-4} \text{ cm/sec} \end{aligned}$$

Table 9-4: Summary of field measurements for Guelph permeameter test #4.

First Set of Readings ($H_1 = 5 \text{ cm}$)					
Reading Number	Time Interval (sec)	Reservoir Water Level		$\Delta(\text{cm})$	$\Sigma R_1 (\text{cm})$
		Start (cm)	End (cm)		
1	30	13.9	14.2	0.3	
2	30	14.2	14.5	0.3	
3	30	14.5	14.6	0.1	
4	30	14.6	15.0	0.4	
5	30	15.0	15.3	0.3	0.3
6	30	15.3	15.5	0.2	0.5
7	30	15.5	15.8	0.3	0.8
8	30	15.8	16.1	0.3	1.1
9	30	16.1	16.3	0.2	1.3
Second Set of Readings ($H_2 = 10 \text{ cm}$)					
Reading Number	Time Interval (sec)	Reservoir Water Level		$\Delta(\text{cm})$	$\Sigma R_2 (\text{cm})$
		Start (cm)	End (cm)		
1	30	7.0	8.0	1.0	
2	30	8.0	8.7	0.7	
3	30	8.7	9.2	0.5	0.5
4	30	9.2	9.8	0.6	1.1
5	30	9.8	10.4	0.6	1.7
6	30	10.4	10.8	0.4	2.1
7	30	10.8	11.4	0.6	2.7
8	30	11.4	11.8	0.4	3.1
9	30	11.8	12.5	0.7	3.8
10	30	12.5	13.0	0.5	4.3
11	30	13.0	13.5	0.5	4.8

9.3 GUELPH PERMEAMETER

Guelph Permeameter Test #5

- Purpose: Test #5 was designed to measure the K_{fs} of a coarse-to-medium-grained clastic injection dike.
- Location: Grout (12/26-1N).
- Test Area: The permeameter was inserted into a borehole 16 cm in depth and 6 cm in diameter. The borehole was located in a coarse-to-medium sand infilling unit of a clastic injection dike. The dike has an east-west trend and dips to the south about 40° (same dike as Guelph permeameter test #4). The clastic injection dike and host sediments (gravel facies, field mapping unit #3, Hanford Formation) are Wisconsin, Pleistocene in age. The permeameter fluid volume reservoir constant (R_c) is 35.4.
- Results:

- The steady-state flow rate for \bar{R}_1 is:

$$\bar{R}_1 = (\Sigma R_1) \left(\frac{1}{n} \right) \left(\frac{1}{t} \right) = (5.5 \text{ cm}) \left(\frac{1}{3} \right) \left(\frac{1}{30_{\text{sec}}} \right) = 6.1 \times 10^{-2} \text{ cm/sec}$$

and for \bar{R}_2 is:

$$\bar{R}_2 = (\Sigma R_2) \left(\frac{1}{n} \right) \left(\frac{1}{t} \right) = (1.49 \times 10^1 \text{ cm}) \left(\frac{1}{4} \right) \left(\frac{1}{30_{\text{sec}}} \right) = 1.2 \times 10^{-1} \text{ m/sec}$$

- The calculated K_{fs} is:

$$\begin{aligned} K_{fs} &= [(4.1 \times 10^{-3})(R_c)(\bar{R}_2)] - [(5.4 \times 10^{-3})(R_c)(\bar{R}_1)] \\ &= [(4.1 \times 10^{-3})(3.54 \times 10^1)(1.2 \times 10^{-1} \text{ cm/sec})] \\ &\quad - [(5.4 \times 10^{-3})(3.54 \times 10^1)(6.1 \times 10^{-2} \text{ cm/sec})] = 5.6 \times 10^{-3} \text{ cm/sec} \end{aligned}$$

First Set of Readings ($H_1 = 5 \text{ cm}$)					
Reading Number	Time Interval (sec)	Reservoir Water Level		$\Delta(\text{cm})$	$\Sigma R_1 (\text{cm})$
		Start (cm)	End (cm)		
1	30	41.8	43.6	1.8	
2	30	43.6	45.5	1.9	
3	30	45.5	47.5	2.0	
4	30	47.5	49.5	2.0	
5	30	49.5	51.1	1.6	
6	30	51.1	53.0	1.9	1.9
7	30	53.0	54.8	1.8	3.7
8	30	54.8	56.6	1.8	5.5

Second Set of Readings ($H_2 = 10 \text{ cm}$)					
Reading Number	Time Interval (sec)	Reservoir Water Level		$\Delta(\text{cm})$	$\Sigma R_2 (\text{cm})$
		Start (cm)	End (cm)		
1	30	7.5	12.3	4.8	
2	30	12.3	16.4	4.1	
3	30	16.4	20.5	4.1	
4	30	20.5	24.5	4.0	
5	30	24.5	28.4	3.9	3.9
6	30	28.4	32.0	3.6	7.5
7	30	32.0	35.8	3.8	11.3
8	30	35.8	39.4	3.6	14.9

Table 9-5: Summary of the field measurements for Guelph permeameter test #5.

9.3 GUELPH PERMEAMETER

Guelph Permeameter Test #6

- Purpose: Test #6 was designed to measure the K_{fs} of a medium-to-fine-grained clastic injection dike.
- Location: Army Loop Road (12/26-34C).
- Test Area: The permeameter was inserted into a shallow borehole less than 20 cm in depth and 6 cm in diameter. The borehole was located in a clastic injection dike with medium-to-fine sand infilling units and silt/clay linings. The dike strikes in a northerly direction and is near vertical. The clastic injection dike and host sediments (sand facies, field mapping unit #3, Hanford Formation) are Wisconsin, Pleistocene in age. The permeameter fluid volume reservoir constant (R_c) is 34.98.
- Results:

- The steady-state flow rate for \bar{R}_1 is:

$$\bar{R}_1 = (\Sigma R_1) \left(\frac{1}{n} \right) \left(\frac{1}{t} \right) = (9.2 \text{ cm}) \left(\frac{1}{7} \right) \left(\frac{1}{30_{\text{sec}}} \right) = 4.4 \times 10^{-2} \text{ cm/sec}$$

and for \bar{R}_2 is:

$$\bar{R}_2 = (\Sigma R_2) \left(\frac{1}{n} \right) \left(\frac{1}{t} \right) = (8.5 \text{ cm}) \left(\frac{1}{4} \right) \left(\frac{1}{30_{\text{sec}}} \right) = 7.1 \times 10^{-2} \text{ cm/sec}$$

- The calculated K_{fs} is:

$$\begin{aligned} K_{fs} &= [(4.1 \times 10^{-3})(R_c)(\bar{R}_2)] - [(5.4 \times 10^{-3})(R_c)(\bar{R}_1)] \\ &= [(4.1 \times 10^{-3})(3.498 \times 10^1)(7.1 \times 10^{-2} \text{ cm/sec})] \\ &\quad - [(5.4 \times 10^{-3})(3.498 \times 10^1)(4.4 \times 10^{-2} \text{ cm/sec})] = 1.9 \times 10^{-3} \text{ cm/sec} \end{aligned}$$

Table 9-6: Summary of field measurements for Guelph permeameter test #6.

First Set of Readings ($H_1 = 5 \text{ cm}$)					
Reading Number	Time Interval (sec)	Reservoir Water Level		$\Delta(\text{cm})$	$\Sigma R_1 (\text{cm})$
		Start (cm)	End (cm)		
1	30	36.0	37.3	1.3	1.3
2	30	38.1	39.5	1.4	2.7
3	30	39.7	41.0	1.3	4.0
4	30	41.5	42.7	1.2	5.2
5	30	43.2	44.5	1.3	6.5
6	30	46.7	48.0	1.3	7.8
7	30	49.9	51.3	1.4	9.2

Second Set of Readings ($H_2 = 10 \text{ cm}$)					
Reading Number	Time Interval (sec)	Reservoir Water Level		$\Delta(\text{cm})$	$\Sigma R_2 (\text{cm})$
		Start (cm)	End (cm)		
1	30	14.9	17.7	2.8	
2	30	18.1	20.7	2.6	
3	30	21.2	23.6	2.4	
4	30	24.0	26.5	2.1	2.1
5	30	26.7	28.9	2.2	4.3
6	30	29.4	31.5	2.1	6.4
7	30	31.9	34.0	2.1	8.5

9.3 GUELPH PERMEAMETER

Guelph Permeameter Test #7

- Purpose: Test #7 was designed to measure the K_{fs} for a silty, clay clastic injection dike.
- Location: Army Loop Road (12/26-34C).
- Test Area: The permeameter was inserted into a shallow borehole less than 20 cm in depth and 6 cm in diameter. The borehole was located in a clastic injection dike filled with fine silt and clay. The test site is adjacent to Guelph permeameter test #6. The dike trends to the north and is nearly vertical. The clastic injection dike and host sediments (sand facies, field mapping unit #3, Hanford Formation) are Wisconsin, Pleistocene in age. The permeameter fluid volume reservoir constant (R_c) is 34.98.
- Results:

- The steady-state flow rate for \bar{R}_1 is:

$$\bar{R}_1 = (\Sigma R_1) \left(\frac{1}{n} \right) \left(\frac{1}{t} \right) = (5.8 \text{ cm}) \left(\frac{1}{10} \right) \left(\frac{1}{30_{\text{sec}}} \right) = 1.9 \times 10^{-2} \text{ cm/sec}$$

and for \bar{R}_2 is:

$$\bar{R}_2 = (\Sigma R_2) \left(\frac{1}{n} \right) \left(\frac{1}{t} \right) = (5.7 \text{ cm}) \left(\frac{1}{5} \right) \left(\frac{1}{30_{\text{sec}}} \right) = 3.8 \times 10^{-2} \text{ cm/sec}$$

- The calculated K_{fs} is:

$$\begin{aligned} K_{fs} &= [(4.1 \times 10^{-3})(R_c)(\bar{R}_2)] - [(5.4 \times 10^{-3})(R_c)(\bar{R}_1)] \\ &= [(4.1 \times 10^{-3})(3.498 \times 10^1)(3.8 \times 10^{-2} \text{ cm/sec})] \\ &\quad - [(5.4 \times 10^{-3})(3.498 \times 10^1)(1.9 \times 10^{-2} \text{ cm/sec})] = 1.9 \times 10^{-3} \text{ cm/sec} \end{aligned}$$

Table 9-7: Summary of field measurements for Guelph permeameter test #7.

First Set of Readings ($H_1 = 5 \text{ cm}$)					
Reading Number	Time Interval (sec)	Reservoir Water Level		$\Delta(\text{cm})$	$\Sigma R_1 (\text{cm})$
		Start (cm)	End (cm)		
1	30	39.1	39.5	0.4	0.4
2	30	39.8	40.4	0.6	1.0
3	30	40.6	41.2	0.6	1.6
4	30	41.4	41.9	0.5	2.1
5	30	42.1	42.8	0.7	2.8
6	30	42.8	43.3	0.5	3.3
7	30	43.6	44.2	0.6	3.9
8	30	44.2	44.9	0.7	4.6
9	30	45.1	45.7	0.5	5.1
10	30	45.8	46.7	0.7	5.8
Second Set of Readings ($H_2 = 10 \text{ cm}$)					
Reading Number	Time Interval (sec)	Reservoir Water Level		$\Delta(\text{cm})$	$\Sigma R_2 (\text{cm})$
		Start (cm)	End (cm)		
1	30	12.5	15.9	3.2	
2	30	15.9	18.9	3.0	
3	30	18.9	20.2	1.3	
4	30	20.2	21.7	1.5	
5	30	21.7	23.2	1.5	
6	30	25.2	27.2	2.0	
7	30	27.2	29.1	1.8	
8	30	29.3	30.8	1.5	
9	30	31.1	32.2	1.1	1.1
10	30	32.5	33.8	1.3	2.4
11	30	34.0	35.1	1.1	3.5
12	30	35.4	36.5	1.1	4.6
13	30	36.8	37.9	1.1	5.7

9.3 GUELPH PERMEAMETER

Guelph Permeameter Test #8

- Purpose: Test #8 was designed to measure the K_{fs} of coarse-to-medium-grained host sediments adjacent to Guelph permeameter tests #6 and #7.
- Location: Army Loop Road (12/26-34C).
- Test Area: The permeameter was inserted into a borehole 16 cm in depth and 6 cm in diameter. The borehole is located in a plane-laminated coarse-to-medium sand. The host sediments (sand facies, field mapping unit #3, Hanford Formation) are Wisconsin, Pleistocene in age. The permeameter fluid volume reservoir constant (R_c) is 34.98.
- Results:

- The steady-state flow rate for \bar{R}_1 is:

$$\bar{R}_1 = (\Sigma R_1) \left(\frac{1}{n} \right) \left(\frac{1}{t} \right) = (5.4 \text{ cm}) \left(\frac{1}{4} \right) \left(\frac{1}{15_{\text{sec}}} \right) = 9.0 \times 10^{-2} \text{ cm/sec}$$

and for \bar{R}_2 is:

$$\bar{R}_2 = (\Sigma R_2) \left(\frac{1}{n} \right) \left(\frac{1}{t} \right) = (6.5 \text{ cm}) \left(\frac{1}{3} \right) \left(\frac{1}{15_{\text{sec}}} \right) = 1.4 \times 10^{-1} \text{ cm/sec}$$

- The calculated K_{fs} is:

$$\begin{aligned} K_{fs} &= [(4.1 \times 10^{-3})(R_c)(\bar{R}_2)] - [(5.4 \times 10^{-3})(R_c)(\bar{R}_1)] \\ &= [(4.1 \times 10^{-3})(3.498 \times 10^1)(1.4 \times 10^{-1} \text{ cm/sec})] \\ &\quad - [(5.4 \times 10^{-3})(3.498 \times 10^1)(9.0 \times 10^{-2} \text{ cm/sec})] = 3 \times 10^{-3} \text{ cm/sec} \end{aligned}$$

Table 9-8: Summary of field measurements for Guelph permeameter test #8.

First Set of Readings ($H_1 = 5 \text{ cm}$)					
Reading Number	Time Interval (sec)	Reservoir Water Level		$\Delta(\text{cm})$	$\Sigma R_1 (\text{cm})$
		Start (cm)	End (cm)		
1	15	40.8	42.1	1.3	1.3
2	15	42.7	44.1	1.4	2.7
3	15	44.5	45.8	1.3	4.0
4	15	46.4	47.8	1.4	5.4
Second Set of Readings ($H_2 = 10 \text{ cm}$)					
Reading Number	Time Interval (sec)	Reservoir Water Level		$\Delta(\text{cm})$	$\Sigma R_2 (\text{cm})$
		Start (cm)	End (cm)		
1	15	13.5	16.7	3.2	
2	15	17.4	20.0	2.6	
3	15	20.6	23.1	2.5	
4	15	23.7	26.1	2.4	
5	15	26.9	29.0	2.1	2.1
6	15	29.8	32.0	2.2	4.3
7	15	32.7	34.9	2.2	6.5

9.4 SMALL-SCALE INFILTRATION TESTS

Test Plan

- Equipment: Single ring infiltrometer that is 7.6 cm in height and 23 cm in diameter, tap water carried to location in 1-gallon plastic containers, shovel, tape measure, watch, American Geophysical Institute (AGI) field book, and field notebook.
- Procedure:
 - Select test area that can easily be excavated to form a level surface and vertical exposure.
 - Clear surface of test area to remove loose sediment, roots, and soil structures.
 - Bury the infiltrometer ring 5 cm into sediments and 8 cm from the edge of the vertical soil exposure.
 - Fill the ring to the top with water and continue adding water to maintain a constant head in the ring for the duration of the test.
 - Measure, at regular intervals, the extent of the moisture front on the vertical soil exposure and the quantity of water added to maintain head in ring.
 - After the final application of water and moisture front measurement, excavate the vertical exposure back to the center line of the infiltrometer ring and remeasure the position of the moisture front.
 - Correct moisture front measurements to the new exposure face.
 - Monitor moisture front 24 hours after final application of water (optional).

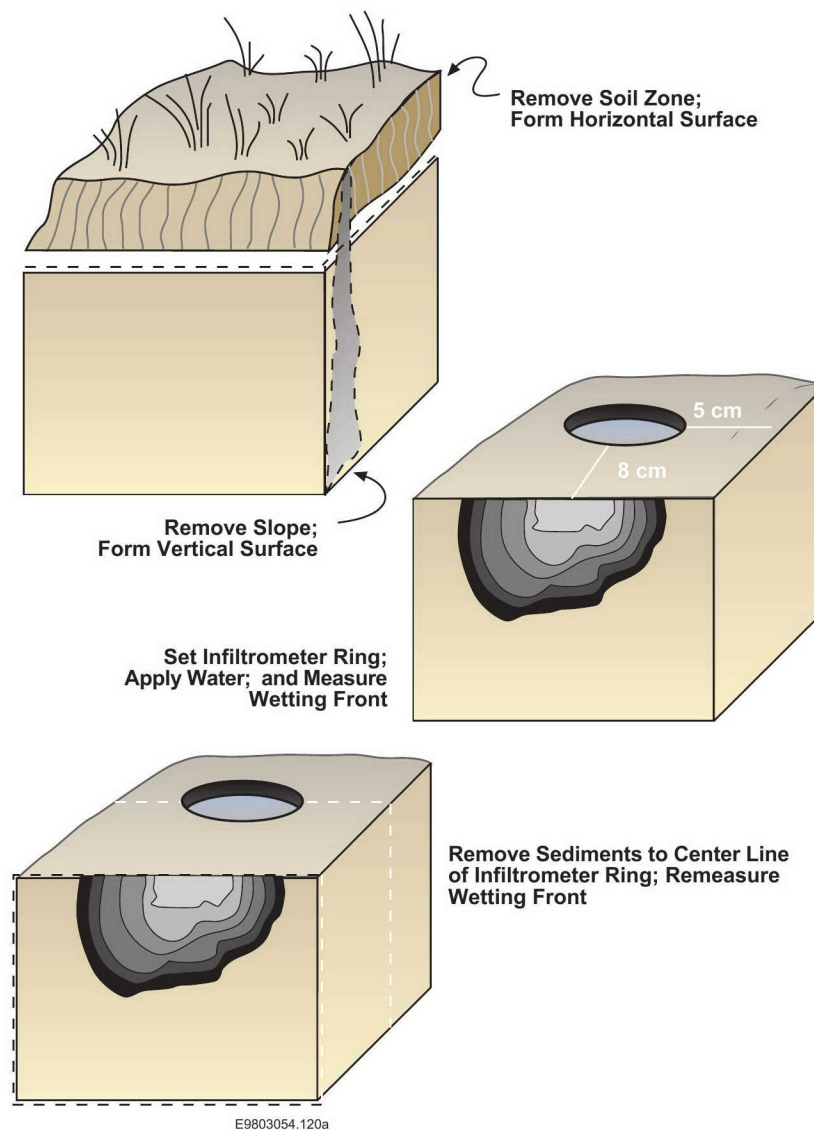


Figure 9-3: General schematic of small-scale infiltration test.

9.4 SMALL-SCALE INFILTRATION TESTS

Selection of Test Sites

- The criteria for site selection were as follows:
 - Walking distance (about 150 m) to road access
 - Horizontal surface to support infiltrometer and vertical exposure to observe moisture front
 - Variety of geographical locations and stratigraphic positions for testing
 - Variety of relationships between clastic injection dikes and host sediments
 - Variety of physical characteristics (e.g., grain size, sorting, shears) of clastic injection dikes.
- The small-scale infiltration test sites that were selected for this study include:

1. Brynes Road	7/32-36G
2. Keene/Kennedy Road	9/28-22M
3. Kiona Railroad Cut	9/27-19G
4. Webber Canyon Road	9/27-33C
- Source: This study.

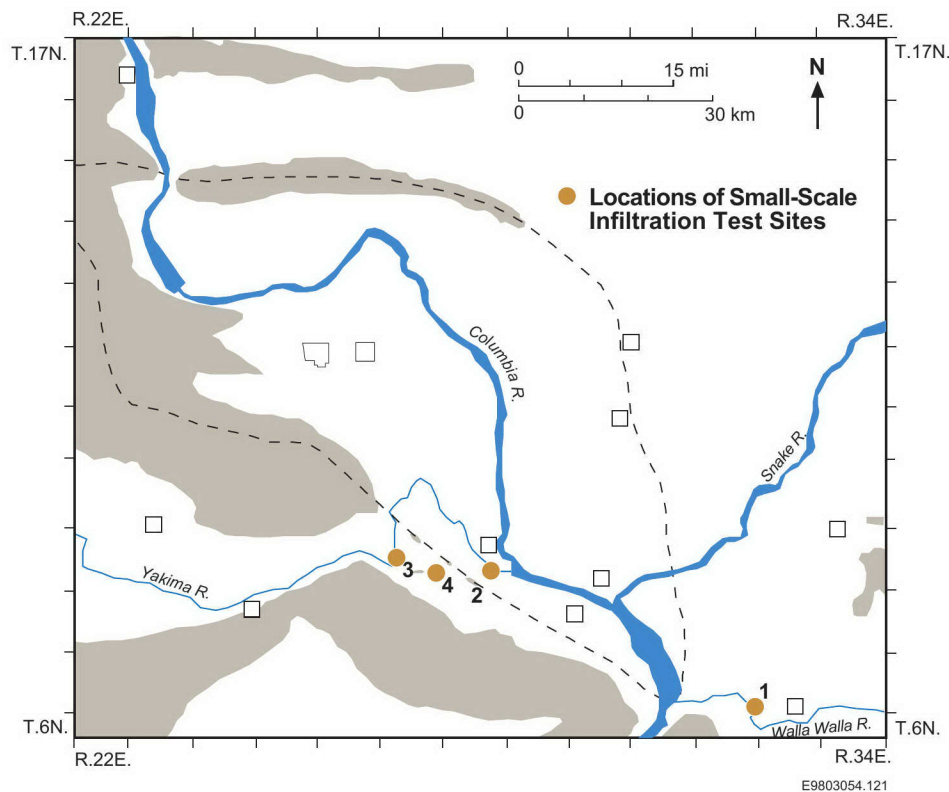


Figure 9-4: Map showing the locations of small-scale infiltration tests.

9.4 SMALL-SCALE INFILTRATION TESTS

Infiltration Test #1

- Purpose: Test #1 was designed to evaluate the variability of infiltration rates through laminated and poorly sorted infilling units within a single clastic injection dike.
- Location: Keene/Kennedy Road (9/28-22M).
- Test Area: An infiltrometer ring was placed across 5 of 13 infilling units centered on a 65-cm-wide dike. The dike occurs in the sand facies (field mapping unit #2) of the Hanford Formation. The dike and host sediment are pre-Wisconsin age. All infilling units contain unconsolidated sediments that are poorly sorted and either cross-laminated or massive.
- Results:
 - The wetting front moved laterally along each of the five infilling units at the same initial velocity of 1×10^{-4} to 2×10^{-4} m/sec.
 - After about 1 hour, the velocity was 3×10^{-5} to 4×10^{-5} m/sec through the end of the 3-hour test.
 - The wetting front moved vertically and laterally in both the massive and the laminated infilling units at about the same velocity (3×10^{-5} to 4×10^{-5} m/sec).

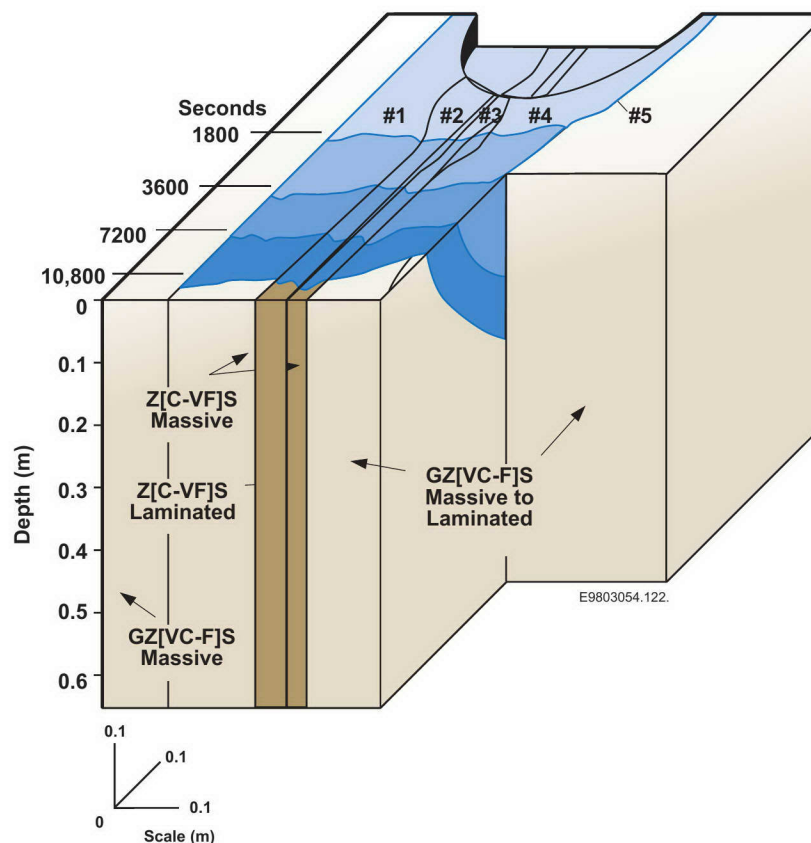


Figure 9-5: Schematic illustrating the corrected results of infiltration test #1.

9.4 SMALL-SCALE INFILTRATION TESTS

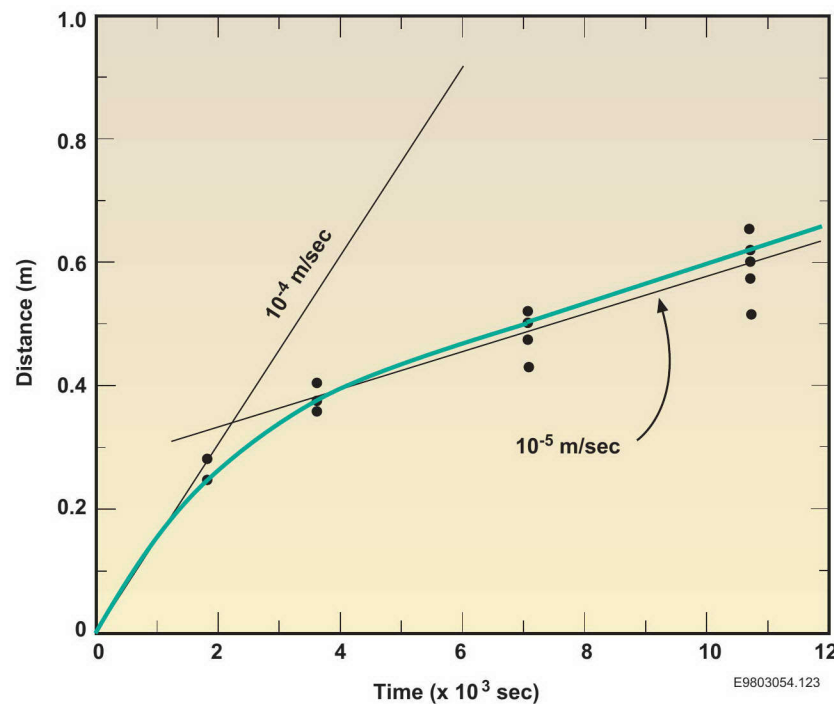
Infiltration Test #1 (Continued)

- Results (Continued)
 - The wetting front did not cross the 3-mm-wide clay/silt linings bounding the outer two infilling units to which water was applied over the duration of the test (10800 sec). This indicates a velocity across linings of less than 1×10^{-7} m/sec.

Table 9-9: Wetting front measurements (corrected) and resulting rates of infiltration for infiltration test #1.

Lateral Wetting Front Measurements						
Time (sec)	#1	#2	#3	#4	#5	Cumulative Liters
	Distance from Ring (m)					
1,800	0.25	0.28	0.28	0.28	0.25	5.7
3,600	0.38	0.38	0.41	0.38	0.36	13.2
7,200	0.51	0.53	0.51	0.48	0.43	24.6
10,800	0.61	0.63	0.66	0.58	0.51	36.0
Initial rate (m/sec)	1×10^{-4}	2×10^{-4}	2×10^{-4}	2×10^{-4}	1×10^{-4}	
3-hour rate (m/sec)	4×10^{-5}	4×10^{-5}	4×10^{-5}	3×10^{-5}	3×10^{-5}	

Figure 9-6: Graph of wetting front measurements (corrected) versus time for infiltration test #1. The 10^{-4} and 10^{-5} m/sec lines are included for reference.



9.4 SMALL-SCALE INFILTRATION TESTS

Infiltration Test #2

- Purpose: Test #2 was designed to evaluate the variability of infiltration rates for laminated infilling units with various grain sizes.
- Location: Kiona Railroad Cut (9/27-19G).
- Test Area: An infiltrometer ring was placed across 2 of 12 infilling groups* near the middle of a 1-m-wide dike. The dike occurs in the sand facies (field mapping unit #3) of the Hanford Formation. The dike and host sediment are Wisconsin in age. All infilling units contain sediments that are unconsolidated, moderately well sorted, cross-laminated or massive, and vary in grain size across the infilling unit groups.
- The test site contains several other dike components including shears, small-scale faults, and slumps.

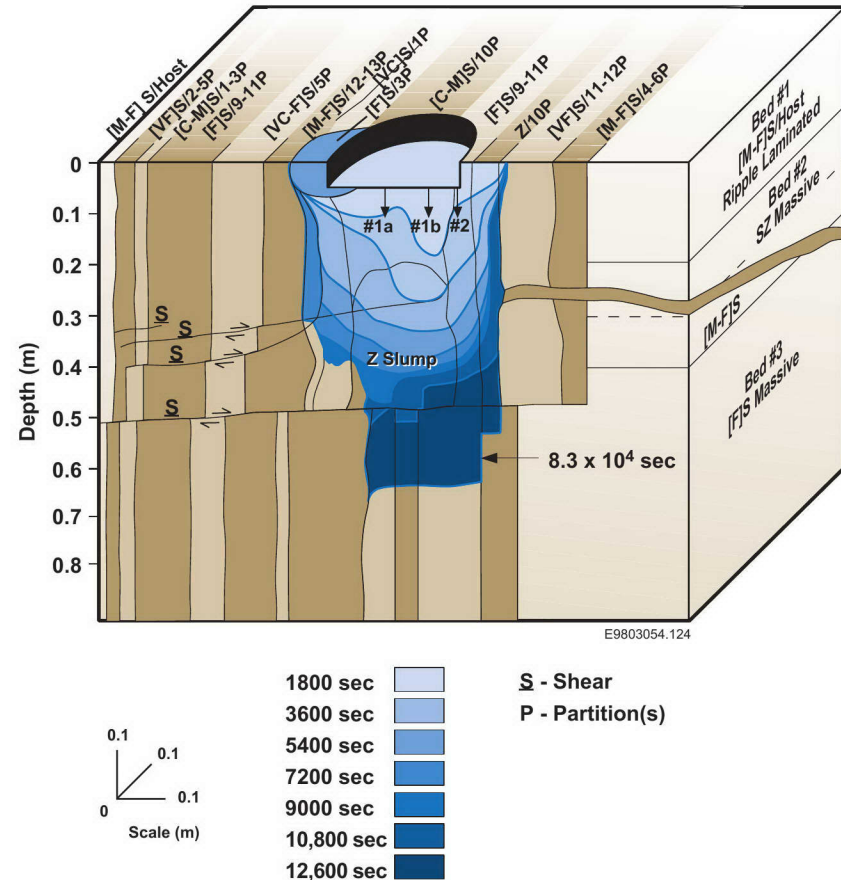


Figure 9-7: Schematic illustrating the corrected results of infiltration test #2.

* Infilling group is several adjacent infilling units with similar textural and bedding characteristics. Individual units within infilling groups are separated by silt/clay linings.

9.4 SMALL-SCALE INFILTRATION TESTS

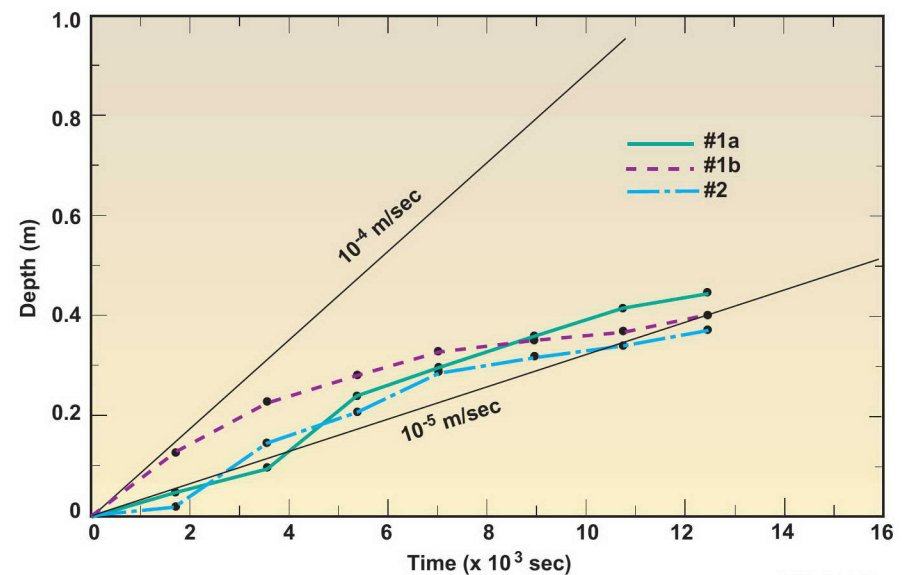
Infiltration Test #2 (Continued)

- Results:
 - The wetting front moved vertically within each infilling group at slightly different rates depending on bedding characteristics and grain size, but at an average rate of 3×10^{-5} m/sec during the 3.5-hour test.
 - The wetting front was temporarily impeded vertically at each encounter with a shear or a slump. The time delay was the same as required to cross distinct grain-size boundaries associated with adjacent laminations in infilling units.
 - On the left side of the dike, the front (1) initially moved laterally across the infilling-unit groups through the [VC]S/1P infilling unit at the same rate as the vertical velocity (3×10^{-5} m/sec), then (2) decreased across the [M-F]S/12-13P infilling-unit group to 3×10^{-6} m/sec.
 - On the right side of the dike, the front moved laterally across the Z/10P infilling group at a velocity of 6×10^{-6} m/sec.

Table 9-10: Wetting front measurements (corrected) and resulting rates of infiltration for infiltration test #2.

Vertical Wetting Front Measurements				
Time (sec)	#1a	#1b	#2	Cumulative Liters
	Distance from Ring (m)			
1,800	0.05	0.13	0.03	6.8
3,600	0.10	0.23	0.15	8.7
5,400	0.26	0.28	0.23	11.4
7,200	0.30	0.33	0.30	14.4
9,000	0.36	0.36	0.33	17.0
10,800	0.43	0.38	0.36	18.9
12,600	0.46	0.41	0.38	22.7
Initial rate (m/sec)	3×10^{-5}	7×10^{-5}	2×10^{-5}	
3.5-hour rate (m/sec)	3×10^{-5}	3×10^{-5}	3×10^{-5}	

Figure 9-8: Graph of vertical wetting front measurements (corrected) versus time for infiltration test #2.



E9803054.125

9.4 SMALL-SCALE INFILTRATION TESTS

Infiltration Test #3

- Purpose: Test #3 was designed to evaluate the variability of infiltration rates among infilling units that have uniform, well-sorted and massive texture and are free of structural features (e.g., slumps, shears, small-scale faults, rip-up clasts, contorted bed forms).
- Location: Keene/Kennedy Road (9/28-22M).
- Test Area: An elongated infiltrometer ring was placed across the two infilling units that comprise an 8-cm-wide dike. The clastic injection dike is associated with the silt facies (field mapping unit #3) of the Hanford Formation and is Wisconsin in age. The dike occurs in a sand facies (field mapping unit #2) sequence that is pre-Wisconsin in age. All infilling units contain unconsolidated sediments that are well-sorted, texturally homogeneous, and free of structural disturbances.
- Results:
 - The wetting front moved vertically and laterally along infilling units at an initial velocity of 2×10^{-4} m/sec, before decreasing to a rate of 4×10^{-5} m/sec.

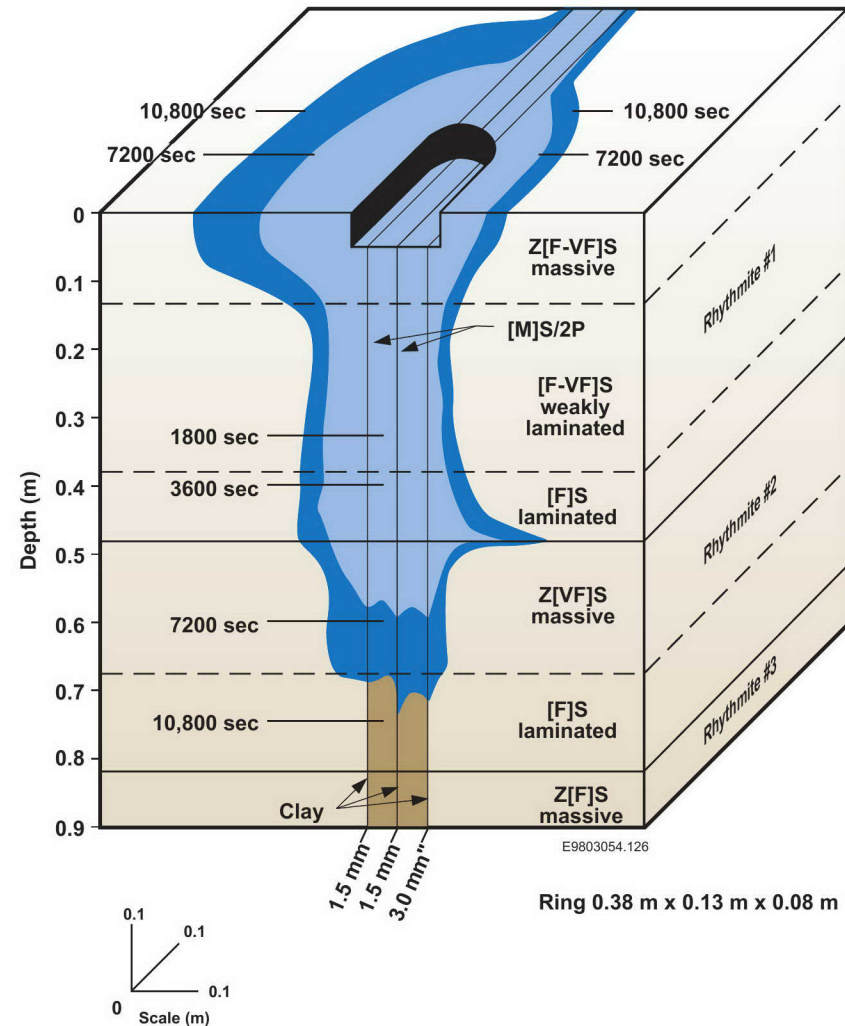


Figure 9-9: Schematic illustrating the corrected results of infiltration test #3.

9.4 SMALL-SCALE INFILTRATION TESTS

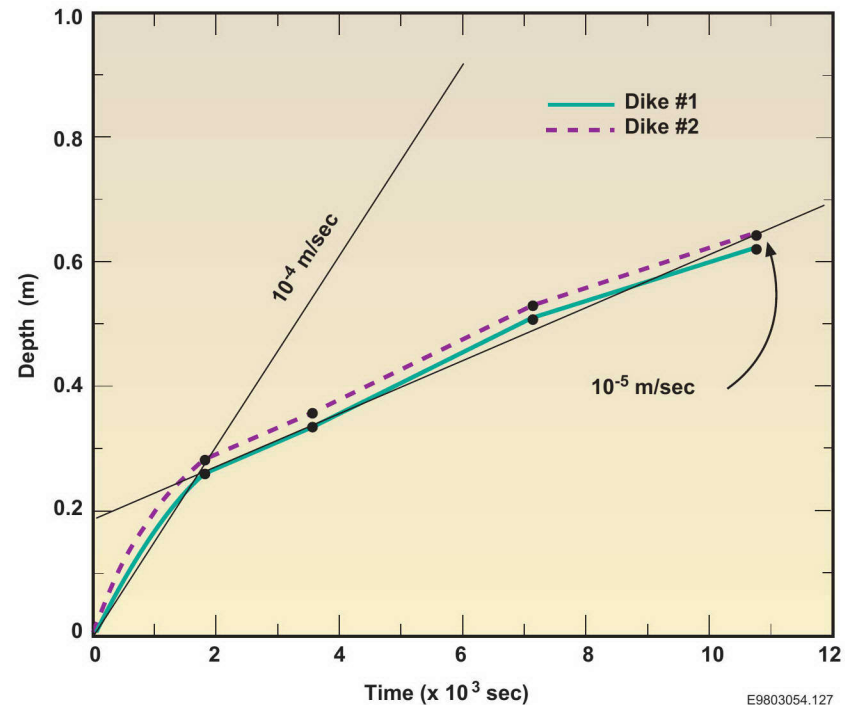
Infiltration Test #3 (Continued)

- Results (Continued):
 - The wetting front moved laterally and vertically in the upper part of rhythmite #1 at a rate of 3×10^{-5} m/sec.
 - The wetting front moved laterally from the left side of the dike into the host sediments at a rate of 1×10^{-5} m/sec.
 - The front moved laterally from the right side of the dike into the host sediments at a rate of 8×10^{-6} m/sec, except at the upper contact of rhythmite #2 where the rate increased to 3×10^{-5} m/sec, before again moving at 8×10^{-6} m/sec.
 - The wetted soil column was calculated to be very near saturation assuming 40% porosity for sediments in both the dike and the surrounding host sediments.

Vertical Wetting Front Measurements			
Time (sec)	#1	#2	Cumulative Liters
	Distance from Ring (m)		
1,800	0.27	0.28	13.2
3,600	0.35	0.35	24.6
7,200	0.52	0.53	37.9
10,800	0.63	0.64	53.0
<hr/>			
Initial rate (m/sec)	2×10^{-4}	2×10^{-4}	
<hr/>			
3-hour rate (m/sec)	4×10^{-5}	4×10^{-5}	
<hr/>			

Table 9-11: Wetting front measurements (corrected) and the resulting rates of moisture movement for infiltration test #3.

Figure 9-10: Graph of wetting front measurements (corrected) versus time for infiltration test #3.



E9803054.127

9.4 SMALL-SCALE INFILTRATION TESTS

Infiltration Test #4

- Purpose: Test #4 was designed to evaluate variability of infiltration rates between fine-grained sediments in infilling units and fine-grained host sediments.
- Location: Webber Canyon Road (9/27-33C).
- Test Area: An infiltrometer ring was placed across an 8-cm-wide dike with multiple thin infilling units (partitions) and a fine-grained host unit surrounding the dike. The dike occurs in a silt facies (field mapping unit #3) of the Hanford Formation. The dike and sediments are Wisconsin in age. The infilling units are unconsolidated and moderately well sorted. Shears occur in the host sediments next to the left side of the dike.
- Results:
 - The wetting front moved vertically and laterally away from the infiltrometer ring in the host sediments at a rate of between 1×10^{-5} to 2×10^{-5} m/sec throughout the 3-hour test.
 - The wetting front moved vertically within the dike at the same vertical and lateral rates as in the host sediments.

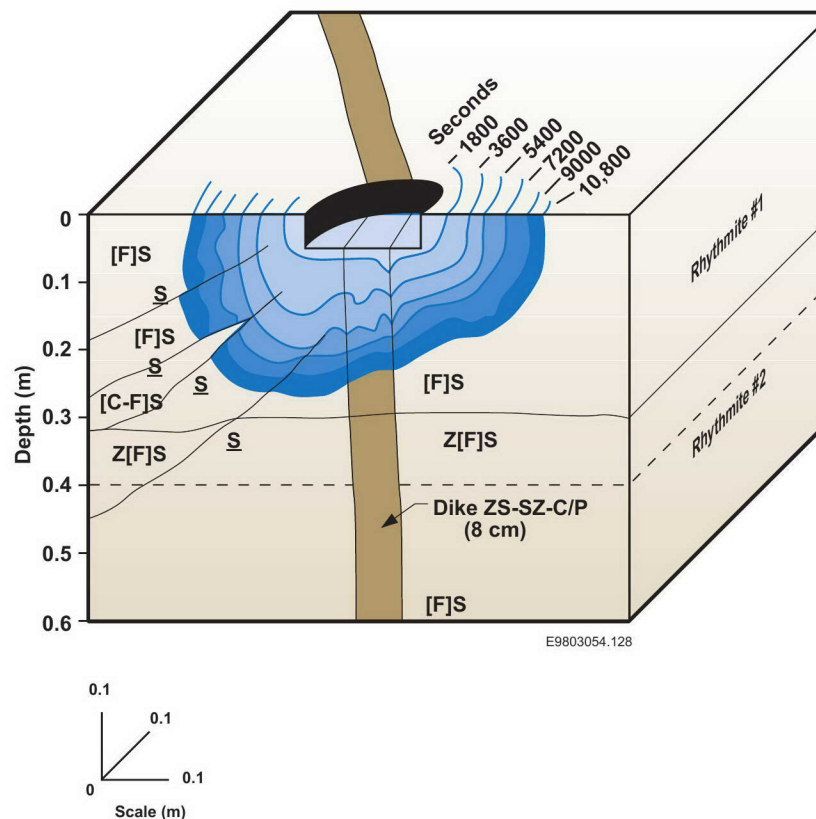


Figure 9-11: Schematic illustrating the corrected results of infiltration test #4.

9.4 SMALL-SCALE INFILTRATION TESTS

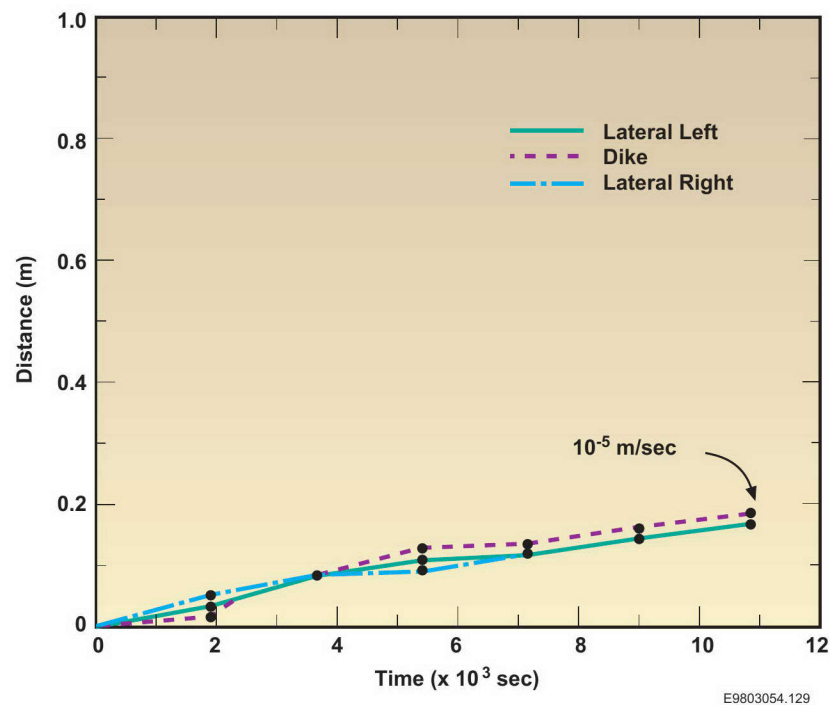
Infiltration Test #4 (Continued)

- Results (Continued):
 - Shears in the host sediments affected the rate of movement of the wetting front. At one location, moisture was channeled between two closely spaced shears and, at another location, moisture moved around sediments bounded by shears.
 - The soil column approached saturated conditions, assuming 40% porosity for sediments in the dike and surrounding host sediments.

Table 9-12: Wetting front measurements (corrected) and the resulting rates for moisture infiltration for infiltration test #4.

Wetting Front Measurements				
Time (sec)	Lateral Left	Dike	Lateral Right	Cumulative Liters
	Distance from Ring (m)			
1,800	0.03	0.02	0.04	3.8
3,600	0.08	0.08	0.08	6.8
5,400	0.11	0.12	0.10	8.7
7,200	0.13	0.14	0.13	10.6
9,000	0.15	0.16	0.15	12.9
10,800	0.17	0.18	0.17	14.4
Initial rate (m/sec)	2×10^{-5}	1×10^{-5}	2×10^{-5}	
3-hour rate (m/sec)	2×10^{-5}	2×10^{-5}	1×10^{-5}	

Figure 9-12: Graph of wetting front measurements (corrected) versus time for infiltration test #4.



9.4 SMALL-SCALE INFILTRATION TESTS

Infiltration Test #5

- Purpose: Test #5 was designed to evaluate variability of infiltration rates between fine-grained sediments in infilling units and fine-grained sediments in surrounding host.
- Location: Byrnes Road (7/32-36G).
- Test Area: An infiltrometer ring was placed across a 20-mm-wide dike containing multiple thin infilling units and all within a fine-grained host. The dike occurs in the silt facies (field mapping unit #3) of the Hanford Formation. The dike and host sediments are Wisconsin in age. The infilling units are unconsolidated and moderately well sorted. A small, thin laminated dikelet (3 mm) merges with the larger dike.
- Results:
 - The wetting front moved vertically and laterally away from the infiltrometer ring in the host sediments at an initial rate between 1×10^{-5} and 3×10^{-5} m/sec.
 - The wetting front moved vertically within the dike at the same rate as the vertical movement in the host sediments.

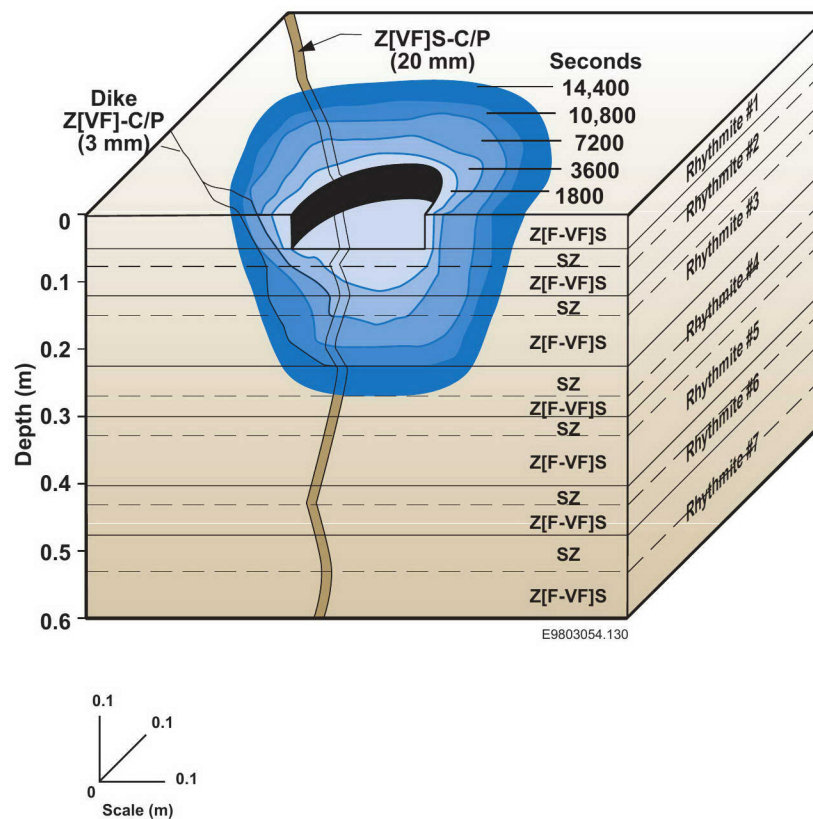


Figure 9-13: Schematic illustrating the corrected results of infiltration test #5.

9.4 SMALL-SCALE INFILTRATION TESTS

Infiltration Test #5 (Continued)

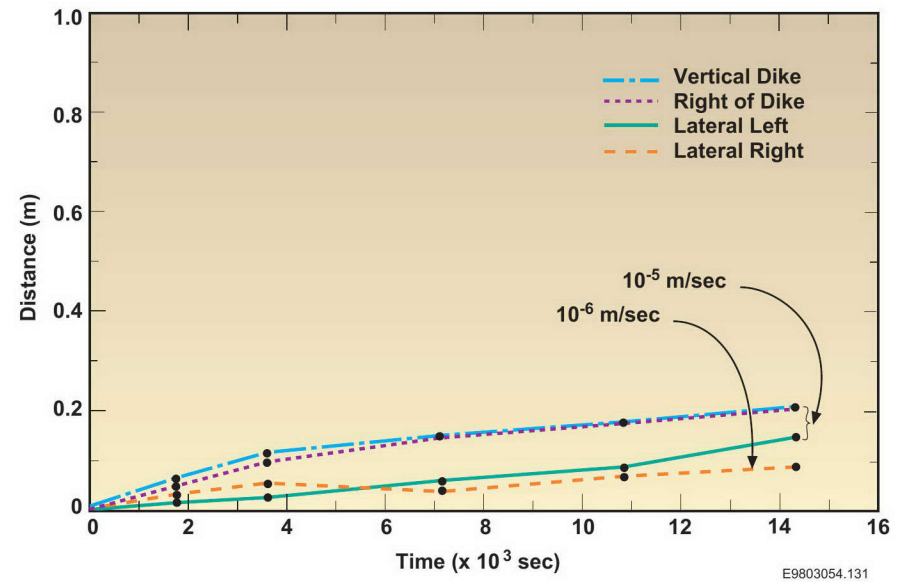
- Results (Continued):
 - The wetting front moved laterally to the right of the infiltrometer ring at a rate of 1×10^{-5} m/sec through the end of the 4-hour test. The lateral movement to the left was at a rate of 4×10^{-6} m/sec through the end of the test.
 - The rate of movement did not appear to be affected as the moisture front moved across a 3-mm-wide dikelet located to the left of the infiltrometer ring.

Table 9-13: Wetting front measurements (corrected) and the resulting rates of infiltration for infiltration test #5.

Time (sec)	Wetting Front Measurements				Cumulative Liters
	Vertical		Lateral		
	Dike	Right of Dike	Left	Right	
	Distance from Ring (m)				
1,800	0.04	0.06	0.03	0.01	3.8
3,600	0.10	0.11	0.05	0.02	5.7
7,200	0.15	0.15	0.05	0.07	9.5
10,800	0.18	0.18	0.07	0.09	ND
14,400	0.22	0.22	0.08	0.15	ND
Initial rate (m/sec)	2×10^{-5}	3×10^{-5}	2×10^{-5}	1×10^{-5}	
4-hour rate (m/sec)	1×10^{-5}	1×10^{-5}	4×10^{-5}	1×10^{-5}	

ND = not determined

Figure 9-14: Graph of wetting front measurements (corrected) versus time for infiltration test #5.



9.4 SMALL-SCALE INFILTRATION TESTS

Infiltration Test #6

- Purpose: Test #6 was designed to evaluate variability of infiltration rates between fine-grained sediments in infilling units and a fine-grained surrounding host.
- Location: Webber Canyon Road (9/27-33C).
- Test Area: An infiltrometer ring was placed across a 13-mm-wide dike containing multiple thin infilling units and a fine-grained host surrounding the dike. The dike bifurcates about 0.1 m beneath the surface of the test area. The dike occurs in the silt facies (field mapping unit #3) of the Hanford Formation. The dike and host sediment are Wisconsin in age. The infilling units are unconsolidated and well sorted.
- Results:
 - The wetting front moved down and to the right more rapidly than to the left because (1) the position of the infiltrometer ring was not centered over the dike, and (2) moisture flow was impeded by the dikes.
 - The wetting front moved vertically and laterally between 1×10^{-5} and 3×10^{-5} m/sec on the right side of the vertical dike.

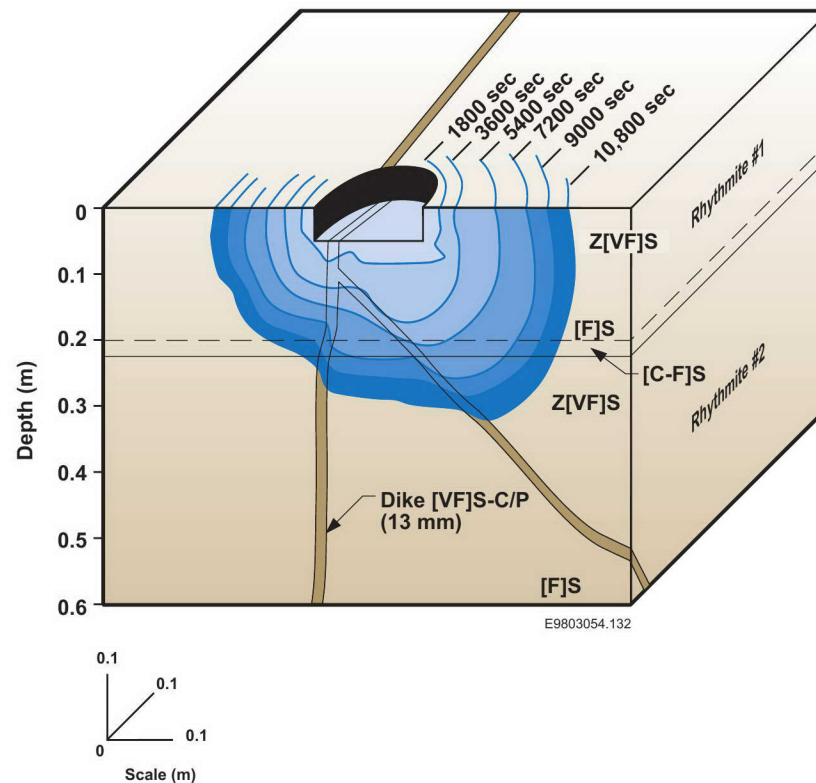


Figure 9-15: Schematic illustrating the corrected results of infiltration test #6.

9.4 SMALL-SCALE INFILTRATION TESTS

Infiltration Test #6 (Continued)

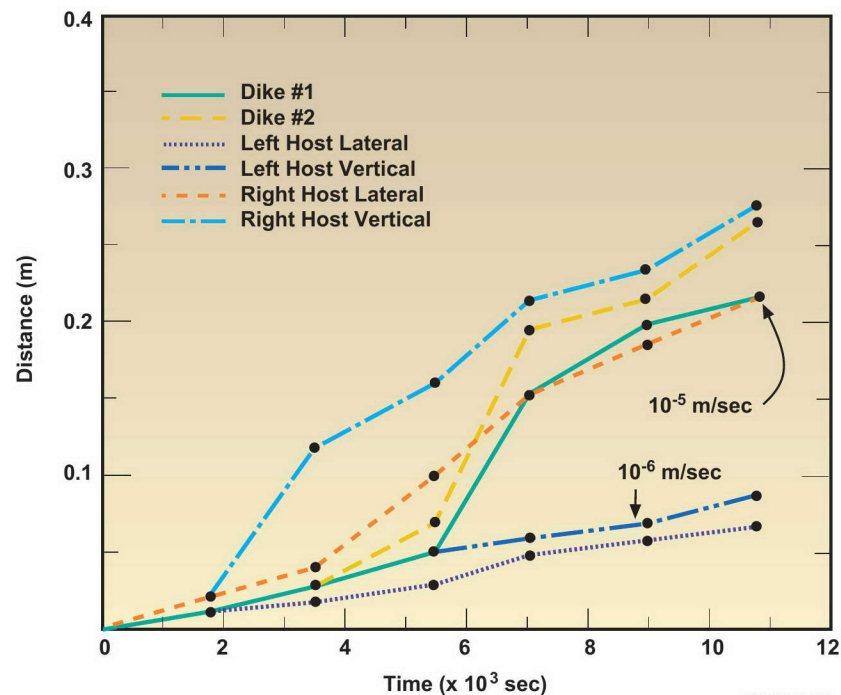
- Results:
 - On the left side of the vertical dike, the wetting front moved vertically and laterally between 6×10^{-6} and 9×10^{-6} m/sec.
 - The wetting front moved along the inclined dike at the same rate as in the host sediments to the right of the vertical dike (i.e., 10^{-5} m/sec).
 - The wetting front moved at different rates within the vertical dike. The rate of movement in the infilling units on the right side of the dike was 3×10^{-5} m/sec. The rate of movement in the units on the left side of the vertical dike was the same as the rates in the host sediments on that side of the dike (i.e., 9×10^{-6} m/sec).

Table 9-14: Wetting front measurements (corrected) and the resulting rates of infiltration for infiltration test #6.

Figure 9-16: Graph of wetting front measurements (corrected) versus time for infiltration test #6.

Wetting Front Measurements							
Time (sec)	Dike #1	Dike #2	Left Host Lateral	Left Host Vertical	Right Host Lateral	Right Host Vertical	Cumulative Liters
1,800	0.01	N/A	0.01	0.01	0.02	0.02	5.7
3,600	0.03	0.03	0.02	0.03	0.04	0.12	9.5
5,400	0.05	0.07	0.03	0.05	0.10	0.16	11.4
7,200	0.16	0.20	0.05	0.06	0.16	0.21	15.1
9,000	0.20	0.22	0.06	0.07	0.19	0.24	19.9
10,800	0.22	0.27	0.07	0.09	0.22	0.28	23.7
Initial rate (m/sec)	6×10^{-6}	--	6×10^{-6}	6×10^{-6}	1×10^{-5}	1×10^{-5}	
3-hour rate (m/sec)	2×10^{-5}	3×10^{-5}	7×10^{-6}	9×10^{-6}	2×10^{-5}	3×10^{-5}	

N/A = not applicable



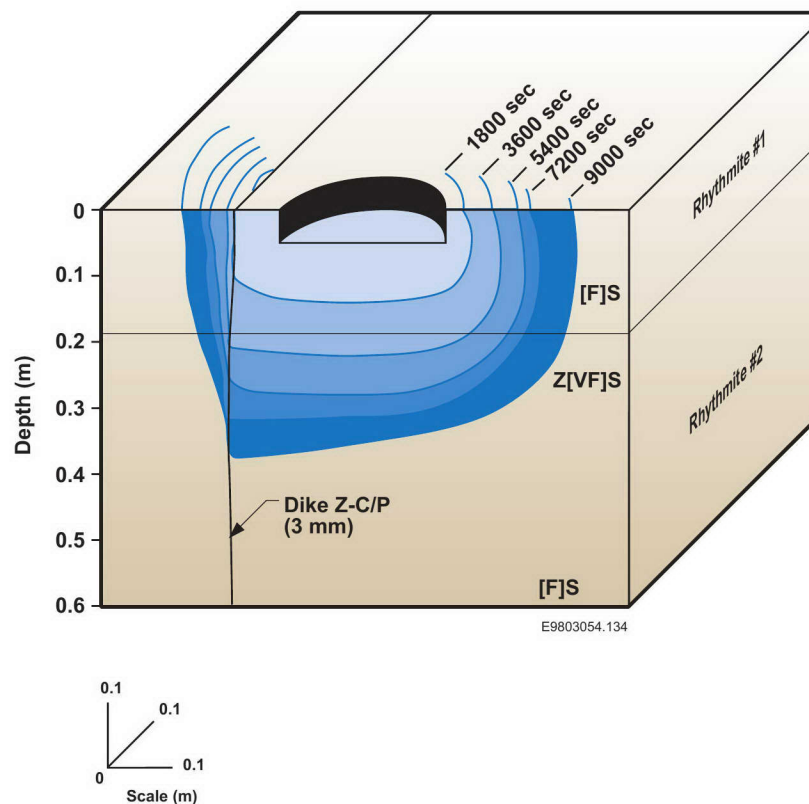
E9803054.133

9.4 SMALL-SCALE INFILTRATION TESTS

Infiltration Test #7

- Purpose: Test #7 was designed to evaluate the lateral migration of a wetting front across a thin, fine-grained dike in a fine-grained host sediment.
- Location: Webber Canyon Road (9/27-33C).
- Test Area: An infiltrometer ring was placed 6 cm to the right of a 3-mm-wide, thinly laminated, fine-grained dike. The dike occurs in the silt facies (field mapping unit #3) of the Hanford Formation. The dike and host sediment are Wisconsin in age. All sediments are unconsolidated and moderately well sorted.
- Results:
 - The wetting front moved vertically and laterally to the right in the host sediments at a rate of 2×10^{-5} to 4×10^{-5} m/sec.
 - The wetting front was not impeded by the sharp bedding contact between the two rhythmites.
 - The wetting front was impeded by the dike; the front slowed to approximately 9×10^{-6} m/sec through the dike and into the host sediments to the left of the dike.

Figure 9-17: Schematic illustrating the corrected results of infiltration test #7.



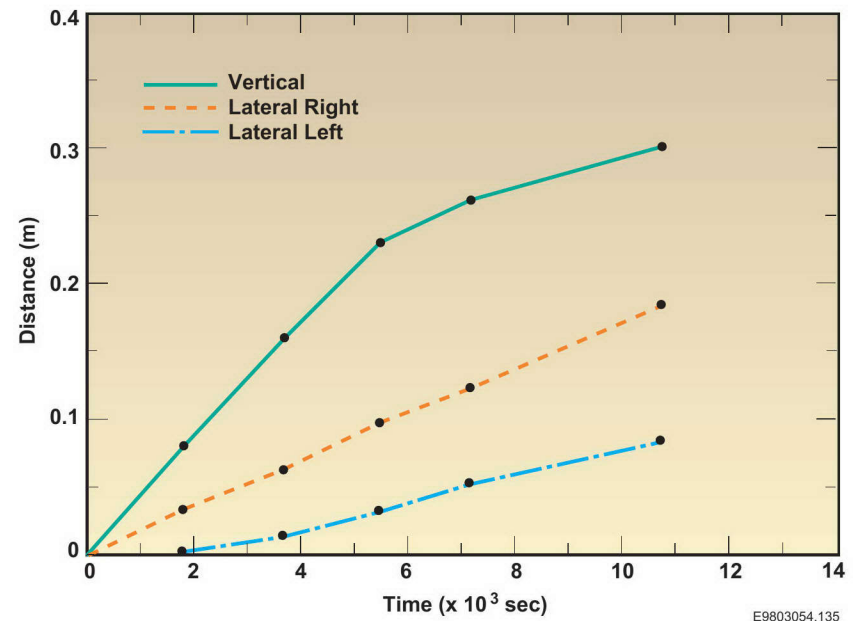
9.4 SMALL-SCALE INFILTRATION TESTS

Infiltration Test #7 (Continued)

Table 9-15: Wetting front measurements (corrected) and the resulting rates of moisture movement for infiltration test #7.

Time (sec)	Wetting Front Measurements			Cumulative Liters
	Vertical	Right Lateral	Left Lateral (Left of Dike)	
	Distance from Ring (m)			
1,800	0.08	0.03	--	5.7
3,600	0.16	0.06	0.00	9.5
5,400	0.23	0.10	0.03	12.3
7,200	0.26	0.12	0.05	15.1
10,800	0.30	0.18	0.08	20.8
Initial rate (m/sec)	4×10^{-5}	2×10^{-5}	--	
3-hour rate (m/sec)	2×10^{-5}	2×10^{-5}	$\sim 9 \times 10^{-5}$	

Figure 9-18: Graph of wetting front measurements (corrected) versus time for infiltration test #7.



9.4 SMALL-SCALE INFILTRATION TESTS

Infiltration Test #8

- Purpose: Test #8 was designed to evaluate the lateral migration of a wetting front across a thin, fine-grained dike that is surrounded by a coarse-grained host sediment.
- Location: Kiona Railroad Cut (9/27-19G).
- Test Area: An infiltrometer ring was placed 6 cm to the left of a 6-mm-wide, thinly laminated, fine-grained dike. The dike occurs in a sand facies (field mapping unit #3) of the Hanford Formation. The dike and host sediments are Wisconsin in age. All sediments are unconsolidated and moderately well sorted.
- Results:
 - The wetting front moved vertically within the host sediments at an initial rate of 1×10^{-4} m/sec.
 - The wetting front moved vertically within the host sediments at a rate of 2×10^{-5} m/sec throughout the 1.25-hour test.
 - The front spread laterally along a thin silt unit capping the lower sedimentary bed of the host sediment.

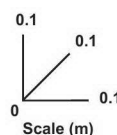
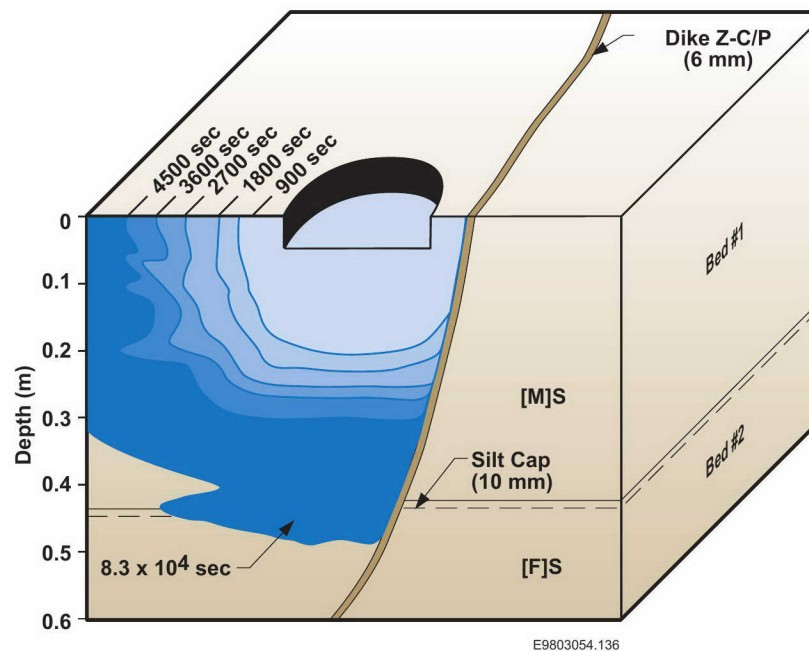


Figure 9-19: Schematic illustrating the corrected results of infiltration test #8.

9.4 SMALL-SCALE INFILTRATION TESTS

Infiltration Test #8 (Continued)

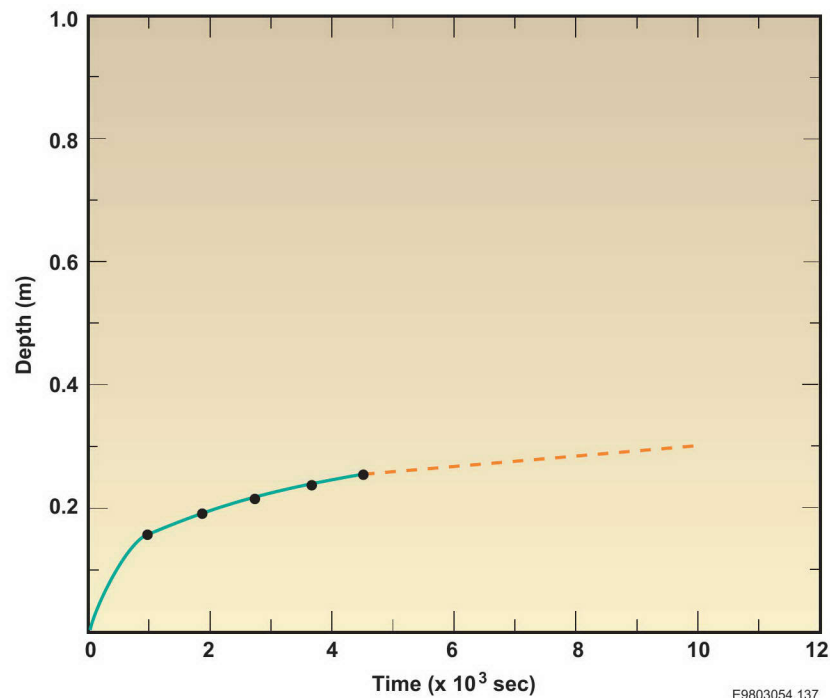
- Results (Continued):
 - The wetting front did not move laterally into the dike or into the host sediments to the right of the dike during the application of water to the infiltrometer or during the continued drainage which was recorded up to 8.3×10^4 sec after the initial water application. The velocity across the silt/clay lining and dike is less than 3×10^{-7} m/sec.

Table 9-16: Wetting front measurements (corrected) and resulting rates of moisture movement for infiltration test #8.

Figure 9-20: Graph of wetting front measurements (corrected) versus time for infiltration test #8.

Wetting Front Measurements		
Time (sec)	Distance from Ring (m)	Cumulative Liters
900	0.16	5.7
1,800	0.19	8.7
2,700	0.21	11.4
3,600	0.23	13.2
4,500*	0.25	15.1
8.3×10^4	0.43	N/A
Initial rate (m/sec)		1×10^{-4}
3-hour rate (m/sec)		2×10^{-5}

*Last application of water into infiltrometer ring.
N/A = not applicable



E9803054.137

9.4 SMALL-SCALE INFILTRATION TESTS

Infiltration Test #9

- Purpose: Test #9 was designed to evaluate the lateral migration of a wetting front across a moderately wide dike with different grain sizes in the infilling units and a host sediment with multiple textural units.
- Location: Kiona Railroad Cut (9/27-19G).
- Test Area: An infiltrometer ring was placed 12 cm to the left of a 12- to 20-mm-wide, thinly laminated, fine-grained dike with three textural units. The dike has three infilling unit groups within the sand facies (field mapping unit #3) of the Hanford Formation. The dike and host sediment are Wisconsin in age. All sediments are unconsolidated and moderately well sorted.
- Results:
 - The wetting front moved vertically at an initial rate of 4×10^{-5} m/sec in the first bed.
 - The downward rate of movement was slightly impeded at the top of the third bed. The overall vertical rate of movement throughout the 3.5-hour test was 3×10^{-5} m/sec.
 - The wetting front moved to the left at slightly different rates depending on textural variations in the bedding, but the front moved at a rate of approximately 3×10^{-5} m/sec throughout the 3.5-hour test. This is the same rate as the vertical movement.

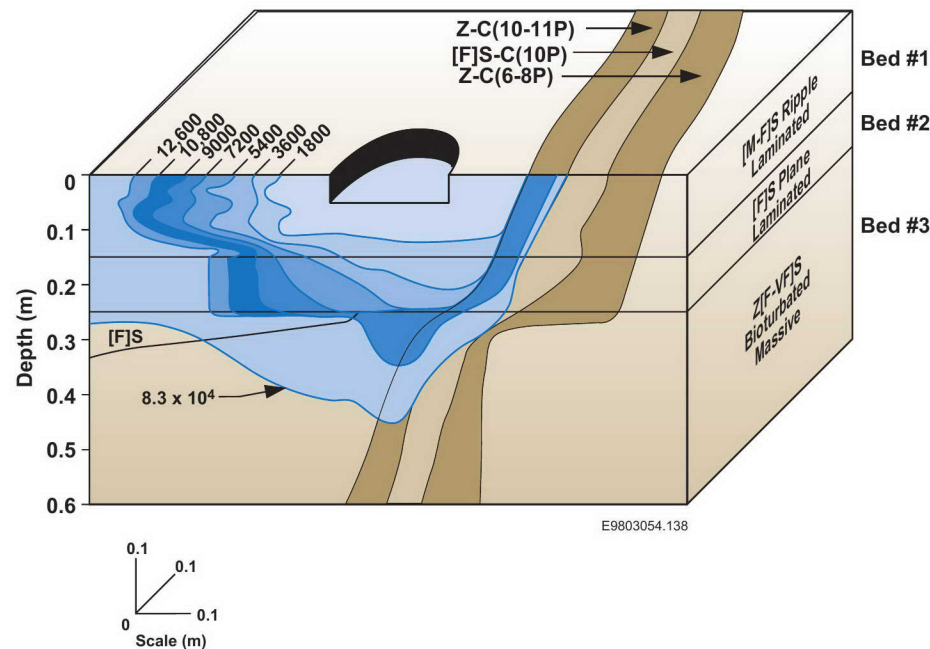


Figure 9-21: Schematic illustrating the corrected results of infiltration test #9.

9.4 SMALL-SCALE INFILTRATION TESTS

Infiltration Test #9 (Continued)

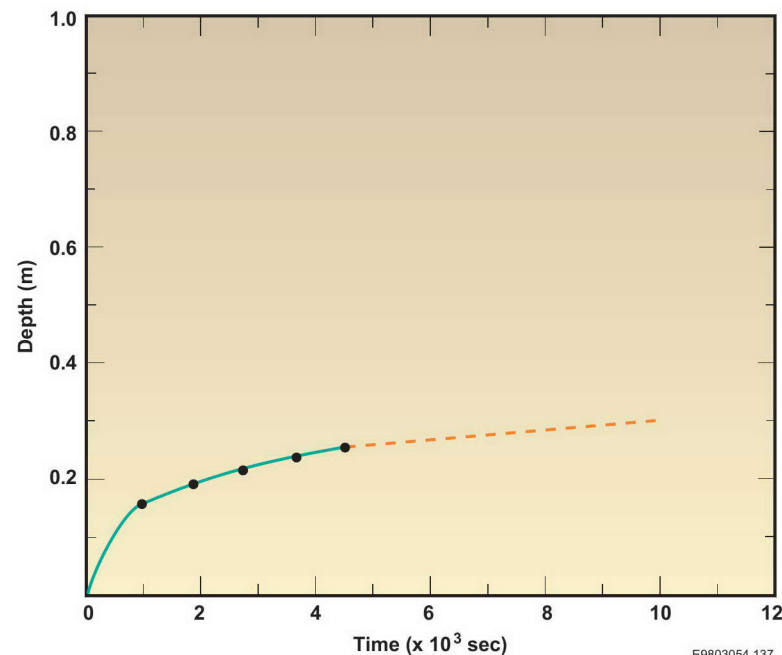
- Results (Continued):
 - The wetting front moved laterally to the right at a rate similar to the vertical and left lateral rates until the front encountered the dike.
 - The wetting front moved laterally into the left infilling group and a portion of the middle infilling group at a rate of 8×10^{-6} m/sec as water was being applied to the infiltrometer during the test.
 - The wetting front did not penetrate into the right infilling unit group of the dike or into the host sediments on the opposite side of the dike from the infiltrometer during the test.
 - Moisture moved down the left infilling unit group during the drainage period.

Table 9-17: Wetting front measurements (corrected) and the resulting rates of moisture movement for infiltration test #9.

Figure 9-22: Graph of wetting front measurements (corrected) versus time for infiltration test #9.

Wetting Front Measurements				
Time (sec)	Lateral Left	Vertical	Lateral Right	Cumulative Liters
	Distance from Ring (m)			
1,800	0.09	0.08	0.13	5.7
3,600	0.14	0.15	0.13	8.7
5,400	0.18	0.20	0.13	13.2
7,200	0.23	0.29	0.13	15.1
9,000	0.26	0.29	0.13	17.8
10,800	0.31	0.29	0.13	20.8
12,600*	0.36	0.29	0.18	22.7
8.3×10^{-4}	>0.50	0.39	0.22	N/A
Initial rate (m/sec)	5×10^{-5}	4×10^{-5}	7×10^{-5}	
3.5-hour rate (m/sec)	3×10^{-5}	3×10^{-5}	8×10^{-6}	

*Last application of water into infiltrometer ring.
N/A = not applicable



E9803054.137

9.5 UNSATURATED FLOW APPARATUS (UFA™) METHOD - MOISTURE

Test Plan

- Objective: The UFA method was selected to measure the unsaturated hydraulic conductivity across silt/clay linings of clastic injection dikes.
- Equipment: UFA instrument, which consists of an ultracentrifuge with a constant ultraflow pump that provides fluid to the sample surface through a rotating seal assembly and microdispersal system. The UFA is used to rapidly determine unsaturated hydraulic conductivity over a range of water content for each sample. The method uses an open-flow centrifuge system to achieve hydraulic steady state for sediments with low water contents.

General Procedure:

- Extract intact core sample from sedimentary unit.

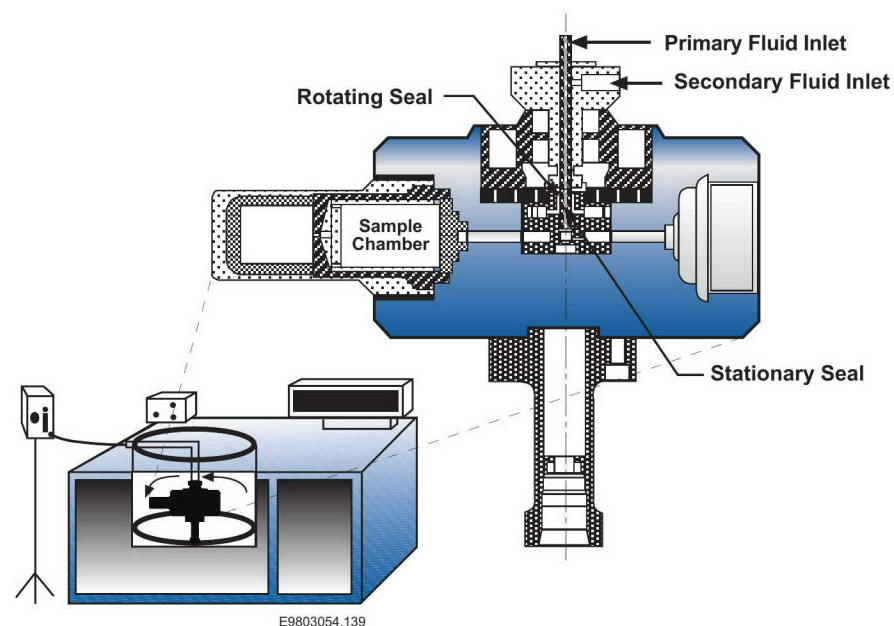
Note: Care must be taken in the collection of samples so as not to disturb the integrity of the delicate structures being sampled from clastic injection dikes (e.g., clay/silt linings, laminations).

- Place core sample directly into UFA Lexan sample container and seal with gas-tight cap.
- Determine the density of the core sample by:

$$D = \frac{W_s}{V_c}$$

where W_s = weight of the sample core (g)

V_c = volume of the Lexan container (cm³)



- Place sample in UFA instrument, progressively desaturate sample, measure changes, and record data.
- Develop characteristic curve [i.e., hydraulic conductivity (cm/sec) versus volumetric water content (percentage)].

Note: Moisture retention curves were not developed as part of this test plan. These curves need to be included in the design of tests to measure hydraulic properties of clastic injection dikes.

- Sources: Conca and Wright (1990, 1992).

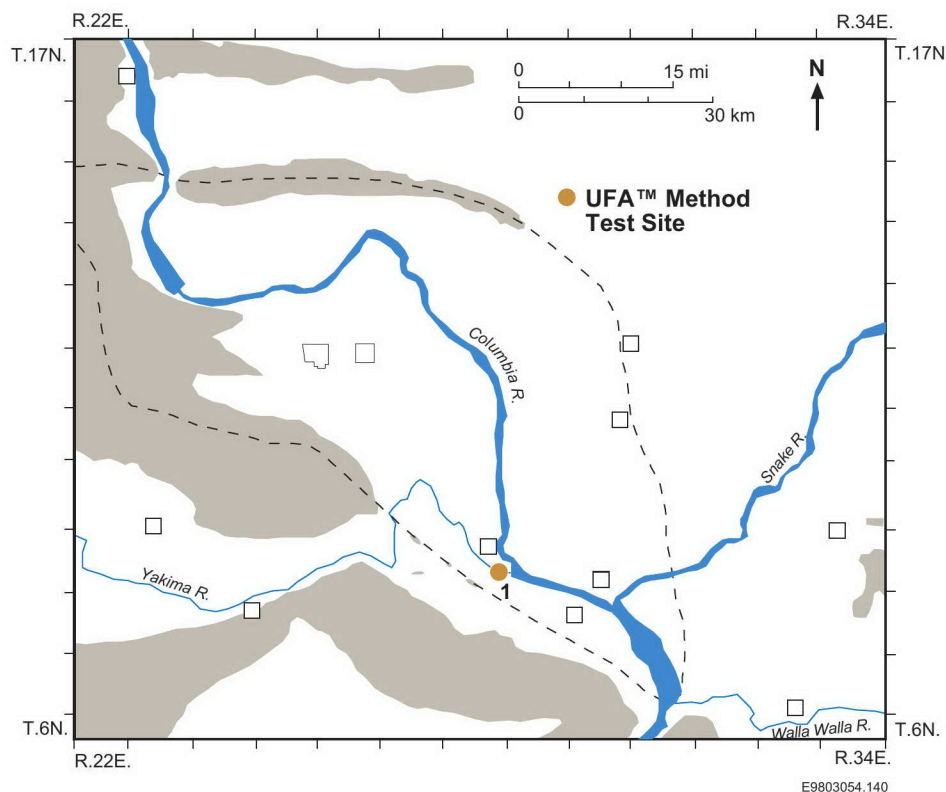
Figure 9-23: Schematic of UFA Hy-Sed 100 Rotor with mechanical seal design (modified from Wright et al. 1994).

9.5 UNSATURATED FLOW APPARATUS (UFA™) METHOD - MOISTURE

Selection of Test Site

- One site was selected for sampling of silt/clay linings of clastic injection dikes. The Keene/Kennedy Road dike network (9/28-22M) was selected because of the then ongoing clastic injection dike investigations at that site.
- The lower unit of the host sediment was a plane-laminated sand sequence from the sand facies (field mapping unit #2) of the Hanford Formation. The unit is pre-Wisconsin, Pleistocene in age. The upper host unit is a finely bedded upward fining medium sand to sandy silt unit that is Wisconsin, Pleistocene in age.
- The clastic injection dikes are part of a polygonal-patterned ground dike network. The dikes are associated with the silt facies (field mapping unit #3) of the Hanford Formation, and are Wisconsin, Pleistocene in age.
- Source: This study.

Figure 9-24: Map showing the location of the samples collected for measuring unsaturated hydraulic conductivity using the UFA method.

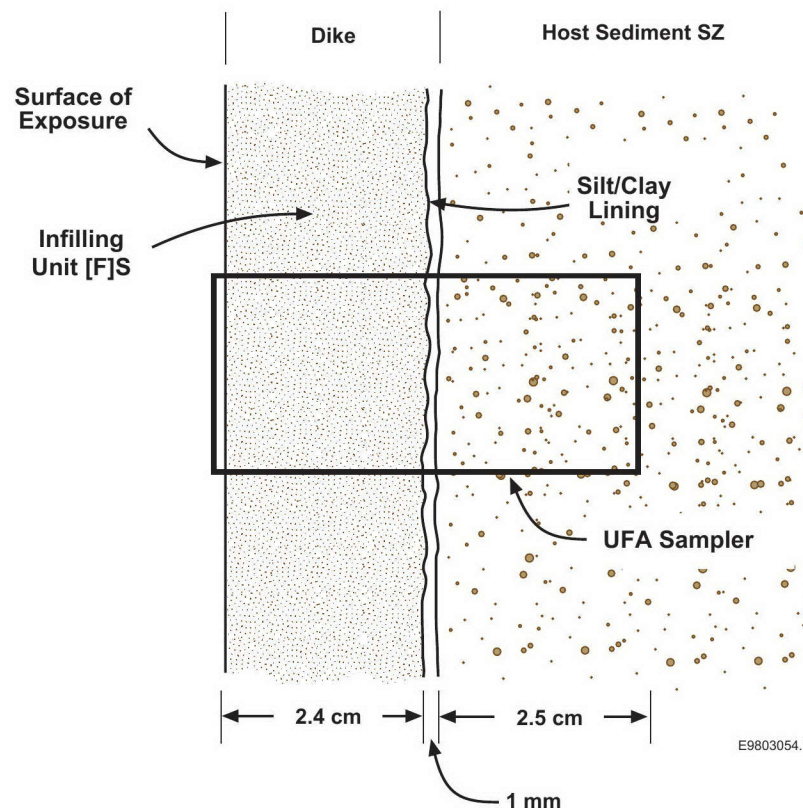


9.5 UNSATURATED FLOW APPARATUS (UFA™) METHOD - MOISTURE

UFA Test #1

- Purpose: The test was designed to measure the hydraulic conductivity across a thin silt/clay lining, bounded by relatively well-sorted, massive, unconsolidated sediments.
- Location: Keene/Kennedy Road (9/28-22M).
- Test Area: A core sampler (3 cm in diameter by 5 cm in length) was driven into an infilling unit, through thin silt/clay lining, and into the host sediment. The infilling unit is an unconsolidated fine sand that is well sorted, uniform in texture, and free of structural disturbances. The silt/clay lining is 1 mm thick. The surface of the silt/clay lining is flat, smooth, and free of undulations or structural features. The infilling unit and silt/clay lining are associated with the silt facies (field mapping unit #3) and are Wisconsin in age. The host sediment is a moderately well-sorted, weakly laminated, unconsolidated sandy silt. The host sediment is the sand facies (field mapping unit #2) and is pre-Wisconsin in age.

Figure 9-25: Cross-section of the sample site for UFA test #1.



**9.5 UNSATURATED FLOW APPARATUS (UFA™)
METHOD - MOISTURE**

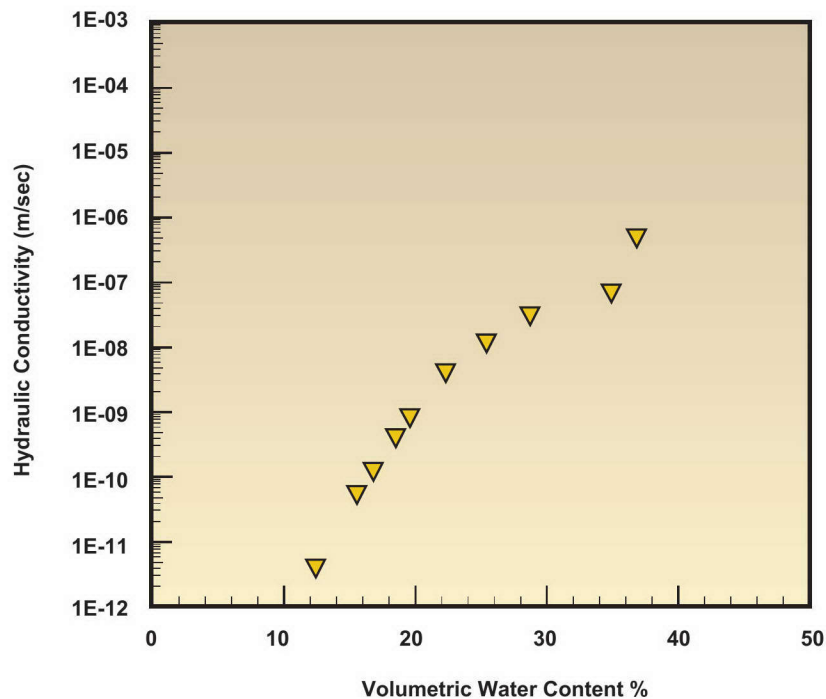
UFA Test #1 (Continued)

- Results:
 - Density of core, 1.58 g/cm³
 - Hydraulic conductivities are shown in Table 9-18 and Figure 9-26.

Table 9-18: Volumetric water content and hydraulic conductivity for UFA test #1.

Volumetric Water Content (%)	Hydraulic Conductivity (m/sec)
36.86	4.90 x 10 ⁻⁷
34.90	7.36 x 10 ⁻⁸
28.76	3.31 x 10 ⁻⁸
25.40	1.24 x 10 ⁻⁸
22.33	4.14 x 10 ⁻⁹
19.62	8.28 x 10 ⁻¹⁰
18.50	4.14 x 10 ⁻¹⁰
16.62	1.28 x 10 ⁻¹⁰
15.26	5.30 x 10 ⁻¹¹
12.40	4.18 x 10 ⁻¹²

Figure 9-26: Graph of volumetric water content versus hydraulic conductivity for UFA test #1.



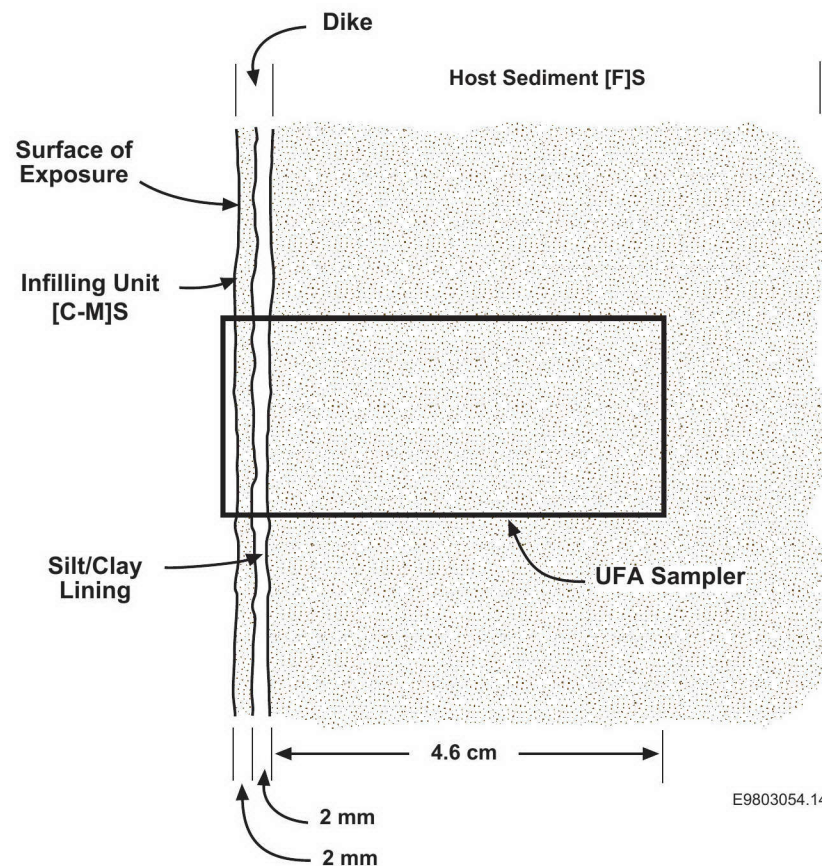
E9803054.142

9.5 UNSATURATED FLOW APPARATUS (UFA™) METHOD - MOISTURE

UFA Test #2

- Purpose: The test was designed to measure the hydraulic conductivity across a thin silt/clay lining, bounded by a relatively well-sorted, massive, unconsolidated sediment. The test was similar to UFA test #1.
- Location: Keene/Kennedy Road (9/28-22M).
- Test Area: A core sampler (3 cm in diameter by 5 cm in length) was driven into an infilling unit through a thin silt/clay lining and into the host sediment. The infilling unit is a thin, unconsolidated, coarse-to-medium sand that is well sorted, uniform in texture, and free of structural disturbances. The silt/clay lining is 2 mm thick. The surface of the silt/clay lining is flat and smooth, free of undulations or structural features. The infilling unit and silt/clay lining are associated with the silt facies (field mapping unit #3) of the Hanford Formation and are Wisconsin in age. The host sediment is a moderately well sorted, weakly laminated, unconsolidated fine sand. The host sediment is from the sand facies (field mapping unit #2) of the Hanford Formation and is pre-Wisconsin, Pleistocene in age.

Figure 9-27: Cross-section of the sample site for UFA test #2.



**9.5 UNSATURATED FLOW APPARATUS (UFA™)
METHOD - MOISTURE**

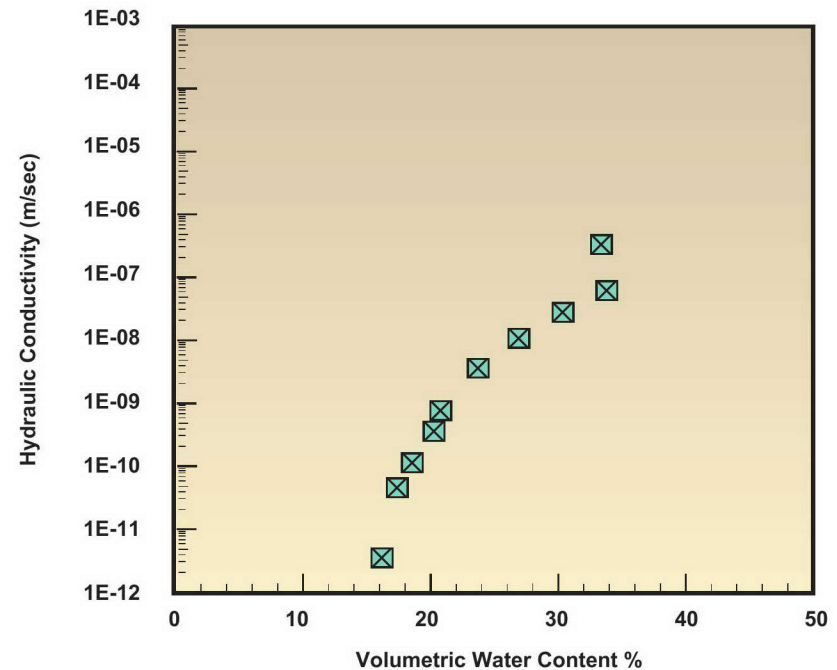
UFA Test #2 (Continued)

- Results:
 - Density of core, 1.55 g/cm³
 - Hydraulic conductivities are shown in Table 9-19 and Figure 9-28.

Table 9-19: Volumetric water content and hydraulic conductivities for UFA test #2.

Volumetric Water Content (%)	Hydraulic Conductivity (m/sec)
33.31	3.68 x 10 ⁻⁷
33.78	7.36 x 10 ⁻⁸
30.24	3.31 x 10 ⁻⁸
26.84	1.24 x 10 ⁻⁸
23.69	4.14 x 10 ⁻⁹
20.68	8.28 x 10 ⁻¹⁰
20.10	4.14 x 10 ⁻¹⁰
18.56	1.28 x 10 ⁻¹⁰
17.17	5.30 x 10 ⁻¹¹
16.01	4.18 x 10 ⁻¹²

Figure 9-28: Graph of volumetric water content versus hydraulic conductivity for UFA test #2.



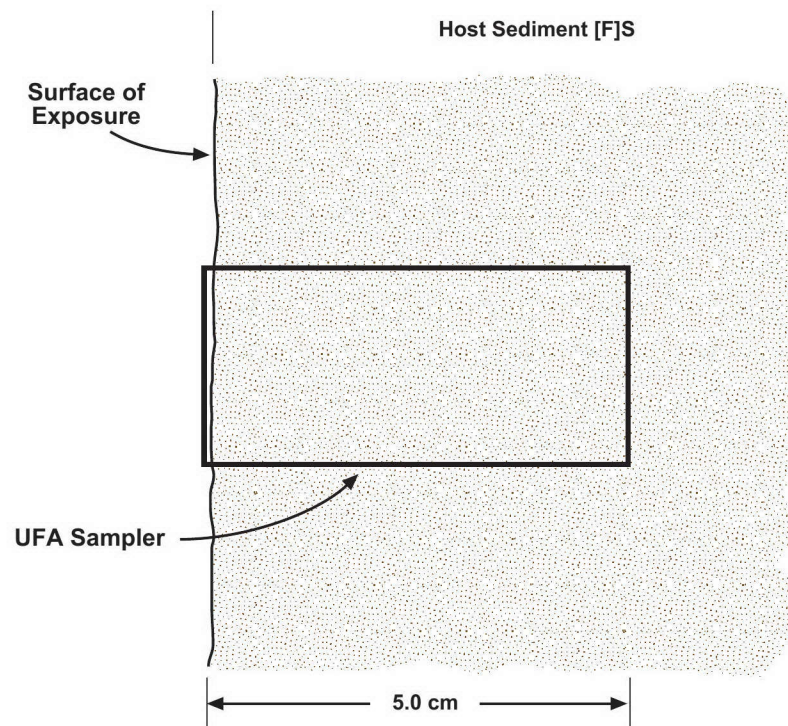
E9803054.144

9.5 UNSATURATED FLOW APPARATUS (UFA™) METHOD - MOISTURE

UFA Test #3

- Purpose: The test was designed to measure the hydraulic conductivity of the host sediments near the UFA tests #1, #2, #4, and #5.
- Location: Keene/Kennedy Road (9/28-22M).
- Test Area: A core sampler (3 cm in diameter by 5 cm in length) was driven into the lower sequence of host sediments at the site. The host sediments are part of the sand facies (field mapping unit #2) of the Hanford Formation. The sands are fine-grained, well-sorted, compact, and plane-laminated. The sediments are pre-Wisconsin, Pleistocene in age.

Figure 9-29: Cross-section of the sample site for UFA test #3.



E9803054.145

**9.5 UNSATURATED FLOW APPARATUS (UFA™)
METHOD - MOISTURE**

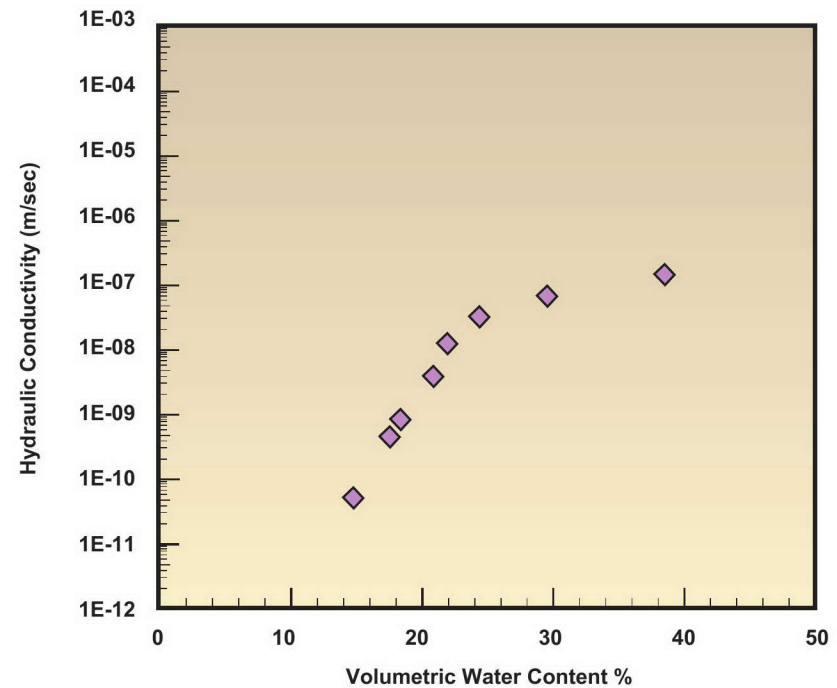
UFA Test #3 (Continued)

- Results:
 - Density of core, 1.47 g/cm³
 - Hydraulic conductivities are shown in Table 9-20 and Figure 9-30.

Volumetric Water Content (%)	Hydraulic Conductivity (m/sec)
38.45	1.66 x 10 ⁻⁷
29.53	7.36 x 10 ⁻⁸
24.33	3.31 x 10 ⁻⁸
21.71	1.24 x 10 ⁻⁸
20.74	4.14 x 10 ⁻⁹
18.36	8.28 x 10 ⁻¹⁰
17.45	4.14 x 10 ⁻¹⁰
15.93	1.25 x 10 ⁻¹⁰
14.83	5.30 x 10 ⁻¹¹

Table 9-20: Volumetric water content and hydraulic conductivities for UFA test #3.

Figure 9-30: Graph of volumetric water content and hydraulic conductivities for UFA test #3.



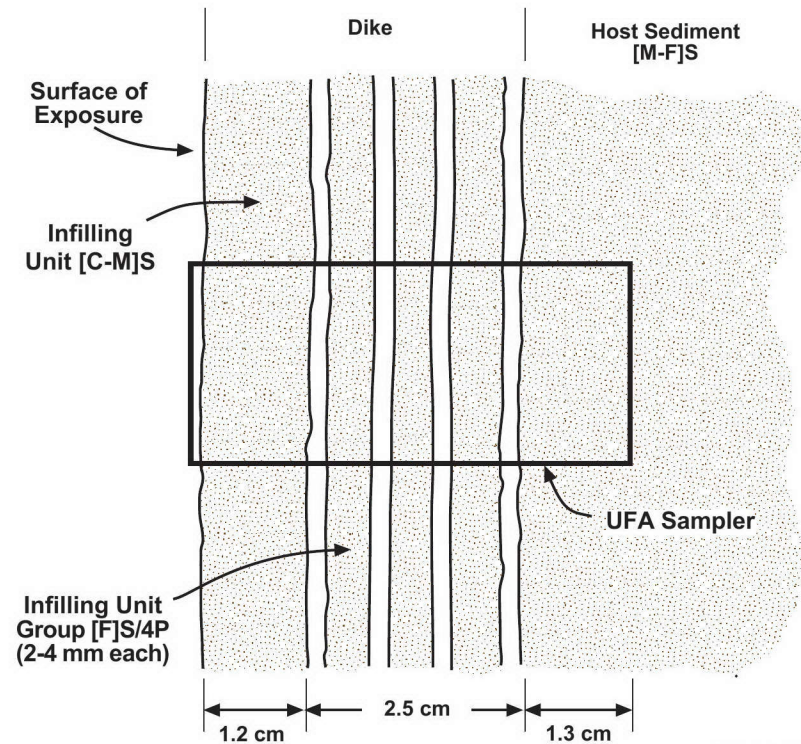
E9803054.146

9.5 UNSATURATED FLOW APPARATUS (UFA™) METHOD - MOISTURE

UFA Test #4

- Purpose: The test was designed to measure the hydraulic conductivity of silt/clay linings across infilling units and the dike wall.
- Location: Keene/Kennedy Road (9/28-22M).
- Test Area: A core sampler (3 cm in diameter by 5 cm in length) was driven into a coarse-to-medium sand infilling unit, through a fine sand and silt/clay lining infilling unit group, and into a medium-to-fine sand host sediment. The dike is associated with the silt facies (field mapping unit #3) of the Hanford Formation and is Wisconsin in age. The host sediment is the sand facies (field mapping unit #2) from the Hanford Formation and is pre-Wisconsin, Pleistocene in age.

Figure 9-31: Cross-section of sample site for UFA test #4.



E9803054.147

**9.5 UNSATURATED FLOW APPARATUS (UFA™)
METHOD - MOISTURE**

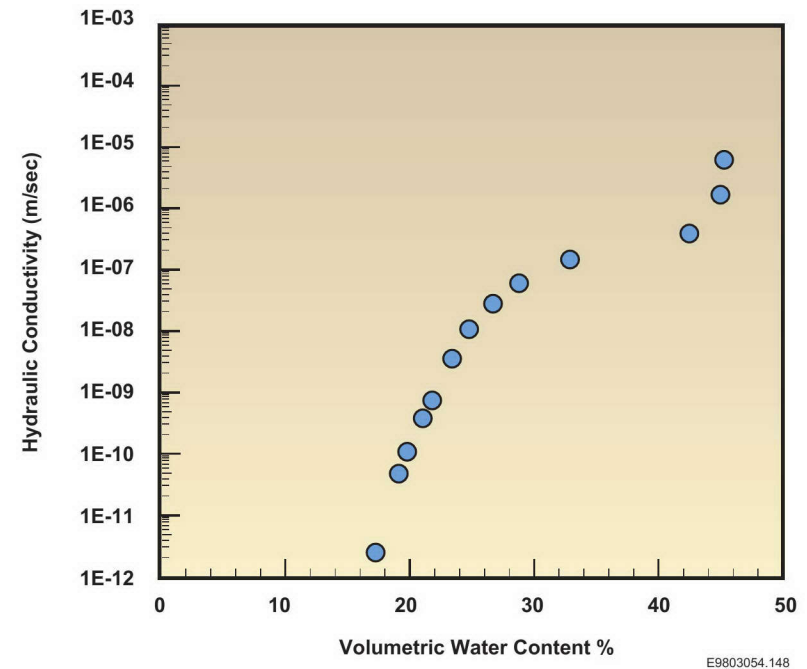
UFA Test #4 (Continued)

- Results:
 - Density of core, 1.39 g/cm³
 - Hydraulic conductivities are shown in Table 9-21 and Figure 9-32.

Table 9-21: Volumetric water content and hydraulic conductivity for UFA test #4.

Volumetric Water Content (%)	Hydraulic Conductivity (m/sec)
45.39	7.20 x 10 ⁻⁶
44.98	1.84 x 10 ⁻⁶
42.48	4.60 x 10 ⁻⁷
32.93	1.66 x 10 ⁻⁷
28.80	7.36 x 10 ⁻⁸
26.70	3.31 x 10 ⁻⁸
24.84	1.24 x 10 ⁻⁸
23.50	4.14 x 10 ⁻⁹
21.76	8.28 x 10 ⁻¹⁰
21.09	4.14 x 10 ⁻¹⁰
19.76	1.25 x 10 ⁻¹⁰
19.04	5.71 x 10 ⁻¹¹
17.01	2.91 x 10 ⁻¹²

Figure 9-32: Graph of volumetric water content versus hydraulic conductivities for UFA test #4.

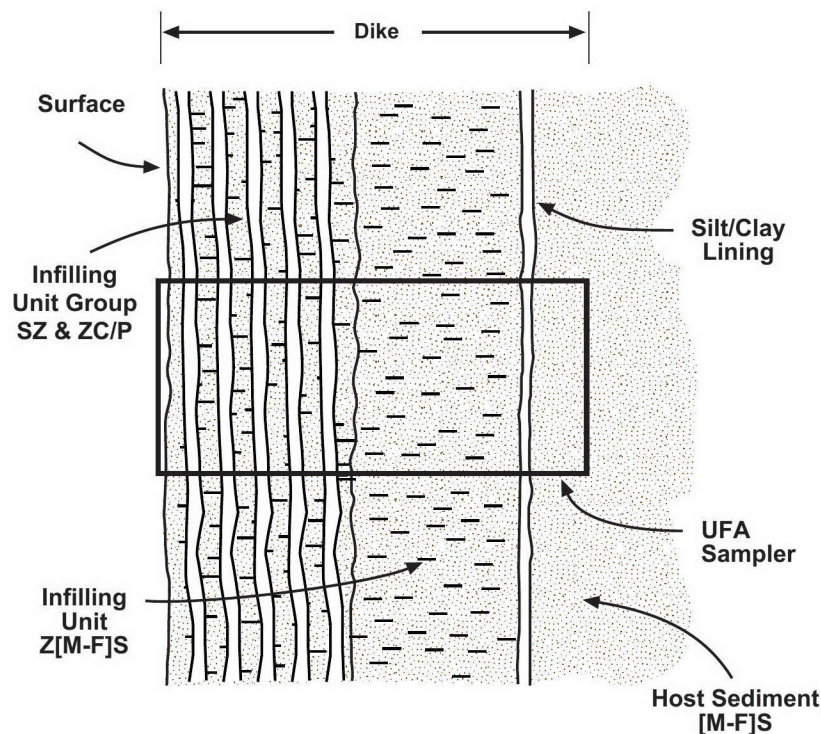


9.5 UNSATURATED FLOW APPARATUS (UFA™) METHOD - MOISTURE

UFA Test #5

- Purpose: The test was designed to measure the hydraulic conductivity across infilling units and silt/clay linings of a clastic injection dike.
- Location: Keene/Kennedy Road (9/28-22M).
- Test Area: A core sampler (3 cm diameter by 5 cm in length) was driven into a silty sand and silt/clay, finely partitioned infilling group, through a silty medium-to-fine sand infilling unit, through a thin silt/clay lining, and into a medium-to-fine sand host sediment. The dike is part of the silt facies (field mapping unit #3) of the Hanford Formation and is Wisconsin in age. The host sediment is the sand facies associated with field mapping unit #2 of the Hanford Formation and is pre-Wisconsin, Pleistocene in age.

Figure 9-33: Cross-section of sample site for UFA test #5.



E9803054.149

9.5 UNSATURATED FLOW APPARATUS (UFA™) METHOD - MOISTURE

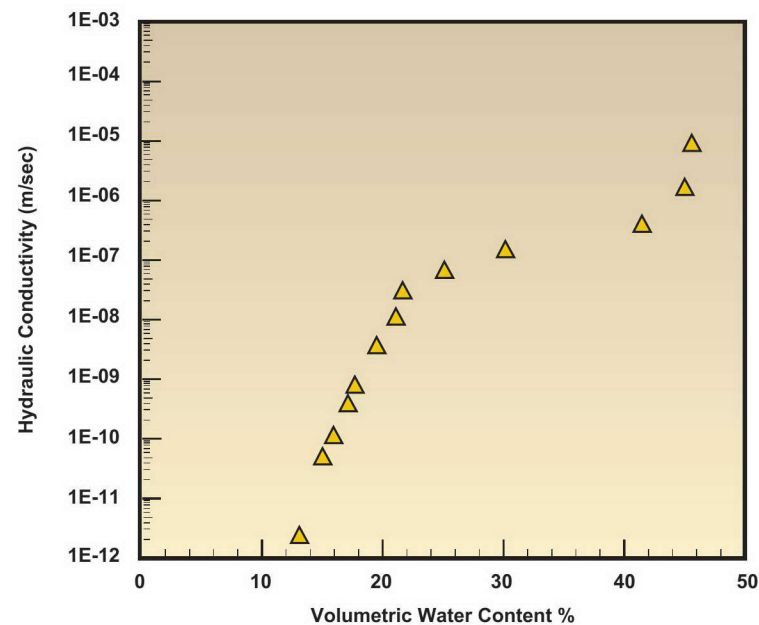
UFA Test #5 (Continued)

- Results:
 - Density of core, 1.39 g/cm³
 - Hydraulic conductivities are shown in Table 9-22 and Figure 9-34.

Table 9-22: Volumetric water content and hydraulic conductivity for UFA test #5.

Figure 9-34: Graph of volumetric water content versus hydraulic conductivity for UFA test #5.

Volumetric Water Content (%)	Hydraulic Conductivity (m/sec)
45.63	9.45 x 10 ⁻⁶
45.01	1.84 x 10 ⁻⁶
41.45	4.60 x 10 ⁻⁷
30.17	1.66 x 10 ⁻⁷
25.24	7.36 x 10 ⁻⁸
21.75	3.31 x 10 ⁻⁸
21.18	1.24 x 10 ⁻⁸
19.54	4.14 x 10 ⁻⁹
17.76	8.28 x 10 ⁻¹⁰
17.14	4.14 x 10 ⁻¹⁰
15.93	1.25 x 10 ⁻¹⁰
15.08	5.71 x 10 ⁻¹¹
13.01	2.91 x 10 ⁻¹²



E9803054.150

9.6 UNSATURATED FLOW APPARATUS (UFA™) METHOD - GAS

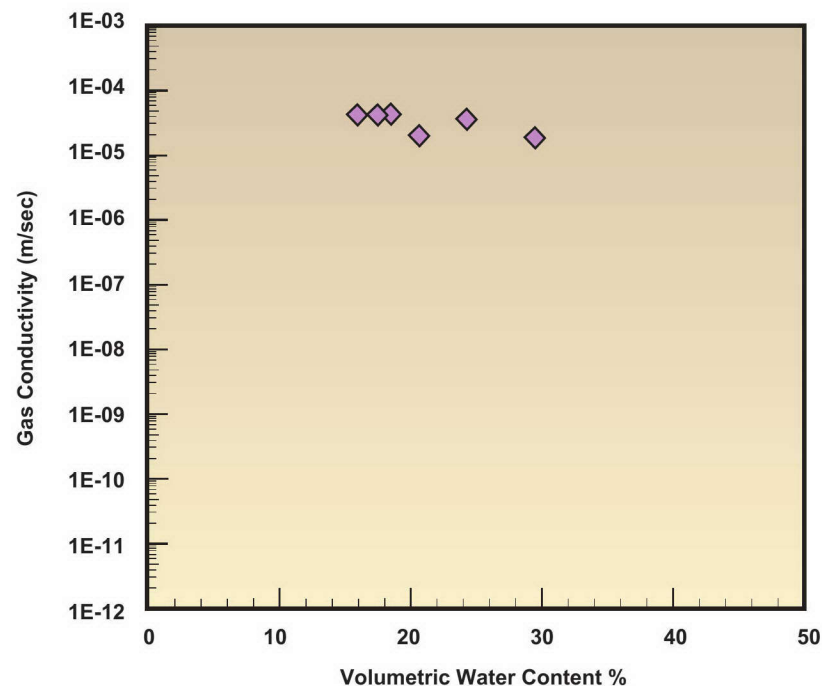
Gas Conductivity Testing

- Objective: Measure the gas permeability across silt/clay linings and infilling units of clastic injection dikes.
- Approach: Use the same UFA equipment, general procedure, and test site for measuring hydraulic conductivity to measure the gas conductivity across silt/clay linings and infilling units. The measurements were made in conjunction with hydraulic conductivity measurements for moisture. Four samples were selected to measure gas conductivity: one host sediment sample (UFA #3) and three dike samples (UFA #2, #4, and #5). The descriptions of the samples are presented in Section 9.5.
- Results:
 - The gas conductivity for the host sediment changed slightly (1.93×10^{-5} to 4.01×10^{-5} m/sec) over the range of volumetric moisture content between 29.53% and 15.93%.

Table 9-23: Volumetric water content and gas conductivity of the host sediment in samples from UFA test #3.

Figure 9-35: Graph showing volumetric water content versus gas conductivity in sample from UFA test #3.

Volumetric Water Content (%)	Gas Conductivity (m/sec)
29.53	1.93×10^{-5}
24.33	3.64×10^{-5}
21.71	--
20.74	2.08×10^{-5}
18.36	4.28×10^{-5}
17.45	3.98×10^{-5}
15.93	4.01×10^{-5}



E9803054.151

**9.6 UNSATURATED FLOW APPARATUS (UFA™)
METHOD - GAS**

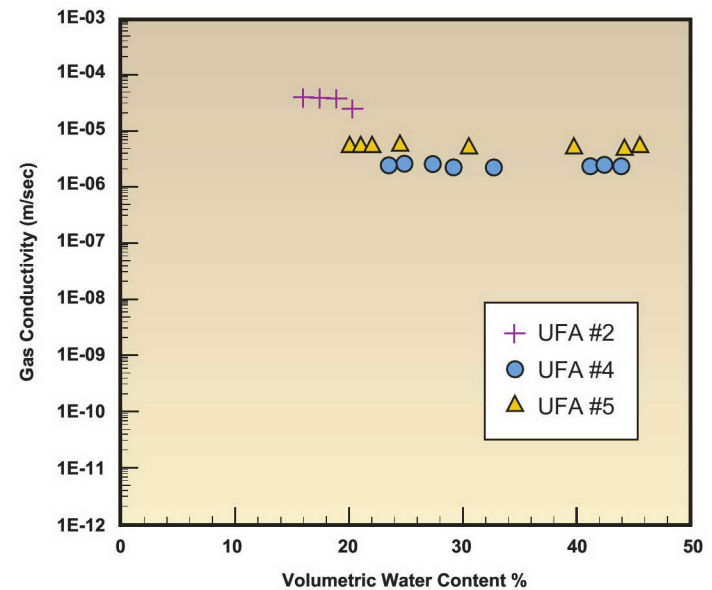
Gas Conductivity Testing (Continued)

- Results (Continued):
 - The gas conductivity across silt/clay linings and infilling units ranges between 1.51×10^{-5} to 3.92×10^{-6} m/sec over the range of measured water content.
 - The gas conductivity for individual samples changes only slightly over the range of measured water content.
 - The gas conductivity for the silt/clay linings (about 10^{-5} to 10^{-6} m/sec) is about equal to or less than the gas conductivity of the host sediments (about 10^{-5}).

Table 9-24: Volumetric water content and gas conductivity measurements across silt/clay linings and infilling units of clastic injection dikes for samples from UFA tests #2, #4, and #5.

Sample #	Volumetric Water Content (%)	Gas Conductivity (m/sec)
UFA #2	20.99	1.51×10^{-5}
	20.01	1.76×10^{-5}
	18.66	1.97×10^{-5}
	17.67	1.95×10^{-5}
UFA #4	45.39	2.70×10^{-6}
	44.98	2.58×10^{-6}
	42.48	2.81×10^{-6}
	32.93	2.82×10^{-6}
	28.80	2.83×10^{-6}
	26.70	3.05×10^{-6}
	24.84	2.48×10^{-6}
	23.50	1.06×10^{-6}
UFA #5	45.63	2.88×10^{-6}
	45.01	3.36×10^{-6}
	41.45	3.72×10^{-6}
	30.17	3.92×10^{-6}
	25.24	3.90×10^{-6}
	21.75	3.88×10^{-6}
	21.18	3.92×10^{-6}
	19.54	1.78×10^{-6}

Figure 9-36: Graph showing volumetric water content versus gas conductivity in samples from UFA tests #2, #4, and #5.



E9803054.152

9.7 DISCUSSION

Introduction

- This section presents a discussion of results from hydraulic testing of silt/clay linings, infilling units, and host sediments. The section provides a discussion of several basic relationships between hydraulic data and physical properties (e.g., grain size, internal bedding) that were gained through this study. The final part of the section presents a comparison of hydraulic testing of clastic injection dikes and host sediments.
- The discussion is intentionally brief, as the data are from a limited number of measurements using several different field and laboratory methods. This atlas assumes that measurements determined by different methods are comparable. A suite of measurements collected from a variety of geologic conditions are necessary to develop high confidence (e.g., precision and accuracy) in the data collected from hydraulic testing of clastic injection dikes.
- The hydraulic testing in this atlas was designed to determine an initial range of hydraulic characteristics over a wide variety of geologic conditions that have been observed in the Pasco Basin and vicinity. The focus of the discussion is on the range of velocities measured for the movement of soil moisture in saturated and unsaturated conditions in and adjacent to clastic injection dikes. The data were collected to support:
 - Revisions of geologic conceptual models for the Hanford Site
 - Numerical modeling of clastic injection dikes as preferential pathways for moisture flow and contaminant transport in the vadose zone
 - Design of follow-on hydraulic testing of clastic injection dikes and other geologic features that form potential preferential pathways.
- Hydraulic testing data collected in this study and presented earlier in this section are summarized in Table 9-25.

9.7 DISCUSSION

Introduction (Continued)

Table 9-25: Summary of hydraulic testing data collected as part of this study.

Test Method	Test No.	Location	Grain Size	Sorting	Age*	Hydrologic Conductivity (m/sec)†		
						Clastic Injection Dike		Host Sediments
						Parallel to Infilling Units	Across Silt/Clay Linings and Infilling Units	
IT	1	Keene/Kennedy Road	PZ[VC-F]S	Poor	W/PW	3×10^{-5}	$<1 \times 10^{-7}$	--
IT	2	Kiona RR Cut	[C-M]&[F]S	Mod. Well	W/W	3×10^{-5}	3×10^{-6} to 6×10^{-6}	--
IT	3	Keene/Kennedy Road	[M]S	Well	W/PW	4×10^{-5}	8×10^{-6}	--
IT	4	Webber Canyon Road	Z&[F]S/[F]S	Mod. Well	W/W	2×10^{-5}	--	2×10^{-5}
IT	5	Brynes Road	SZ/Z[FVF]S&SZ	Mod. Well	W/W	1×10^{-5}	--	1×10^{-5}
IT	6	Webber Canyon Road	[VF]S/Z[VF]S	Well	W/W	2×10^{-5} to 3×10^{-5}	--	2×10^{-5}
IT	7	Webber Canyon Road	[F]S to Z[VF]S/Z	Mod. Well	W/W	--	9×10^{-6}	2×10^{-5} to 4×10^{-5}
IT	8	Kiona RR Cut	[M]S/Z	Mod. Well	W/W	--	$<3 \times 10^{-7}$	2×10^{-5}
IT	9	Kiona RR Cut	[M-F]S/-	Mod. Well	W/W	--	8×10^{-6}	3×10^{-5}
GP	1	Goose Egg Hill	[M-F]S/-	Mod. Well	W/W	1×10^{-5}	--	--
GP	2	Goose Egg Hill	[VP]S/-	Mod. Well	W/W	2×10^{-5}	--	--
GP	3	Goose Egg Hill	-/Z&Z[F]S	Mod. Well	-/W	--	--	2×10^{-5}
GP	4	Grout Excavation	[M-F]S/-	Mod. Well	W/W	9×10^{-6}	--	--
GP	5	Grout Excavation	[C-M]S-	Well	W/W	6×10^{-5}	--	--
GP	6	Army Loop Road	[M-F]S/-	Mod. Well	W/W	2×10^{-5}	--	--
GP	7	Army Loop Road	[F]S/-	Mod. Well	W/W	5×10^{-5}	--	--
GP	8	Army Loop Road	-/[C-M]S	Mod. Well	-/W	--	--	3×10^{-5}
UFA	1	Keene/Kennedy Road	[F]S/SZ	Mod. Well	W/W	--	5×10^{-7}	--
UFA	2	Keene/Kennedy Road	[C-M]S/[F]S	Mod. Well	W/PW	--	4×10^{-7}	--
UFA	3	Keene/Kennedy Road	-/[F]S	Mod. Well	-/PW	--	--	2×10^{-7}
UFA	4	Keene/Kennedy Road	[C-M]S to [F]S/[M-F]S	Mod. Well	W/PW	--	7×10^{-6}	--
UFA	5	Keene/Kennedy Road	SZ&Z[M-F]S/[M-F]S	Mod. Well	W/PW	--	9×10^{-6}	--

*Age information includes age of dike/age of host sediment (W = Wisconsin; PW = pre-Wisconsin).

†Saturated hydraulic conductivity rounded to one significant factor.

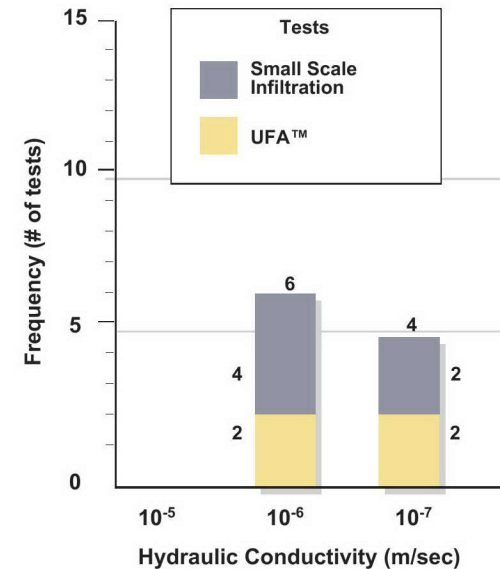
9.7 DISCUSSION

Hydraulic Conductivity of Silt/ Clay Linings

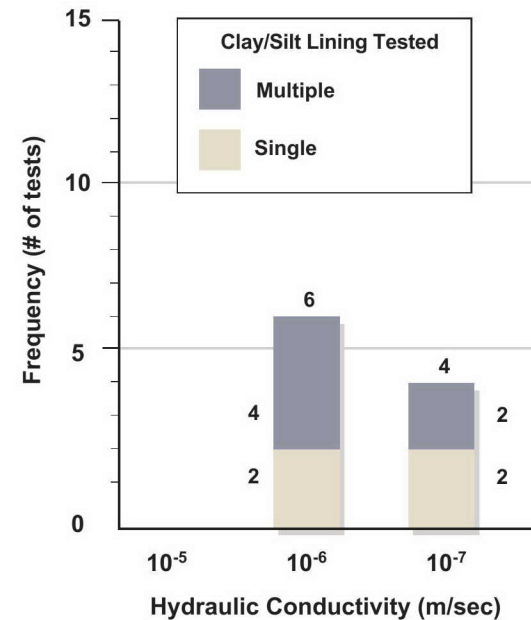
- The saturated hydraulic conductivity for water measurements across silt/clay linings and infilling units of elastic injection dikes ranged from 10^{-6} to less than 10^{-7} m/sec. The range of velocities is based on ten hydraulic conductivity measurements that were made as part of this study. Six of the measurements were calculated based on infiltration tests and four on UFA tests.
- The thickness of the silt/clay linings that were tested ranged between 1 and 3 mm in thickness. Six tests were conducted on single linings. Four tests were made on multiple groups of silt/clay linings separated by thin infilling units. The grain size of the silt/clay linings were all finer than the grain size of the infilling units.
- The hydraulic conductivity measurements were made from silt/clay linings with flat or slightly undulating surfaces. Silt/clay linings with ridge and trough, V-tapered, bulbous, mudcracks, or sheared structures were not tested.

Figure 9-37: Frequency of occurrence of hydraulic conductivities across silt/clay linings and infilling units by testing method.

Figure 9-38: Frequency of occurrence of hydraulic conductivities across multiple and single silt/clay linings and associated infilling units.



E9905060.1



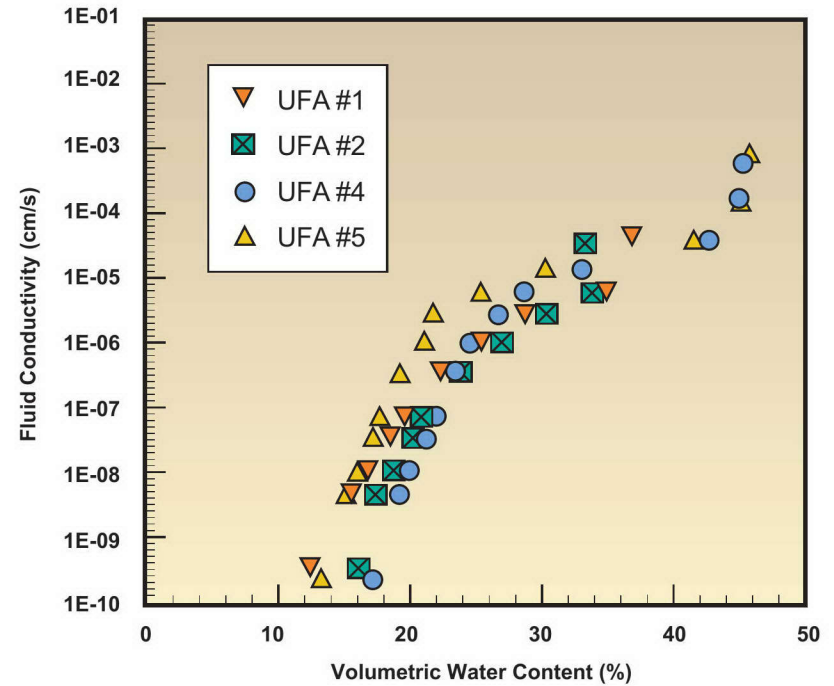
E9905060.2

9.7 DISCUSSION

Hydraulic Conductivity of Silt/Clay Linings (Continued)

- The moisture curves from hydraulic testing across silt/clay linings and infilling units using the UFA method were all similar in shape and position on the graph. The hydraulic conductivity gradually increased with increasing volumetric water content.

Figure 9-39: Graph of volumetric water content versus hydraulic conductivities across silt/clay linings.



E9803054.152a

9.7 DISCUSSION

Gas Conductivity of Silt/Clay Linings

- Twenty gas conductivity measurements were determined across silt/clay linings and infilling units in three samples. The gas conductivity ranged from 10^{-5} to 10^{-6} m/sec.
- The gas conductivity of each sample tested remained relatively constant over the range of volumetric water content from 17% to 46%. It is expected that gas conductivity values would change inversely with soil moisture measurements.
- Four gas conductivity measurements of 10^{-5} m/sec are from the UFA test #2 sample. The measurements were taken across a single silt/clay lining that was 2 mm thick. The integrity of this sample is questionable due to the percussion sampling method that was used to collect thin and fragile silt/clay lining.
- The gas conductivity measurements measured across multiple silt/clay linings and infilling units were no greater than the maximum gas conductivity measurements across single silt/clay linings and associated infilling units.
- The gas conductivity measurements taken across multiple silt/clay linings and infilling units are considered more representative of gas flow through a clastic injection dike since most clastic injection dikes are composed of multiple infilling units with each infilling unit separated by a silt/clay lining, and multiple clay skins are less likely to be adversely affected by sampling. The samples collected for gas conductivity measurements may have been adversely affected by the percussion sampling methods.

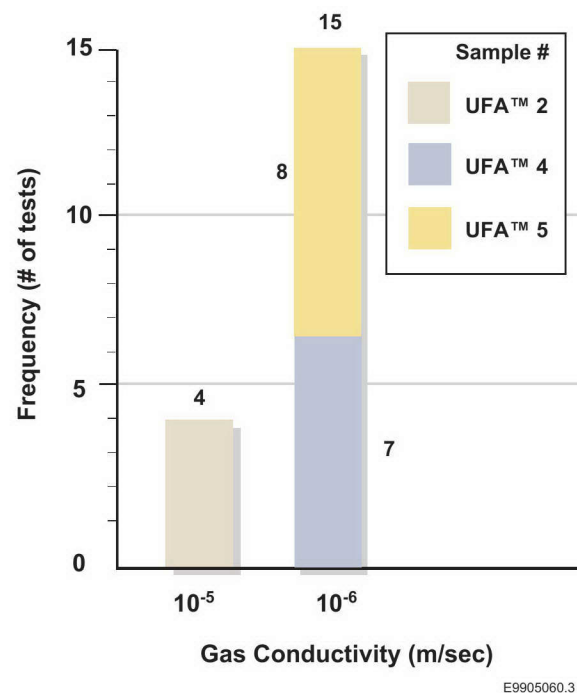
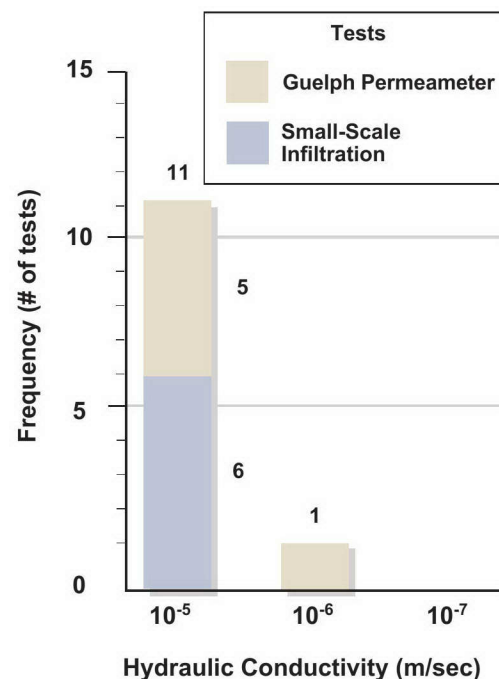


Figure 9-40: Frequency of gas conductivities from samples analyzed using the UFA method.

9.7 DISCUSSION

Hydraulic Testing of Infilling Units

- The vertical- and lateral-saturated hydraulic conductivity within infilling units of clastic injection dikes varied between 10^{-5} to 10^{-6} m/sec. Twelve saturated hydraulic conductivity measurements were made for this study. Six were calculated from infiltration tests, and six were from Guelph permeameter tests.
- The saturated hydraulic conductivity measurements of infilling units are based on a wide variety of textural characteristics including:
 - Poorly to well sorted
 - Highly structured (cross- and plane-laminated) to structureless (massive)
 - Fine-grained (silty sand) to coarse-grained (medium-to-coarse sand).
- Across structural discontinuities (e.g., shears and small-scale faults), the saturated hydraulic conductivities within infilling units were not significantly different than elsewhere in infilling units.
- All saturated hydraulic conductivity measurements were made in unconsolidated sediments of Wisconsin age.



E9905060.4

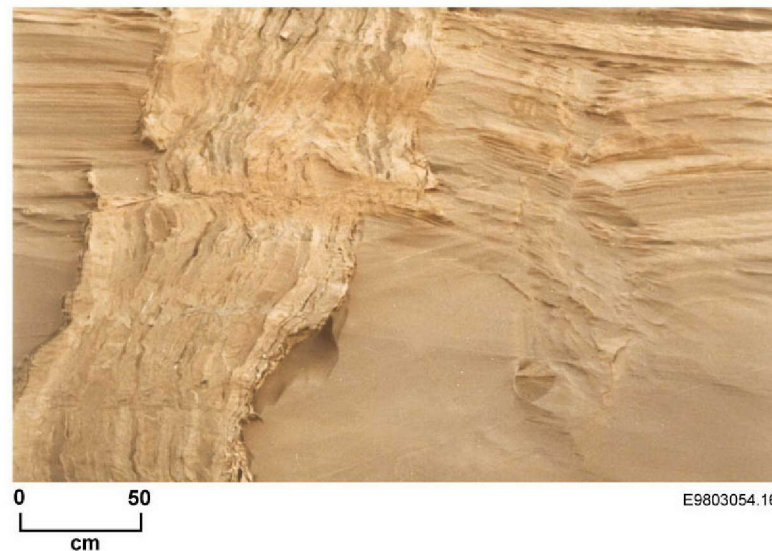
Figure 9-41: Frequency of occurrence of saturated hydraulic conductivities within infilling units of clastic injection dikes.

9.7 DISCUSSION

Hydraulic Testing of Infilling Units (Continued)

- Most infilling units varied in saturated hydraulic conductivity from 9×10^{-6} to 3×10^{-5} m/sec. The chief physical characteristics of the infilling units with these moderate velocities are:
 - Fine-grained (silts, very fine-to-coarse sand)
 - Poor to moderately well sorted
 - Laminated and massive
 - Variable thickness
 - Limited continuity
 - Structural discontinuities.

Figure 9-42: Photograph of clastic injection dikes from the Richland Landfill (10/28-17N) showing physical characteristics typical of most infilling units.



9.7 DISCUSSION

Hydraulic Testing of Infilling Units (Continued)

- The highest measured saturated hydraulic conductivities were 4×10^{-5} to 5×10^{-5} m/sec. The characteristics of the infilling units with the higher saturated hydraulic conductivities are:
 - Coarse-to-medium sand
 - Well sorted
 - Massive
 - Uniform in thickness
 - Vertical or lateral continuity
 - Free of structural discontinuities.
- Infilling units with higher velocity characteristics are relatively uncommon. Many infilling units have one or more characteristic of higher velocity units, but most infilling units do not have all of the high velocity characteristics. The characteristics that are most often missing are lateral and vertical continuity and massively bedded. Generally, infilling units are not laterally continuous and terminate within several centimeters to several meters and are commonly laminated or graded.
- The initial velocities measured during infiltration tests were often greater than longer term rates. After the initial set of measurements, the velocities decreased to relatively constant rates for the duration of the test.



E9803054.160

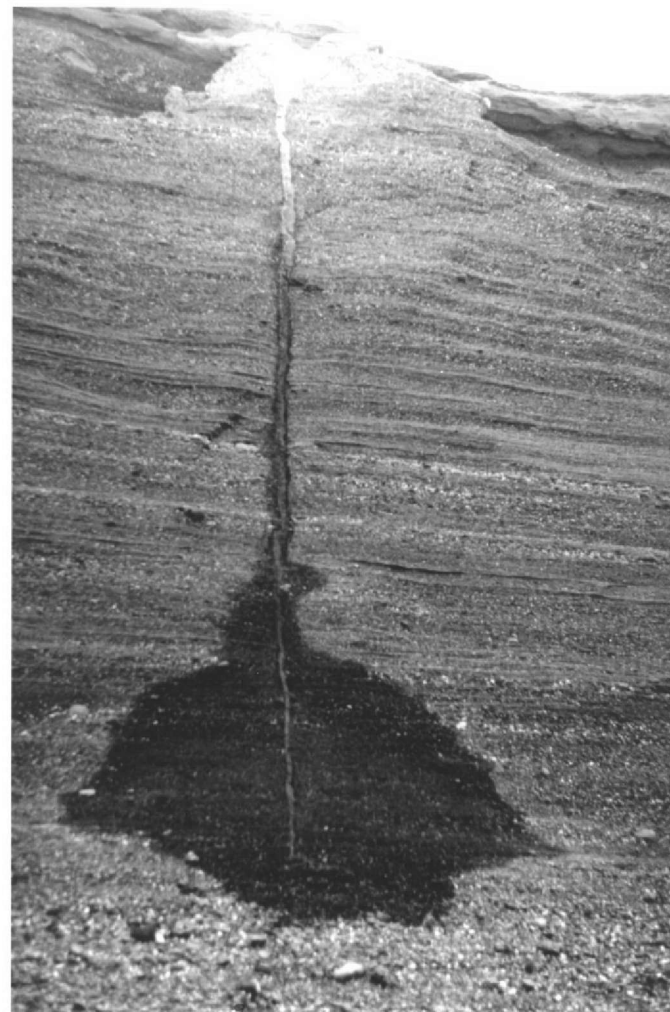
Figure 9-43: Photograph of a clastic injection dike with physical characteristics of infilling units with high saturated hydraulic conductivities. The clastic injection dike is located at Keene/Kennedy Road (9/28-22M).

9.7 DISCUSSION

Hydraulic Testing of Infilling Units (Continued)

- The highest observed hydraulic infiltration within an infilling unit was in a random occurrence dike network located in Lind Coulee east of Warden, Washington (32 km north of the Pasco Basin).
- The clastic injection dike occurs in a 8-m vertical exposure on the south wall of the coulee located below an irrigated alfalfa field.
- The host sediment consists of poorly sorted, horizontally bedded, silty, sandy gravel deposited by glaciofluvial floods during the late Pleistocene. The gravel unit is equivalent to the gravel facies (field mapping unit #3) of the Hanford Formation in the Pasco Basin. The gravel unit is capped by 50- to 70-cm-thick loess of Holocene age.
- A 10-cm-wide, 6.5-m-high, single infilling unit bounded by 8- to 10-mm-thick clay/silt linings forms the clastic injection dike. The texture of the infilling unit is primarily a slightly silty sandy gravel that is unconsolidated and moderately well sorted. The dike extends to the top of the gravel sequence, but does not penetrate into the loess.
- Irrigation water from runoff percolated into the dike at the contact with the loess and was observed trickling down the infilling unit to the root of the dikes where the water migrated into the host sediment.
- The rate of moisture movement was not measured, but water could be observed moving down the dike at rates estimated at least 10 times the rates observed in other dikes in this study. The clastic dike acted as a conduit to transmit soil moisture downward through a preferential pathway to the base of the dike before spreading out into the host sediments.
- The very high moisture velocity in the infilling unit that was observed is due to the unconsolidated, moderately well-sorted nature of the sediments. The characteristics of this infilling unit is unique compared to infilling units observed in the Pasco Basin and vicinity.

Figure 9-44: Photograph of a clastic injection dike in the southern wall of Lind Coulee with irrigation runoff percolating downward through the dike.



E9803054.159

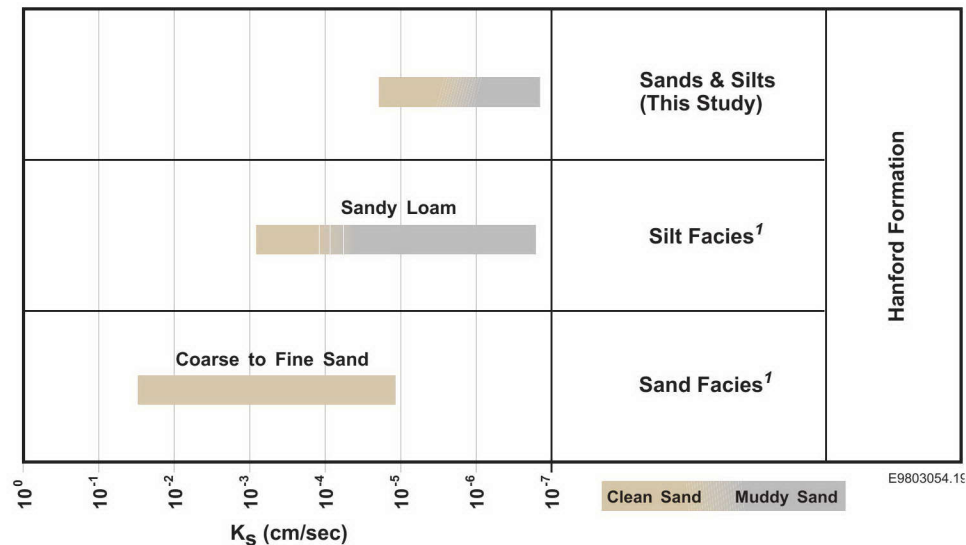
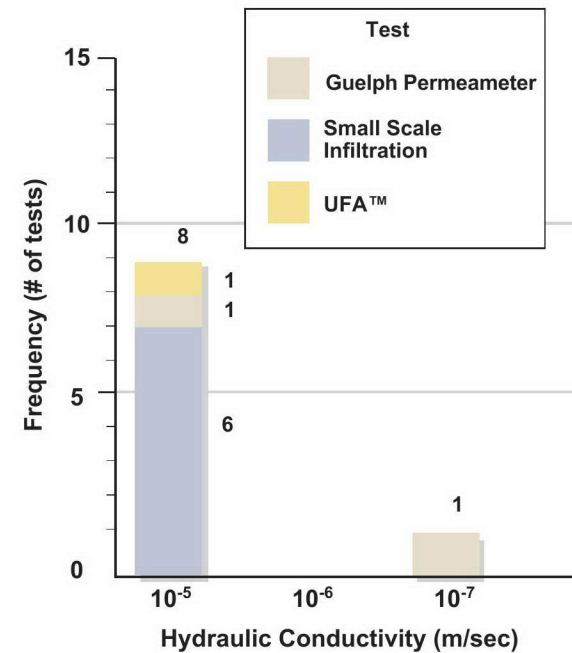
9.7 DISCUSSION

Hydraulic Conductivity of Host Sediments - Saturated

- The vertical- and lateral-saturated hydraulic conductivity within infilling units of clastic injection dikes was calculated at 10^{-5} m/sec. One measurement was calculated at 10^{-7} m/sec. Nine measurements of saturated hydraulic conductivity were made from this study, including:
 - Six measurements from small-scale infiltration tests
 - Two measurements from Guelph permeameter tests
 - One measurement from UFA tests.
- The saturated hydraulic conductivity measurements of 10^{-5} m/sec were made in the sand and silt facies of the Hanford Formation. The glaciofluvial sediments are unconsolidated and from Wisconsin stage of the Pleistocene age.
- The single saturated hydraulic conductivity measurement of 10^{-7} m/sec was from a sediment sample from the sand facies of the Hanford Formation. The measurement was made in a sample collected near the top of a pre-Wisconsin stage of the Pleistocene. The glaciofluvial sediments are more oxidized and compact than the Wisconsin-age glaciofluvial sediments.

Figure 9-45: Frequency of occurrence of saturated hydraulic conductivities within the host sediments adjacent to clastic injection dikes.

Figure 9-46: Range of saturated hydraulic conductivities in host sediments from this atlas and data summarized in Khaleel and Freeman (1995).



¹ Sources include: Bergeron 1987, Bjornstad 1990, Delaney 1992, Gee et al. 1989, Heller 1989, Hoffman 1992, Khaleel and Freeman 1995, Relyea 1995, Rockhold et al. 1993, Volk 1993

9.7 DISCUSSION

Hydraulic Conductivity of Clastic Injection Dikes - Saturated

- Saturated hydraulic conductivities have been measured in most sediment types that form the host for many clastic injection dikes. Most measurements of saturated hydraulic conductivity in host sediments associated with dikes are from other studies. The results of these studies are summarized in Figure 9-47. A fundamental assumption of this atlas is the data that are based on measurements from multiple analytical methods are comparable.
- A comparison of saturated hydraulic conductivity values from infilling units measured parallel to the dike walls (and silt/clay linings) and host sediments indicates conductivities in clastic injection dikes are:
 - Greater than values in silt facies, silt beds, and some sandy gravels in the Hanford Formation (primarily field mapping unit #3)
 - Within the range of values for coarse-to-fine and coarse sands of the sand facies of the Hanford Formation (primarily field mapping unit #3)
 - At the top of the range of values for sand units within the deposits of upper Cold Creek
 - Greater than the values for sands and silty sands of the member of Taylor Flat
 - Within the range of values for sandy gravels, but greater than the values for silty sandy gravels of the member of Wooded Island.

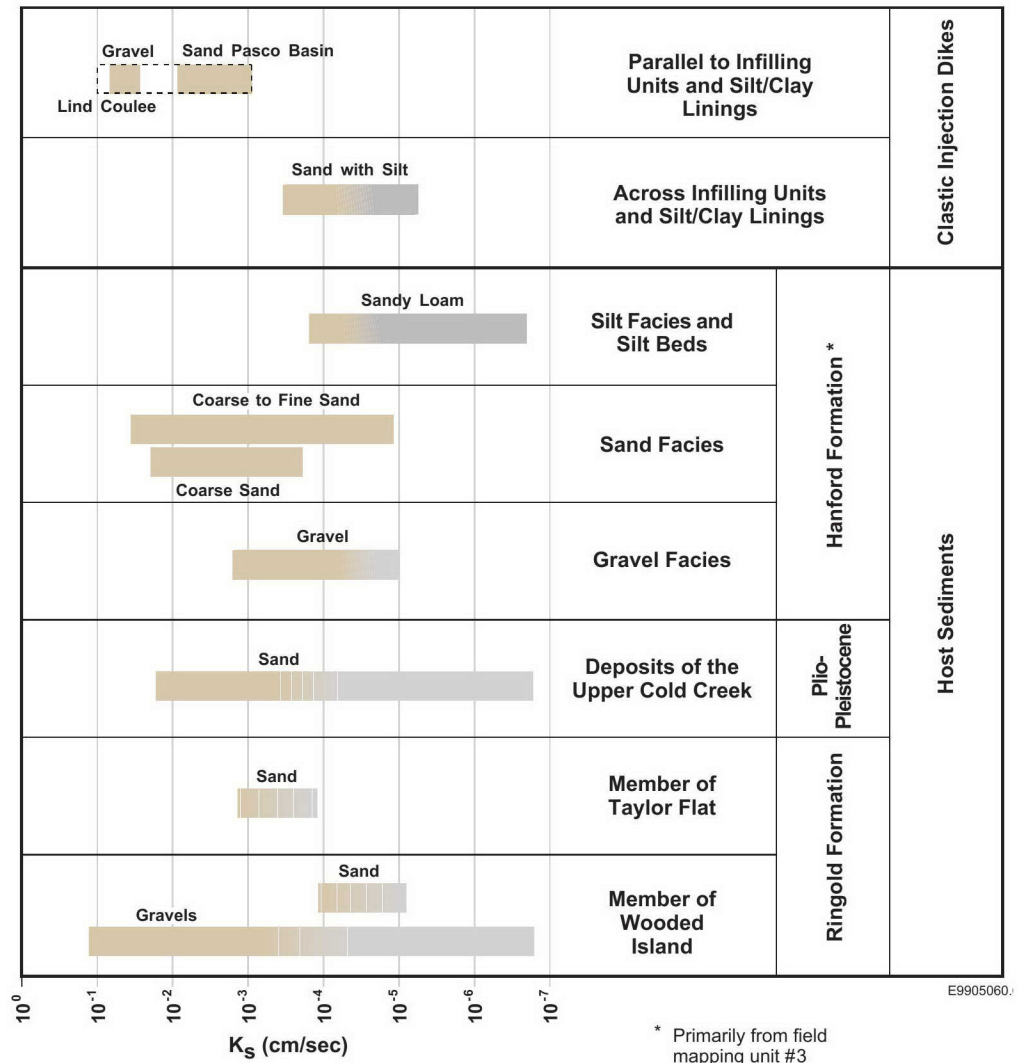


Figure 9-47: Range of saturated hydraulic conductivities in clastic injection dikes and host sediments. Data from host sediments are summarized from Khaleel and Freeman (1995).

9.7 DISCUSSION

Hydraulic Conductivity of Clastic Injection Dikes - Saturated (Continued)

- A comparison of saturated hydraulic conductivity values from infilling units and silt/clay linings measured perpendicular to dike walls and host sediments indicates conductivities in clastic injection dikes are:
 - Greater than to similar to values of sandy loam, but generally greater than values from silty sandy loam of the silt facies and silt beds of the Hanford Formation (primarily field mapping unit #3)
 - Generally equal to the lower range of values from the coarse to fine and coarse sand of the sand facies of the Hanford Formation (primarily field mapping unit #3)
 - Generally similar to values of sandy gravels and silty sandy gravels of the gravel facies of the Hanford Formation (primarily field mapping unit #3)
 - Less than values of sands in deposits of the upper Cold Creek and within the range of values of silty sands of deposits of the upper Cold Creek
 - Equal to the lower range of silty sands of the member of Taylor Flat and similar to the sands of the member of Wooded Island
 - Less than values of sandy gravels of the member of Wooded Island and within the upper range of values of the silty sandy gravel of the member of Wooded Island.
- Clastic injection dikes have the potential to be preferential pathways to vertical saturated hydraulic flow under the following conditions:
 - Clastic injection dikes with infilling units that are sufficiently wide, massive, coarse-grained, well sorted, and vertically continuous (i.e., free of faults, shears, other discontinuities)
 - Host sediment sequence in which all or a significant part of the sequence consists of fine-grained sediments or coarse-grained with a high mud (silt/clay) content.
 - The highest observed saturated hydraulic conductivity in clastic injection dikes was observed in Lind Coulee, north of the Pasco Basin. The dike consists of a moderately well sorted, slightly silty sandy gravel infilling unit that is vertically continuous over the entire dike and bounded by silt/clay linings. Dikes with these characteristics have not been observed in the central Pasco Basin or in the Walla Walla and Yakima River Valleys. The grain size of infilling units in clastic injection dikes within the study area consist of silt, sand, and occasionally poorly sorted silty sandy gravel. The high saturated hydraulic conductivity values observed at Lind Coulee would not be expected to occur within polygonal-patterned ground dike networks in the Pasco Basin and vicinity.
 - Clastic injection dikes can impede saturated flow in the horizontal direction under the following conditions:
 - Silt/clay linings and associated infilling units with lower saturated hydraulic conductivity values than the host sediments
 - Dikes with alternating coarser grained infilling units and silt/clay linings
 - Dikes with few discontinuities (e.g., faults, shears) and vertical continuity
 - Highest potential in areas with the highest conductivity values in host sediments and the lowest values across dikes.

9.7 DISCUSSION

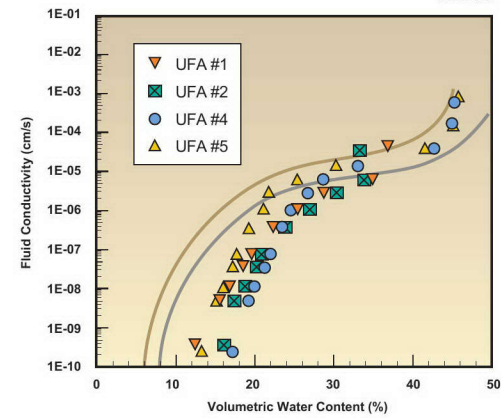
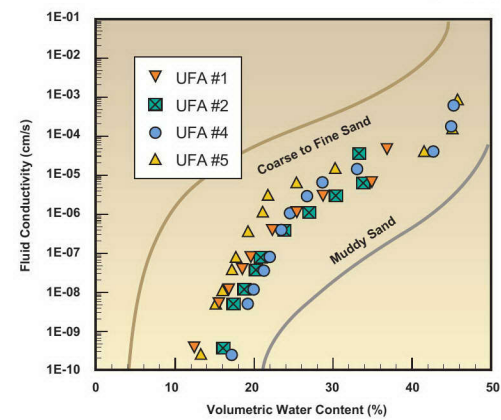
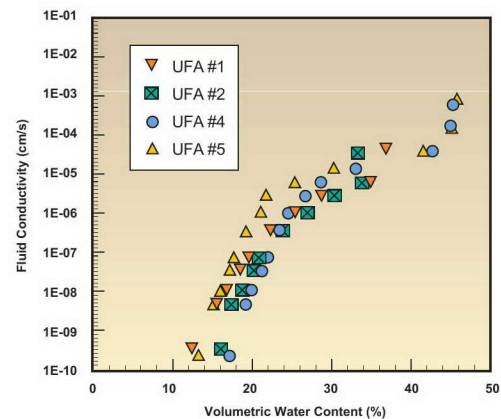
Hydraulic Conductivity of Clastic Injection Dikes - Unsaturated

- A comparison of unsaturated hydraulic conductivity values of silt/clay linings and infilling units measured across clastic injection dikes and in host sediments indicates similar relationships in moisture content and conductivity and shape of the moisture curves based on measurements from this study.
- A comparison of unsaturated hydraulic conductivity values between measurements across clastic injection dikes from this study and measurements in host sediments from the 200 Areas from Connelly et al. (1992a, 1992b) indicates that moisture curves from clastic injection dikes are:
 - Mid-range to curves for the sand facies (primarily field mapping unit #3) of the Hanford Formation, but lower than many clean coarse to fine sand and higher than most muddy (silty/clayey) sands
 - Similar to the upper range ($>10^{-6}$ cm/sec) moisture curves for early Palouse soils (deposits of the upper Cold Creek?) and below the curves of the soils at the lower range

Figure 9-48: Graph of moisture curves from hydraulic testing across clastic injection dikes and from host sediments measured in this study.

Figure 9-49: Graph of moisture curves from hydraulic testing across clastic injection dikes (symbols) and the range of moisture curves from sand of the Hanford Formation in the 200 Areas (solid lines).

Figure 9-50: Graph of moisture curves from hydraulic testing across clastic injection dikes (symbols) and the range of moisture curves from the early Palouse soil (deposits of the upper Cold Creek?) (solid lines).



9.7 DISCUSSION

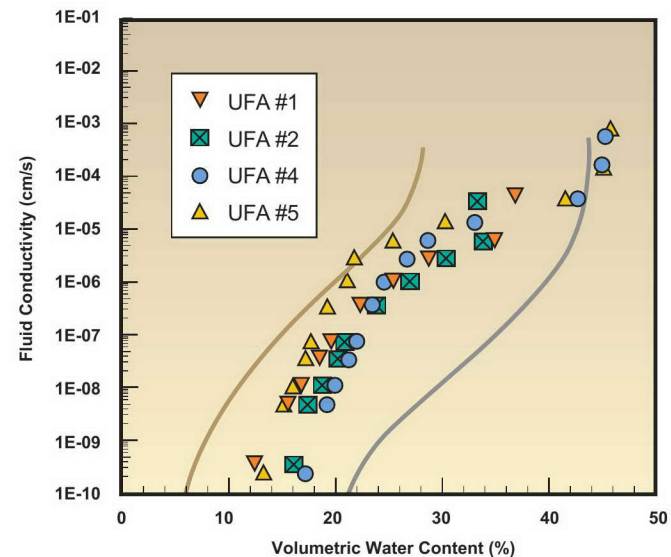
Hydraulic Conductivity of Clastic Injection Dikes - Unsaturated (Continued)

- Similar to curves for deposits of the upper Cold Creek, although the general shape of the curves are different
- At the lower range of curves for sands from the member of Taylor Flat.
- Clastic injection dikes have the potential to be preferential pathways to vertical unsaturated hydraulic flow where dikes intruded into or through:
 - Many poorly sorted muddy sands of the Hanford Formation
 - Deposits of the upper Cold Creek at selected moisture values.

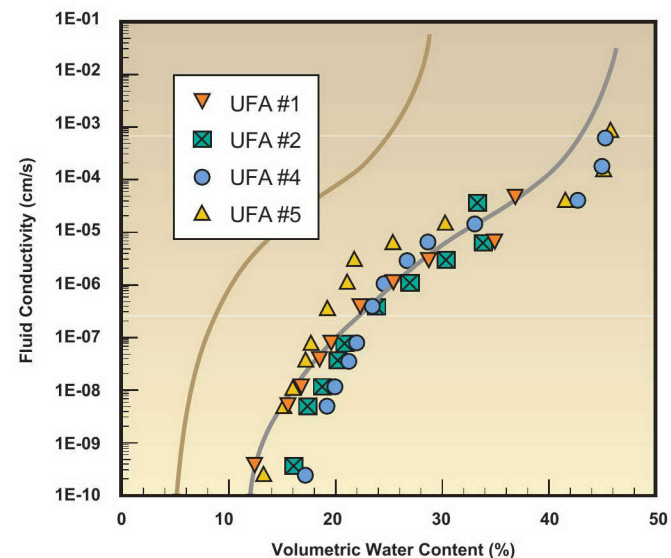
In the muddy sands of the Hanford Formation and in deposits of the upper Cold Creek, the conductivities across silt/clay linings and infilling units are greater than specified host sediments. In other geologic units there is insufficient unsaturated hydraulic testing data parallel to infilling units of clastic injection dikes to determine the potential for preferential pathways.

Figure 9-51: Graph of moisture curves from hydraulic testing across clastic injection dikes (symbols) and the range of moisture curves from the deposits of the upper Cold Creek (solid lines).

Figure 9-52: Graph of moisture curves from hydraulic testing across clastic injection dikes (symbols) and the range of moisture curves from sands of the member of Taylor Flat (solid lines).



E9803054.200



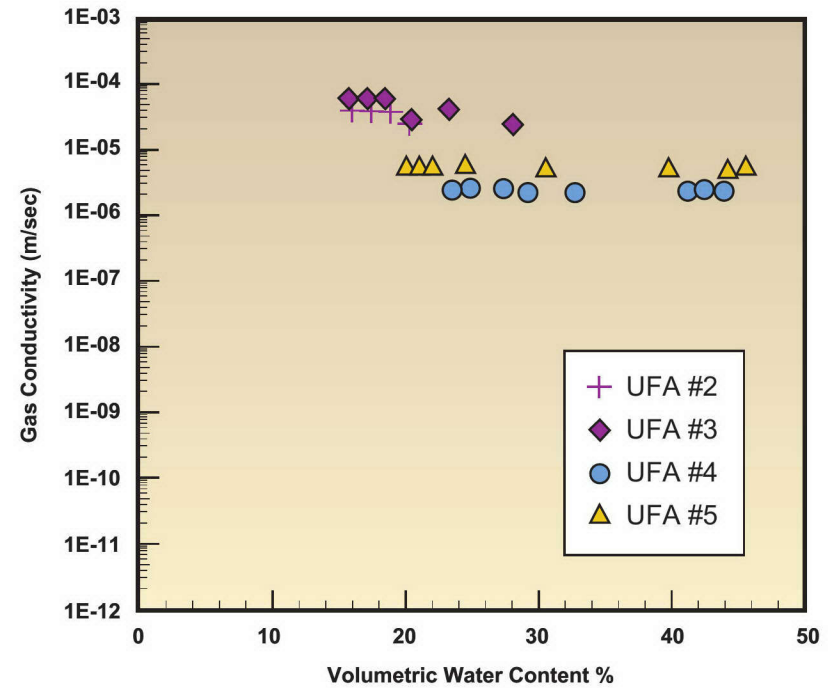
E9803054.201

9.7 DISCUSSION

Hydraulic Conductivity of Clastic Injection Dikes - Unsaturated (Continued)

- Gas conductivity values across clastic injection dikes with multiple silt/clay linings and infilling units are about 10^{-1} less than values in the sand facies (field mapping unit #2) of the Hanford Formation.
- Gas conductivity was not measured in clastic injection dikes parallel to infilling units or in other geologic units.

Figure 9-53: Graph of gas conductivity values and moisture contents for clastic injection dikes and host sediments.



E9803054.198

10.0 SUMMARY AND CONCLUSIONS

PHYSICAL DESCRIPTION

- Clastic injection dikes are fissures filled with sand, silt, clay, and minor coarser debris. Many dikes occur as sharp-walled, near-vertical, tabular bodies filled with multiple layers of unconsolidated sediments. The margins of dikes and internal layers within dikes are separated by thin clay/silt linings.
- Clastic injection dikes include both dike and sill structures that are filled with single or multiple infilling units. The infilling units are composed of clastic sediments and are aligned parallel or subparallel to the structure walls.
- The key components of a clastic injection dike are clay/silt linings, infilling sediments, small-scale slumps, small-scale faults and shears, slickensides, rip-up clasts, and soft-sediment flow features.
- Clastic injection dikes range in vertical (continuous) extent from less than 30 cm to more than 45 m. The maximum depth below ground surface that clastic injection dikes have been encountered in exposures or boreholes in the Pasco Basin is 75 m. There are more than 30 known localities in the Pasco Basin and vicinity where clastic injection dikes have been traced from the surface to a depth of at least 20 m.
- The deepest known occurrence of clastic injection dikes below the ground surface in the Pasco Basin and vicinity is greater than 75 m on the 200 Area Pleistocene Glaciofluvial Flood Bar in the 200 West Area on the Hanford Site (12/25-12F). The total vertical extent of this clastic injection dike is not known.
- In cross-section, clastic injection dikes range from less than 1 mm to over 2 m in width. The millimeter-scale dikes consist entirely of clay/silt linings.
- In plan view, clastic injection dikes range from less than 0.3 m to more than 100 m along strike.

- Clastic injection dikes terminate as follows:
 - Truncation against another clastic injection dike, at bedding planes, at small-scale faults, or at small-scale slumps.
 - Thinning and pinching out at the top, bottom, or lateral extent of a dike.
 - Gradually losing definition into a superimposed soil horizon. The soil horizon is associated with Holocene soils or older paleosols.
 - Merging and fading into host sediment.
 - Bending and merging with another dike or sill.
 - Splaying into dikelets (i.e., narrow dikes) and sills.
- Clastic injection dikes in the Pasco Basin and vicinity can be divided into dike networks based on the context of the fissures and the interrelationship of individual clastic dikes. A dike network occurs where stratigraphic units have consistent textural and bedding characteristics, topographic relief, and structural features or fabric over a large area (many square kilometers).
- Types of networks that are defined in this study are:
 - Regular-shaped, polygonal-patterned ground: Clastic injection dikes form regular polygonal patterns in clastic host sediments in plan view. Dikes merge at intersections with other dikes in the network.
 - Irregular-shaped, polygonal-patterned ground (slumps): Clastic injection dikes form irregular and complex forms in clastic host sediments in plan view. Dikes merge, but primarily cross-cut at intersections with other dikes in the network.
 - Pre-existing fissure: Clastic injection dikes form along fissures that were established in the host sediments/rocks long before emplacement of the infilling dike material. Clastic injection dikes merge or cross-cut at intersections with other clastic injection dikes.

PHYSICAL DESCRIPTION (Continued)

- Random occurrence: Clastic injection dikes form in randomly oriented and distributed fissures in clastic host sediments in both plan view and cross-section. Few dikes have been observed intersecting with other dikes in the “network.”
- Many clastic injection dikes penetrate to or very near the top of the three field mapping units of the Hanford Formation (field mapping units #1, #2, and #3) in most dike networks. Clastic injection dikes in random occurrence dike networks may not intrude to the top of field mapping units.

LOCATION (Within Study Area)

- The upper limit of clastic injection dikes is higher than 275 m elevation. Clastic injection dikes are scarce above 275 m, and are often obscured by developing soils (bioturbation), deposition of a veneer of loess, and disking of farm land.
- Clastic injection dikes are not found above the maximum Pleistocene glaciofluvial flood level, which is about 380 m elevation.
- The lower limit of clastic injection dikes is about river level or near the elevation of the historic water table in the southern Pasco Basin prior to filling of reservoirs behind Ice Harbor, McNary, Priest Rapids, and Wanapum Dams (i.e., 104 m).
- Clastic injection dikes occur in several geomorphic terrains in the Pasco Basin and vicinity, including river and basin, lower slope, coulees and scabland, and low-relief ridges.
- Clastic injection dikes have been observed in the Columbia River Basalt Group, Ellensburg Formation, Ringold Formation, Plio-Pleistocene Unit, and Hanford Formation. Clastic injection dikes have not been observed in Holocene sediments.

AGE

- Clastic injection dikes were emplaced during at least three different periods of injection based on evaluation of dike networks. Clastic injection dikes in each period appear to have formed over short time spans and, in the youngest dikes, essentially simultaneously. The ages of emplacement are:
 - Between 12.5 and 15.7 Ka
 - Approximately 200 Ka
 - Greater than 770 Ka.

GEO PHYSICAL METHODS TESTING

- Electromagnetic induction and ground-penetrating radar methods can be used to detect clastic injection dikes below a veneer (<1 m) of Holocene-age sands and should be detectable to several meters depending on soil conditions.

HYDRAULIC CHARACTERISTICS

- Guelph permeameter, small-scale infiltration, and unsaturated flow apparatus methods were used in this study to measure hydraulic properties of clastic injection dikes.
- The saturated hydraulic conductivities of clastic injection dikes in this study are:
 - 10^{-6} to 10^{-7} cm/sec across silt/clay linings and infilling units
 - 10^{-5} to 10^{-6} cm/sec for infilling units parallel to dike walls.
- The unsaturated hydraulic conductivities of clastic injection dikes measured across silt/clay linings and infilling units ranged from about 10^{-10} cm/sec up to about 10^{-3} cm/sec from volumetric water contents that ranged from 12% to 46%.

HYDRAULIC CHARACTERISTICS (Continued)

- Clastic injection dikes have the potential to be preferential pathways to vertical saturated hydraulic flow under the following conditions:
 - Clastic injection dikes with infilling units that are sufficiently wide, massive, coarse-grained, well sorted, and vertically continuous (i.e., free of faults, shears, other discontinuities)
 - Host sediment sequence in which all or a significant part of the sequence consists of highly bedded fine-grained sediments or coarse-grained with a high mud (silt/clay) content.
- Clastic injection dikes can impede saturated flow in the horizontal direction under the following conditions:
 - Silt/clay linings with lower saturated hydraulic conductivity values than the host sediments
 - Dikes with alternating coarser grained infilling units and silt/clay linings
 - Dikes with few discontinuities (e.g., faults, shears) and vertical continuity
 - Highest potential in areas with the highest conductivity values in host sediments and the lowest values across dikes.
- Clastic injection dikes have the potential to be preferential pathways to vertical unsaturated hydraulic flow where dikes intruded into or through:
 - Poorly sorted muddy sands of the Hanford Formation
 - Deposits of the upper Cold Creek at selected moisture values (i.e., volumetric water content <30%).

ORIGIN

- Clastic injection dikes were formed as a relatively continuous process in each type of dike network. The process included:
 - Development of fissure systems that formed immediately before sediment infilling, except for dikes associated with pre-existing fissure systems

- Gradual widening of fissure apertures with injection of sediments
- Continual injection of sediments along separate flowpaths; each flowpath is preserved as an individual infilling unit within a dike.
- The primary mechanism for infilling of open fissures associated with clastic injection dikes is by water (and probably air) under hydraulic pressure. Eolian processes did not play a significant role in formation of clastic injection dikes.
- Clastic injection dikes are interpreted to be the result of rapid dewatering of a wetted sediment/rock sequence. Fissures (other than pre-existing fissures) were formed as a result of ground failure caused by the compaction, translocation, or extension of the wetted sediment/rock mass. The wetted character of the sediment/rock mass is interpreted to be the result of partial drainage of water within the vadose zone following proglacial cataclysmic flooding of the Pasco Basin and vicinity.
- Many older clastic injection dikes (i.e., pre-late Wisconsin) formed in the Pasco Basin and vicinity in one or more glaciofluvial floods during at least two glacial events. Wisconsin- and Holocene-age sediments obscure exposures of sediments and rocks penetrated by older clastic injection dikes and limit the ability to define a single geologic process/event that could be responsible for the formation of older clastic injection dikes and dike networks. The geologic processes considered significant in the formation and infilling of fissures in older clastic injection dikes are unloading of Pleistocene floodwaters and seismically-induced ground motion.
- In the late Wisconsin, most clastic injection dikes and associated dike networks formed essentially simultaneously, over a very large area, and in different geographic terrain. Formation of the late Wisconsin dikes appears to be related to a geologic event (i.e., ground motion from a large earthquake) that occurred during proglacial cataclysmic flooding of the basin and vicinity.

11.0 REFERENCES

- Alwin, J. A., 1970, "Clastic Dikes of the Touchet Beds, Southeastern Washington," Master's thesis, Washington State University, Pullman, Washington, 87 p.
- Alwin, J. A. and W. F. Scott, 1970, "Clastic Dikes of the Touchet Beds, Southeastern Washington (abstract)," in *Northwest Science*, Vol. 44, No. 1, p. 58.
- Baker, V. R., 1973, *Paleohydrology and Sedimentology of Lake Missoula Flooding in Eastern Washington*, Special Paper 144, Geological Society of America, Boulder, Colorado, 79 p.
- Baker, V. R., B. N. Bjornstad, A. J. Busacca, K. R. Fecht, E. P. Kiver, U. L. Moody, J. G. Rigby, D. F. Stradling, and A. M. Tallman, 1991, "Quaternary Geology of the Columbia Plateau," in R. B. Morrison (ed.), *Quaternary Nonglacial Geology - Conterminous U.S.*, Geological Society of America, DNAG Geology of North America, Vol. K-2.
- Bechtel, 1971, "A Discussion of Sand Dikes," in *FFTF Excavation*, HEDL-TME71-101, prepared for Westinghouse Atomic Development Company, Richland, Washington, by Bechtel Incorporated, San Francisco, California, 12 p.
- Bergeron, M. P., G. V. Last, and A. E. Reisenauer, 1987, *Geohydrology of a Commercial Low-Level Radioactive Waste Disposal Facility Near Richland, Washington*, prepared for US Ecology, Richland, Washington, by Pacific Northwest Laboratory, Richland, Washington.
- Bjornstad, B. N., 1980, "Sedimentary and Depositional Environment of the Touchet Beds, Walla Walla River Basin, Washington," Master's thesis, Eastern Washington University, Cheney, Washington.
- Bjornstad, B. N., 1990, *Geohydrology of the 218-W-5 Burial Ground, 200 West Area, Hanford Site*, PNL-7336, Pacific Northwest Laboratory, Richland, Washington.
- Black, R. F., 1976, "Periglacial Features Indicative of Permafrost: Ice and Soil Wedges," in *Quaternary Research*, Vol. 6, pp. 3-26.
- Black, R. F., 1979, *Clastic Dikes of the Pasco Basin, Southeastern Washington*, RHO-BWI-C-64, Rockwell Hanford Operations, Richland, Washington, 65 p.
- Bretz, J. H., 1923, "The Channeled Scablands of the Columbia Plateau," in *Journal of Geology*, Vol. 31, No. 8, pp. 617-649.
- Bretz, J. H., H. T. U. Smith, and G. E. Neff, 1956, "Channeled Scabland of Washington; New Data and Interpretations," in *Geological Society of America Bulletin*, Vol. 67, pp. 956-1049.

Brown, R. E., 1975, "Ground-Water and the Basalts in the Pasco Basin," in *Proceedings of the Thirteenth Engineering Geology and Soils Symposium*, April 2, 3, 4, 1975, Moscow, Idaho.

Brown, R. E. and D. J. Brown, 1962, *Touchet Clastic Dikes in the Ringold Formation*, HW-SA-2851, General Electric Company, Richland, Washington, 11 p.

Brown, R. E. and D. J. Brown, 1968, *The Geology of the Pasco Basin*, BNWL-947, Battelle Northwest Pacific Northwest Laboratory, Richland, Washington.

Bunker, R. C., 1980, "Catastrophic Flooding in the Badger Coulee Area, South-Central Washington," Master's thesis, University of Texas, Austin, Texas.

Carson, R. J., C. F. McKhann, and M. H. Pizey, 1978, "The Touchet Beds of the Walla Walla Valley," in V. R. Baker and D. Nummedal (eds.), *The Channeled Scabland*, Planetary Geology Program, National Aeronautics and Space Administration, Washington, D.C., pp. 173-177.

CDA, 1969, *Logs of Exploratory Trenches on Gable Mountain at the Hanford Works of the U.S. Atomic Energy Commission*, prepared by Converse, Davis, and Associates, Pasadena, California, for Atlantic Richfield Hanford Company, Richland, Washington.

CDA, 1971, *Logs of Exploratory Trenches on Gable Mountain at the Hanford Works of the U.S. Atomic Energy Commission*, Converse, Davis, and Associates, Pasadena, California, for Atlantic Richfield Hanford Company, Richland, Washington.

Conca, J. L. and J. V. Wright, 1990, "Diffusion Coefficients in Gravel Under Unsaturated Conditions," in *Water Resources Research*, Vol. 26, pp. 1055-1066.

Conca, J. L. and J. V. Wright, 1992, "Diffusion and Flow in Gravel, Soil, and Whole Rock," in *Applied Hydrogeology*, Vol. 1, pp. 15-24.

Connelly, M. P., B. H. Ford, and J. V. Borghese, 1992a, *Hydrogeologic Model for the 200 West Groundwater Aggregate Area*, WHC-SD-EN-TI-014, Westinghouse Hanford Company, Richland, Washington.

Connelly, M. P., B. H. Ford, J. W. Lindberg, S. J. Trent, and C. D. Delaney, 1992b, *Hydrogeologic Model for the 200 East Groundwater Aggregate Area*, WHC-SD-EN-TI-019, Westinghouse Hanford Company, Richland, Washington.

Dapples, E. C., 1959, *Basic Geology for Science and Engineering*, Wiley and Sons, Inc., New York, New York, 609 p.

Delaney, C., 1992, *W-049H Borehole Summary Report*, WHC-SD-EN-DP-068, Westinghouse Hanford Company, Richland, Washington.

- Dionne, J. C., 1976, "Miniature Mud Volcanoes and Other Injection Features in Tidal Flats, James Bay, Quebec," in *Canadian Journal of Earth Sciences*, Vol. 13, No. 3, pp. 422-428.
- Dionne, J. C. and W. W. Shilts, 1974, "A Pleistocene Clastic Injection Dike, Upper Caudiere Valley, Quebec," in *Canadian Journal of Science*, Vol. 11, pp. 1594-1605.
- Fairbridge, R. H. (ed.), 1968, *The Encyclopedia of Geomorphology*, Reinhold Book Corporation, New York, New York, pp. 761-763.
- Farooqui, S. M., 1979, *Evaluation of Faulting in the Warm Springs Canyon Area, Southeast Washington*, prepared by Shannon and Wilson, Inc., Portland, Oregon, for Washington Public Power Supply System, Richland, Washington.
- Fecht, K. R., D. B. Barnett, A. G. Law, K. A. Lindsey, and V. J. Rohay, 1994, *Pleistocene Clastic Dikes and Their Influence on Moisture Flow in the Vadose Zone of South-Central Washington State*, in Abstracts with Program, Geological Society of America, Vol. 26, No. 7, p. 204.
- Fecht, K. R., S. P. Reidel, and A. M. Tallman, 1987, "Paleodrainage of the Columbia River System on the Columbia Plateau of Washington State - A Summary," in J. E. Schuster (ed.), *Selected Papers on the Geology of Washington*, Bulletin 77, Washington State Division of Geology and Earth Resources, Olympia, Washington.
- Fecht, K. R. and D. C. Weekes, 1996, *Geologic Inspection of the Sedimentary Sequence at the Environmental Restoration Disposal Facility*, BHI-00230, Bechtel Hanford, Inc., Richland, Washington, 17 p.
- Flint, R. F., 1938, "Summary of Late Cenozoic Geology and Space of Southeastern Washington," in *American Journal of Science*, Vol. 35, p. 223.
- Gee, G. W., M. L. Rockhold, and J. L. Downs, 1989, *Status of FY 1988 Soil-Water Study on the Hanford Site*, PNL-6750, Pacific Northwest Laboratory, Richland, Washington.
- Geomatrix, 1996, *Probabilistic Seismic Hazard Analysis, DOE Hanford Site, Washington*, WHC-SD-W2364-TI-002, Rev. 1, prepared by Geomatrix Consultants for Westinghouse Hanford Company, Richland, Washington.
- Grolier, M. J. and J. W. Bingham, 1978, *Geology of Parts of Grant, Adams, and Franklin Counties, East-Central Washington*, Bulletin 71, Washington State Division of Geology and Earth Resources, Olympia, Washington, 91 p.
- Gustafson, E. P., 1978, "The Vertebrate Fauna of the Pliocene Ringold Formation, South-Central Washington," University of Oregon Museum of Natural History Bulletin 23, 62 p.

- Heller, P. R., 1989, "Physical Analysis for Grout Study," in Smoot, J. L., J. E. Szecsody, B. Sagar, G. W. Gee, and C. T. Kincaid, *Simulation of Infiltration of Meteoric Water and Contaminant Plume Movement in the Vadose Zone at the Single-Shell Tank 241-T-106 at the Hanford Site*, WHC-EP-0332, Westinghouse Hanford Company, Richland, Washington.
- Hoffman, K. M., 1992, *200-BP-1 Borehole Summary Report for Tasks 2, 4, and 6*, WHC-SD-EN-TI-054, Westinghouse Hanford Company, Richland, Washington.
- Jenkins, O. P., 1925, "Clastic Dikes of Eastern Washington and Their Geologic Significance," in *American Journal of Science*, Vol. 10, pp. 234-246.
- Jones, F. O. and R. J. Deacon, 1966, *Geology and Tectonic History of the Hanford Area and its Relation to the Geology and Tectonic History of the State of Washington and the Active Seismic Zones of Western Washington and Western Montana*, DUN-1400, Douglas United Nuclear, Richland, Washington.
- Kanamori, H., 1977, "The Energy Release in Great Earthquakes," in *Journal of Geophysical Research*, Vol. 9, No. 20, pp. 2981-2987.
- Khaleel, R. and E. J. Freeman, 1995, *Variability and Scaling of Hydraulic Properties for 200 Area Soils, Hanford Site*, WHC-EP-0883, Westinghouse Hanford Company, Richland, Washington.
- Kittleman, L. R., 1973, "Mineralogy, Correlation, and Grain-Size Distribution of Mazama Tephra and Other Postglacial Pyroclastic Layers, Pacific Northwest," in *Geological Society of America Bulletin*, Vol. 84, No. 9, pp. 2957-2980.
- Last, G. V. and K. R. Fecht, 1986, "Clastic Dikes of the Pasco Basin, South-Central Washington" (abstract), in R. M. Iverson and H. A. Martinson (eds.), *Mount St. Helens American Geomorphological Field Group Field Trip Guidebook and Abstracts*, Cirpos Center, Washington, p. 173.
- Lindsey, K. A., 1991, *Revised Stratigraphy for the Ringold Formation, Hanford Site Washington, South-Central Washington*, WHC-SD-EN-EE-004, Westinghouse Hanford Company, Richland, Washington.
- Lindsey, K. A., 1995, *Miocene- to Pliocene-Aged Suprabasalt Sediments of the Hanford Site, South-Central Washington*, BHI-00184, Bechtel Hanford, Inc., Richland, Washington.
- Lindsey, K. A., 1996, *The Miocene to Pliocene Ringold Formation and Associated Deposits of the Ancestral Columbia River System, South-Central Washington and North-Central Oregon*, Washington Division of Geology and Earth Sciences, Open-File Report 96-8, Olympia, Washington.
- Lindsey, K. A., S. P. Reidel, K. R. Fecht, J. L. Slate, A. G. Law, and A. M. Tallman, 1994, "Geohydrologic Setting of the Hanford Site, South-Central Washington," in D. A. Swanson and R. A. Haugerud (eds.), *Geologic Field Trips in the Pacific Northwest*, Geological Society of America Annual Meeting, published by the University of Washington, Seattle, Washington, Vol. 1, pp. 1C-1-16.

Long, P. E. and B. J. Wood, 1986, "Structures, Textures, and Cooling Histories of Columbia River Basalt Flows," in *Geological Society of America Bulletin*, Vol. 97, pp. 1144-1155.

Lupher, R. L., 1944, "Clastic Dikes of the Columbia Basin Region, Washington and Idaho," in *Geological Society of America*, Vol. 55, pp. 1431-1462.

McKee, E. H., D. A. Swanson, and T. L. Wright, 1977, "Duration and Volume of Columbia River Basalt Volcanism, Washington, Oregon, and Idaho" (abstract), in *Geological Society of America Abstracts with Programs*, Vol. 9, No. 4, pp. 463-464.

Mehring, P. J., J. C. Shepard, and F. F. Foit, 1984, "The Age of Glacier Peak Tephra in West-Central Montana," in *Quaternary Research*, Vol. 21, pp. 36-41.

Mullineaux, D. R., R. E. Wilcox, W. F. Ebaugh, R. Fryxell, and R. Meyer, 1978, "Age of the Last Major Scabland Flood of the Columbia Plateau in Eastern Washington," in *Quaternary Research*, Vol. 10, No. 2, pp. 171-180.

Myers, C. W., S. M. Price, J. A. Caggiano, M. P. Cochran, W. J. Czimer, N. J. Davidson, R. C. Edwards, K. R. Fecht, G. E. Holmes, M. G. Jones, J. R. Kunk, R. D. Landon, R. K. Ledgerwood, J. T. Lillie, P. E. Long, T. H. Mitchell, E. H. Price, S. P. Reidel, and A. M. Tallman, 1979, *Geologic Studies of the Columbia Plateau: A Status Report*, RHO-BWI-ST-4, Rockwell Hanford Operations, Richland, Washington.

Newcomb, R. C., 1962, "Hydraulic Injection Dikes in the Touchet Beds, Washington, Oregon, and Idaho" (abstract), in *Geological Society of the Oregon Country Newsletter*, Vol. 28, p. 70.

Newcomb, R. C., J. R. Strand, and F. J. Frank, 1972, "Geology and Groundwater Characteristics of the Hanford Reservation of the U.S. Atomic Energy Commission," U.S. Geological Survey Professional Paper 717, 78 p.

Packer, D. R. and J. M. Johnson, 1979, *A Preliminary Investigation of the Magnetostratigraphy of the Ringold Formation*, RHO-BWI-C-46, Rockwell Hanford Operations, Richland, Washington.

Price, W. H. and K. R. Fecht, 1976a, *Geology of the 241-A Tank Farm*, ARH-LD-127, Atlantic Richfield Hanford Company, Richland, Washington.

Price, W. H. and K. R. Fecht, 1976b, *Geology of the 241-AX Tank Farm*, ARH-LD-128, Atlantic Richfield Hanford Company, Richland, Washington.

Price, W. H. and K. R. Fecht, 1976c, *Geology of the 241-B Tank Farm*, ARH-LD-129, Atlantic Richfield Hanford Company, Richland, Washington.

Price, W. H. and K. R. Fecht, 1976d, *Geology of the 241-BX Tank Farm*, ARH-LD-130, Atlantic Richfield Hanford Company, Richland, Washington.

- Price, W. H. and K. R. Fecht, 1976e, *Geology of the 241-BY Tank Farm*, ARH-LD-131, Atlantic Richfield Hanford Company, Richland, Washington.
- Price, W. H. and K. R. Fecht, 1976f, *Geology of the 241-C Tank Farm*, ARH-LD-132, Atlantic Richfield Hanford Company, Richland, Washington.
- Price, W. H. and K. R. Fecht, 1976g, *Geology of the 241-S Tank Farm*, ARH-LD-133, Atlantic Richfield Hanford Company, Richland, Washington.
- Price, W. H. and K. R. Fecht, 1976h, *Geology of the 241-SX Tank Farm*, ARH-LD-134, Atlantic Richfield Hanford Company, Richland, Washington.
- Price, W. H. and K. R. Fecht, 1976i, *Geology of the 241-T Tank Farm*, ARH-LD-135, Atlantic Richfield Hanford Company, Richland, Washington.
- Price, W. H. and K. R. Fecht, 1976j, *Geology of the 241-TX Tank Farm*, ARH-LD-136, Atlantic Richfield Hanford Company, Richland, Washington.
- Price, W. H. and K. R. Fecht, 1976k, *Geology of the 241-TY Tank Farm*, ARH-LD-137, Atlantic Richfield Hanford Company, Richland, Washington.
- Price, W. H. and K. R. Fecht, 1976l, *Geology of the 241-U Tank Farm*, ARH-LD-138, Atlantic Richfield Hanford Company, Richland, Washington.
- Price, W. H. and K. R. Fecht, 1976m, *Geology of the 241-SY Tank Farm*, ARH-LD-139, Atlantic Richfield Hanford Company, Richland, Washington.
- PSPL, 1981, "Gable Mountain: Structural Investigations and Analysis," Appendix 2.0, in *Puget Power, Skagit/Hanford Nuclear Project Preliminary Safety Analysis Report*, Puget Power Sound and Light, Bellevue, Washington, Vol. 4.
- Reidel, S. P., N. P. Campbell, K. R. Fecht, and K. A. Lindsey, 1994, *Late Cenozoic Structure and Stratigraphy of South-Central Washington*, Bulletin 80, Washington Division of Geology and Earth Resources, Olympia, Washington.
- Reidel, S. P. and K. R. Fecht, 1981, "Wanapum and Saddle Mountains Basalts of the Cold Creek Syncline Area," in C. W. Myers and S. M. Price (eds.), *Subsurface Geology of the Cold Creek Syncline*, RHO-BWI-ST-14, Rockwell Hanford Operations, Richland, Washington.
- Reidel, S. P. and K. R. Fecht, 1994a, *Geologic Map of the Priest Rapids 1:100,000 Quadrangle, Washington*, Open-File Report 94-13, Washington State Division of Geology and Earth Resources, Olympia, Washington.
- Reidel, S. P. and K. R. Fecht, 1994b, *Geologic Map of the Richland 1:100,000 Quadrangle, Washington*, Open-File Report 94-8, Washington State Division of Geology and Earth Resources, Olympia, Washington.

- Relyea, J., 1995, *Laboratory Reports, Project Files for WHC-EP-0883*, Westinghouse Hanford Company, Richland, Washington.
- Richman, L. R., 1981, "Sedimentary Analysis of Pre-Missoula Gravels in the Southeastern Part of the Pasco Basin, Washington," Master's thesis, Washington State University, Pullman, Washington, 82 p.
- Rockhold, M. L., M. J. Fayer, and P. R. Heller, 1993, *Physical and Hydraulic Properties of Sediments and Engineered Materials Associated with Grouted Double-Shell Tank Waste Disposal at Hanford*, PNL-8813, Pacific Northwest Laboratory, Richland, Washington.
- Rubey, W. W., 1933, "Settling Velocities of Gravel, Sand, and Silt Particles," in *American Journal of Science*, Vol. 224, pp. 325-338.
- Schuster, R. L. and R. J. Krizek (eds.), 1978, *Landslides, Analysis and Control*, Transportation Research Board Special Report 176, National Academy of Sciences, Washington, D.C., 234 p.
- Shannon and Wilson, Inc., 1974, *Supplemental Geologic Investigations for Carty West Site Report on Trenching and Clastic Dikes, Boardman Nuclear Project, Morrow County, Oregon*, prepared for Portland General Electric Company, Portland, Oregon, by Shannon and Wilson, Inc., Portland, Oregon.
- Singleton, K. M. and K. A. Lindsey, 1994, *Groundwater Impact Assessment Report for the 216-U-14 Ditch*, WHC-EP-0698, Westinghouse Hanford Company, Richland, Washington.
- Slate, J. L., 1996, "Buried Carbonate Paleosols Developed in Pliocene-Pleistocene Deposits of the Pasco Basin, South-Central Washington, U.S.A." in *Quaternary International*, Vols. 34-36, pp. 191-196.
- Smith, G. A., 1993, "Missoula Flood Dynamics and Magnitudes Inferred from Sedimentology of Slack-Water Deposits on the Columbia Plateau, Washington," in *Geological Society of America Bulletin*, Vol. 105, pp. 77-100.
- Smith, G. A., B. N. Bjornstad, and K. R. Fecht, 1989, "Neogene Terrestrial Sedimentation on and Adjacent to the Columbia Plateau; Washington, Oregon, and Idaho," in S. P. Reidel and P. R. Hooper (eds), "Volcanism and Tectonism in Columbia River Flood Basalt Province," *Geological Society of America Special Paper 239*, Geological Society of America, Boulder, Colorado.
- Stokes, G. G., 1851, "On the Effect of Internal Friction on the Motion of Pendulums," in *Cambridge Philosophy Transactions*, Vol. 9, No. 2, pp. 8-106.
- Terzaghi, K. and R. B. Peck, 1948, *Soil Mechanics in Engineering Practice*, John Wiley and Sons, New York, New York, 566 p.

- Tolan, T. L. and S. P. Reidel, 1989, "Structural Map of a Portion of the Columbia River Flood-Basalt Province," in S. P. Reidel and P. R. Hooper (eds.), *Volcanism and Tectonism in the Columbia River Flood Basalt Province*, Geological Society of America Special Paper 239, Geological Society of America, Boulder, Colorado.
- Tolan, T. L., S. P. Reidel, M. H. Beeson, J. L. Anderson, K. R. Fecht, and D. A. Swanson, 1989, "Revisions to the Estimates of the Aerial Extent and Volume of the Columbia River Basalt Group," in S. P. Reidel and P. R. Hooper (eds.), *Volcanism and Tectonism in the Columbia River Flood Basalt Province*, Geological Society of America Special Paper 239, Geological Society of America, Boulder, Colorado.
- Van Alstine, D. R., 1982, *Paleomagnetic Investigation of Pre-Missoula Gravels, Pasco Basin and Vicinity, Washington*, SGI-R-82-055, Sierra Geophysics, Redmond, Washington, for Golder Associates, Redmond, Washington.
- Volk, B. W., 1993, "Relating Particle Size Distribution to Moisture Retention Data for Hanford Soils," Master's thesis, Washington State University, Pullman, Washington.
- Waitt, R. B., 1980, "About Forty Last-Glacial Lake Missoula Jokulhlaups through Southern Washington," in *Journal of Geology*, Vol. 88, pp. 653-679.
- Waitt, R. B., 1994, "Scores of Gigantic, Successively Smaller Lake Missoula Floods Through Channeled Scabland and Columbia Valley," in D. A. Swanson and R. A. Haugerud (eds.), *Geologic Field Trips in the Pacific Northwest*, 1994 Geological Society of America Annual Meeting, Seattle, Washington, Vol. 1, pp. 1K-1-88.
- Walsh, T. J., R. A. Combellick, and G. L. Black, 1995, *Liquefaction Features from a Subduction Zone Earthquake: Preserved Examples from the 1964 Alaska Earthquake*, Report of Investigations No. 32, Washington Division of Geology and Earth Resources, Olympia, Washington, 80 p.
- WCC, 1980, *Potential for Reservoir Induced Seismicity, Chulac Dam Site*, prepared by Woodward-Clyde Consultants, San Francisco, California, for Instituto Nacional de Electrificación, Guatemala.
- WCC, 1981, *Quaternary Sediments Study of the Pasco Basin and Adjacent Areas*, prepared by Woodward-Clyde Consultants, San Francisco, California, for Washington Public Power Supply System, Richland, Washington.
- Weekes, D. C., G. K. Jaeger, and B. H. Ford, 1995, *Preoperational Baseline and Site Characterization Report for the Environmental Restoration Disposal Facility*, BHI-00270, Bechtel Hanford, Inc., Richland, Washington.
- Wright, J., J. L. Conca, and X. Chen, 1994, *Hydrostratigraphy and Recharge Distributions From Direct Measurements of Hydraulic Conductivity Using the UFA© Method*, PNL-9424, Pacific Northwest Laboratory, Richland, Washington.

LIST OF FIGURES

Figure	Page
1-1	1-2
1-2	1-2
1-3	1-4
1-4	1-6
1-5	1-7
1-6	1-8
1-7	1-9
1-8	1-10
1-9	1-11
1-10	1-12
1-11	1-13
1-12	1-14
1-13	1-15
2-1	2-1
2-2	2-2
2-3	2-3
2-4	2-3
2-5	2-4
2-6	2-4
2-7	2-5
2-8	2-6
2-9	2-7
2-10	2-8
3-1	3-1
3-2	3-1

Figure	Page	
3-3	Top: Thin clay/silt linings along the margins of infilling sediments and across infilling units in a clastic injection dike in south Richland [Keene/Kennedy Road (9/28-22M)]. Bottom: Thick clay/silt linings that comprise the majority of the clastic injection dikes in a coarse sand and granule unit in north Pasco [Transtate Gravel Pit (9/30-6F)]	3-2
3-4	Photographs of relatively smooth and flat (top) and undulating clay/silt linings (bottom) in vertical exposures of clastic injection dikes.	3-3
3-5	Photographs of deformed surfaces of clay/silt linings in vertical exposures that occur in the Pasco Basin and vicinity (clockwise from upper right): ridge and trough, V-tapered ridges, bulbous ridges, and filled mudcracks.	3-4
3-6	Photographs of vertical exposures showing dike infilling sediments and host rock with similar particle sizes at the Keene/Kennedy Road exposure located at 9/28-22M (top) and different particle sizes at the Yakima Bluffs site located at 9/28-16G (bottom).	3-5
3-7	Frequency of grain sizes within infilling sediments encountered in clastic injection dikes in the Pasco Basin.	3-5
3-8	Photographs of a vertical exposure (top) and surface exposure (bottom) of infilling sediments from a clastic injection dike in the sand facies of the Hanford Formation at Keene/Kennedy Road (9/28-22M).	3-6
3-9	Photographs of bedding structures of infilling sediments (clockwise from upper right): massive, normally graded, cross-laminated, and complex bed form.	3-7
3-10	Photograph of a small-scale slump adjacent to a clastic injection dike at the Environmental Restoration Disposal Facility excavation on the 200 Area Pleistocene Glaciofluvial Flood Bar, Hanford Site (12/26-7K).	3-8
3-11	Photograph of shears adjacent to a clastic injection dike in the sand facies (field mapping unit #3) of the Hanford Formation in the Environmental Restoration Disposal Facility excavation (12/26-7K)	3-9
3-12	Photograph of a small-scale horizontal fault with 8 cm of offset that cuts across a clastic injection dike.	3-9
3-13	Photograph of slickensides on a clay/silt lining of a thin clastic injection dike along a preexisting tear fault on the north-central flank of Gable Mountain, Hanford Site [Gable Mountain North (13/27-19A)]	3-10
3-14	Photographs of multiple rip-up clasts in infilling units at two clastic injection dikes located along Touchet Road, north of Touchet [Touchet Road (7/33-22Q)].	3-11
3-15	Photograph of soft-sediment flow features in the sand facies of the Hanford Formation (field mapping unit #3)	3-12
3-16	Photograph of contorted bedding associated with a laminated silty sand in the sand facies of the Hanford Formation (field mapping unit #2) at Keene/Kennedy Road (9/28-22M).	3-12
3-17	Map showing several localities of clastic injection dikes that extend more than 20 m in depth.	3-13
3-18	Photograph of a clastic injection dike complex that exceeds 2 m in width. The dike occurs in the sand facies (field mapping unit #2) in the Hanford Formation at the Fuels and Materials Examination Facility excavation (11/28-18N).	3-13
3-19	Truncation of a clastic injection dike at a bedding plane at Cummings Bridge (7/32-35Q)	3-14
3-20	Truncation of a clastic injection dike at a small-scale fault at Touchet Road (7/33-22Q).	3-14
4-1	Map showing the distribution of clastic injection dikes used in this study on a topographic map of the Pasco Basin and vicinity.	4-1
4-2	Map showing the geographic distribution of clastic dikes used in this study associated with geomorphic terrains in the Pasco Basin.	4-2
4-3	Photograph of a clastic injection dike along cooling fractures in the interior of a basalt flow from the Frenchman Springs Member.	4-4
4-4	Photograph of a clastic injection dike in the main channel sand facies of the Rattlesnake Ridge interbed of the Ellensburg Formation	4-5

Figure	Page	
4-5	Photograph of a clastic injection dike that extends down from lacustrine deposits of the member of Savage Island into a conglomerate unit of the member of Wooded Island	4-6
4-6	Photograph of the upper portion of the greatest known continuous vertical exposure of a clastic injection dike in the Pasco Basin (45 m)	4-7
4-7	Photograph of a clastic injection dike that penetrates the member of Savage Island along the Wahluke Landing Road (14/26-3N).	4-7
4-8	Photograph of a clastic injection dike in the deposits of the Yakima River.	4-8
4-9	Photograph of a clastic injection dike in deposits of the upper Cold Creek located in an interfluvium between sidestreams near Wahluke Landing Road (14/26-3N).	4-8
4-10	Photograph of a clastic injection dike in the gravel facies of the Hanford Formation (field mapping unit #3) along the Columbia River at the 100-N Area, Hanford Site (14/26-28C).	4-9
4-11	Photograph of a clastic injection dike that filled open-framework gravels at the top of a pre-13,000-year-old gravel facies of the Hanford Formation (field mapping unit #1 or #2?)	4-9
4-12	Photograph of a clastic injection dike in the sand facies of the Hanford Formation (field mapping unit #3) at the US Ecology excavation on the 200 Area Pleistocene Glaciofluvial Flood Bar, Hanford Site (12/26-9R).	4-10
4-13	Map showing the location of the major deposits of the sand facies of the Hanford Formation (field mapping units #3 and #4).	4-10
4-14	Photograph of clastic injection dikes in the silt facies of the Hanford Formation (field mapping unit #3) in the Burlingame Canyon (6/34-5M).	4-11
4-15	Photograph of clastic injection dikes in a host of glaciofluvial sediment at the Environmental Restoration Disposal Facility excavation (12/26-7K)	4-12
4-16	Map showing the locations of clastic injection dikes exposed in multiple stratigraphic units.	4-13
4-17	Figures illustrating the relationship of clastic injection dikes from two different intervals of emplacement, including (from top to bottom) older dike as host, older sediments as host, and bifurcation.	4-15
5-1	Photographs of clastic injection dike networks that occur in the Pasco Basin and vicinity (clockwise from top: regular-shaped polygons, irregular-shaped polygons, pre-existing fissures, and random dikes).	5-1
5-2	Aerial oblique photographs of regular-shaped, polygonal-patterned ground from the Goose Egg Hill area (12/26-33C)	5-2
5-3	Map showing the location of large exposures of regular-shaped, polygonal-patterned ground dike networks in the Pasco Basin.	5-3
5-4	Schematic of master dikes associated with a regular-shaped, polygonal-patterned ground dike network	5-4
5-5	Photograph of a simple merger of three master dikes segments at the Keene/Kennedy Road regular-shaped, polygonal-patterned ground dike network in the southern Pasco Basin (9/28-22M).	5-5
5-6	Photograph of a complex merger of three master dike segments at Touchet Road (7/33-22Q).	5-5
5-7	Aerial photograph illustrating examples of straight and curvilinear master dike segments in the regular-shaped, polygonal-patterned ground dike network near the Richland Landfill (10/28-17N).	5-6
5-8	Frequency of the number of sides forming polygons in the regular-shaped, polygonal-patterned ground dike network at Goose Egg Hill (12/26-33C).	5-6
5-9	Strike of master dikes in the Goose Egg Hill regular-shaped, polygonal-patterned ground dike network in the lower Cold Creek Valley (12/26-33C).	5-7
5-10	Dip of master dikes in regular-shaped, polygonal-patterned ground dike networks in the Pasco Basin and vicinity.	5-7

Figure	Page
5-11 Color near-infrared photograph of a portion of the Goose Egg Hill regular-shaped, polygon-patterned ground dike network in the lower Cold Creek Valley (12/26-33C)	5-8
5-12 Frequency plot of the area of polygons in the Goose Egg Hill regular-shaped, polygonal-patterned ground dike network (12/26-33C).	5-8
5-13 Relationship between dike width and the long (top) and short (bottom) polygon dimensions for regular-shaped, polygonal-patterned ground dike networks in the Pasco Basin and vicinity	5-9
5-14 Vertical photograph of a dikelet (right side of photograph) merging with a master dike (center of photograph) in a regular-shaped, polygonal-patterned ground dike network at Keene/Kennedy Road (9/28-22M)	5-10
5-15 Frequency of dikelets across a polygon as a function of distance from a master dike in a regular-shaped, polygonal-patterned ground dike network at Keene/Kennedy Road (9/288-22M)	5-10
5-16 Photograph of random dikelets in a central polygonal area at a regular-shaped, polygonal-patterned ground dike network at Keene/Kennedy Road (9/28-22M)	5-11
5-17 Photograph of a dikelet merging on the left side of the photograph that changes orientation into a sill in a silt lens.	5-11
5-18 Photograph of a sill along a bedding plane between two plane-laminated sand units in the sand facies of the Hanford Formation (field mapping unit #3)	5-12
5-19 Frequency of small-scale faults and shears as a function of distance across a regular-shaped polygon from the master dike at Keene/Kennedy Road (9/28-22M)	5-13
5-20 Photograph of small-scale faults and shears in a master dike and sand facies (field mapping unit #2) sequence at Keene/Kennedy Road (9/28-22M).	5-13
5-21 Photographs of a conjugate shear set with minor faulting associated within a master dike in a regular-shaped, polygonal-patterned ground dike network	5-14
5-22 Schematics of vertical offsets that have been observed at master dikes in regular-shaped, polygonal-patterned ground dike networks	5-15
5-23 Photograph of cross-cutting clastic injection dikes in an irregular-shaped, polygonal-patterned dike network in the silt facies of the Hanford Formation from the Touchet Road area (7/33-22Q).	5-16
5-24 Photograph of deformed (slumped) sediments and clastic injection dikes in an irregular-shaped, polygonal-patterned ground dike network along Touchet Road (7/33-22Q)	5-16
5-25 Map showing the location of several irregular-shaped, polygonal-patterned ground dike networks in the Pasco Basin and vicinity.	5-17
5-26 Photograph showing cross-cutting relationships among clastic injection dikes associated with irregular-shaped, polygonal-patterned ground	5-18
5-27 Photograph of highly deformed and contorted clastic injection dikes in an irregular-shaped, polygonal-patterned ground dike network along Touchet Road (7/33-22Q)..	5-18
5-28 Frequency of dike widths from a segment of an irregular-shaped, polygonal-patterned ground dike network along Touchet Road (7/33-22Q).	5-19
5-29 Strike of clastic injection dikes in a segment of an irregular-shaped, polygonal-patterned ground dike network along Touchet Road (7/33-22Q).	5-19
5-30 Dip of clastic injection dikes in a segment of an irregular-shaped, polygonal-patterned ground dike network along Touchet Road (7/33-22Q).	5-19

Figure	Page	
5-31	Frequency of distance between clastic injection dikes in a segment of an irregular-shaped, polygonal-patterned ground dike network along Touchet Road (7/33-22Q)	5-20
5-32	Photograph of the clastic injection dikes in an irregular-shaped, polygonal-patterned ground dike network in the sand facies of the Hanford Formation	5-20
5-33	Photograph of slumped sediments with deformed beds and low-angle, small-scale faults cutting across a clastic injection dike at an irregular-shaped, polygonal-patterned ground dike network along Touchet Road (7/33-22Q)	5-21
5-34	Dip of shears in an irregular-shaped, polygonal-patterned ground dike network along Touchet Road (7/33-27)	5-21
5-35	Photograph of clastic injection dikes in the hanging wall of the Horse Heaven Hills fault zone	5-22
5-36	Map showing locations of key exposures of pre-existing fissure dike networks in the Pasco Basin and vicinity.	5-23
5-37	Photograph of 40-cm-wide dike with multiple infilling units located in a pre-existing fracture within the CRBG	5-24
5-38	Photograph of a clastic injection dike within a fault of a flow-top breccia in the Elephant Mountain flow [Gable Mountain North (13/27-19A)]	5-25
5-39	Photograph of clastic injection dike that splays and pinches out downward into enhanced, pre-existing fissures in the Elephant Mountain flow of the CRBG	5-25
5-40	Photograph of a clastic injection dike penetrating vertically through the silt facies of the Hanford Formation	5-26
5-41	Photograph of clastic injection dikes that occur as a set of sills trending parallel to the surface of the CRBG at the south end of Weaver Pit (6/33-17H)	5-26
5-42	Extended cooling joints in a Frenchman Springs flow of the CRBG filled with a clastic injection dike	5-27
5-43	Photograph of clastic injection dikes in tectonic joints within the member of Wooded Island, Ringold Formation	5-27
5-44	Orientation of joints and shears that are filled with clastic injection dikes at Iowa Beef South (8/31-36D) and Weaver Pit (6/33-17H)	5-27
5-45	Photograph of a clastic injection dike along a zone of weakness in a brecciated zone within the Pomona Member, CRBG at Meadow Hills (9/28-35R)	5-28
5-46	Photograph of a clastic injection dike along a shear within a breccia zone	5-28
5-47	Photograph of a random occurrence dike that penetrates an upper silt facies and a lower gravel facies of the Hanford Formation.	5-29
5-48	Map showing the location of several random occurrence dike networks.	5-30
5-49	Photograph of a random occurrence clastic injection dike (coarse-grained dike) that penetrates the upper gravel facies (field mapping unit #2) of the Hanford Formation, middle silt facies (field mapping unit #3) of the Hanford Formation, and the overbank sediments of the deposits of the Yakima River, Plio-Pleistocene deposits [Yakima Bluffs (9/28-16G)]	5-31
5-50	Photograph of a single, random-occurrence clastic injection dike in bedded sand and silt sequence within a gravel facies of the Hanford Formation (field mapping unit #3)	5-32
5-51	Photograph of an isolated clastic injection dike complex associated with a random dike in Smith Coulee North (9/30-13N)	5-33
5-52	Map of the Pasco Basin and vicinity showing the location of the types of dike networks that are identified in this atlas	5-36
5-53	Map showing the location of clastic injection dikes that occur vertically in more than one type of dike network.	5-38
6-1	Photograph of a clastic injection dike in a regular-shaped, polygonal-patterned ground dike network	6-2
6-2	Stratigraphic column of Yakima Bluffs (9/28-16G) with at least two older glaciofluvial events and two ages of clastic injection dike emplacement	6-3
6-3	Photograph of a clastic injection dike in an irregular-shaped, polygonal-patterned ground dike network	6-4

Figure	Page
6-4 Photograph of a clastic injection dike in silt facies of the Hanford Formation (field mapping unit #3) unconformably overlying an older clastic injection dike in an earlier silt facies of the Hanford Formation	6-5
6-5 Photograph of an older clastic injection dike penetrating the silt facies of the Hanford Formation (equivalent to field mapping unit #1 or #2) and lower loess horizon in Touchet Valley (7/33-2F)	6-5
6-6 Photograph of clastic injection dikes of two different ages in the member of Wooded Island, Ringold Formation.	6-6
6-7 Stratigraphic column of Kiona Quarry (9/27-20K) with three glaciofluvial flooding events and two and perhaps three ages of clastic injection dike emplacement	6-7
7-1 Photograph of mud cracks on Pleistocene silt-dominated flood sediments in upper Cold Creek Valley (13/25-30M).	7-3
7-2 Photograph of large recent mud cracks that formed in the bottom of a large excavation located within lower Smith Canyon in the southeastern Pasco Basin (9/30-13L)	7-4
7-3 Photograph of downward-tapering fissures in desiccation cracks in a Saddle Mountains wasteway pond [Saddle Mountain Lakes (14/26-18J)]	7-4
7-4 Photograph of an ice wedge in permafrost, Yukon Territory, Canada (http://res.agr.ca/CANSIS/TAXA/LANDSCAPE/GROUND/yukon.html)	7-5
7-5 Aerial photograph of polygonal-patterned ground that occurs in a modern permafrost region south of Prudhoe Bay in northern Alaska, north of the Arctic Circle	7-6
7-6 Photograph of an ice-melt feature in the sand facies (field mapping unit #3) of the Hanford Formation in the Richland Landfill (10/28-17N).	7-7
7-7 Photograph of an ice-melt feature in the gravel facies (field mapping unit #2) of the Hanford Formation at a borrow pit located in Amon Canyon (9/28-25F)	7-8
7-8 Photograph of clastic injection dikes that formed during two different cataclysmic flooding events and penetrate to the top of their respective sequence.	7-10
7-9 Photograph of clastic injection dikes along tectonic joints within the member of Wooded Island, Ringold Formation, that are oriented N50°W	7-11
7-10 Photograph of tension fractures associated with the uplift of a doubly plunging anticline in the Rattlesnake Hills south of Richland at Meadow Hills (9/28-35R).	7-12
7-11 Photograph of an excavation in floodplain alluvium exposing a clastic injection dike that formed in the 1964 Alaska earthquake	7-13
7-12 Photograph of an alluvium with polygonal-patterned ground that formed during the 1964 Alaska earthquake	7-14
7-13 Photograph of a clastic dike located south of Finley in the Rattlesnake Hills.	7-17
7-14 Graph of Settling Velocities Versus Particle Size (from Dapples 1959).	7-21
8-1 Map of EMI survey showing two orthogonal clastic injection dikes in the lower Cold Creek Valley [Goose Egg Hill area (12/26-33C)]	8-1
8-2 Cross-section of an anomaly associated with a clastic injection dike in the Goose Egg Hill area (12/26-33C)	8-2
9-1 Photograph of Guelph permeameter equipment.	9-1
9-2 Map showing the location of Guelph permeameter tests.	9-4
9-3 General schematic of small-scale infiltration test.	9-13
9-4 Map showing the locations of small-scale infiltration tests.	9-14
9-5 Schematic illustrating the corrected results of infiltration test #1.	9-15

Figure	Page	
9-6	Graph of wetting front measurements (corrected) versus time for infiltration test #1	9-16
9-7	Schematic illustrating the corrected results of infiltration test #2.	9-17
9-8	Graph of vertical wetting front measurements (corrected) versus time for infiltration test #2.	9-18
9-9	Schematic illustrating the corrected results of infiltration test #3.	9-19
9-10	Graph of wetting front measurements (corrected) versus time for infiltration test #3.	9-20
9-11	Schematic illustrating the corrected results of infiltration test #4.	9-21
9-12	Graph of wetting front measurements (corrected) versus time for infiltration test #4.	9-22
9-13	Schematic illustrating the corrected results of infiltration test #5.	9-23
9-14	Graph of wetting front measurements (corrected) versus time for infiltration test #5.	9-24
9-15	Schematic illustrating the corrected results of infiltration test #6.	9-25
9-16	Graph of wetting front measurements (corrected) versus time for infiltration test #6.	9-26
9-17	Schematic illustrating the corrected results of infiltration test #7.	9-27
9-18	Graph of wetting front measurements (corrected) versus time for infiltration test #7.	9-28
9-19	Schematic illustrating the corrected results of infiltration test #8.	9-29
9-20	Graph of wetting front measurements (corrected) versus time for infiltration test #8.	9-30
9-21	Schematic illustrating the corrected results of infiltration test #9.	9-31
9-22	Graph of wetting front measurements (corrected) versus time for infiltration test #9.	9-32
9-23	Schematic of UFA Hy-Sed 100 Rotor with mechanical seal design (modified from Wright et al. 1994).	9-33
9-24	Map showing the location of the samples collected for measuring unsaturated hydraulic conductivity using the UFA method.	9-34
9-25	Cross-section of the sample site for UFA test #1.	9-35
9-26	Graph of volumetric water content versus hydraulic conductivity for UFA test #1.	9-36
9-27	Cross-section of the sample site for UFA test #2.	9-37
9-28	Graph of volumetric water content versus hydraulic conductivity for UFA test #2.	9-38
9-29	Cross-section of the sample site for UFA test #3.	9-39
9-30	Graph of volumetric water content and hydraulic conductivities for UFA test #3.	9-40
9-31	Cross-section of sample site for UFA test #4.	9-41
9-32	Graph of volumetric water content versus hydraulic conductivities for UFA test #4.	9-42
9-33	Cross-section of sample site for UFA test #5.	9-43
9-34	Graph of volumetric water content versus hydraulic conductivity for UFA test #5.	9-44
9-35	Graph showing volumetric water content versus gas conductivity in sample from UFA test #3.	9-45
9-36	Graph showing volumetric water content versus gas conductivity in samples from UFA tests #2, #4, and #5.	9-46
9-37	Frequency of occurrence of hydraulic conductivities across silt/clay linings and infilling units by testing method.	9-49
9-38	Frequency of occurrence of hydraulic conductivities across multiple and single silt/clay linings and associated infilling units.	9-49
9-39	Graph of volumetric water content versus hydraulic conductivities across silt/clay linings.	9-50
9-40	Frequency of gas conductivities from samples analyzed using the UFA method.	9-51
9-41	Frequency of occurrence of saturated hydraulic conductivities within infilling units of clastic injection dikes.	9-52
9-42	Photograph of clastic injection dikes from the Richland Landfill (10/28-17N) showing physical characteristics typical of most infilling units	9-53

Figure	Page
9-43 Photograph of a clastic injection dike with physical characteristics of infilling units with high saturated hydraulic conductivities	9-54
9-44 Photograph of a clastic injection dike in the southern wall of Lind Coulee with irrigation runoff percolating downward through the dike.	9-55
9-45 Frequency of occurrence of saturated hydraulic conductivities within the host sediments adjacent to clastic injection dikes.	9-56
9-46 Range of saturated hydraulic conductivities in host sediments from this atlas and data summarized in Khaleel and Freeman (1995). . .	9-56
9-47 Range of saturated hydraulic conductivities in clastic injection dikes and host sediments	9-57
9-48 Graph of moisture curves from hydraulic testing across clastic injection dikes and from host sediments measured in this study.	9-59
9-49 Graph of moisture curves from hydraulic testing across clastic injection dikes (symbols) and the range of moisture curves from sand of the Hanford Formation in the 200 Areas (solid lines)	9-59
9-50 Graph of moisture curves from hydraulic testing across clastic injection dikes (symbols) and the range of moisture curves from the early Palouse soil (deposits of the upper Cold Creek?) (solid lines)	9-59
9-51 Graph of moisture curves from hydraulic testing across clastic injection dikes (symbols) and the range of moisture curves from the deposits of the upper Cold Creek (solid lines)	9-60
9-52 Graph of moisture curves from hydraulic testing across clastic injection dikes (symbols) and the range of moisture curves from sands of the member of Taylor Flat (solid lines).	9-60
9-53 Graph of gas conductivity values and moisture contents for clastic injection dikes and host sediments.	9-61

LIST OF TABLES

Table	Page	
1-1	List of typical geological and geotechnical investigations that were sources for much of the published and unpublished data used in this study.	1-3
1-2	A summary of selected information from previous studies on clastic injection dikes.	1-16
2-1	Location of polygonal-patterned ground in the Pasco Basin and vicinity identified from aerial photographs from several earlier studies.	2-4
2-2	List of borehole clusters and boreholes that are known to have encountered clastic injection dikes during drilling.	2-6
4-1	Stratigraphic units in the Pasco Basin that are known to be intruded by clastic injection dikes.	4-3
4-2	Selected geologic sequences within the Pasco Basin and vicinity that contain clastic injection dikes in multiple sediment/rock types and units in a single geologic section.	4-14
6-1	Age of key stratigraphic units and tephra horizons in the Pasco Basin and vicinity important to determining the age and timing of emplacement of clastic injection dike networks.	6-1
6-2	Age of clastic injection dikes based on dike networks from the Pasco Basin and vicinity.	6-8
7-1	Selected moderate-sized earthquakes detected with filling of large reservoirs (from Bolt 1978).	7-13
9-1	Summary of field measurements for Guelph permeameter test #1.	9-5
9-2	Summary of field measurements for Guelph permeameter test #2.	9-6
9-3	Summary of field measurements for Guelph permeameter test #3.	9-7
9-4	Summary of field measurements for Guelph permeameter test #4.	9-8
9-5	Summary of the field measurements for Guelph permeameter test #5.	9-9
9-6	Summary of field measurements for Guelph permeameter test #6.	9-10
9-7	Summary of field measurements for Guelph permeameter test #7.	9-11
9-8	Summary of field measurements for Guelph permeameter test #8.	9-12
9-9	Wetting front measurements (corrected) and resulting rates of infiltration for infiltration test #1.	9-16
9-10	Wetting front measurements (corrected) and resulting rates of infiltration for infiltration test #2.	9-18
9-11	Wetting front measurements (corrected) and the resulting rates of moisture movement for infiltration test #3.	9-20
9-12	Wetting front measurements (corrected) and the resulting rates for moisture infiltration for infiltration test #4.	9-22
9-13	Wetting front measurements (corrected) and the resulting rates of infiltration for infiltration test #5.	9-24
9-14	Wetting front measurements (corrected) and the resulting rates of infiltration for infiltration test #6.	9-26
9-15	Wetting front measurements (corrected) and the resulting rates of moisture movement for infiltration test #7.	9-28
9-16	Wetting front measurements (corrected) and resulting rates of moisture movement for infiltration test #8.	9-30
9-17	Wetting front measurements (corrected) and the resulting rates of moisture movement for infiltration test #9.	9-32
9-18	Volumetric water content and hydraulic conductivity for UFA test #1.	9-36
9-19	Volumetric water content and hydraulic conductivities for UFA test #2.	9-38
9-20	Volumetric water content and hydraulic conductivities for UFA test #3.	9-40
9-21	Volumetric water content and hydraulic conductivity for UFA test #4.	9-42
9-22	Volumetric water content and hydraulic conductivity for UFA test #5.	9-44
9-23	Volumetric water content and gas conductivity of the host sediment in samples from UFA test #3.	9-45

Table		Page
9-24	Volumetric water content and gas conductivity measurements across silt/clay linings and infilling units of clastic injection dikes for samples from UFA tests #2, #4, and #5.	9-46
9-25	Summary of hydraulic testing data collected as part of this study.	9-48

DISTRIBUTION

U.S. Department of Energy, Richland Operations Office

K. M. Thompson† H0-12
RL Reading Room‡ H2-53

ERC Team

R. Boutin*	H0-19	R. M. Pawlowicz*	H0-02
L. A. Dietz*	H0-20	W. H. Price*	H0-18
K. R. Fecht† (3)	H0-02	V. J. Rohay*	H0-19
B. H. Ford*	H0-19	L. C. Swanson*	H9-02
R. L. Jackson*	H9-02	D. C. Weekes*	H9-02
Document and Information Services‡ (3)	H0-09		

Fluor Daniel Northwest

R. Khaleel* B4-43

Lockheed Martin Hanford

A. J. Knepp* H0-02

Pacific Northwest National Laboratory

D. B. Barnett*	K6-81	G. W. Gee*	K9-33
B. N. Bjornstad†	K6-81	D. G. Horton†	K6-81
B. W. Bryce*	K6-75	V. G. Johnson*	K6-96
M. J. Fayer*	K9-33	G. V. Last†	K6-91
Hanford Technical Library‡	P8-55	S. P. Reidel†	K6-81

Daniel B Stephens & Associates

719 Jadwin
Richland, WA 99352

K. A. Lindsey†
T. L. Tolan*

HydroGeologic, Inc.
3250 Port of Benton Blvd.
Richland, WA 99352

M. P. Connelly*

SAIC
3250 Port of Benton Blvd.
Richland, WA 99352

A. M. Tallman*

Jacobs Engineering Group Inc.
601 Williams Blvd. #4-A
Richland, WA 99352

P. Rogers*

Waste Management Federal Services Northwest Operations

K. D. Reynolds* H1-12

Washington Division of Ecology and Earth Resources

P. O. Box 47007
Olympia, Washington 98504-7007

J. E. Schuster*

*CD only.
†Hardcopy and CD.
‡Hardcopy only.

BHI-011103
Rev. 0
OU: N/A
TSD: N/A
ERA: N/A

APPROVAL PAGE

Title: Clastic Injection Dikes of the Pasco Basin and Vicinity: Geologic Atlas Series

Approval: W. H. Price
Site Assessments and Closure Manager

W. H. Price
Signature

7/27/99
Date

The approval signature on this page indicates that this document has been authorized for information release to the public through appropriate channels. No other forms or signatures are required to document this information release.

BHI-DIS done **JUL 27 1999**